

THE EFFECTS OF FIRE ON SOIL AND
SEDIMENT MAGNETISM.

Thesis submitted in accordance with the
requirements of the University of Liverpool
for the degree of Doctor in Philosophy by,

Timothy Andrew Rummery(12/1/81)

ABSTRACT

The present study examines the effects of fire on soil and sediment magnetism. Measurements of magnetic susceptibility (χ), saturated isothermal remanent magnetisation (S.I.R.M.) and coercivity of S.I.R.M. ((Bo)CR) have been undertaken on soil, stream bedload, suspended stream sediment and lake sediment samples. Samples were collected from 5 lake drainage basins which at some time in their history have been subject to forest fires.

The study was undertaken in 2 parts; the first examined in a recently burnt catchment (Llyn Bychan) the effects of fire on soil, where it was found to produce a large increase in χ and S.I.R.M. The increase was of the order of 2 to 3 times the values of unburnt soils. The increase was due to the production, in the fire-induced soil environment, of magnetically enhanced secondary ferrimagnetic oxides from low intensity magnetic forms of iron. Mossbauer and magnetic studies suggest the formation of non-stoichiometric magnetite from antiferromagnetic minerals in the soil.

The enhanced magnetic properties of the oxides were used to examine the main sediment pathways acting within an upland catchment following burning. Erosion from the soils ranged from rain splash erosion to sheet erosion on the steeper slopes. Input of the secondary ferrimagnetic oxides into the lake was examined, where they form at the mud-water interface a layer of magnetically enhanced material which is easily and rapidly distinguishable.

The second part of the study examined the persistence of the secondary ferrimagnetic oxides in the lake and soil environment. The persistence of enhanced oxides, formed in 1951, in the lake environment is shown in the Llyn Goddionduon sediments. The Landes case study shows the persistence of secondary ferrimagnetic oxides, formed in 1949, in both the lake and soil environment. The enhanced magnetic layer in the lake sediments is shown to correlate with known pollen and charcoal fire indicators enabling the magnetic technique to be used as a quick and accurate method of detecting and dating fires as recorded in lake sediments.

The use of enhanced χ and S.I.R.M. values as a rapid means of identifying past forest fires as recorded in lake sediments is examined further in the Lake Laukunlampi case study. The lake has a fire history of over 600 years and an attempt is made at examining the frequency and periodicity of fire events in the annually laminated sediment using the magnetic technique.

The increased magnetic properties of the oxides is used in a series of experiments investigating the use of artificially enhanced material as a natural stream bedload tracer.

<u>LIST OF CONTENTS</u>	<u>PAGE NO.</u>
List of Tables	ii
List of plates	ii
List of figures	iii
List of Appendices	vi
Acknowledgements	vii
Chapter 1 Introduction and Objectives	1
Chapter 2 Llyn Bychan. A case study.	32
Chapter 3 Llyn Goddionduon. A case study.	98
Chapter 4 Le Landes. A case study.	104
Chapter 5 Lake Laukunlampi. A case study.	155
Chapter 6 Plynlimon. A case study.	178
Chapter 7 Summary and general conclusion.	204
APPENDICES	205
PLATES	238
REFERENCES	239

<u>LIST OF TABLES</u>	<u>PAGE NO.</u>
1.2.1 Magnetic properties and crystal structure of certain minerals.	6
2.2.1 Morphometric data. Llyn Bychan.	40
2.6.1 χ values of eroded burnt soil material	51
2.6.2 S.I.R.M., χ , S.I.R.M./ χ , colour and depth for burnt erosion wash material.	55
2.8.1 S.I.R.M., χ and S.I.R.M./ χ for burnt and unburnt soils.	61
2.8.2 Mössbauer spectra results.	63
2.11.1 Lake bottom sediment trap results.	73
2.15.1 Rescaled S.I.R.M. and χ for bedload material from the Afon Abrach.	89
4.2.1 Morphometric data Lake Biscarrosse and Lake Sanguiret.	116
5.4.1 Peak number, depth, S.I.R.M. and time interval between S.I.R.M. peaks Lake Laukunlampi.	163
6.3.1 Magnetic enhancement Plynlimon bedload 200 ⁰ C-800 ⁰ C.	185
 <u>LIST OF PLATES</u>	
Plate 1 Llyn Bychan study area.	238
Plate 2 Llyn Goddionduon study area.	238

<u>LIST OF FIGURES</u>	<u>PAGE NO.</u>
1.2.1 χ plotted against grain size and domain type.	9
1.3.1 The hysteresis loop.	11
1.5.1 χ and S.I.R.M. plotted against grain size.	17
1.5.2 χ plotted against S.I.R.M.	18
1.5.3 Coercivity curves.	19
1.6.1 Magnetic minerals in the soil Fe-cycle.	22
2.1.1 Location of Llynau Bychan and Goddionduon.	33
2.2.1 Geology of Llynau Bychan and Goddionduon drainage basins.	35
2.2.2 Vegetation of the Llyn Bychan study area.	37
2.2.3 Llyn Bychan morphometry and lake sediment coring sites	39
2.2.4 Hydrology of the Llyn Bychan catchment.	41
2.3.1 The area around Llyn Bychan destroyed in the 1976 forest fire.	43
2.4.1 Location of soil sites sampled.	46
2.5.1 χ profiles for unburnt soils; B79:1, B79:2, B79:3, B79:10	48
2.5.2 S.I.R.M. profiles for unburnt soils BY17, BY19, BY20.	49
2.6.1 χ values for burnt soils.(probably soil wash).	52
2.6.2 χ profiles for burnt soils BY2, TB23.	53
2.8.1 Coercivity curves for burnt soils, stream and lake sediments from the Llyn Bychan catchment.	59
2.8.2 Thermomagnetic curve on extract BY6.	62
2.11.1 Continuous core K traces for LB1, 3, 4 and 5 and B79:1	63
2.11.2 S.I.R.M./depth profile for core LB6.	69
2.11.3 S.I.R.M./depth profiles for cores B79:3,4 and 5.	71
2.11.4 Coercivity curves for recent and older sediments. Core B79:4	72
2.11.5 Lake bottom sediment trap results.	74
2.13.1 Stream sediment trap results.	78
2.15.1 Location of bedload shoals sampled in the Afon Abroch.	86
2.15.2 Unscaled mass specific, total and average χ against distance for bedload shoals sampled.	87

2.15.3	Afon Abrach bedload rescaled S.I.R.M. regression lines.	90
2.15.4	Afon Abrach bedload rescaled χ regression lines.	91
3.2.1	χ , S.I.R.M, N.R.M. and ^{137}Cs for Llyn Goddionduon core 50/-43.	100
4.2.1	Location of the Landes.	106
4.2.2	Soils of the Landes.	110
4.2.3	Areas of the Landes destroyed by fire 1940-48 and 1949	114
4.2.4	Hydrology of Lake Biscarrosse and Lake Sanguinet.	117
4.2.5	Morphometry of Lake Biscarrosse.	118
4.2.6	Morphometry of Lake Sanguinet.	119
4.3.1	S.I.R.M. depth profiles for soil profiles from the Lake Biscarrosse catchment.	122
4.3.2	S.I.R.M. depth profiles for soil profiles from the Lake Sanguinet catchment.	124
4.5.1	Continuous K traces for Lake Biscarrosse cores BP1, 2, 6, 7, 8.	129
4.5.2	Location of coring sites Lake Biscarrosse.	130
4.5.3	Location of coring sites Lake Sanguinet.	131
4.5.4	S.I.R.M. depth profile cores BP6 and BP9.	133
4.5.5	S.I.R.M. depth profile cores S4, S6 and S15.	135
4.6.1	^{137}Cs profile core BP6.	137
4.6.2	^{210}Pb , ^{137}Cs and sedimentation rate Core S6.	139
4.8.1	Pollen and charcoal diagram core BP6.	142
4.8.2	Pollen and charcoal diagram core S4.	144
4.9.1	Fire indicators and S.I.R.M. core BP6.	148
4.9.2	Fire indicators and S.I.R.M. core S4.	150
5.2.1	Location Lake Laukunlampi.	158
5.4.1	S.I.R.M. profile for sediment core.	164
5.4.2	Sedimentation rate (mm. yr ⁻¹) depth curve for core.	166

	<u>PAGE NO.</u>
5.4.3 S.I.R.M. results 0.25 and 0.5 cm samples for the lake Laukunlampi sediments.	168
5.4.4 Corrected S.I.R.M. 0.25 cm samples and 0.5 cm sample. Rejected samples shown by a star.	170
6.2.1 Location of test reaches.	182
6.3.1 χ against temperature for toasted material.	186
6.3.2 Effects of alternative toasting procedures.	187
6.3.3 χ /grain size for toasted bedload used in the pilot study.	189
6.4.1 Control/mean χ values for each size range versus percentage concentration.	193
6.4.2 Estimated percentage concentration of enhanced material size ranges 710 μ m., 2.8mm. and 11.2mm.	194
6.4.3 Percentage concentrations for each fraction at each trap emptying. L.Tan and L. TanA.	196
8.2 Lake bottom sediment trap.	207
8.3 Stream sediment trap.	209

<u>LIST OF APPENDICES</u>	<u>PAGE NO.</u>
APPENDIX 1 - Magnetic extraction technique	205
APPENDIX 2 - Lake bottom sediment trap	206
APPENDIX 3 - Stream sediment traps	208
APPENDIX 4 - Some of the authors publications	210
APPENDIX 5 - Identification of cores used for analysis	237A

ACKNOWLEDGEMENTS

I would like to thank my supervisor, Professor Frank Oldfield for his continual help and encouragement at all stages of my work. Special thanks are due to Drs. R. Battarbee, K. Edwards, P. Huttunen, J. Meralianen, M. Newson and R. Thompson for their help and constructive comments.

I am grateful to Dr. J. Dearing and J. Bloemendal for allowing the inclusion of their unpublished data.

I am also grateful to the Department of Geophysics, University of Edinburgh for allowing access to measuring equipment, the Forestry Commission for access to their land and records, Pilkington Brothers for the use of their ovens and the R.A.F (University of Liverpool Air Squadron) for help in obtaining the aerial photographs. I would like to mention the help of the Gilchrist Educational Trust and the Sidney Perry Foundation towards field work assistance.

I would like to thank my fellow postgraduates Jan, Ann, John, Annie, Brian and Sandra for their comments and help on field work. In this respect I am indebted to Jan who also proof read the final draft. Thanks are also due to Sandra Mather for her help with the diagrams.

Finally I would like to thank Julie who has helped and encouraged me at all stages of my work and at times has shown great patience.

The work was carried out in the Geography Department University of Liverpool whilst in receipt of a Liverpool University Post graduate studentship.

INTRODUCTION

Palaeomagnetism is the study of the history of the earth's magnetic field as recorded in the permanent magnetisation of rocks and sediments. Palaeomagnetic studies are based on the natural remanent magnetisation properties of samples and they have been widely applied to the problems of sea floor spreading, continental drift and archaeomagnetic dating. (McElhinney, 1973. Thompson, 1974). Oldfield (1977) outlines the value of natural remanent magnetic properties as an aid to drainage basin interpretation. The production of a geomagnetic master curve calibrated with observatory, archaeomagnetic and radiocarbon dates has enabled lake sediments to be dated using the common variations that exist in the inclination and declination records in the sediments.

The application of magnetic measurements to the study of environmental problems in a relatively new field of investigation, differing from palaeomagnetic studies by the emphasis it places on non-naturally remanent and non-directional magnetic properties. The main magnetic properties used have been induced in artificially applied low and high strength magnetic fields. Thompson et al., in a recent paper (1980) have described the various environmental applications of induced magnetic properties to problems in geophysics, meteorology, climatology, hydrology, limnology, oceanography, sedimentology, geomorphology, soil science and land-use studies.

The application to lake sediment studies ranges from multiple core correlation and sediment accumulation studies (Thompson et al., 1975; Bloemendal et al., 1979) to the construction and extension of

tephrachronologies in the New Guinea Highlands (Thompson et al., 1978; Oldfield et al., in press). Rummery et al., (1979a) have used the enhanced magnetic properties of burnt inwashed soil to provide a datum for future studies.

Sediment process studies include the magnetic fingerprinting of suspended stream sediments (Oldfield et al., 1979) thereby enabling the identification of the sediment type, source areas and the contribution each area makes to the suspended load during a flood event (Walling et al., 1979). Stream bedload tracing using natural material magnetically enhanced artificially in ovens has been successfully demonstrated by Rummery et al., (1979b). They have shown that the technique may yield insight into the storage and delivery rates of such material, therefore making an important contribution to studies in fluvial geomorphology and hydrology.

Dearing (1979) has demonstrated the application of environmental magnetism to soil science and to land-use studies in contrasting magnetic environments. Thompson and Morton (1979) demonstrated the association of sediment particle size, susceptibility changes, and environmental changes in the drainage basin as reflected in the limnic deposits.

The distinctive magnetic properties of most industrial and domestic atmospheric particulate pollutants have been used (i) to allow the volume of post -1840 influx of pollutants to ombrotrophic peat deposits to be determined; (ii) to identify the source areas of the industrial and domestic pollutants and (iii) to calculate the variations in the post - 1840 magnetic flux density. (Oldfield, et al., in press)

In the marine environment magnetic analysis may enable a more detailed timescale to be constructed within which the effects of climatic changes on weathering, soil development and erosion rates can be studied.

PRINCIPLES OF MAGNETISATION 1.2

Electromagnetic theories are based on the fundamental observation that a magnetic field is produced when an electrically charged particle is in motion (Tarling, 1971). The movement of an electron in orbit around a nucleus produces a magnetic dipole moment which is the product of the orbital magnetic moment and the spin magnetic moment from the rotation of the electron on its own axis. All substances are magnetically active to some degree, the type and level of activity being determined by the nature of the alignment between the atomic moments when the substance is placed in a magnetic field.

Substances which possess a weak magnetic moment when placed in an applied field are either diamagnetic if there is an alignment of the moments in the opposite direction to that of the applied field, or paramagnetic if the alignment of the moments is in the direction of the applied field but breaks down after its removal. Water, organic matter, limestone and most siliceous minerals fall into these two groups and need only be considered here when they effectively 'dilute' the magnetic effects of low concentrations of 'highly' magnetic minerals.

Ferro-Ferri and Antiferromagnetism:

Ferromagnetic substances such as iron, cobalt and nickel exhibit spontaneous magnetisation due to the parallel alignment of the magnetic moments in the absence of an applied field.

Antiferromagnetic and ferrimagnetic substances exhibit a similar behaviour but are characterised by two sublattices, A and B. In antiferromagnetic substances the two sublattices have equal atomic moments aligned antiparallel to each other resulting in the ferromagnetic effects of the two sublattices cancelling each other out.

It is also possible that a substance may have equal atomic moments in the two sublattices which are not exactly antiparallel producing a weak spontaneous magnetisation. Such a substance exhibits a canted antiferromagnetic behaviour, e.g. hematite.

Ferrimagnetic substances possess the same antiparallel alignment but the magnetic moments of the lattices are unequal resulting in a net ferromagnetism.

The crystal structure will determine the type of magnetic behaviour. A simple cubic spinel structure as in magnetite consists of alternating layers of anions and cations but due to an imbalance of Fe^{2+} cations in the B lattice the crystal acts as a ferrimagnet. In contrast, hematite and ilmenite have hexagonal, corundum type crystal structures which allow a balance of Fe^{3+} ions in both lattices to occur; however the antiparallel alignment of the alternate lattices results in the crystal having an antiferromagnetic spin alignment.

Table 1.2.1 lists the different magnetic minerals, their magnetic properties, crystal type and typical magnetic susceptibility (χ) values. The important soil magnetic minerals possess either ferrimagnetic or antiferromagnetic behaviour, the two most important being magnetite and maghemite (Mullins, 1977). The magnetic properties of these are extensively covered in Stacey and Banerjee (1974).

The properties of anti-, ferro- and ferrimagnetism are dependant upon crystal structure, the elements present, and may be further modified by lattice defects and impurities in the crystal structure.

SAMPLE	FORMULA	MAGNETIC PROPERTIES OF MINERALS	TYPICAL χ VALUES $\times 10^{-6} \text{G.Oe.cm}^3 \text{g}^{-1}$	CRYSTAL TYPE
Ilmenite	FeTiO_3	Antiferromagnetic	136	HEXAGONAL
Hematite	Fe_2O_3	Antiferromagnetic	22-50	HEXAGONAL
Goethite	FeO.OH	Antiferromagnetic	10-101	ORTHORHOMBIC
Lepidocrocite	FeO.OH	Antiferromagnetic	40-60	HEXAGONAL
Pyrrhotite	FeS_{1+x}	Ferrimagnetic	4240	HEXAGONAL
Magnetite	Fe_3O_4	Ferrimagnetic	32,000-80,000	CUBIC-SPINEL
Maghemite	Fe_2O_3	Ferrimagnetic	32,800	CUBIC-SPINEL

TABLE 1.2.1

AFTER MULLINS

Above a temperature (the Curie Point) specific to ferro and antiferromagnetic materials, the magnetic behaviour of the materials reverts to paramagnetism. Curie point temperatures are diagnostic, and are typically 575°C for magnetite and 680°C for hematite.

Domain theory

Grains of ferrimagnetic material can be magnetised more easily in some directions than others, this leads to the material possessing a demagnetising field which arises from the shape of the grain.

Magnetic domains are spontaneously formed in an effort to reduce the overall demagnetising field of a grain. The number of domains formed is dependant on the size of the grain. (McElhinney, op cit).

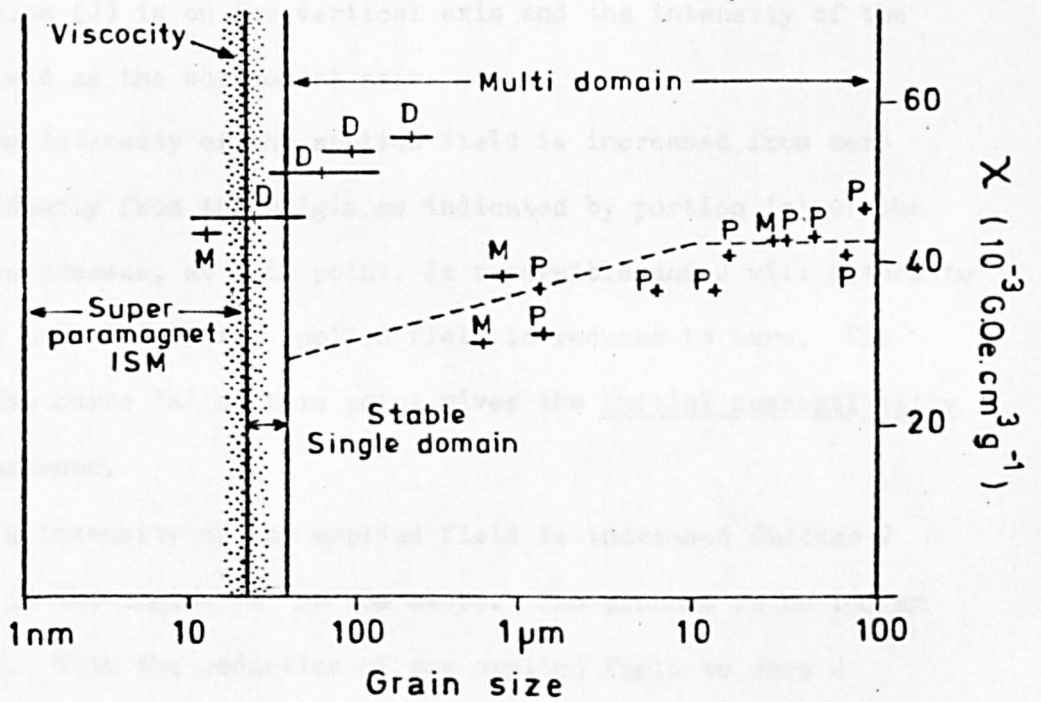
Large grains of ferrimagnetic material are physically large enough to be able to subdivide into two or more magnetic domains and are termed multidomain. Below a certain size limit, between 50 nm and $1\ \mu\text{m}$, a grain has only sufficient volume for a single domain to form and has magnetic properties specific to this state. (Dunlop, 1972). It is commonly expected that stable single domain and small multidomain grains will have smaller magnetic susceptibilities (χ) per unit volume than that of larger grains. However, Stacey and Banerjee (op cit) state that a given volume of superparamagnetic grains will make a bigger contribution to χ than an equal volume of stable single domain grains.

If a single domain grain is sufficiently small it becomes thermally unstable; a state in which the whole magnetic moment of the grain flips from one easy axis of magnetisation to another at room temperature. The application of an applied field in a specific direction will cause the grain magnetic moment to spend longer periods of time in that direction. The alignment of the grains in the direction of the applied field results in a χ value per unit volume greater than that expected for a paramagnetic

substance. Such behaviour is termed superparamagnetism.

Magnetic grains around the stable single domain/superparamagnetic boundary display a time dependence of magnetisation, termed magnetic viscosity. This can be observed by measuring the decay of saturation isothermal remanent magnetisation (S.I.R.M.) in these grains over a period of time. The decrease in S.I.R.M. is not arithmetic but linear when plotted against $\log t$ e.g. Oldfield et al., (in press).

The size ranges for the different domain types is still the subject of much discussion; the results of the main workers in the field are covered in Mullins (op cit). Fig. 1.2.1. plots the grain size, χ and domain type for magnetite and includes the results of Mullins (op cit), Parry (1965) and Dunlop (op cit).



(M=Mullins; P=Parry; D=Dunlop)

fig1.2.1 χ plotted against grain size and domain type.

with results of Mullins, Parry and Dunlop.

MAGNETIC PROPERTIES 1.3

Most of the fundamental magnetic properties used in this study can be defined using a hysteresis loop. The loop is simply the plot of induced magnetisation against the strength of the field applied. The following definitions, units and methods of measurement are presented in a shortened form in the appendix to Oldfield et al. (1978a).

Fig. 1.3.1. plots a typical initial magnetisation curve and hysteresis loop for a ferromagnetic substance. The intensity of magnetisation (J) is on the vertical axis and the intensity of the applied field as the horizontal axis.

As the intensity of the applied field is increased from zero J rises linearly from the origin as indicated by portion 'a' of the curve. The process, at this point, is reversible and J will return to zero along path 'a' if the applied field is reduced to zero. The slope of the curve 'a' at this point gives the initial susceptibility of the substance.

If the intensity of the applied field is increased further J increases in the region 'b' on the slope. The process is no longer reversible. With the reduction of the applied field to zero J does not follow the path 'b' but follows the curve 'c' producing an isothermal remanent magnetisation given by the point IRM.

Subsequent increases in the strength of the applied field take J up to point S, beyond which any further increases in the strength of the applied field produce no further increases in the intensity of magnetisation. The sample is said to be magnetically saturated. When the applied magnetic field is reduce to zero, J ,

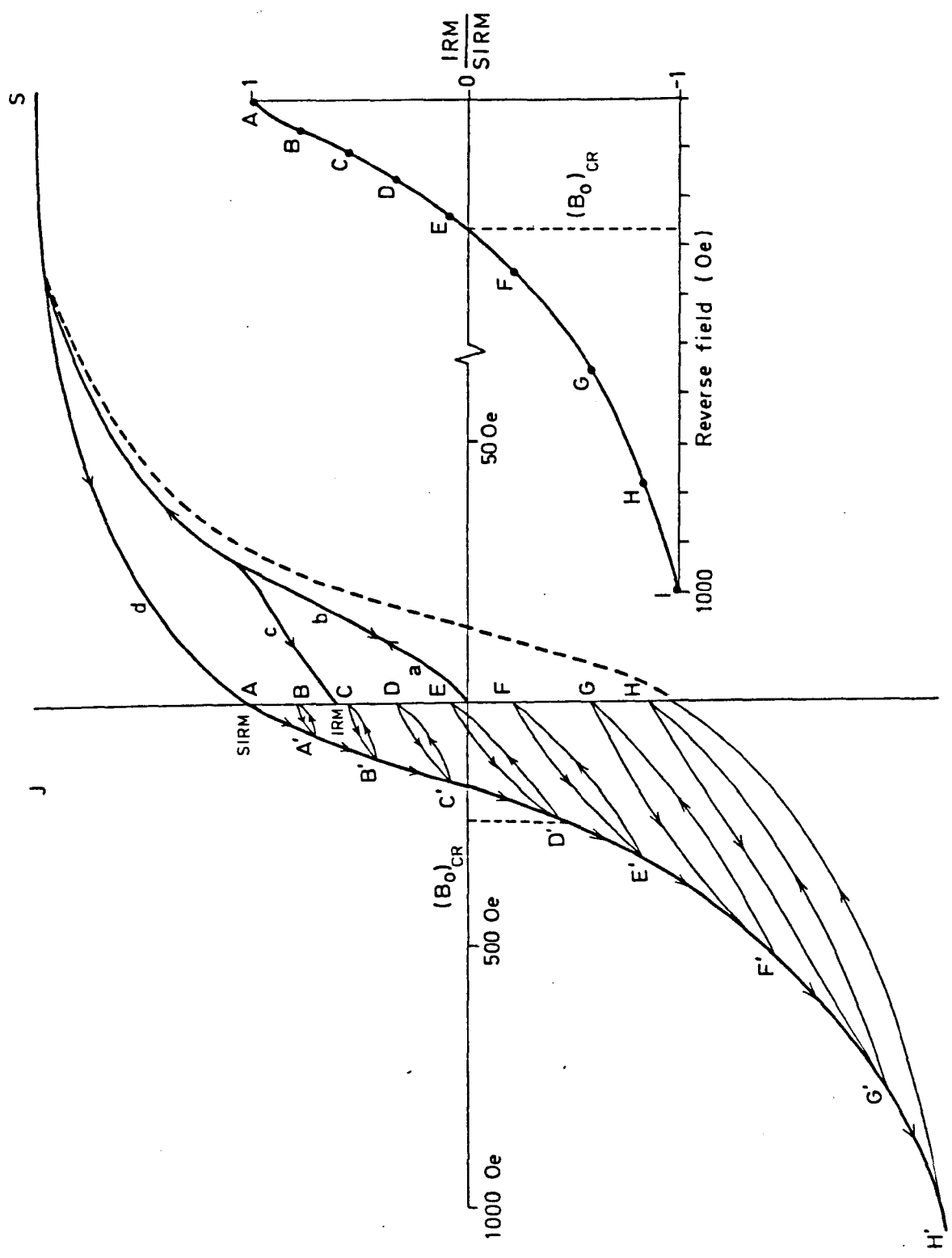


fig. 1.3.1. The hysteresis loop

the intensity of magnetisation, follows the path 'd' to point A which corresponds to the Saturation Isothermal Remanent Magnetisation (S.I.R.M.).

The application of a reversed magnetic field at this point leads to a growth of magnetisation that is plotted 'downwards' on the J axis. From A to A¹ on the curve the sample is in the applied field. The resulting intensity of magnetisation reflects the amount of reversed stable domains in the sample and the proportion of magnetised grains that are thermally unstable in a zero field. In an applied field these grains will align themselves in the direction of that field.

Upon removal of the reverse field the intensity of magnetisation will follow that path A¹ to B on the curve with a loss of 'downward' magnetisation. The loss is the result of the randomization of any alignment of the thermally unstable grains when the field was removed (i.e. field equals zero strength). The arrow, therefore, goes up to B.

If the strength of the reversed field is increased still further the intensity of 'downward' magnetisation follows the path B to B¹ as a result of the alignment of some of the stable domains and all the thermally unstable grains in the direction of the applied field. On removal of the field the direction of the thermally aligned grains is destroyed and the consequent loss of intensity is indicated by the curve moving upwards to C.

At a point just beyond D¹ on the hysteresis loop the reversed direction applied field is sufficient to overcome the direction of magnetisation of the majority of grains acquired at point S (saturation magnetisation). The product of the reversed stable domains is now greater than the number of stable domains that were originally aligned at S.

However, on removal of the applied field the intensity of magnetisation imparted by the alignment of the thermally unstable grains is lost and the number of reversed single domain grains equals the number of aligned grains in the original direction. The stable domains in the oppositely aligned directions cancel each other out. The reversed field at which this occurs is known as the coercivity of SIRM ($(B_0)_{CR}$) and helps to characterize different minerals and grain size.

If the reversed field is increased in steps until H , increases in J follow the course from E^1 to F up to G^1 to H . At all times there is a decrease in intensity on removal of the applied field. At H^1 the sample is completely saturated in the reversed direction with all the stable domains commonly aligned. At this point, if the direction of the applied field is again reversed the hysteresis loop will follow the course shown by the broken line and will exhibit the same changes in intensity on removal of the applied field.

The magnetic susceptibility (χ) of a sample can be most easily visualized as a function of the volume of ferrimagnetic minerals such as magnetite or maghemite, present in the sample. Thompson et al., (op cit) have demonstrated that for suites of samples with similar magnetic assemblages the S.I.R.M. is directly proportional to the χ . For this reason, in certain circumstances, S.I.R.M. can be used as a surrogate for χ where samples have a low χ value.

MEASUREMENT 1.4

Magnetic susceptibility can be measured on whole long cores of unextruded sediment or on extruded, soil and rock samples, wet or dry (volume K or specific χ). A digico long-core susceptibility bridge, detailed by Molyneux and Thompson (1973) is used for measuring whole cores. Single sample measurements are made on a smaller bridge (modified from Molyneux and Thompson). The equipment gives repeatable χ values down to a level of c. $2 \times 10^{-6} \text{G.Oe.cm}^3.\text{g}^{-1}$ with a noise level of c. $0.2 \times 10^{-6} \text{G.Oe.cm}^3.\text{g}^{-1}$.

S.I.R.M. is the magnetic moment induced in and retained by a sample after it has been placed in a high strength magnetic field at room temperature (section 1.3). S.I.R.M. is determined by grain size, type and shape. The coercivity of S.I.R.M. ($(B_o)_{CR}$) is used for detecting different magnetic mineral assemblages in single samples (section 1.5).

Units. (c.g.s.)	S.I.R.M.	$\text{G.Oe.cm}^3.\text{g}^{-1}$.
	$(B_o)_{CR}$	Oe.

Sample holders are marked with an inked arrow to facilitate orientation within the applied field and magnetometer. The samples are placed between the pole pieces of an electromagnet and saturated in a field of 10.k.Oe. The samples are then transferred to a Digico slow-speed balanced flux-gate magnetometer (modified form Molyneux, 1971) with a noise level of c. $0.1 \times 10^{-6} \text{G.Oe.cm}^3.\text{g}^{-1}$.

To avoid internal disorientation during measurement, samples of volumes smaller than the sample holders require packing with material (polythene foam) which has an insignificant S.I.R.M. value.

For (B_0) CR determinations the sample is first saturated and the S.I.R.M. measured. The sample is placed in a reversed field strength e.g. 100.Oe., and transferred to a magnetometer for measurement of I.R.M. The strength of the reversed field is increased to 200.Oe. and the sample is placed in the field and measured. The procedure continues for each increase in reverse field strength until all the stable domains in the sample are aligned in the direction of the reversed field.

The I.R.M. of the sample at each reversed field strength is divided by the original S.I.R.M. of the sample, the result indicating the proportion of grains in the sample aligned in the reversed direction. The (B_0) CR value is then determined graphically.

All single samples of soils and lake sediments were dried in an oven at 80°C for 12 hours and when dry placed in 10cc. plastic containers for χ measurement and the container marked with an arrow for S.I.R.M. and (B_0) CR determinations (to permit orientation within the electromagnet).

The magnetic measurements were made at the Department of Geophysics, University of Edinburgh U.K.

INTERPRETATION OF MAGNETIC MEASUREMENTS 1.5

The major magnetic parameters of χ , S.I.R.M., S.I.R.M./ χ ratio, $(B_0)_{CR}$ (coercivity of S.I.R.M.) and 'S' ratios (see below) used in this study are rapidly measured and make possible the differentiation of samples on the basis of magnetite-hematite ratios (ferrimagnetic vs. antiferromagnetic) and grain size contrasts. Dearing (op cit) extensively discusses the interpretation of the above parameters in their application to the study of particulate flux in lake watershed ecosystems.

χ is a basic measure of the volume of ferrimagnetic minerals in a sample and varies slightly with the size and shape of the magnetic grains. For spherical grains χ varies very little with grain volume and for magnetite or maghemite is c. $2 \times 10^{-6} \text{G.Oe.cm}^3.\text{g}^{-1}$ which represents a ferrimagnetic concentration by volume of 0.0001%. Therefore, only when the ferrimagnetic concentration is extremely low will antiferromagnetic or paramagnetic minerals sufficiently contribute to the total χ value.

Fig. 1.5.1 plots S.I.R.M., χ and S.I.R.M./ χ against grain size for spherical magnetite. Single and multi-domain grains show little variation in χ whereas S.I.R.M. varies considerably with grain size. Viscous and superparamagnetic grains possess very low S.I.R.M./ χ ratios. Fig. 1.5.2. summarizes the relationship between S.I.R.M./ χ and grain size.

Fig. 1.5.3 plots typical coercivity curves for fine and coarse grained magnetite and hematite. The degree of saturation when the applied back field in 1 KOe. after saturation in a forward field is denoted by an 'S' ratio which is a useful indicator of the ratio of low coercivity (e.g. ferrimagnetics) to high coercivity (e.g. antiferromagnetics) in a specimen (Stober and Thompson 1979). 'S' is usually negative.

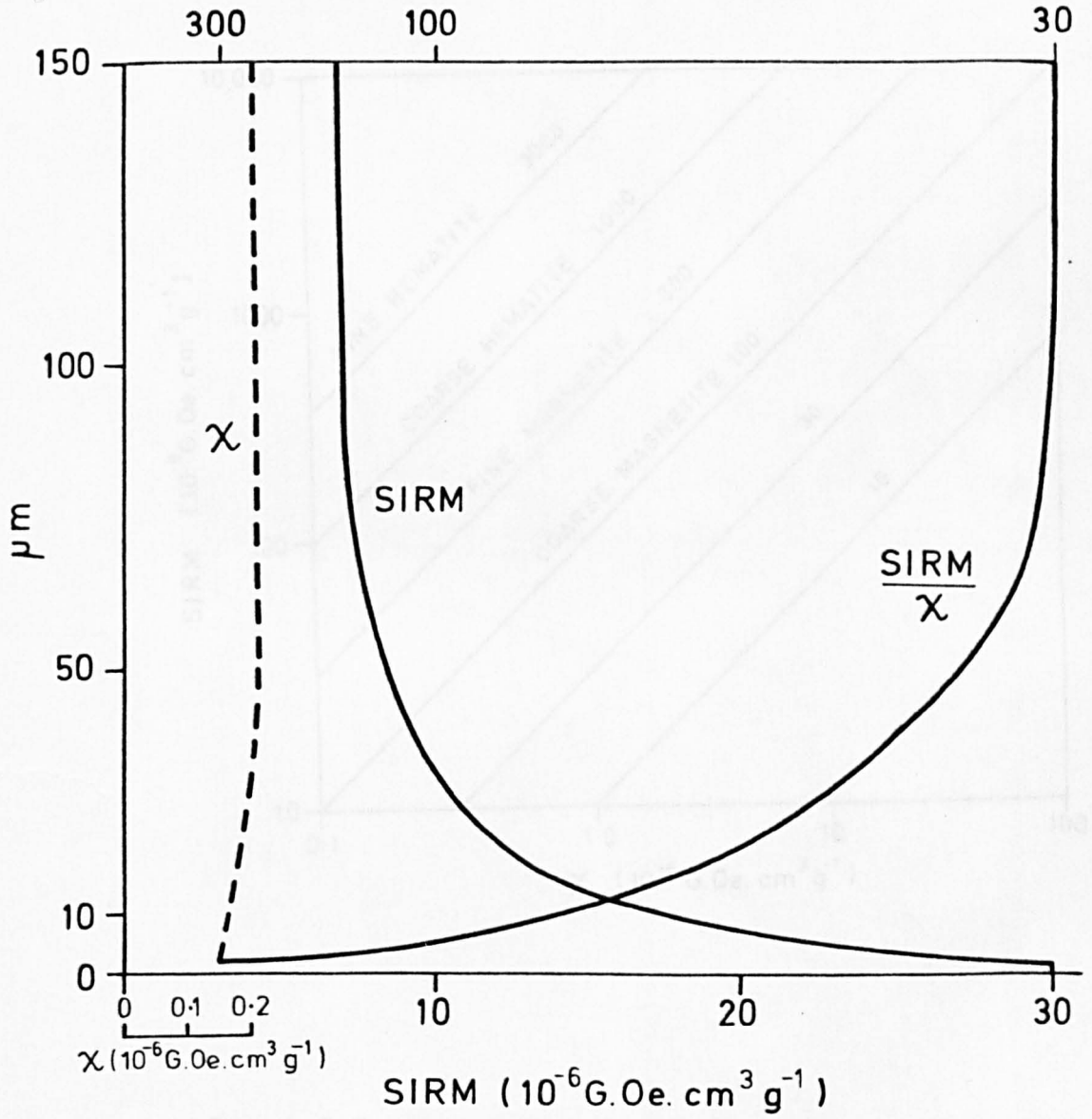


fig. 1.5.1 χ and S.I.R.M. plotted against grain size.

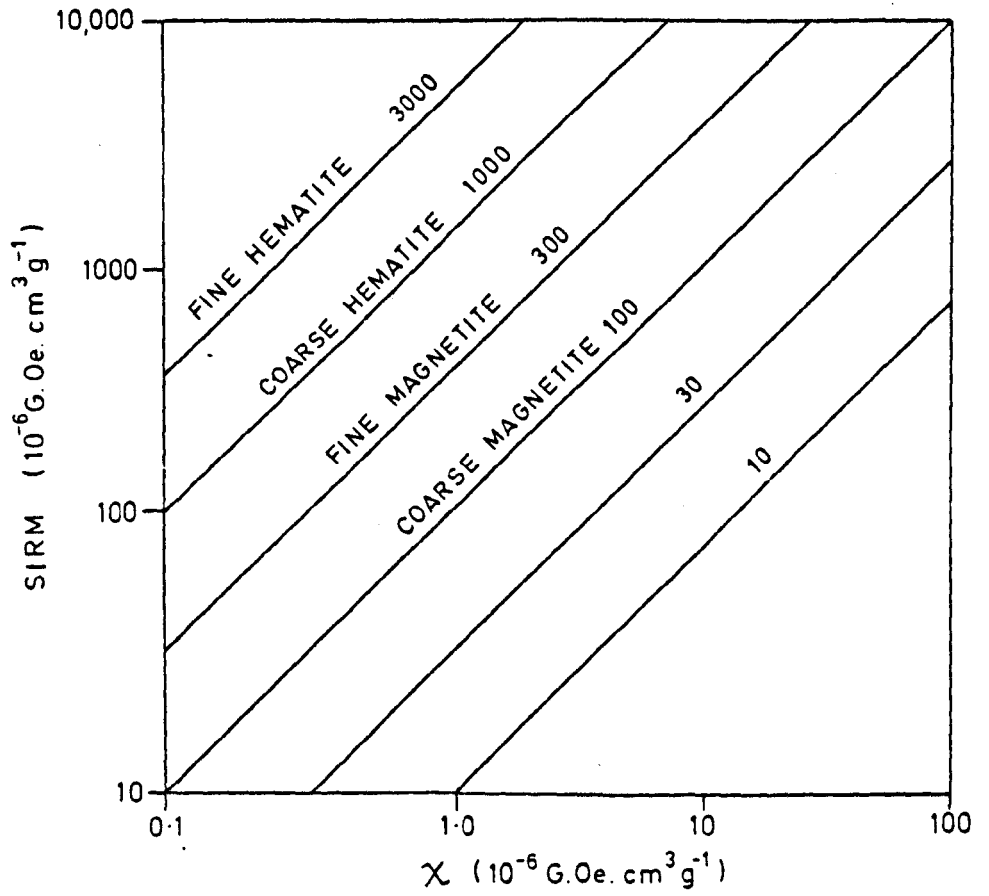


fig 1.5.2. χ against S.I.R.M.

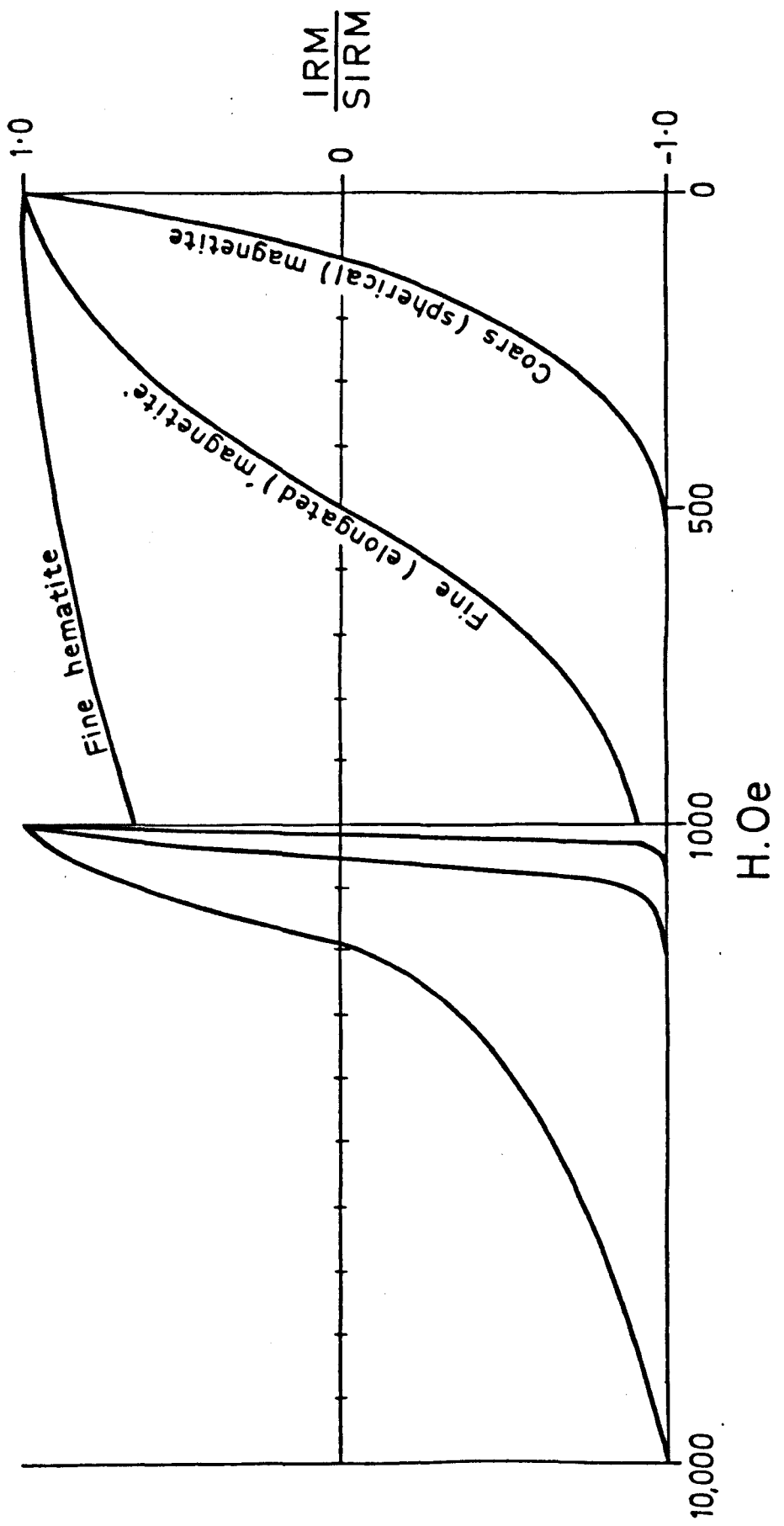


fig 1.5.3. Coercivity curves

Interpretation of coercivity curves is complicated by two factors.

(i) Grain shape; elongate grains have higher ^(Bo)CR values than spherical grains due to the increased resistance of the grains to demagnetisation (section 1.2). (ii) Due to the different mineral combinations in a sample a compound curve is produced. The identification of the constituents is not always obvious from the shape of the coercivity curves.

MAGNETIC MINERALS IN THE SOIL 1.6

The main ferri and antiferromagnetic soil forming minerals of importance are the oxides and hydroxides of iron, the iron titanium oxides and the iron sulphides. The magnetic properties of all are discussed in detail in Stacey and Banerjee (op cit).

In nearly all soils there are only two strongly magnetic minerals that are likely to be of any significance. Magnetite (Fe_3O_4) including oxidized titanomagnetites, and maghemite ($\gamma\text{Fe}_2\text{O}_3$) including oxidized titanomaghemites.

Fig. 1.6.1 describes the magnetic minerals in the soil iron cycle. The cycle falls into two main categories : (i) Primary ferrimagnetic minerals, which are essentially lumps of bedrock resistant to weathering that have become incorporated in the soil matrix. (ii) Secondary ferri and antiferromagnetic minerals which are the product of various pedogenic processes.

Le Borgne (1960) was the first to observe the increase in χ in the top few cm of the soil, which he attributed to the formation of secondary ferrimagnetic maghemite. Mullins (op cit) lists four different ways in which maghemite can be formed.

(i) By low temperature oxidation of magnetite present in rocks or in the soil. Stacey and Banerjee (op cit) have demonstrated the oxidation of magnetite to maghemite at low temperatures between 150°C and 250°C . Particles above 600 nm convert to hematite whereas smaller particles oxidize to maghemite (Feitknecht, 1965). Titanomaghemites oxidize to a two-phase solution, a titanium poor titanomagnetite with titanohematite lamellae. The low temperature oxidation process is not important in temperate climates but may be of significance in tropical areas. (Fitspatrick and Le Roux, 1975).

MAGNETIC MINERALS IN THE SOIL - Fe CYCLE

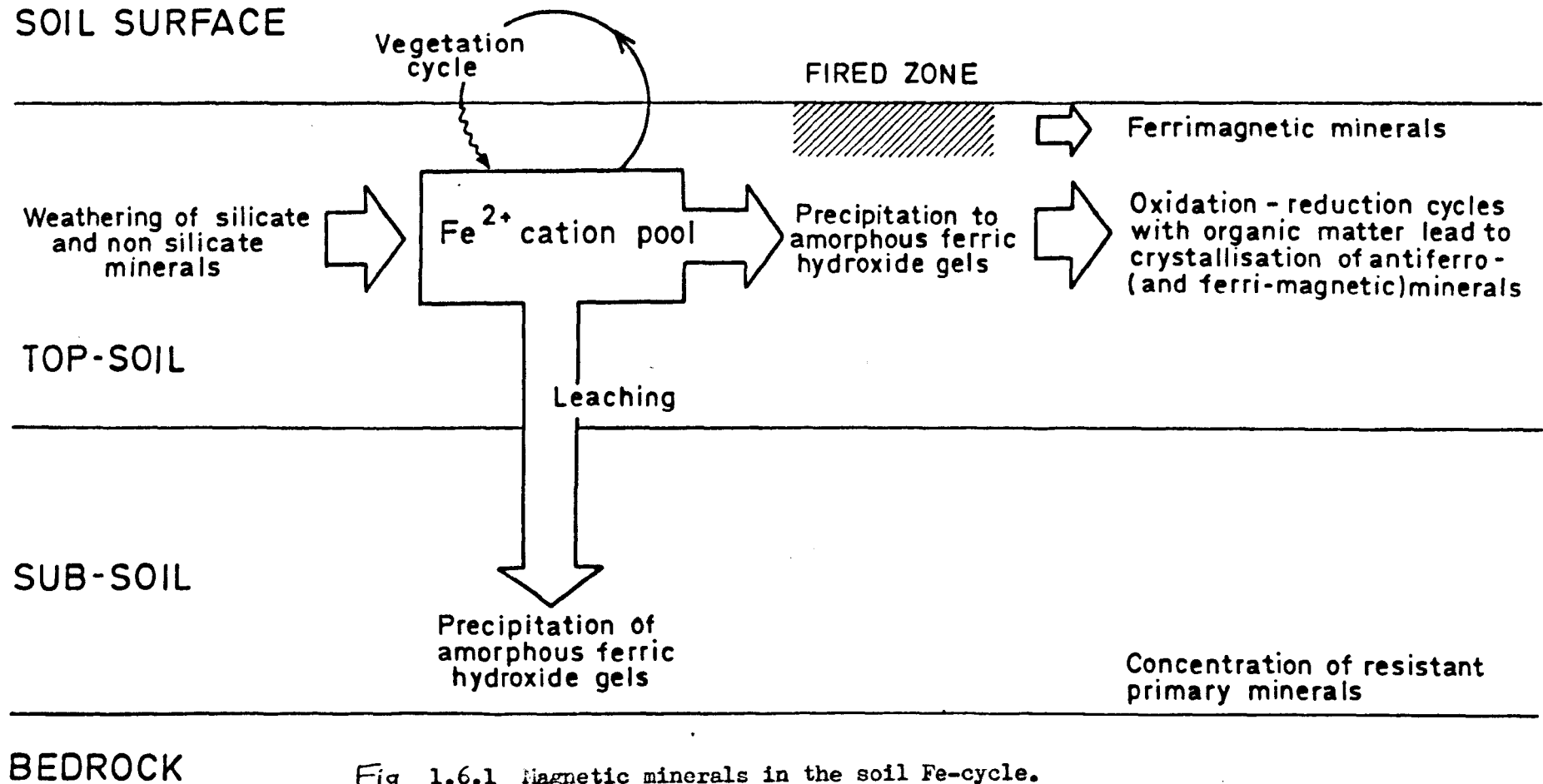


Fig. 1.6.1 Magnetic minerals in the soil Fe-cycle.

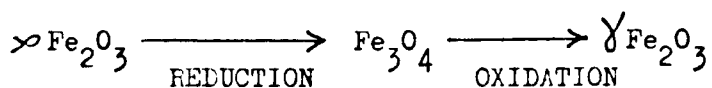
(ii) Dehydration of lepidocrocite : In poorly draining soils lepidocrocite dehydrates to maghemite within a temperature range 275°C to 410°C. (Scheffer et al., 1959)

(iii) Reduction - oxidation cycles under pedogenic conditions.

The mechanism involved in the magnetic enhancement of topsoils has been studied by a number of authors, (Oades, and Townsend, 1963; Mullins, 1974; Vadyunima and Babanin, 1972) and although not properly understood it is generally accepted that magnetic enhancement is due to the in-situ conversion of weakly magnetic forms of iron oxide and hydroxides to a strongly magnetic form. Schwertmann and Taylor (1976) demonstrated the production of maghemite from solutions of ferrous and ferric iron and showed that microbial activity is necessary to produce the reducing conditions essential for the solution of some forms of iron.

The discovery of magnetotactic bacteriam with grains of single domain magnetite in their structure by Blakemore (1975) points to the possibility that bacteria and soil fauna may be a source of magnetite production/synthesis and hence magnetic enhancement in soils. The discovery of single domain magnetite in bees and higher animals (Walcott et al., 1979) indicates that this source of magnetite may be of greater significance than was once supposed (Gould, 1979). In some soils, therefore, with a high faunal and microbial activity rate, the magnetic enhancement observed may be due to the magnetite present in the animals as well as that formed by other pedogenic processes.

(iv) As a result of burning : The production of magnetic enhancement as a result of burning was first demonstrated by Le Borgne (1955). The process involved is likely to be the main mechanism of magnetic enhancement in many soils and the resulting products form the main subject matter of this Thesis. Le Borgne demonstrated that under the action of reducing gases weakly magnetic forms of iron reduce to strongly ferrimagnetic magnetite and may subsequently be oxidized to maghemite on cooling, when air enters the soil, he inferred the following process :



Recent studies by the author and others (Tite and Lillington, 1975, Graham and Schollar, 1976) on natural magnetic enhancement by forest fires and artificial enhancement in ovens, has demonstrated the importance of burning as a mechanism of magnetic enhancement. Longworth et al., (1979) and the author have found that the end product of the burning process is magnetite, although of an impure form, and not maghemite. Rummery et al., (1979b) and Oldfield et al., (op cit) have demonstrated the production of maximum magnetic enhancement in soils or stream bedload material by heating is a complex procedure with a large number of variables. It can therefore be expected that the end product of the burning process could be either magnetite or maghemite. The nature of the original magnetic minerals in the soil before heating and the method used to differentiate between the two minerals are likely to be the factors governing whether maghemite or magnetite is found.

For the purpose of this study the end product of the burning process is termed magnetite.

THE EFFECTS OF FIRE ON SOILS AND VEGETATION 1.7

The ecological effects of fires on soils and vegetation have been extensively documented in a review article by Ahlgren and Ahlgren (1960). Wright (1976) has demonstrated the disruption of the nutrient cycling processes in terrestrial watersheds and lakes following a fire. Fire physically affects the soil in a number of ways; the extent is dependant on the severity of the burn and the temperatures reached. Komarek (1973) lists the main fire producing factors as the season, the prevailing weather conditions, fuel moisture and the type and quantity of the fuel.

A late summer fire following a prolonged period of drought is potentially the most disastrous due to the accumulation of litter and organic matter that has become 'tinder dry' (Heinselmann, 1973). The type of fire that results is both a surface and canopy fire consuming the ground and aerial fuel sources (Heyward, 1938).

The temperatures reached during a fire are the subject of much literature, (Heyward, (op cit)., Elpatievsky, (1934); Isaac and Hopkins, (1937); Whittaker, (1963)). Generally the temperatures attained above the surface exceed 600°C whereas below a depth of 5cm in the soil the temperatures reached are not great, around 28°C . Such temperature observations are usually made during controlled burns where the insulating properties of the soil litter layer are not destroyed. During an uncontrolled fire the temperatures attained in the mineral soil, after the combustion of the litter layer fuel source, may therefore exceed 600°C . Magnetic evidence is available confirming the high temperatures reached in the mineral soil during an uncontrolled fire (Rummary, 1978).

The high temperatures attained in the soil may be maintained for a long period of time after the initial fire. The author has personally observed localized hotspots of 'red hot' soil five days after a fire event in 1980.

The physical effects on the soil of high temperatures are well documented (Dryness, 1967) and include a removal of up to 75% of soil organic matter, resulting in the destruction of the soil structure, a destruction of the water stable aggregates (Dryness and Youngsberg, 1957) and a reduction in the soil macroscopic pore volume. (Tarrant, 1958). The net result of the effects as reported by many workers e.g. Fuller (1955); Beaton (1959) is a decrease in soil infiltration rates that is apparently proportional to the intensity of the fire. Mutch (1970) has shown that during an intense fire all the surface fuel is consumed and that the exposure of mineral soil will often result in decreased infiltration rates, largely due to the destruction of any surface structure by raindrop impact.

EFFECTS OF FIRE ON EROSION RATES 1.8

Fire in forested watersheds is often followed by increased rates of soil erosion. Hendricks and Johnson (1944), Connaughton (1935), Dryness (op cit) and Rich (1962) all reported increases in soil erosion following burning. The magnitude of accelerated erosion is controlled by many factors; two of the most important are inherent soil erodability and severity of the burn.

The atmospheric transport of material during a fire has only been studied from a pollution aspect. Several workers have recorded strong updrafts during a fire which transport not only the products of burning but also fine grained soil material (Section 2.13). The destruction of the soil structure and the binding properties of the organic matter exposes the soil to constant erosion by the wind until restabilization by vegetation growth. Locally, therefore, wind erosion may be an important erosive pathway and the author has observed its effectiveness on all recently burnt sites.

Exposure of the mineral soil coupled with decreased infiltration rates results in (i) the removal of surface material by raindrop impaction and eventually leads to gullyng. (ii) Soil creep and mass movement of the soils on steeper slopes. Wright (op cit) and Tiedemann and Helvey (1973) working in Minnesota and Washington respectively, found a 60% increase in runoff two years after a fire event, although Fredriksonn (1970) reports an increase of up to 250 times normal runoff immediately following logging.

Work in the paired catchments at Hubbard Brook, New Hampshire, has demonstrated the dramatic changes in particulate and solute export following a major disturbance of the forest ecosystem. To date a

major disturbance has not included fire but their findings give an insight into what might be expected after such an event. Borman et al., (1969); Likens et al., (1970); Hobbie and Likens (1973); Likens and Borman (1974).

The type of soil movement following a fire is naturally controlled by the characteristics of the individual area, i.e. topography, climate, inherent soil erodability and the amount of protection provided by the remaining litter and plant cover. Values of soil loss range from 32 to 165 tons per acre (Hendricks and Johnson, op cit) to a total loss from a 60 acre burn of about 1 foot per acre (Rich, op cit). Krammes (1960) working in Southern California found that fire caused erosion increases of from 4 to 17 times the pre-burn rates.

DISCUSSION AIMS AND OBJECTIVES 1.9

Mullins (op cit) concluded that the production of magnetic minerals in the soil by the burning mechanism may be of considerable importance since most soils at some stage in the last few thousand years have been subject to natural or man made fires. The mechanism is of prime importance in areas that have been devastated by forest fires, dominating all the other soil magnetic mineral forming processes operating in the soil.

The immediate environmental and erosional consequences of such a dramatic event in a lake drainage basin are well known and are usually studied using time consuming techniques such as soil, soil water, stream water and lake sediment chemistry. Elaborate surveying and resurveying exercises may be needed to measure the amount of erosion after a fire event. Similar chemical techniques coupled with laborious pollen, diatom and charcoal analyses are the main methods of investigating the fire histories of lake basins.

The earliest examples of the application of magnetic measurements to studies of lake watershed ecosystems (Thompson et al., op cit) used whole core K in a lake core correlation study in which K was shown to correlate with the diatom biostratigraphies as well as the pollen and chemical erosion indicators. Dearing (op cit) studied the application of magnetic measurements to the study of particulate flux in lake watershed ecosystems: He demonstrated the advantages of being able to rapidly, and non-destructively measure large numbers of soil, sediment and rock samples together with the consequent increases in accuracy that such an approach gives when constructing source-sediment linkages and making estimations of total sediment influx.

From section 1.6 it has been shown that burning produces magnetic minerals in the soil that are magnetically distinct from those formed by other processes.

The present study was prompted by the works of Le Borgne (op cit) and Mullins (op cit) together with the promising results from investigations of the links between environmental changes and changes as recorded in lake sediment cores. Many lakes from contrasting environments had been studied.

There are three specific questions in any study of the effect of fire on soil magnetism that have to be answered.

(i) Did the burning of the soil produce persistent secondary ferrimagnetic oxides and hence magnetic enhancement? (ii) if magnetic enhancement was produced how was it related to soil and site conditions at the time of the burn? (iii) What are the processes and variables involved in the formation and persistence of the secondary ferrimagnetic oxides in the soil and how may one identify these oxides?

A 1976 summer forest fire in North Wales provided the first site for these investigations.

Once the three basic questions had been satisfactorily examined and answered the further objectives of the study were by using magnetic techniques:

(a) Identify by the enhanced magnetic properties, burnt soils within the catchment and to relate the degree of enhancement to soil and other environmental conditions.

(b) To study the erosional processes acting within the drainage basin examining soils, streams and lake sediments in an effort to examine the inputs and outputs of the enhanced material in the system.

- (c) To study the short term persistence of the enhanced material in the lake environment (over a period of 3 years) and to examine the implications of a magnetically distinct layer in the sediment for multiple core correlation studies and as a fixed datum.
- (d) To study the long term persistence of the fire created secondary ferrimagnetic minerals in the soil and lake environment in a lake basin with an earlier well documented forest fire.
- (e) To examine the application of the magnetic technique as a complimentary method to palaeoecological studies in examining and establishing fire chronologies of lake basins with long undocumented fire histories.
- (f) To investigate the use of artificially magnetically enhanced material as a stream bedload tracing method.

CHAPTER 2 LLYN BYCHANINTRODUCTION 2.1

In section 1.6 the four possible sources of magnetic minerals in the soil were discussed. It is the fourth mechanism, the action of burning, that is to be examined in this chapter. The 1976 drought in Great Britain led to a series of forest fires in North Wales and provided suitable areas where the effects of the fire upon the soil and sediment magnetism could be studied.

A substantial part of the drainage basin of a small lake, Llyn Bychan (Grid ref: SH 753593), located in the Gwydyr Forest area of North Wales approximately 10km north west of Betws-y-Coed was devastated by a forest fire. (Fig. 2.1.1, plate 1). The fire consisted of both a ground and canopy element destroying not only the vegetation cover but inflicting severe damage to the soil cover.

The catchment constituted an ideal site for examining the effects of fire on the soil magnetism, i.e. the production of secondary ferrimagnetic oxides; the transportation of the material and its deposition as lake sediment and the dominant pathways of erosion acting within an upland catchment following burning.

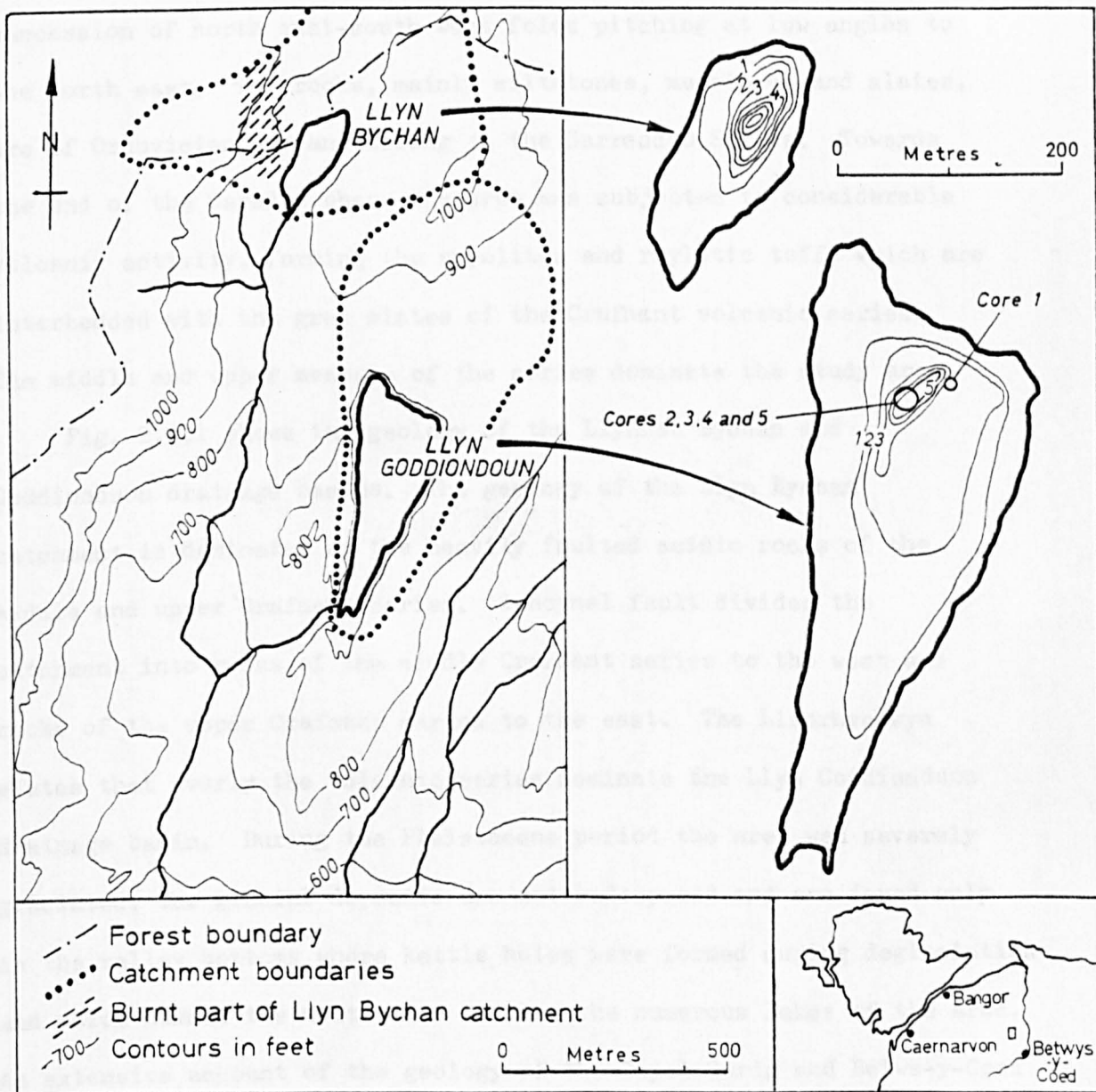


fig. 2.1.1 Location of Llynau Bychan and Goddioundou.

SITE CHARACTERISTICS 2.2

Geology

The area of the Glynn can be considered as part of the eastward dipping monocline of eastern Gwynedd, upon which is super-imposed a succession of north east-south west folds pitching at low angles to the north east. The rocks, mainly siltstones, mudstones and slates, are of Ordovician age and belong to the Garreddau Series. Towards the end of the Caradoc phase the area was subjected to considerable volcanic activity, forming the rhyolites and rhylitic tuffs which are interbedded with the grey slates of the Crafnant volcanic series. The middle and upper members of the series dominate the study area.

Fig. 2.2.1 shows the geology of the Llynnau Bychan and Goddionduon drainage basins. The geology of the Llyn Bychan catchment is dominated by the heavily faulted acidic rocks of the middle and upper Crafnant series. A normal fault divides the catchment into rocks of the middle Crafnant series to the west and rocks of the upper Crafnant series to the east. The Llanrhychwyn slates that overly the volcanic series dominate the Llyn Goddionduon drainage basin. During the Pleistocene period the area was severely glaciated; the glacial deposits are not widespread and are found only in the valley bottoms where kettle holes were formed during deglaciation and which dammed the meltwaters forming the numerous lakes of the area. An extensive account of the geology of the Capel Curig and Betws-y-Coed area can be found in Howells et al., (1978).

GEOLOGY OF THE LLYN BYCHAN AND LLYN GODDIONUON AREA

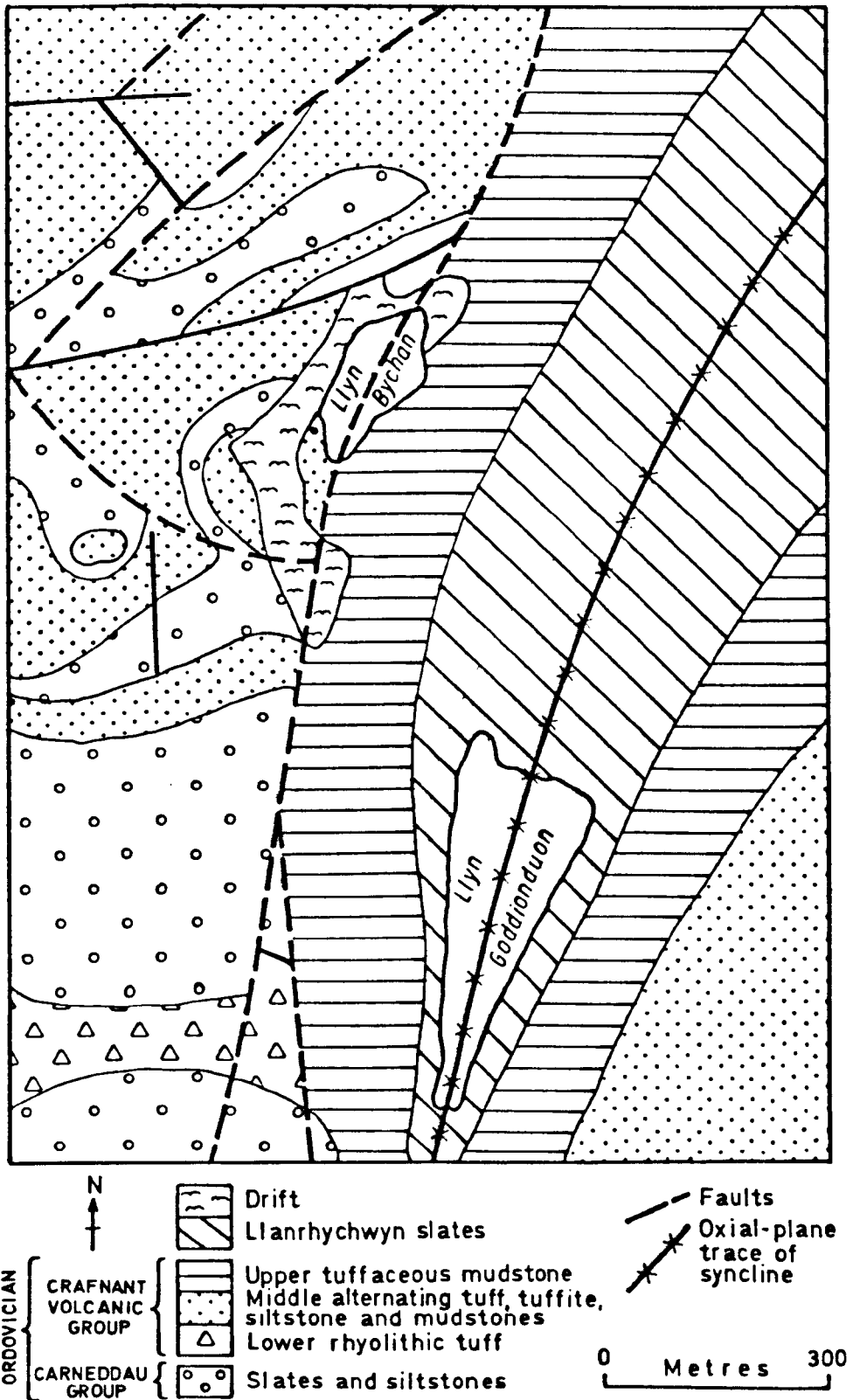


fig. 2.2.1 Geology of Llynau Bychan and Goddienduon drainage basins.

Soils

The main soil type found within the catchment is acidic podsol. Steep slopes are characterized by freely draining immature soils whereas the deeper more mature soils dominate the less steep slopes and the tops of ridges and spurs. On the ridge tops where drainage is imperfect peat development occurs. Peat development is also associated with the water logged land immediately adjacent to the lakes and with the flushes that occur along the wall to the north of the catchment. (see fig. 2.2.2)

The eastern half of the catchment is characterized by deep podsol with large quantities of rock fragments and poor profile differentiation. These soils have developed on the Llanrhychwyn slates and are the main soil type found in the Llyn Goddionduon drainage basin except for some peat development around the lake fringes.

Vegetation and land-use

The vegetation of the catchment can be grouped into three categories (Fig. 2.2.2) moorland, mire and aquatic species and forestry plantation. Calluna vulgaris, Molinia caerulea, Erica and Ulex species and Vaccinium myrtillus typify the moorland areas with Pteridium aquilinum colonizing the deeper soils at the base of the slopes. The peaty areas around the lake edge are dominated by Sphagnum Spp. and Myrica gale, although in the relatively drier areas these species grow along with Calluna vulgaris and Juncus species. Together, the moorland and peat areas constitute c.42% on the catchment area, the remaining 36% of ground area is under Forestry Commission plantation.

LLYN BYCHAN - VEGETATION

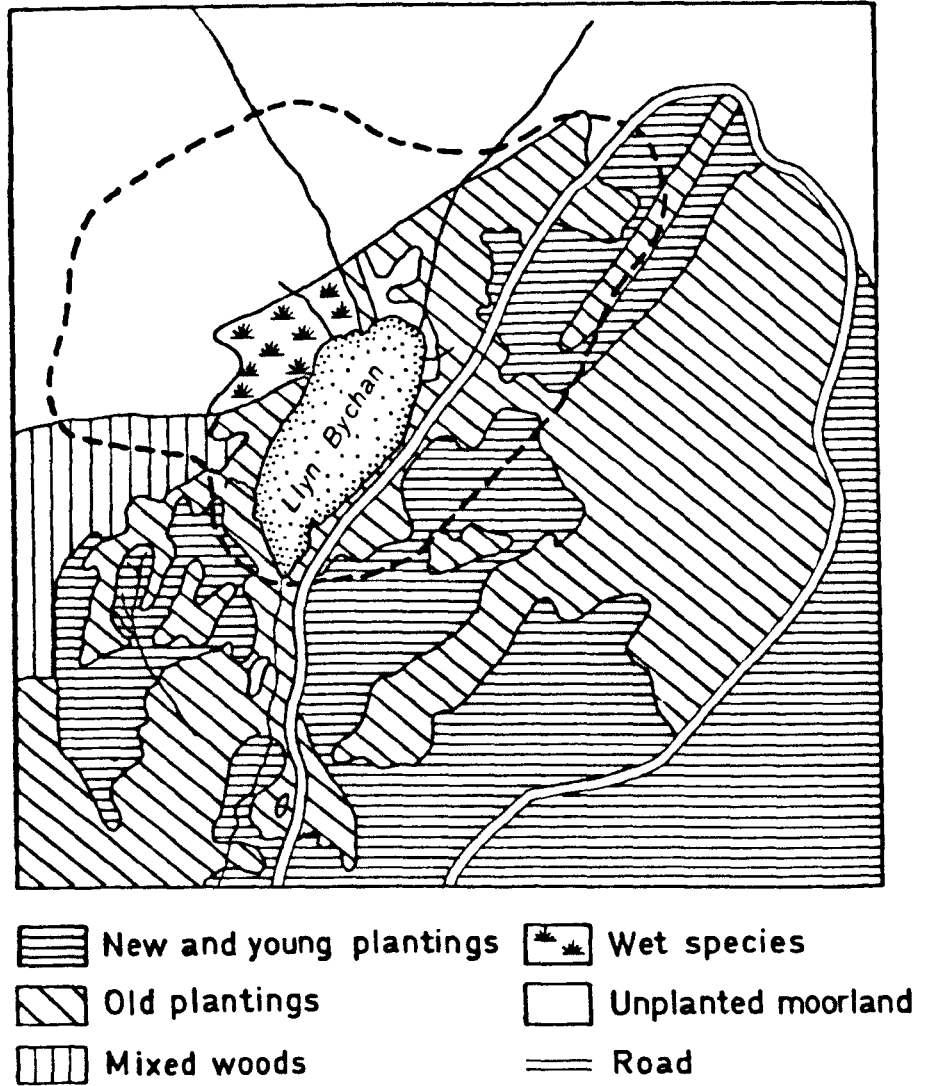


Fig. 2.2.2 Vegetation of the Llyn Bychan study area.

Planting of the Gwydyr Forest began in 1921 and by 1932 the areas around the Llynau Bychan and Goddionduon were completely forested, forming part of a total afforestation programme of over 410 ha. (Shaw, 1971). The Forestry Commission designated the rugged land to the west of Llyn Bychan as being of marginal value for forestry. Japanese larch and Lodgepole pine were planted on the steepest slopes and in the most exposed locations. Silka and Norway spruce were planted on the lower, more protected slopes. The eastern side of the catchment and the whole of the Llyn Goddionduon catchment was classified as prime forestry land and now support mixed plantations of Norway spruce, Silka spruce and Scots pine. (Taylor, pers. comm.).

The Glynn area has always been noted as an area of high fire risk and even before afforestation the 'dry' years previous to 1942 saw several large moorland fires. As extensive 7 year forest road construction programme was initiated in 1951 as a means of reducing the high fire risk. The need for a good communications system was made evident in 1951 when fire ravaged the Glynn inflicting great damage to the forested areas around Llyn Goddionduon. The fire did not enter the Llyn Bychan drainage basin. Replanting of the 265 ha. destroyed in the fire and restocking following fellings in 1965 has produced the mozaic of old and young plantations that is typical of the Glynn today.

Hydrology

Llyn Bychan is a small lake formed in a kettle hole. The lake origins are reflected in a maximum depth of 9m. in relation to a mean depth of 1.35m. (Liddle, 1974). The lake morphometry is shown in Fig. 2.2.3. The trench in the centre of the lake produces an

BASIN MORPHOLOGY OF LLYN BYCHAN WITH LOCATION OF THE LAKE SEDIMENT CORING SITES

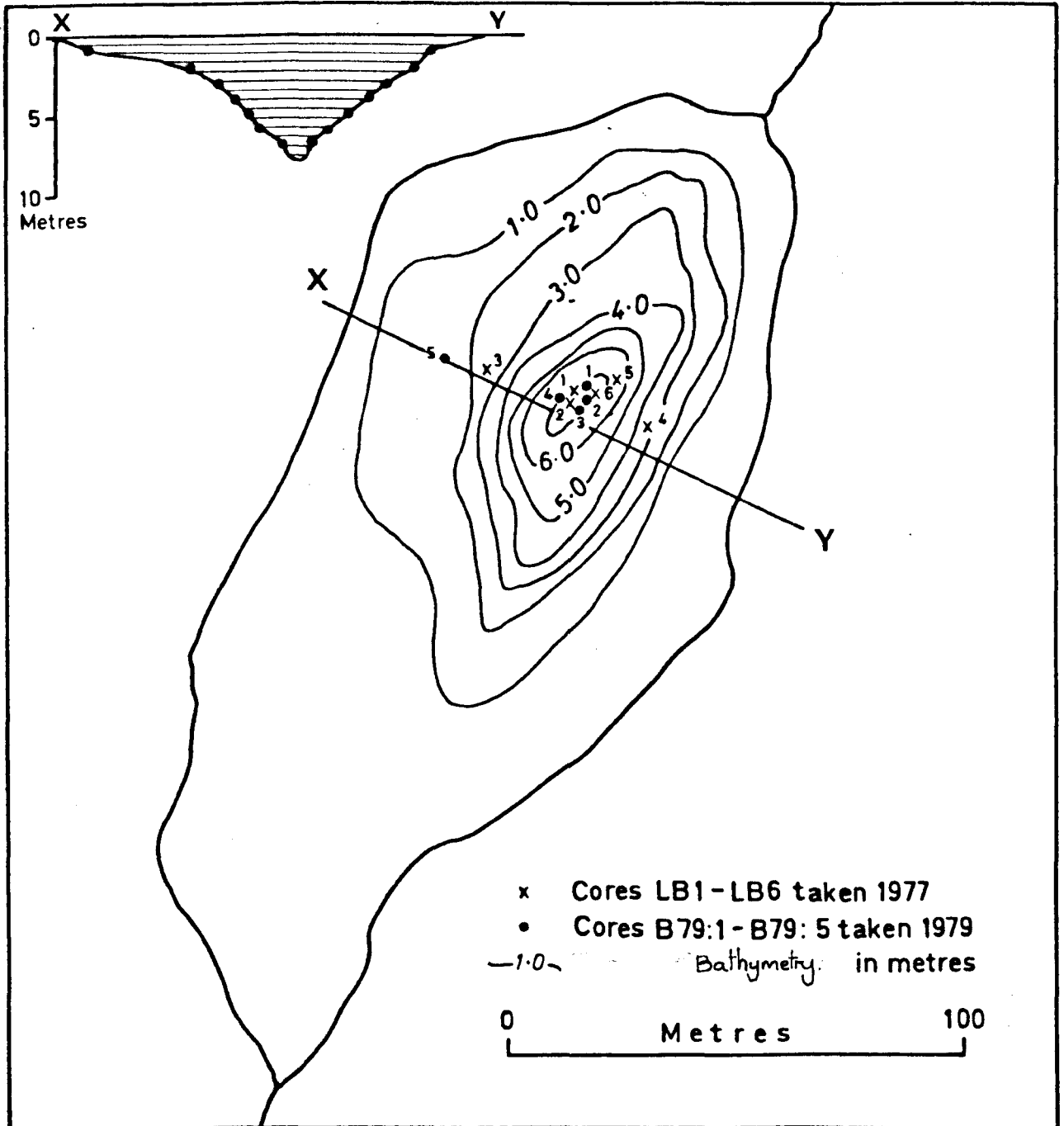


fig.2.2.3 Llyn Bychan morphometry and lake sediment coring sites.

inverted 'Mexican hat' profile with the majority of the lake less than 2m. deep.

Table 2.2.1 lists the lakes parameters.

Surface area	m ²	16,759	
Length	m	243	
Breadth	m	98	
Max. depth	m	9	TABLE 2.2.1
Mean depth	m	1.35	
Volume	m ³	22,978	
<i>Theoretical</i> turnover time	days	62.3	

After Liddle, 1974.

Fig. 2.2.4 shows the hydrology of the lake. There are two inflowing streams, both at the northern end. The stream draining the eastern half of the catchment is a Forestry Commission drainage channel, while the stream draining the western half is natural and drains through a heavily waterlogged area. The lake outflow is at the southern end of the lake. Initially the outflow channel drained via an artificial channel (constructed during the Victorian period. Shaw pers. comm.) into Llyn Goddionduon; however the construction of a forest road in 1958 severed the link allowing the outflow stream to follow its original course.

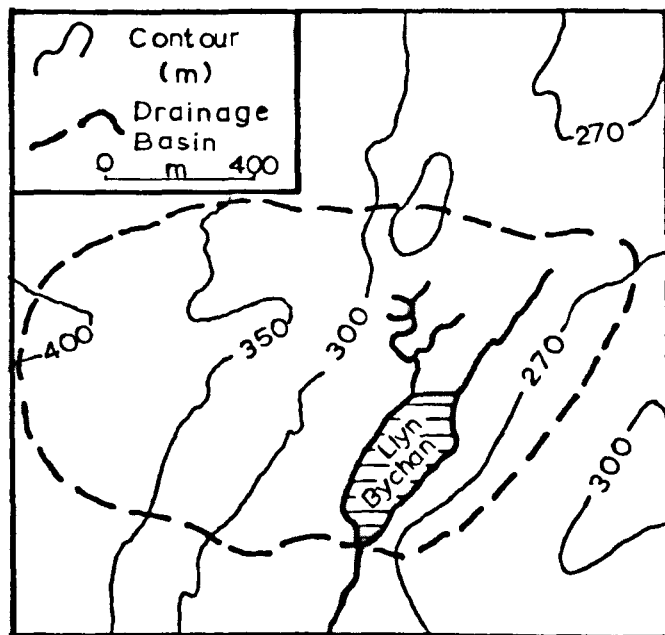


fig. 2.2.4 Stream network of the Llyn Bychan catchment.

FIRE HISTORY 2.3

As mentioned in section 2.2, the Glynn has always been considered an area of high fire risk, especially during periods of dry weather. The summer drought of 1976 was so severe in North Wales that the soils and vegetation of the study area was completely dessicated and the fire risk became considerable. In August 1976 a fire started.

Fig. 2.3.1 plots the extent of the area destroyed in the 1976 fire. The following account is an edited summary of the official fire report reproduced with the permission of the Forestry Commission. The fire is described in detail to illustrate its severity.

The fire was first observed on the 25th August in the moorland to the west of Llyn Bychan and was brought under control with the aid of the fire service and army personnel. However, the fire restarted in the morning on the 26th August and despite efforts by fire fighters entered the Glynn plantation at 1500 hours. The fire became completely out of control, forcing the Forestry Commission to clear a fire line along the forest road leading to Llyn Bychan.

By 2400 hours the wind speed had decreased and altered direction, moving the fire back towards the burnt areas, slowing the speed of travel. At the same time the fire started to break up due to the terrain.

At 0900 hours on the 27th August the Forestry Commission was confident that the fire could be contained at or before the fire line, providing that the wind conditions did not deteriorate. The fire was contained but it was not until the 8th September, when a period of heavy rain commenced that the fire was considered to have been completely extinguished.

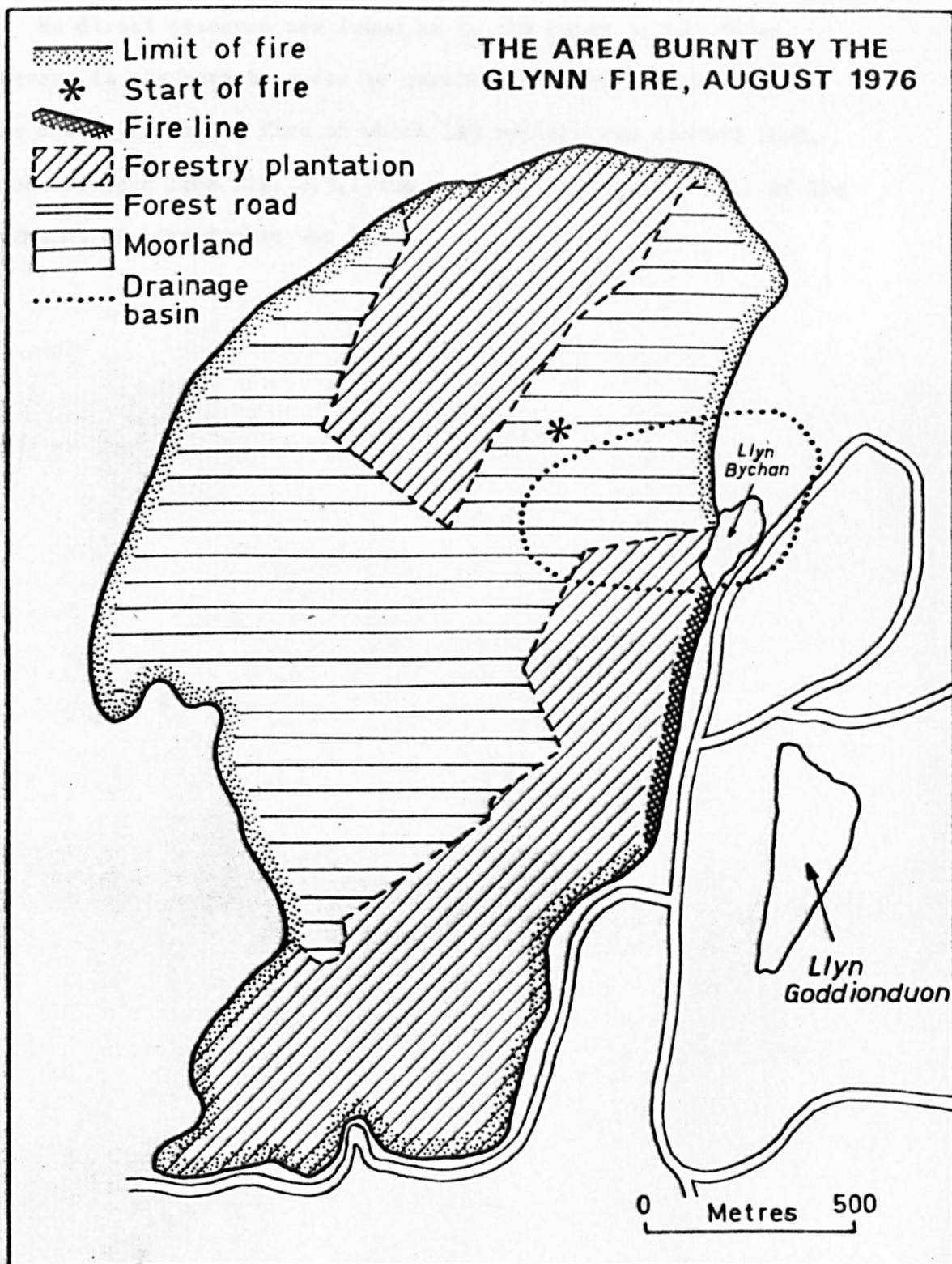


fig. 2.3.1. The area around Llyn Bychan destroyed in the 1976 forest fire.

No direct evidence was found as to the cause of the fire; however, it may have been due to careless hikers. 239 hectares were destroyed in the fire of which 113 hectare was stocked land. As can be seen from fig. 2.3.1 the whole of the western half of the catchment of Llyn Bychan was burnt.

SOIL MAGNETISM 2.4

The soils of the study area were repeatedly sampled from October 1976 to October 1979. Soil profiles were sampled either from different horizons, if present, or from specified depths if no profile differentiation was visible. All samples were placed in labelled polythene bags until preparation for magnetic measurements as outlined in section 1.4

χ and S.I.R.M. were measured on all samples and $(B_o)_{CR}$ measurements made on selected samples. Loss on ignition measurements were made on the samples and the results are expressed on an ash basis.

Fig. 2.4.1 plots the locations from which the soil samples were taken. Soils from both the unburnt (east) and burnt (west) sides of the catchment were sampled.

LLYN BYCHAN LOCATION OF THE SOIL AND STREAM BEDLOAD SAMPLES

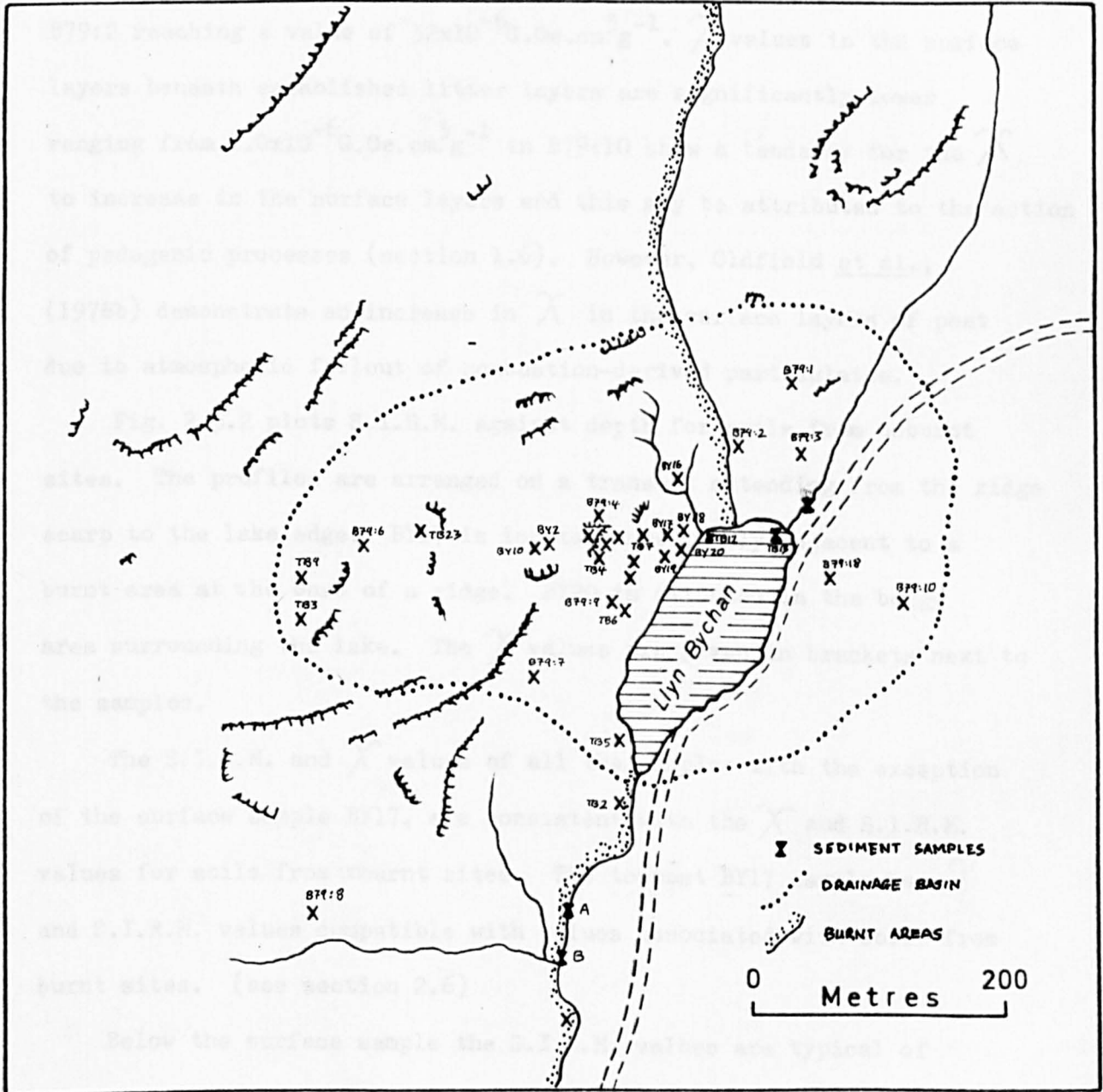


fig. 2.4.1 Location of soil sites sampled

MAGNETIC RESULTS FOR SOILS COLLECTED FROM UNBURNT SITES 2.5

Fig. 2.5.1 plots χ against depth for four soil profiles collected from unburnt sites in the Llyn Bychan catchment. The soils sampled exceeded 30cm. in depth. All the soil profiles with the exception of B79:10 display an overall increase in χ with depth, B79:2 reaching a value of $32 \times 10^{-6} \text{G.Oe.cm}^3 \text{g}^{-1}$. χ values in the surface layers beneath established litter layers are significantly lower ranging from $1.0 \times 10^{-6} \text{G.Oe.cm}^3 \text{g}^{-1}$ in B79:10 show a tendency for the χ to increase in the surface layers and this may be attributed to the action of pedogenic processes (section 1.6). However, Oldfield *et al.*, (1978b) demonstrate an increase in χ in the surface layers of peat due to atmospheric fallout of combustion-derived particulates.

Fig. 2.5.2 plots S.I.R.M. against depth for soils from unburnt sites. The profiles are arranged on a transect extending from the ridge scarp to the lake edge. BY17 is located immediately adjacent to a burnt area at the base of a ridge. BY20 is situated in the boggy area surrounding the lake. The χ values are given in brackets next to the samples.

The S.I.R.M. and χ values of all the samples with the exception of the surface sample BY17, are consistent with the χ and S.I.R.M. values for soils from unburnt sites. The topmost BY17 sample has χ and S.I.R.M. values compatible with values associated with soils from burnt sites. (see section 2.6)

Below the surface sample the S.I.R.M. values are typical of unburnt soils as are the surface samples of BY19 and BY20. The increase in S.I.R.M. in the surface samples may be due to normal pedogenic

LLYN BYCHAN : χ /DEPTH FOR UNBURNT SOIL PROFILES

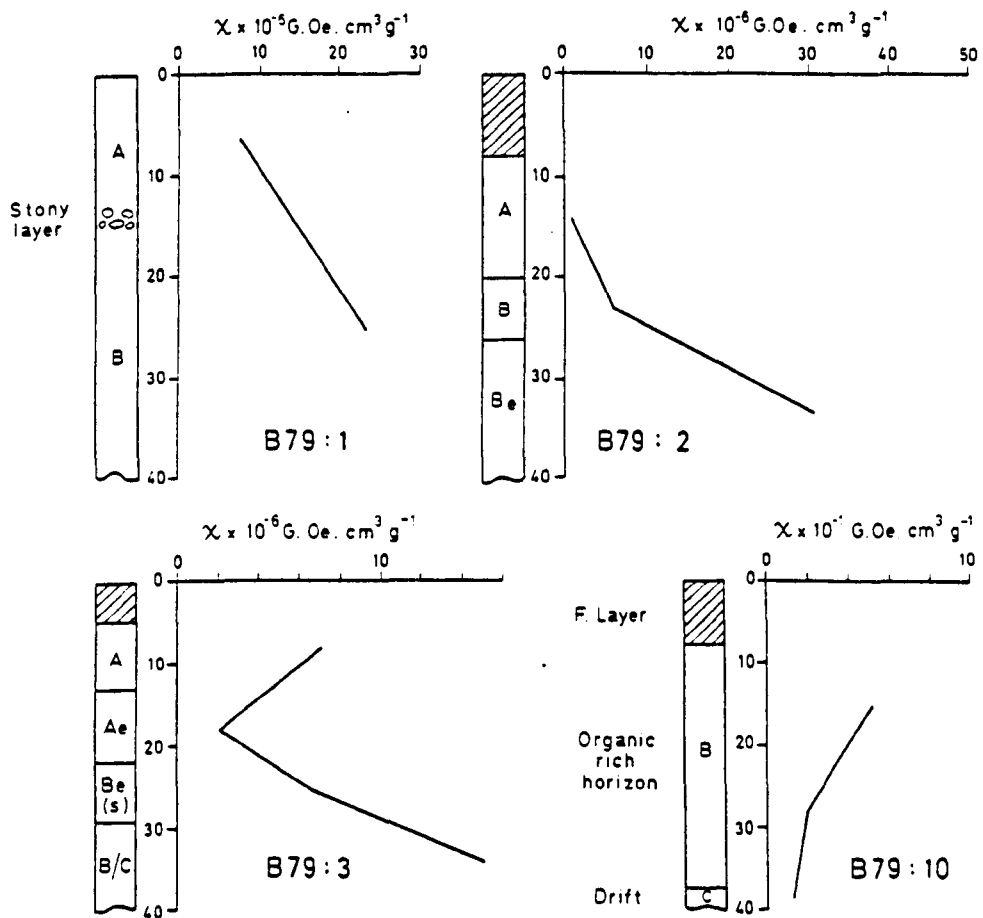


fig. 2.5.1 χ profiles for unburnt soils;
B79:1, B79:2, B79:3, B79:10

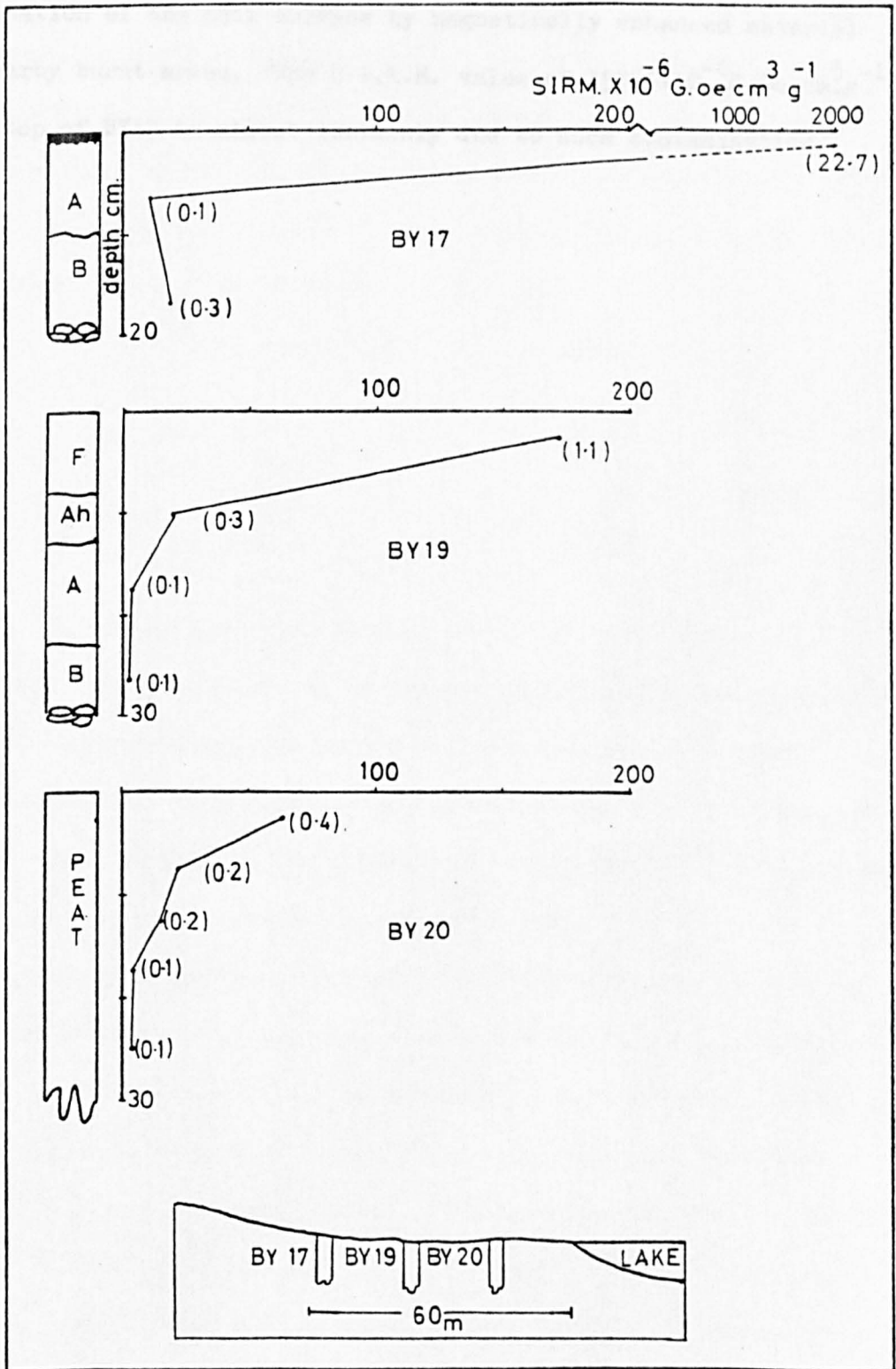


fig.2.5.2. S.I.R.M. profiles for unburnt soils BY17, BY19, BY20.

processes, atmospheric fallout of particulate pollutants or contamination of the soil surface by magnetically enhanced material from nearby burnt areas. The S.I.R.M. value of $15066 \times 10^{-6} \text{ G.Oe.cm}^3\text{-}^{-1}$ at the top of BY17 is almost certainly due to such contamination.

MAGNETIC RESULTS FOR SOILS COLLECTED FROM BURNT SITES 2.6

Due to the immediate erosion of the soils after burning, samples were either collected from complete in situ soil profiles or from areas where the eroded material had collected. (e.g. in gullies).

Table 2.6.1 lists the χ values of eroded burnt material. The samples are probably a mixture of both burnt and unburnt soils that have collected at the bottom of slopes and gullies.

<u>Sample</u>	<u>$\chi \times 10^{-6} \text{G.Oe.cm}^3 \text{g}^{-1}$</u>	<u>Colour</u>
TB3	3785.0	ORANGE
TB7	630.0	ORANGE
BY1	399.0	BLACK
BY9	100.0	BLACK
B79:7	61.0	GREY
B79:8	6000.0	ORANGE
B79:9	94.0	GREY

TABLE 2.6.1

The χ values vary from between 61 and 399 $\times 10^{-6} \text{G.Oe.cm}^3 \text{g}^{-1}$ for the grey and black samples to between 630 and 6000 $\times 10^{-6} \text{G.Oe.cm}^3 \text{g}^{-1}$ for the orange samples. The colouration implies that the orange samples relate to material from mineral soil horizons before erosion and the grey and black samples to the organic-humic layers of the soil column which correspondingly have a lower iron content.

Complete soil profiles sampled from burnt sites can be typified by the two types of soil profiles illustrated in Figs. 2.6.1 and 2.6.2. The soil profiles are situated at the base of a steep slope; field evidence suggests that they are complete soil units that have moved downslope and have remained intact. All have been subject to burning.

All the soil profiles consist of two components; a black/grey ash type layer and a friable orange/pink layer. Higher χ values are recorded for the pink layers reaching $4515 \times 10^{-6} \text{G.Oe.cm}^3 \text{g}^{-1}$ in profile BY10 and $3265 \times 10^{-6} \text{G.Oe.cm}^3 \text{g}^{-1}$ for BY5. The χ is considerably lower in the samples from the black/grey layers: $246 \times 10^{-6} \text{G.Oe.cm}^3 \text{g}^{-1}$ in B79:4, rising to $1450 \times 10^{-6} \text{G.Oe.cm}^3 \text{g}^{-1}$ in B79:6

X FOR BURNT SOILS COLLECTED AT BASE OF SLOPE

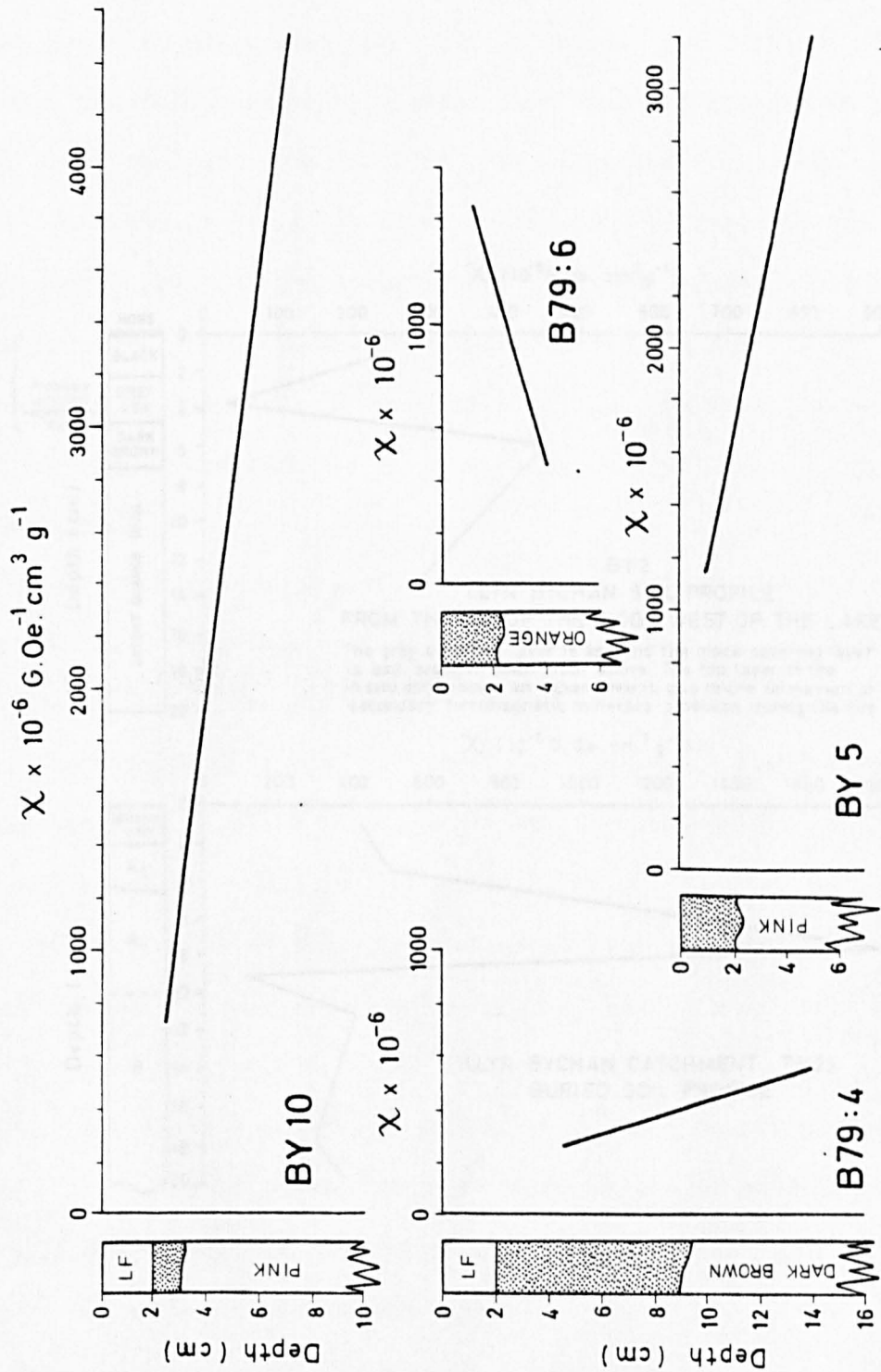


fig.2.6.1. X values for burnt soils.(probably soil wash).

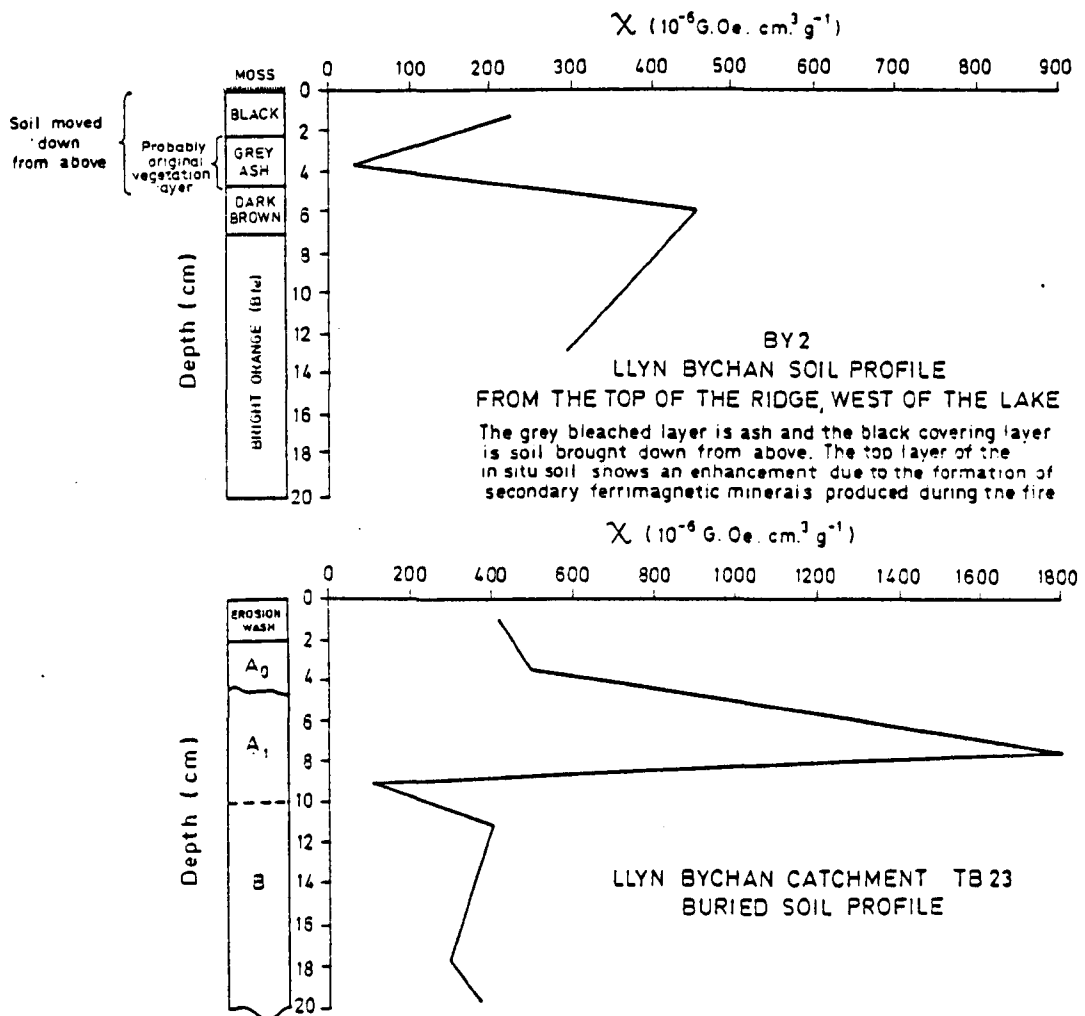


fig.2.6.2 χ profiles for burnt soils BY2, TB23.

Fig. 2.6.2 plots χ against depth for two soil profiles that had not, at the time of sampling, been subject to erosion BY2 and TB23. Both profiles are typical of the burnt area. The original soil profile has been covered by erosion wash that has moved down from the burnt areas upslope. The profiles were collected from ridge tops where soil development has taken place on the flatter areas (section 2.2).

Soil profile TB23 is characterized by a χ peak of $1843 \times 10^{-6} \text{G.Oe.cm}^3 \cdot \text{g}^{-1}$ in the upper parts of the mineral horizons. Above 6cm the χ values decrease to below $400 \times 10^{-6} \text{G.Oe.cm}^3 \cdot \text{g}^{-1}$. At a depth of 19.5cm in the B horizon of the soil the χ value rises to about $400 \times 10^{-6} \text{G.Oe.cm}^3 \cdot \text{g}^{-1}$.

Soil profile BY2 shows a similar trend in χ but the values do not reach the levels recorded in TB23. The maximum χ value of $450 \times 10^{-6} \text{G.Oe.cm}^3 \cdot \text{g}^{-1}$ is recorded in the mineral soil decreasing below this level to $250 \times 10^{-6} \text{G.Oe.cm}^3 \cdot \text{g}^{-1}$. Above the maximum χ level (7cm) the values decrease to $25 \times 10^{-6} \text{G.Oe.cm}^3 \cdot \text{g}^{-1}$ but increase in the erosion wash material to $225 \times 10^{-6} \text{G.Oe.cm}^3 \cdot \text{g}^{-1}$.

All the soil profiles from burnt sites exhibit an increase in the surface layers corresponding to zones in the soil affected by the high temperatures reached during the forest fire.

Table 2.6.2 plots S.I.R.M., χ , S.I.R.M./ χ ratio, colour and depth for a selection of burnt erosion wash material and clearly shows the relationship between colour and degree of enhancement, the pink material relating to the soil mineral horizons.

Sample	S.I.R.M. $\times 10^{-6}$ G.Oe.cm ³ g ⁻¹	χ $\times 10^{-6}$ G.Oe.cm ³ g ⁻¹	Colour	depth	S.I.R.M.
BY5/1	16773	1168	BLACK	1	14
BY5/2	108390	3264	PINK	5	33
BY10/1	40024	713	BLACK	2.5	56
BY10/2	175736	4516	PINK	7	39

TABLE 2.6.2

DISCUSSION 2.7

Using the magnetic properties of χ and S.I.R.M it is possible to magnetically distinguish between the soils subject to heating during the fire and those which were not. All the burnt soils have χ values between two to three orders of magnitude greater than those for the unburnt soils. The greatest increases are found in the orange and pink horizons of the soils and which correspond to the mineral horizons before erosion. The high χ values in the mineral horizons of TB 3 indicate their origins. The χ of the grey and black samples is much lower and corresponds to the litter layers of the unburnt soils. The litter layers have a very low iron content and consequently during the fire the possible volume of converted secondary ferrimagnetic oxides was strictly limited, resulting in the lower χ values.

The increased sensitivity of S.I.R.M. measurements is well illustrated when comparing burnt and unburnt soils. The maximum measured S.I.R.M. value for an unburnt soil sample was $207 \times 10^{-6} \text{G.Oe.cm}^3 \text{g}^{-1}$. compared with S.I.R.M. values of greater than $10,000 \times 10^{-6} \text{G.Oe.cm}^3 \text{g}^{-1}$, reaching $175,736 \times 10^{-6} \text{G.Oe.cm}^3 \text{g}^{-1}$ in BY10, for soils sampled from burnt sites. An increase in S.I.R.M. in the burnt soils of between two to three orders of magnitude over the values recorded for unburnt soils is in evidence.

The volume of available iron in the soils for conversion to a secondary ferrimagnetic form probably accounts for much of the great variation in the enhanced χ and S.I.R.M. values both within burnt zones in the soils and between burnt soils from different parts of the catchment. However, consideration must also be given to other soil

factors that probably influence the conversion of iron to a secondary ferrimagnetic form: The temperature reached in the soil, for instance, will be dependant upon numerous site conditions and the availability and amount of fuel for burning which will also govern the production of a reducing and oxidizing soil environment.

The maximum magnetic enhancement in χ and S.I.R.M. in the soil profiles BY5, BY10, TB3 and in the burnt zone of TB23 indicates the burnt areas where the optimum conversion conditions in the soil environment prevailed at the time of the fire.

IDENTIFICATION OF THE ENHANCED FERRIMAGNETIC OXIDES 2.8

From section 1.6 it can be seen that the end product of the heating mechanism is commonly thought to be maghemite. Attempts were made to identify the secondary ferrimagnetic oxide responsible for the increases in χ and S.I.R.M. observed in the burnt soils from the Llyn Bychan catchment. Experiments were performed on whole samples and on magnetic extracts from samples. (Appendix 1)

Fig. 2.8.1 plots the coercivity of S.I.R.M. ($^{(Bo)}CR$) profiles for a selection of soil samples from the Llyn Bychan catchment and includes some stream and lake sediments. All the samples have profiles that show a rapid decline in S.I.R.M. in low fields (<400 . Oe.) and all become 90 - 100% reverse saturated in a back field of 1000.Oe.. ('S' values of $>-.9$). Coercivities of between 100 Oe, and 400 Oe. coupled with the high percentage saturation in a field of 1000 Oe. indicate that the material measured, including the bedrock is relatively poor in antiferromagnetic minerals. Burnt soils and bedload samples from forestry drainage ditches possess the lowest coercivities (100-200 Oe) and are fully saturated in fields at or below 1000 Oe. These factors together with the greatly increased χ and S.I.R.M. values associated with the burnt material indicate the formation of secondary ferrimagnetic oxides from soils and parent material rich in iron but initially poor in both ferri and antiferromagnetic minerals.

Table 2.8.1 lists the χ and χ_{max}/X ratios for a collection of burnt and unburnt soils. The χ_{max}/X ratios for both the burnt and unburnt soils are similar but the high χ values and low ratios for some of the burnt soils reflects crystal sizes ranging from superparamagnetic to stable single domains in size (Dunlop 1972, 1973).

LLYN BYCHAN CATCHMENT - COERCIVITY OF SIRM PROFILES FOR A VARIETY OF MATERIALS

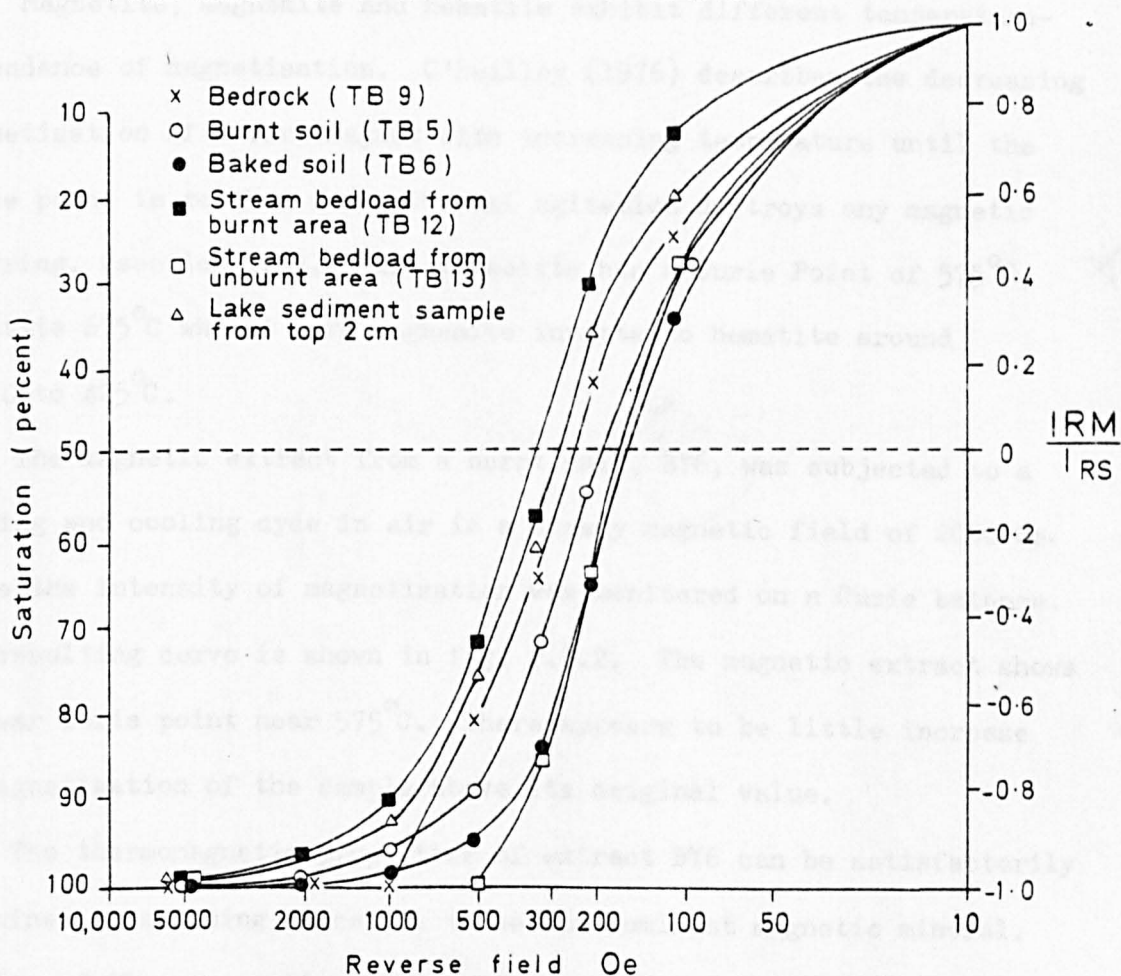


fig. 2.8.1

Coercivity curves for burnt soils, stream and lake sediments from the Llyn Bychan catchment.

Table 2.8.1 lists the S.I.R.M., χ and S.I.R.M./ χ ratios for a collection of burnt and unburnt soils. The S.I.R.M./ χ ratios for both the burnt and unburnt soils are similar but the high χ values and low ratios for some of the burnt soils indicate crystal sizes ranging from superparamagnetic to stable single domain in size (Dunlop 1972,1973).

Thermomagnetic Experiments

Magnetite, maghemite and hematite exhibit different temperature-dependence of magnetisation. O'Reilly (1976) describes the decreasing magnetisation of a ferromagnet with increasing temperature until the Curie point is reached where thermal agitation destroys any magnetic ordering. (section 1.3). Pure magnetite has a Curie Point of 575°C, hematite 675°C whilst pure maghemite inverts to hematite around 255°C to 425°C.

The magnetic extract from a burnt soil, BY6, was subjected to a heating and cooling cycle in air in a steady magnetic field of 2000 Oe. while the intensity of magnetisation was monitored on a Curie balance. The resulting curve is shown in fig. 2.8.2. The magnetic extract shows a clear Curie point near 575°C. There appears to be little increase in magnetisation of the sample above its original value.

The thermomagnetic properties of extract BY6 can be satisfactorily explained by assuming magnetite to be the dominant magnetic mineral. Results of thermomagnetic experiments on material from other burnt areas in Longworth et al., (op cit) suggest similar conclusions : Magnetite is the dominant magnetic mineral and not maghemite.

Mössbauer effect studies

Mössbauer effect studies have been performed on samples TB1, TB3 and TB7 from the Llyn Bychan catchment. TB3 and TB7 are magnetic extracts

S.I.R.M./ χ RATIOS

TABLE 2.8.1

BURNT	S.I.R.M. $-10^{-6}\text{G.Oe.cm}^3\text{g}^{-1}$	$\chi \times 10^{-6}\text{G.Oe.cm}^3\text{g}^{-1}$	$\frac{\text{S.I.R.M.}}{\chi}$	UNBURNT	S.I.R.M. $\times 10^{-6}\text{G.Oe.cm}^3\text{g}^{-1}$	$\chi \times 10^{-6}\text{G.Oe.cm}^3\text{g}^{-1}$	$\frac{\text{S.I.R.M.}}{\chi}$
BY1	23051	399	57	BY20/2	211	2.0	106
BY5/1	16733	1168	14	BY20/3	156	2.0	78
BY5/2	108390	3264	33	BY19/2	200	3.0	67
BY9	11528	100	115	BY19/3	47	1.0	47
BY10/1	40024	713	56	BY19/4	49	1.0	49
BY10/2	175736	4516	39	BY17/2	100	0.7	142
TB3	7320	378	19	BY17/3	207	0.3	69

from burnt soils, TEL is a magnetic extract from a stream
crossing an industrial area. The results from these studies and from
studies on samples from other burnt sites in F.B. England are
documented in Longworth et al., (op cit). A summary of the findings is
shown in table 2.8.2.

SAMPLE BY6 - MAGNETIC EXTRACT

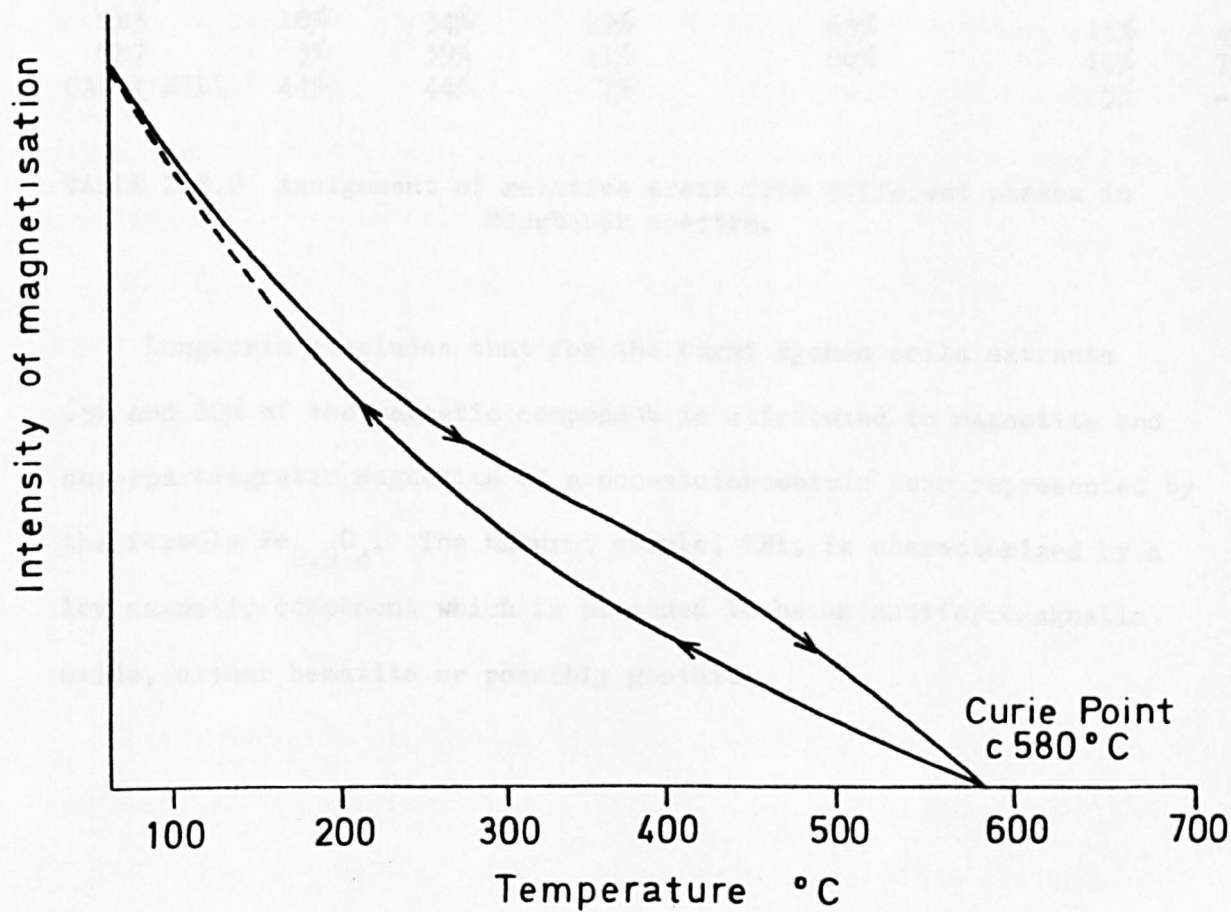


fig. 2.8.2 Thermomagnetic curve on extract BY6

from burnt soils, TBl is a magnetic extract from a stream draining an unburnt area. The results from these studies and from studies on samples from other burnt sites in N.W. England are documented in Longworth et al., (op cit). A summary of the findings is shown in table 2.8.2.

	<u>Hematite</u>	<u>Magnetite</u>	<u>Superpara magnetic</u>	<u>total magnetic iron component</u>	<u>Structural ferric</u>	<u>Iron Ferrous</u>
TB3	18%	34%	29%	63%	15%	4%
TB7	3%	39%	41%	80%	10%	7%
CALDY HILL	44%	44%	7%	-	5%	-

TABLE 2.8.2 Assignment of relative areas from different phases in Mössbauer spectra.

Longworth concludes that for the burnt Bychan soils extracts 63% and 80% of the magnetic component is attributed to magnetite and superparamagnetic magnetite of a non-stoichiometric form represented by the formula $Fe_{2.9}O_4$. The unburnt sample, TBl, is characterized by a low magnetic component which is presumed to be an antiferromagnetic oxide, either hematite or possibly goethite.

DISCUSSION 2.9

χ and S.I.R.M. measurements allow a differentiation to be made between burnt and unburnt soils. The basis for differentiation is the degree of magnetic enhancement: Burnt soils have χ and S.I.R.M. peaks in the burnt layers of between two to three orders of magnitude higher than the χ and S.I.R.M. values for the corresponding layers in unburnt soils. The high χ and S.I.R.M. values are caused by the production of highly magnetic secondary ferrimagnetic oxides from weakly magnetic para- and antiferromagnetic forms of iron in the fire created soil environment.

The formation of secondary ferrimagnetic oxides in the burnt soils is indicated not only by the greatly increased χ and S.I.R.M. values but also by the low coercivity values of the samples (between 100-200 Oe), and which are fully reverse saturated in backfields of below 1000. Oe. (\bar{S} values of above -.95). Sample TB12 taken from a stream draining a burnt area has an 'S' value of 1; the sample was fully reverse saturated at 500 Oe.

Thermomagnetic and Mössbauer studies indicate that the magnetic component of the burnt soils is dominated by a superparamagnetic form of iron. The S.I.R.M./ χ ratios indicate that as a whole the samples have a magnetic component ranging from stable single domain to superparamagnetic and presumably include some magnetically viscous material (Mullins op cit).

The non-stoichiometry of the secondary ferrimagnetic oxide suggests impurity as a result of isomorphic substitution of the iron by the commonly occurring soil cations such as sodium and aluminium. Other factors that may affect the degree of magnetic enhancement in a burnt soil are

- (i) dilution of the secondary ferrimagnetic oxide by non or less magnetic forms of iron. (ii) the effectiveness of the fire in producing conditions required in the soil environment for maximum magnetic enhancement. (iii) The volume of iron available in the soil for conversion to a secondary ferrimagnetic form.

In this respect sample B79:8 may be considered to have had optimum conditions necessary for the production of secondary ferrimagnetic oxides as reflected in the high χ value of $6,000 \times 10^{-6} \text{G Oe cm}^3 \text{g}^{-1}$. Sample TB7, a similar soil sample to B79:8, but from a different location, has a χ value of $630 \times 10^{-6} \text{G.Oe.cm}^3 \text{g}^{-1}$ and may be taken to indicate that the site and soil conditions at the time of the fire were not favourable to the maximum production of secondary ferrimagnetic oxides.

It is therefore possible to detect burnt zones in soils by the detection of secondary ferrimagnetic oxides as reflected in the magnetic enhancement in χ and S.I.R.M. that they produce.

Lake and Stream Sediments

METHODS 2.10

A 1m. pneumatic Mackereth corer (Mackereth, 1969) was used to take six sediment cores from Llyn Bychan in December 1976. Further cores were taken in 1979; one with a Mackereth corer and four with a Gilson corer. Both cores, carefully used, will preserve an undisturbed mud-water interface. Water depth was recorded at each coring site using an echo sounder. The basin morphometry was established from Liddle (op.cit.) and an echo sounder.

The sediment cores retrieved with the Mackereth cover were kept in the perspex core tubes for long core k (volume susceptibility) measurements. All the cores were extruded for single sample χ and S.I.R.M. measurements. The sediment was extruded in 1cm slices to a depth of 10 cm and then in 2 cm slices to the end of the core.

A sediment trap (Appendix 2) was constructed and placed on the lake bottom in December 1976, being raised in June 1977 and June 1978.

Three stream sediment traps of simple design (Appendix 3) were constructed and placed in position in October 1977. One trap was placed in the inflow stream draining the burnt area, one in the stream draining the unburnt area and one in the lake outflow. The traps were emptied in April 1978, and April 1979. Emptying of the traps could not be made on a more systematic basis due to vandalism of the traps.

Stream bedload samples were collected from shoals in the outflow stream, draining the lake. The samples were fractioned into ten different sizes ranging from -1.0ϕ to $>4.0\phi$.

All samples were prepared for magnetic measurements as outlined in Section 1.4.

LAKE SEDIMENT RESULTS 2.11Whole core K traces

Fig. 2.2.3 locates the position of the coring sites. Fig. 2.11.1 plots the continuous core K traces for five sediment cores from Llyn Bychan. Cores LB1,2, 4 and 5 were taken in 1976 and core B79:1 in 1979.

The continuous core traces show that the marginal cores and core LB5 have similar K profiles with no prominent peaks, LB5 however, exhibits a slight increase in K at the surface. Core LB1 has a similar K profile up to 10cm. above which the K increases dramatically from 15 units to 265 units. Core B79:1, taken from the trench three years later displays a similar K profile to core LB1 with a low constant K until around 10cm. when the K increases to 140 units at the surface.

Single sample χ and S.I.R.M. measurements

Fig. 2.11.2 plots S.I.R.M. against depth for core LB6. χ measurements for the core ranged from $69.5 \times 10^{-6} \text{G.Oe.cm}^3 \cdot \text{g}^{-1}$ at 1-2 cm to less than $1.0 \times 10^{-6} \text{G.Oe.cm}^3 \cdot \text{g}^{-1}$ at 3-4 cm and continuing at this low level to the end of the core. Since the measured values of χ were below the limit of repeatable readings S.I.R.M. was used as a substitute for χ measurements.

The single sample S.I.R.M. plot shows little variation from the bottom of the core up to about 2-3 cm. where the S.I.R.M. increases from $200 \times 10^{-6} \text{G.Oe.cm}^3 \cdot \text{g}^{-1}$ to $790 \times 10^{-6} \text{G.Oe.cm}^3 \cdot \text{g}^{-1}$ and rises to $4270 \times 10^{-6} \text{G.Oe.cm}^3 \cdot \text{g}^{-1}$ at the mud water interface. The surface sample has a level of magnetic enhancement nearly 40 times greater than the samples beneath the zone of enhancement. Single sample S.I.R.M. against depth plots for cores taken from the marginal areas of the lake in 1976 do not show any enhancement in the surface layers of the sediment.

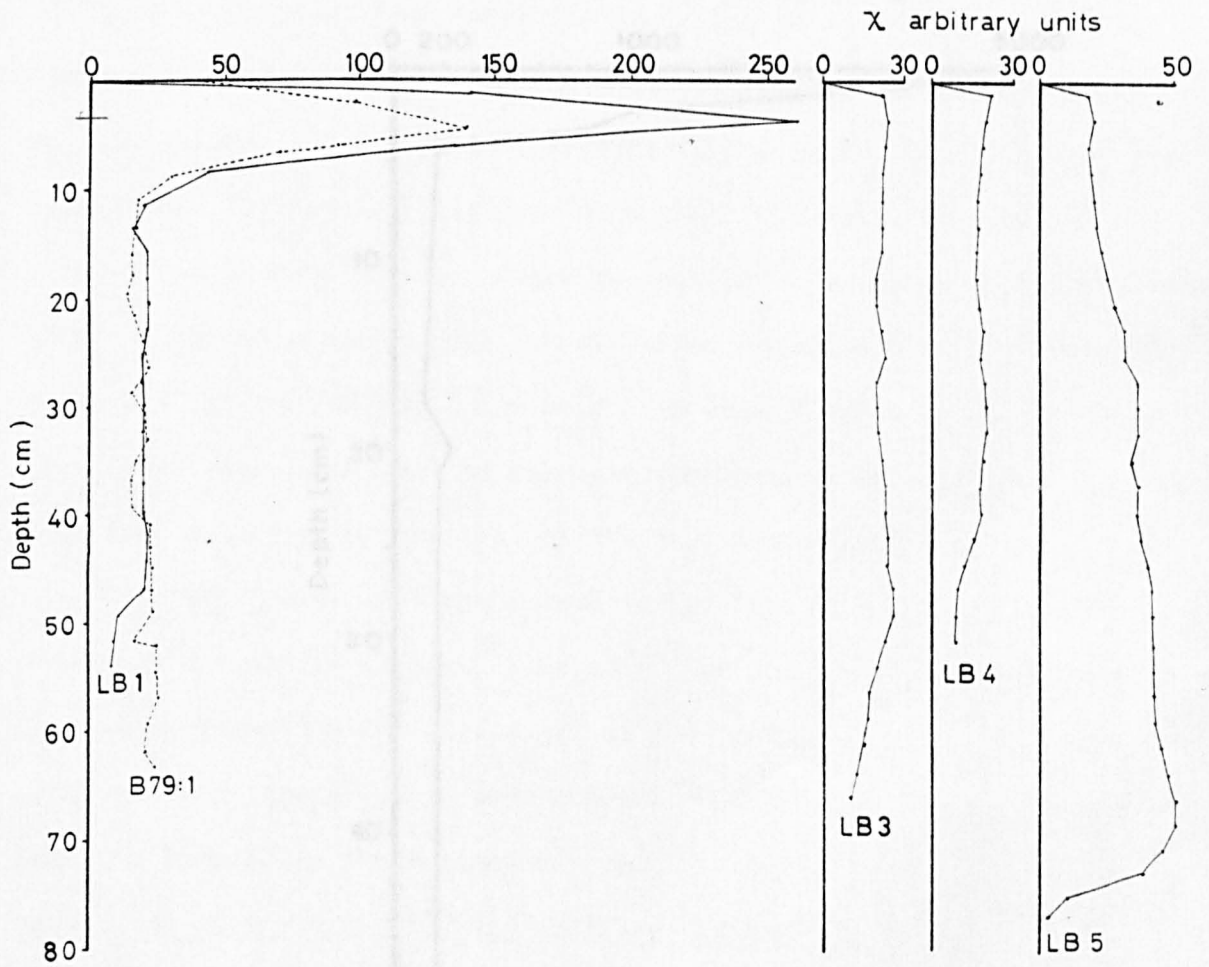


fig. 2.11.1 Continuous core χ traces for LB1, 3, 4 and 5 and B79:1

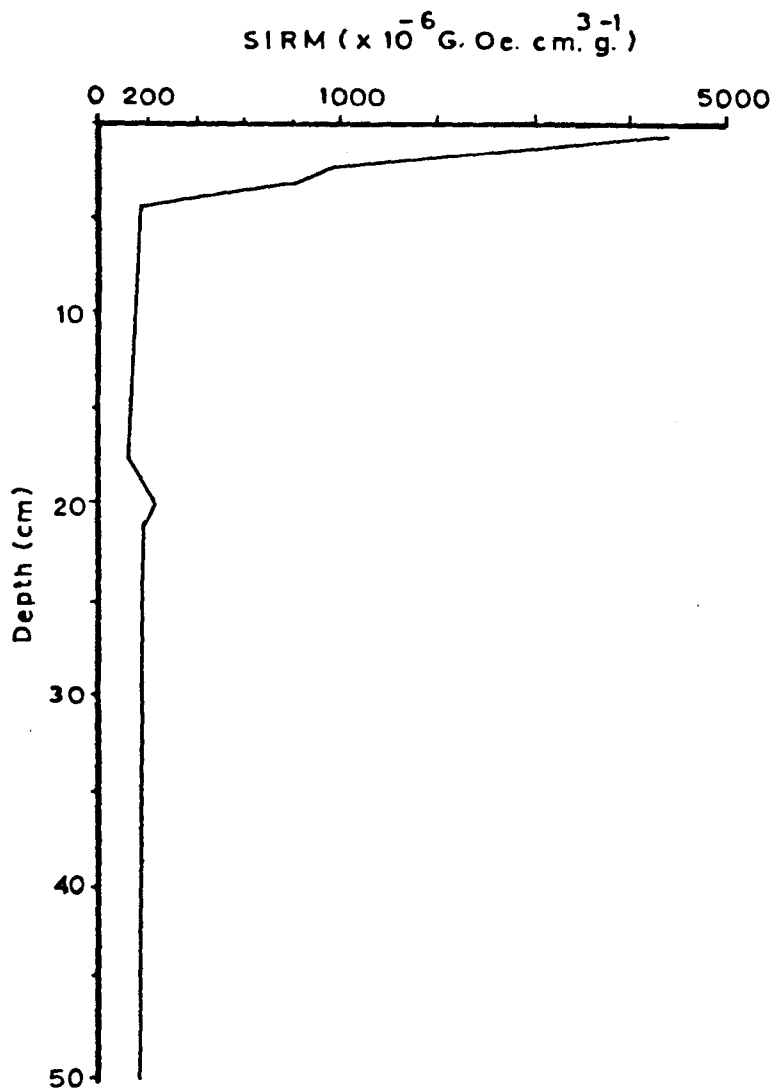


fig. 2.11.2 S.I.R.M./depth profile for core L6g.

Sediment cores LB1 to LB6 were taken from the lake some four months after the fire. Sediment cores B79:1 to B79:5 were taken three years later and display a more interesting S.I.R.M./depth profile.

Fig. 2.11.3 plots S.I.R.M. against depth for sediment cores B79:3, 4 and 5 taken from water depths of 9m, 7m and 2m respectively. Cores B79:3 and B79:4 have similar S.I.R.M. profiles, i.e. relatively uniform values, up to 3 cm in core B79:3 and 6 cm in core B79:4, of less than $350 \times 10^{-6} \text{G.Oe.cm}^3 \cdot \text{g}^{-1}$ (except for a peak of $919 \times 10^{-6} \text{G.Oe.cm}^3 \cdot \text{g}^{-1}$ at 10-12 cm in core B79:4). Above these depths the sediment in both cores has a greatly increased S.I.R.M. value, reaching $7403 \times 10^{-6} \text{G.Oe.cm}^3 \cdot \text{g}^{-1}$ in core B79:3 and $5603 \times 10^{-6} \text{G.Oe.cm}^3 \cdot \text{g}^{-1}$ in core B79:4. At the mud-water interface there is a level of magnetic enhancement over 30 times greater than that recorded for the rest of the sediment beneath it.

Core B79:5 also displays a peak in S.I.R.M. in the top 3 cm, attaining a value of $6148 \times 10^{-6} \text{G.Oe.cm}^3 \cdot \text{g}^{-1}$ at the mud water interface increasing from $455 \times 10^{-6} \text{G.Oe.cm}^3 \cdot \text{g}^{-1}$ at 3-4 cm depth. Below this level the S.I.R.M. value increases to over $4000 \times 10^{-6} \text{G.Oe.cm}^3 \cdot \text{g}^{-1}$ but the values are never as high as in the surface sample.

Coercivity of S.I.R.M. ($^{(Bo)}$ CR) profiles for the lake sediments

Fig. 2.11.4 plots the $^{(Bo)}$ CR profiles for both recent and older sediments from Llyn Bychan. The recent sediments have coercivity values of less than 400 Oe. and 'S' values of $> -.60$, and the surface samples have coercivity values of less than 200 Oe. with 'S' values of c. $-.90$. The older sediments predating the fire have higher coercive fields; greater than 700.Oe. with 'S' values of $< -.40$. Sample B79:4, 2-3 cm has an intermediate coercivity value and an 'S' ratio between the two extremes indicating a mixture of burnt and unburnt material.

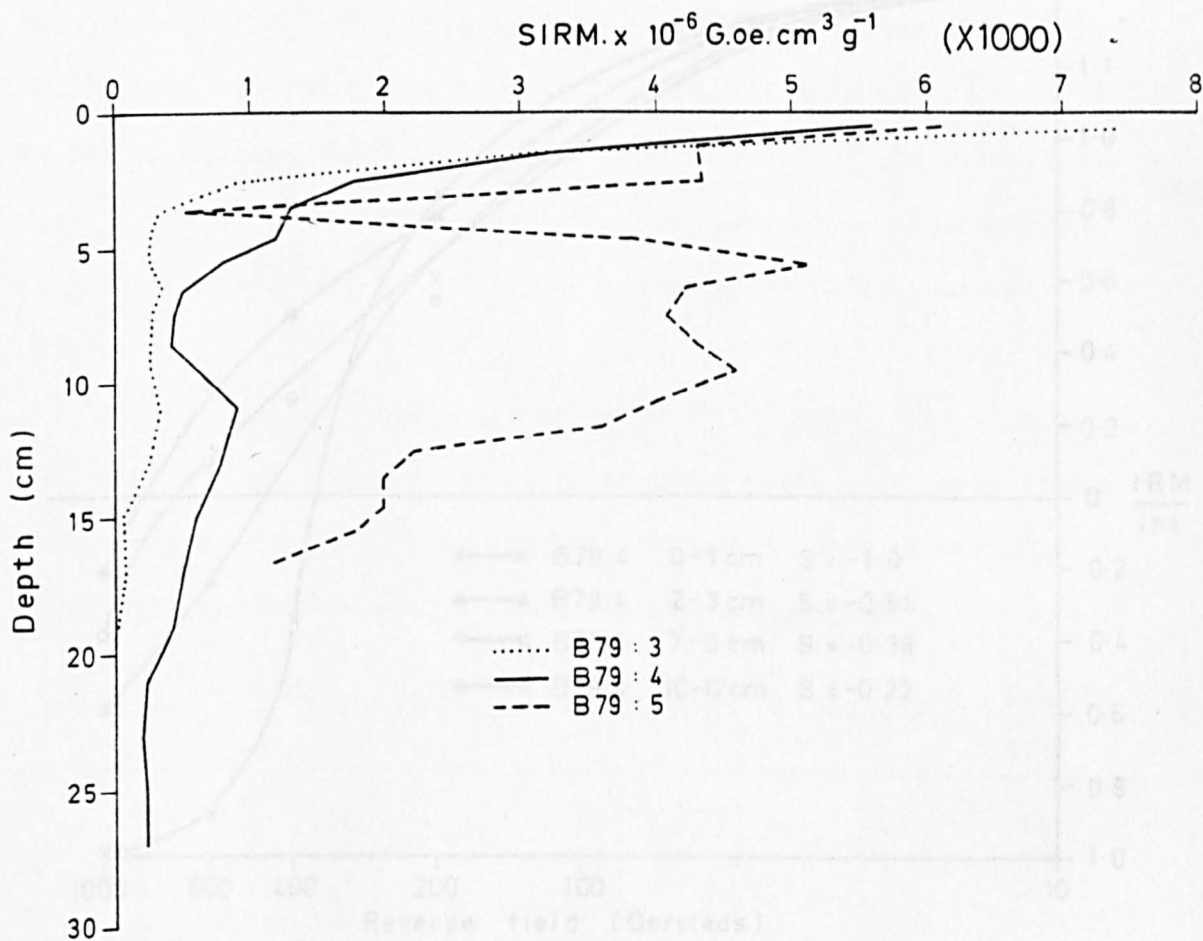


fig. 2.11.3 S.I.R.M./depth profiles for cores B79:3,4 and 5.

Lake bottom sediment trap results

To examine the type of sediment entering the lake system an orientated sediment trap was placed on the lake bottom four months after the fire event. The trap was emptied in 1977 and 1978, six and eighteen months after emplacement.

Fig. 2.11.3 and table 2.11.1 tabulate the results from the two liftings. All the compartments have similar values of χ of $25,000 \times 10^{-6} \text{ g}^{-1} \text{ cm}^3$ or greater. The spread of the S.I.M. values exceeding $10 \times 10^{-6} \text{ g}^{-1} \text{ cm}^3$ is so large that it can be considered that there is no preferred direction of magnetization of the magnetically enhanced material.

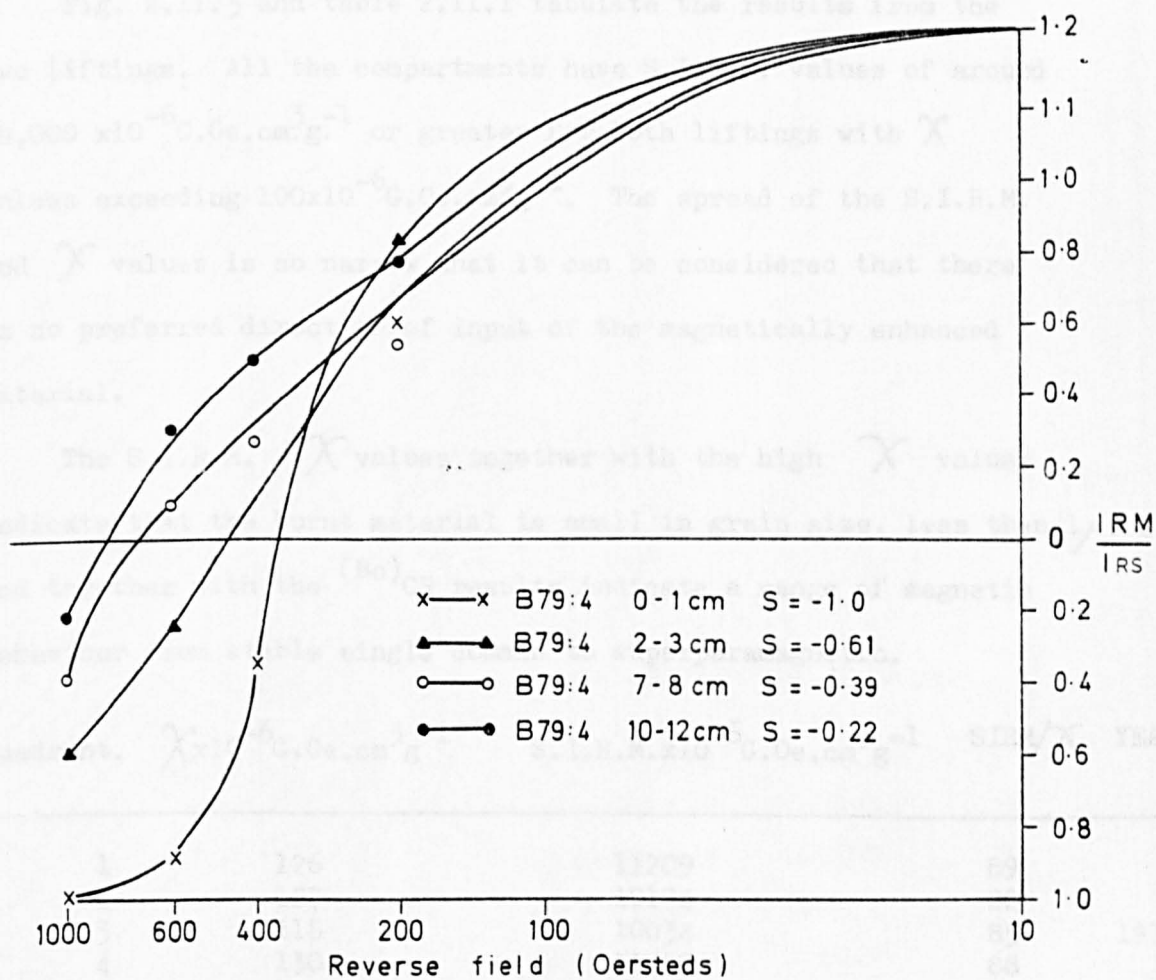


fig 2.11.4 Coercivity curves for recent and older sediments. Core B79:4

Lake bottom sediment trap results

To examine the type of sediment entering the lake system an orientated sediment trap was placed on the lake bottom four months after the fire event. The trap was emptied in 1977 and 1978, six and eighteen months after emplacement.

Fig. 2.11.5 and table 2.11.1 tabulate the results from the two liftings. All the compartments have S.I.R.M. values of around $10,000 \times 10^{-6} \text{G.Oe.cm}^3 \text{g}^{-1}$ or greater for both liftings with χ values exceeding $100 \times 10^{-6} \text{G.Oe.cm}^3 \text{g}^{-1}$. The spread of the S.I.R.M. and χ values is so narrow that it can be considered that there is no preferred direction of input of the magnetically enhanced material.

The S.I.R.M. / χ values together with the high χ values indicate that the burnt material is small in grain size, less than $1 \mu\text{m}$. and together with the $(B_0)_{CR}$ results indicate a range of magnetic behaviour from stable single domain to superparamagnetic.

Quadrant.	$\chi \times 10^{-6} \text{G.Oe.cm}^3 \text{g}^{-1}$	S.I.R.M. $\times 10^{-6} \text{G.Oe.cm}^3 \text{g}^{-1}$	SIRM/ χ	YEAR
1	126	11209	89	1977
2	127	10174	80	
3	118	10034	85	
4	130	11457	88	
CENTRE 5	-	9777	-	
1	140	11550	83	1980
2	146	11030	76	
3	129	11509	89	
4	240	12214	51	
CENTRE 5	125	10250	82	

TABLE 2.11.1

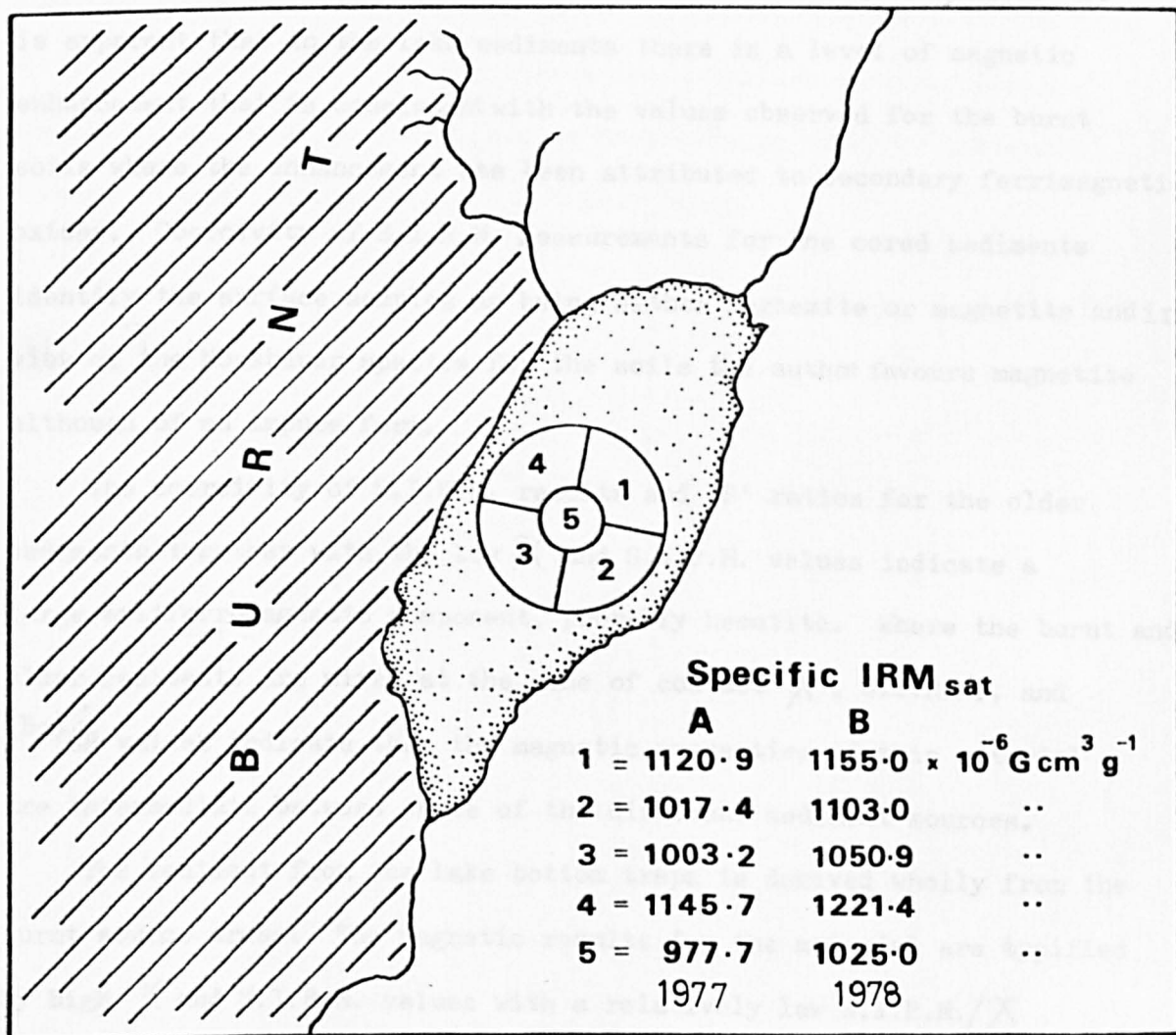


fig. 2.11.5 Lake bottom sediment trap results.

DISCUSSION 2.12

A zone of magnetic enhancement in the surface sediments of Llyn Bychan has been identified using both whole core and single sample measurements. The low volumes of the samples necessitated the use of S.I.R.M. measurements where the values of the surface samples were nearly 40 times greater than the background S.I.R.M. values. It is apparent that in the lake sediments there is a level of magnetic enhancement that is consistent with the values observed for the burnt soils where the enhancement has been attributed to secondary ferrimagnetic oxides. Coercivity of S.I.R.M. measurements for the cored sediments identify the surface samples as being either maghemite or magnetite and in view of the Mössbauer spectra for the soils the author favours magnetite although of an impure form.

The coercivity of S.I.R.M. results and 'S' ratios for the older sediments together with the low χ and S.I.R.M. values indicate a large antiferromagnetic component, probably hematite. Where the burnt and older sediments are mixed at the zone of contact χ , S.I.R.M., and $(Bo)_{CR}$ values indicate that the magnetic properties of this material are intermediate between those of the different sediment sources.

The sediment from the lake bottom traps is derived wholly from the burnt source areas: The magnetic results for the material are typified by high χ and S.I.R.M. values with a relatively low S.I.R.M./ χ ratio and low coercivities. The results indicate that the enhanced material is of a secondary ferrimagnetic form with a magnetic component consisting of material exhibiting a range of behaviour from stable single domain to superparamagnetic.

The similarities of the magnetic properties of the recent lake sediments and the burnt soils provide persuasive evidence that the recent sediments are almost wholly derived from the burnt soils in the catchment. It can therefore be assumed that the magnetically enhanced surface sediments are derived from the burnt soils. The magnetically enhanced secondary ferrimagnetic oxides formed in the soils at the time of the fire have been eroded and have moved through various pathways into the lake where they have become incorporated into the sediments forming a magnetically distinct sediment layer.

SEDIMENT PATHWAYS 2.13

The incorporation of secondary ferrimagnetic oxides in the lake sediments from sources in the burnt part of the catchment leads to some consideration of the sediment pathways within an upland burnt and deforested lake drainage basin.

The magnetic measurements indicate that the secondary ferrimagnetic oxides in the modern sediments accumulated in the deepest part of the lake four months after the fire event. The phenomenon of sediment focusing is known to occur commonly in lakes with the 'Kettle-hole' type morphometry, and other simple basins where the sediment accumulates fastest in the central deepest part of the lake (Likens and Davis, 1975). Three years after the fire event the magnetically enhanced material was detected on the shallow 'shelf' areas of the lake; however, maximum accumulation of the magnetically enhanced material had again occurred in the 'trench', perhaps indicating that the least dense material moves into the lake first and more rapidly than the more dense material.

To investigate the possible transport pathways into the lake, simple stream sediment traps were placed in the two inflowing streams and the lake outflow. The results from the two emptying's (fig. 2.13.1) show that the sediment from the inflowing stream draining the burnt part of the catchment has S.I.R.M. values higher than those for the sediment from the stream draining the unburnt area. The high values of the outflow stream sediment are of great interest. The first two emptyings have a substantially higher S.I.R.M. value than the sediment emptyings from traps 1 and 2

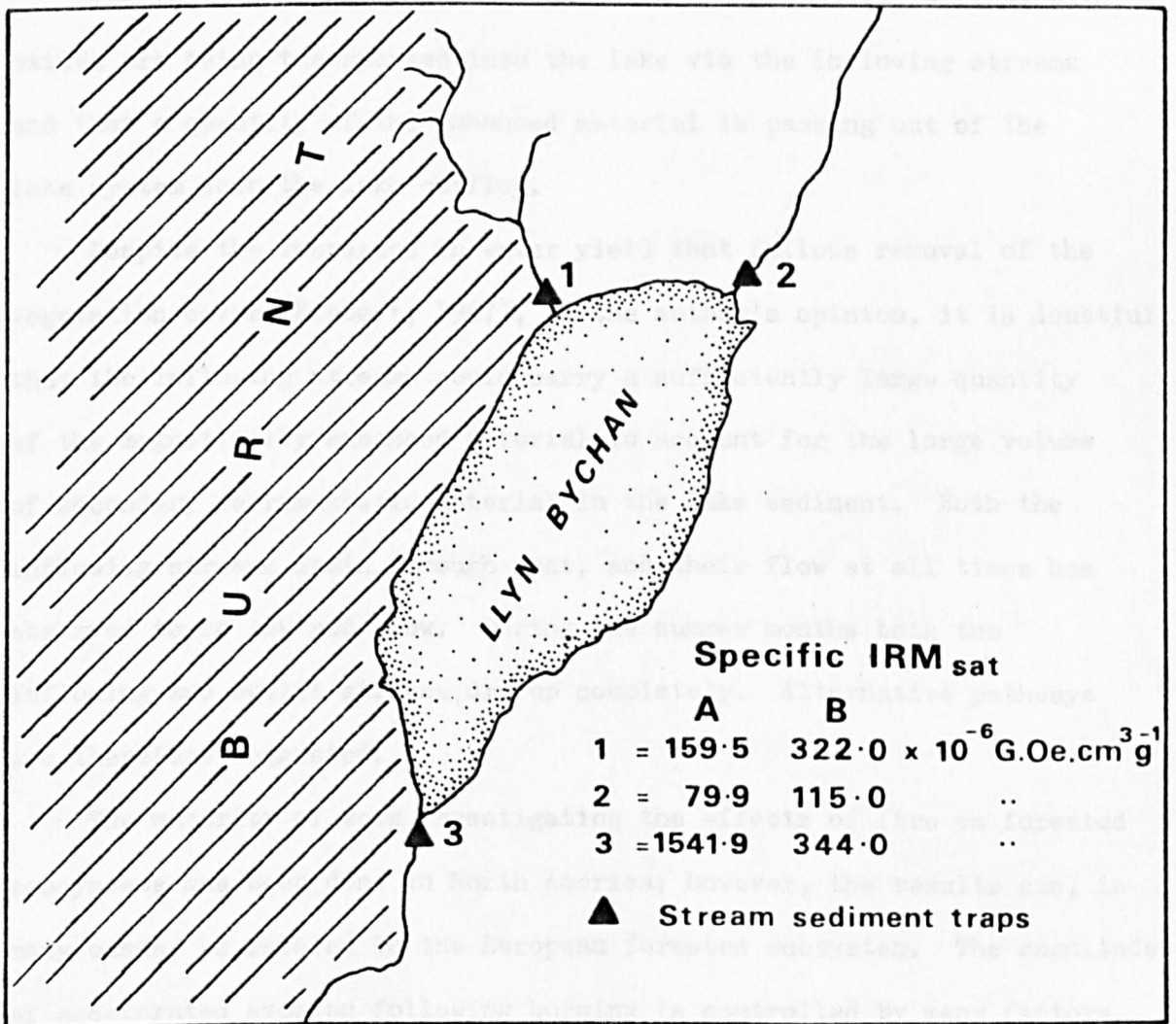


fig.2.13.1 Stream sediment trap results

The second emptying has similar S.I.R.M. values to the sediment from trap 1 draining the burnt part of the catchment. In all cases the S.I.R.M. values for stream traps 1 and 3 are higher than those for the sediment from trap 2 draining the unburnt part of the catchment.

The results can be taken to indicate that secondary ferrimagnetic oxides are being transported into the lake via the inflowing streams and that a quantity of the enhanced material is passing out of the lake system down the lake outflow.

Despite the increases in water yield that follows removal of the vegetation cover (Hibbert, 1967), in the author's opinion, it is doubtful that the inflowing streams could carry a sufficiently large quantity of the magnetically enhanced material to account for the large volume of secondary ferrimagnetic material in the lake sediment. Both the inflowing streams drain through peat, and their flow at all times has been observed to be low and slow. During the summer months both the inflowing and outlet streams dry up completely. Alternative pathways are therefore suggested.

The majority of work investigating the effects of fire on forested ecosystems has been done in North America; however, the results can, in many cases, be related to the European forested ecosystem. The magnitude of accelerated erosion following burning is controlled by many factors. Two of the most important are inherent soil erodability and the severity of the burn (section 1.8).

Burning alters the physical characteristics of the soil increasing erodability. Many workers (Fuller, op cit, and Beaton, op cit) have reported decreased soil infiltration rates as a result of burning.

The decrease is roughly proportional to the intensity of the fire. Dryness and Youngsberg (op. cit.) have shown that fire destroys a portion of the water stable aggregates in the surface soil. As organic matter is an important cementing agent in soil aggregate formation, any removal by fire will have an adverse effect on structural stability. As much as 75% of organic matter in the surface soil is consumed by an intense fire (section L8), and the resulting exposure of the mineral soil often results in decreased infiltration rates, largely due to the destruction of the surface structure by raindrop impact.

The erosion may range from almost imperceptible sheet erosion on denuded slopes to mass soil movement downslope. The type of soil movement is controlled by such site characteristics as topography, climate, inherent soil erodability and the amount of protection provided by litter and plant cover. Willen (1965) and Wallis and Willen (1963) have demonstrated that soils derived from acid igneous rock types are considerably more erodable than soils derived from other parent materials.

Wright (op cit) in studying the effects of fire on the nutrient influxes to a small lake in N.E. Minnesota has shown that two years after a fire, runoff was 60% greater than at a control site and was probably even greater one year after the fire.

The effect of devegetation and destruction of the soil structure by impact is firstly to increase the amount of material dislodged by rainfall impact and therefore available for transport by overland flow. The reduced infiltration capacity of the burnt soils also increases the amount of overland flow. The high rainfall of the area

(average 196 cm. per annum) coupled with the steep slopes of the catchment and the large amount of water available after the winter snowmelts have led to considerable gullying and soil creep on the slopes. The process is demonstrated by the magnetic profiles of the erosion wash overlying insitu soils; this is clearly shown in soil profile TB23.

The movement of the secondary ferrimagnetic oxides by soil creep and overland flow is probably the dominant transport mechanism operating in the catchment. It has now been observed to occur on the shallow slopes around the lake margins. The surface samples of unburnt soil profiles BY17, BY19 and BY20 have S.I.R.M. values consistent with burnt soils and it is possible that soil creep and overland flow have moved the burnt material including the secondary ferrimagnetic oxides downslope over the unburnt soils to the lake edge.

In areas of maximum gradient the large volumes of water released after the snowmelts in the Winters of 1977, 1978 and 1979 may have carried large amounts of loose material downslope.

An additional explanation for the transport of large quantities of burnt material into the lake may be by the movement of the material by wind around and possibly outside the catchment. Observations in the field by the author and others have noted large volumes of material being moved by the wind. During the summer after the fire when the soil was still structureless and friable, the action of hikers and ramblers walking over the burnt slopes disturbed large quantities of burnt soil forming dustclouds behind them as they come downslope. The material was seen to move up to 600 metres in the wind and to move downslope towards the lake.

Observations studying the air quality during forest fires in America (Komarek, 1970; Schaeffer, 1973; Vines, 1973) have noted large updrafts around a fire transporting large volumes of material into the atmosphere. The composition of the smoke was observed by Vines to be made up of 55% tar, 25% soot and 20% ash, although certainly particulate matter from the soil is included in these figures. Vines also noted that the majority of the particulates were $1\mu\text{m}$ or less in diameter. The magnetic results and Mossbauer spectra identify the secondary ferrimagnetic oxide as including a major fraction less than $1\mu\text{m}$. It is possible, therefore, that quantities of the enhanced material were transported in upcurrents during the fire and were then deposited around the catchment and in the lake itself.

There was probably an immediate deposition of the enhanced material around the catchment during the fire followed by a longer term deposition of wind-blown material until the soils were stabilized by vegetation, thereby reducing the source areas available for this mode of transportation.

DISCUSSION 2.14

The movement of the magnetically enhanced secondary ferrimagnetic oxides from the burnt soils into the lake began during the fire when the upcurrents in the fire lifted the material into the air dispersing and depositing it around the catchment.

Large amounts of material in the burnt part of the catchment have been moved downslope by gullying and soil creep. Three years after the initial erosion a series of erosion lobes is beginning to spread out over the flat land adjacent to the lake margins. The stream draining the burnt area of the catchment probably contributed a significant quantity of enhanced material to the lake although this was probably limited to the period immediately following burning, which is typified by increased streamflows.

The relatively high S.I.R.M. values for the material in the stream sediment trap draining the unburnt area may be explained by the contamination of that part of the drainage basin by windblown magnetically enhanced material that has been washed off the plant and soil surfaces into the stream.

Once the material has entered the lake system there appears to be a certain amount of sediment focusing into the deepest part of the lake. Three years after the fire event a more general spread of material around the lake floor was beginning to occur.

The magnetic results from the outflow sediment trap indicate that a significant amount of enhanced material stays in suspension passing through the lake and down the outflow. No quantitative measurements have been made of the volume of material that is lost from the lake system.

The small grain size of the enhanced material and the change in specific density (section 6.3) after burning should facilitate suspension in the lake water.

During periods of high lake level the outflow stream is at bankfull stage; however if the water level in the lake is below full level then the outflow stream is reduced to a 'trickle'. It is therefore reasonable to assume that removal of the suspended enhanced material down the outflow stream only occurs when the lake water level is at a maximum. It is also probable that while at lake bankfull level, resuspension of shallow water marginal surface sediment will occur increasing the amount of enhanced material available to travel down the outflow. Below full level the outflow is dramatically reduced allowing the suspended and resuspended material to settle out in the lake waters and at the same time focusing into the centre of the lake.

MOVEMENT OF THE MAGNETICALLY ENHANCED MATERIAL DOWN THE OUTFLOW.
AFON ABRACH. 2.15

Fig. 2.15.1 locates the bedload shoals sampled on the outflow stream of Llyn Bychan. Road construction works below shoal T prevented further shoals being sampled down the Afon Llugwy, as a result of contamination of the lower reaches by road building material. The main source of burnt material is the ridge to the south west of Llyn Bychan. The ridge is drained by a stream entering the Afon Abrach approximately 200m below Llyn Bychan.

The samples, after collection, were wet sieved into ten different size fractions, dried and a 10cc aliquot from each fraction was measured for χ and S.I.R.M. Time and practical constraints would not allow all the shoal material to be measured and it was decided to rescale the χ and S.I.R.M. results to reflect the contribution each size fraction made to the total shoal weight, e.g. the three coarsest size fractions averaged 93% on the total shoal weight.

The results were rescaled using the formula:

$$Kf \times \frac{\text{total st of size fraction}}{\text{Total wt of shoal}}$$

$$\text{where } Kf = \frac{\chi}{wt} \times \text{total wt of size fraction.}$$

(S.I.R.M. can be substituted for χ)

Fig. 2.15.2 plots the unscaled mass specific χ values against distance for the 0.0 ϕ and <4.0 ϕ fractions, the total and average shoal values and the rescaled total shoal χ . The distribution of the data may be considered bi-modal, high χ values at H which decrease downstream to shoal X. The χ values at this point increase at shoal T.

POSITION OF THE STREAM BEDLOAD SAMPLING SITES FOR AFON ABRACH

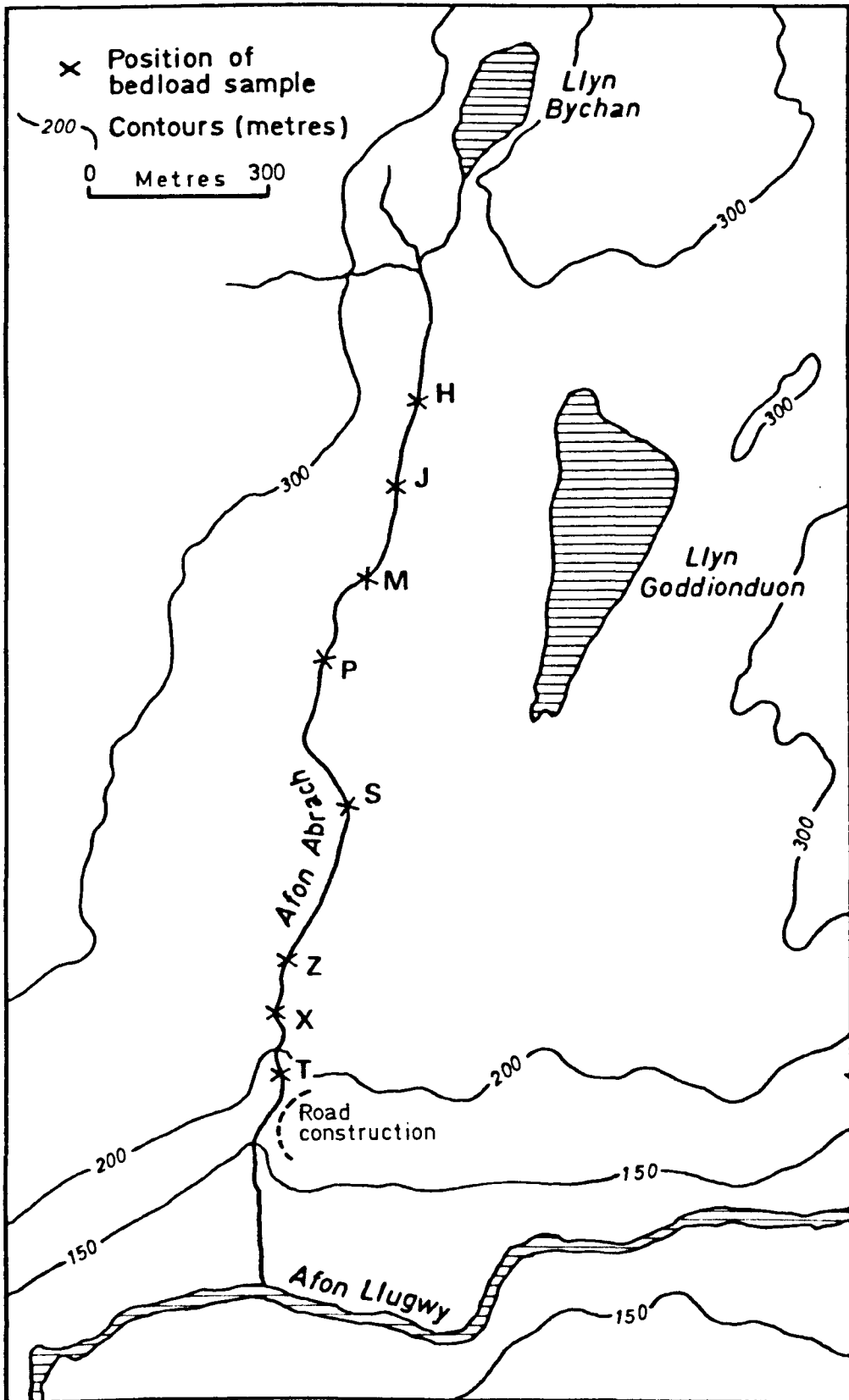


fig. 2.15.1 Location of bedload shoals sampled in the Afon Abroch.

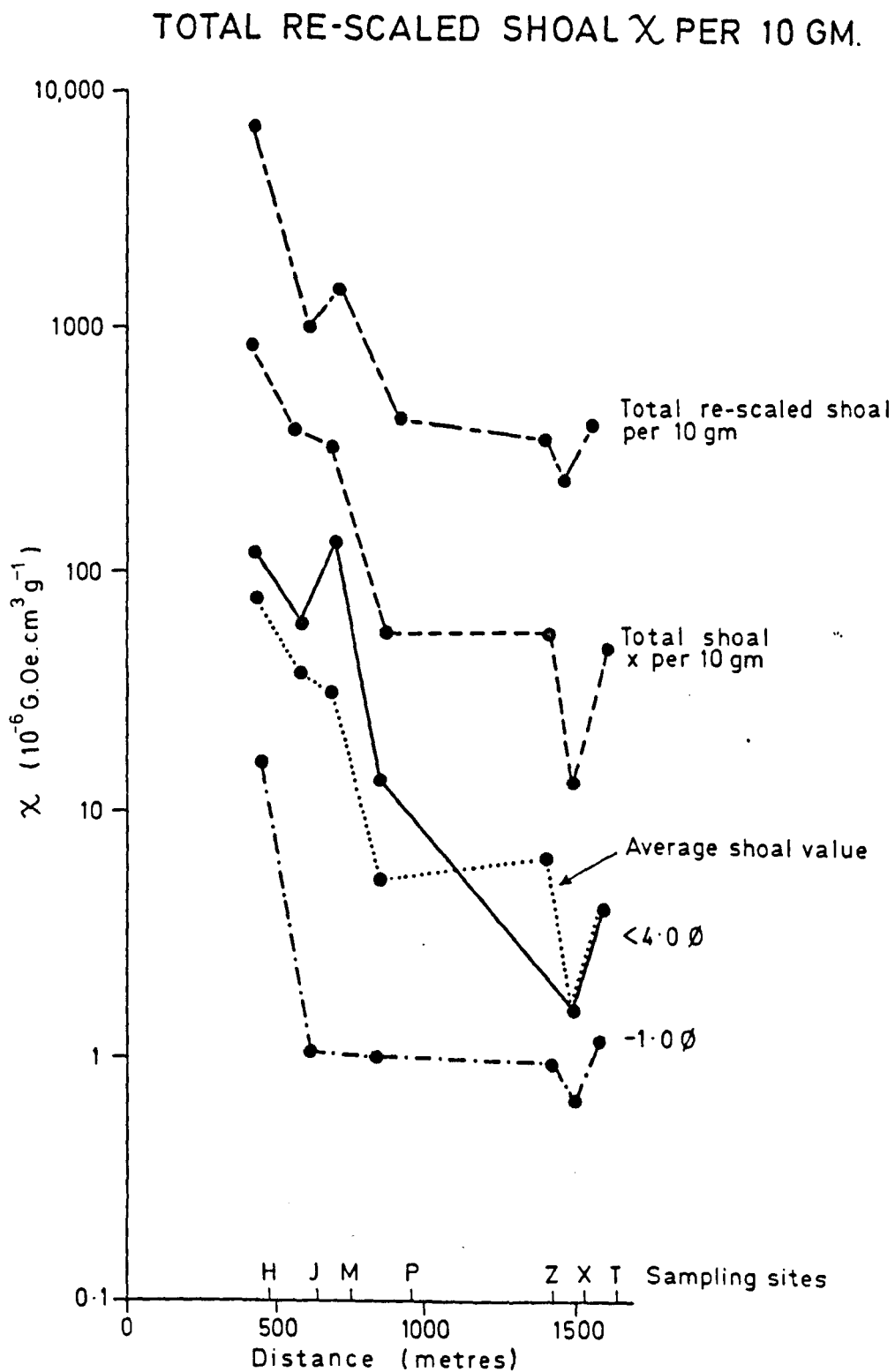


fig2.15.2 Unscaled mass specific, total and average χ against distance for bedload shoals sampled.

The 0.0 ϕ fraction curve is below the average χ curve and $< 4.0\phi$ fraction curve lies above it indicating that the finer fractions have higher specific values. The effect of rescaling the specific data is to increase the χ values of the coarser fractions but not to alter the χ distribution down the reach, the rescaled total curve being similar to the specific curve.

Table 2.15.1 lists the rescaled χ and S.I.R.M. values for each size fraction for the shoals sampled. The highest χ and S.I.R.M. values are recorded at shoal H decreasing downstream to shoal X, although in the size fractions 1.0 ϕ to $< 4.0\phi$ an increase in χ , S.I.R.M. or both is evident in shoal Z. The S.I.R.M. values at shoal T are higher than at shoal X in the -1.0 ϕ and 0.0 ϕ fractions, but the values at shoal T are higher for the size fractions 2.5 ϕ to $> 4.0\phi$ than at shoal X.

The magnitude of the decrease in χ from shoal H to T ranges in χ from 4 times for the 0.0 ϕ fraction to 372 times in the $< 4.0\phi$ fraction and in S.I.R.M. from 6 times (0.0 ϕ) to 209 times (4.0ϕ). The table also shows a domination of the magnetic properties of the shoal by the coarser size fractions but with a significant contribution from the $< 4.0\phi$ fraction.

Figs. 2.15.3 and 2.15.4 plot the regression lines and correlation coefficients for the rescaled S.I.R.M. and χ values respectively. The 0.0 ϕ shoal Z value was omitted from the S.I.R.M. regression calculations.

Both figures show a negative correlation of S.I.R.M. and χ and increasing distance from the source. The regression analysis for S.I.R.M. against distance exhibits a distinct ordering from the

STATION	H		J		M		P		Z		X		T	
CORRECTED VALUES	SIRM $\times 10^{-6}$ G.Oe.cm ³ g ⁻¹	χ emu.g ⁻¹	SIRM	χ	SIRM	χ	SIRM	χ	SIRM	χ	SIRM	χ	SIRM	χ
-1.0 ϕ	36982	1143	1613	128	5430	268	6399	276	1410	197	630	142	5598	268
0.0 ϕ	62368	2417	10060	440	5593	201	4061	109	6244	99	2083	53	11647	70
1.0 ϕ	13939	863	5713	251	2160	89	2400	70	12253	96	4810	55	1020	15
1.5 ϕ	5804	228	1471	69	441	23	426	13	1875	20	322	6	237	5
2.0 ϕ	3756	190	1006	59	220	14	206	8	973	13	71	2	69	.8
2.5 ϕ	3113	157	551	39	225	12	209	6	517	8	48	.3	39	.4
3.0 ϕ	2447	137	597	38	196	11	134	6	291	6	32	.2	12	.6
3.5 ϕ	2222	120	437	30	95	7	84	5	201	4	24	.2	13	.6
4.0 ϕ	1698	88	416	24	107	7	73	3	100	2	11	.7	7	1
4.0 ϕ	50303	2233	10156	408	22847	812	2044	65	557	14	399	10	241	6

TABLE 2.15.1

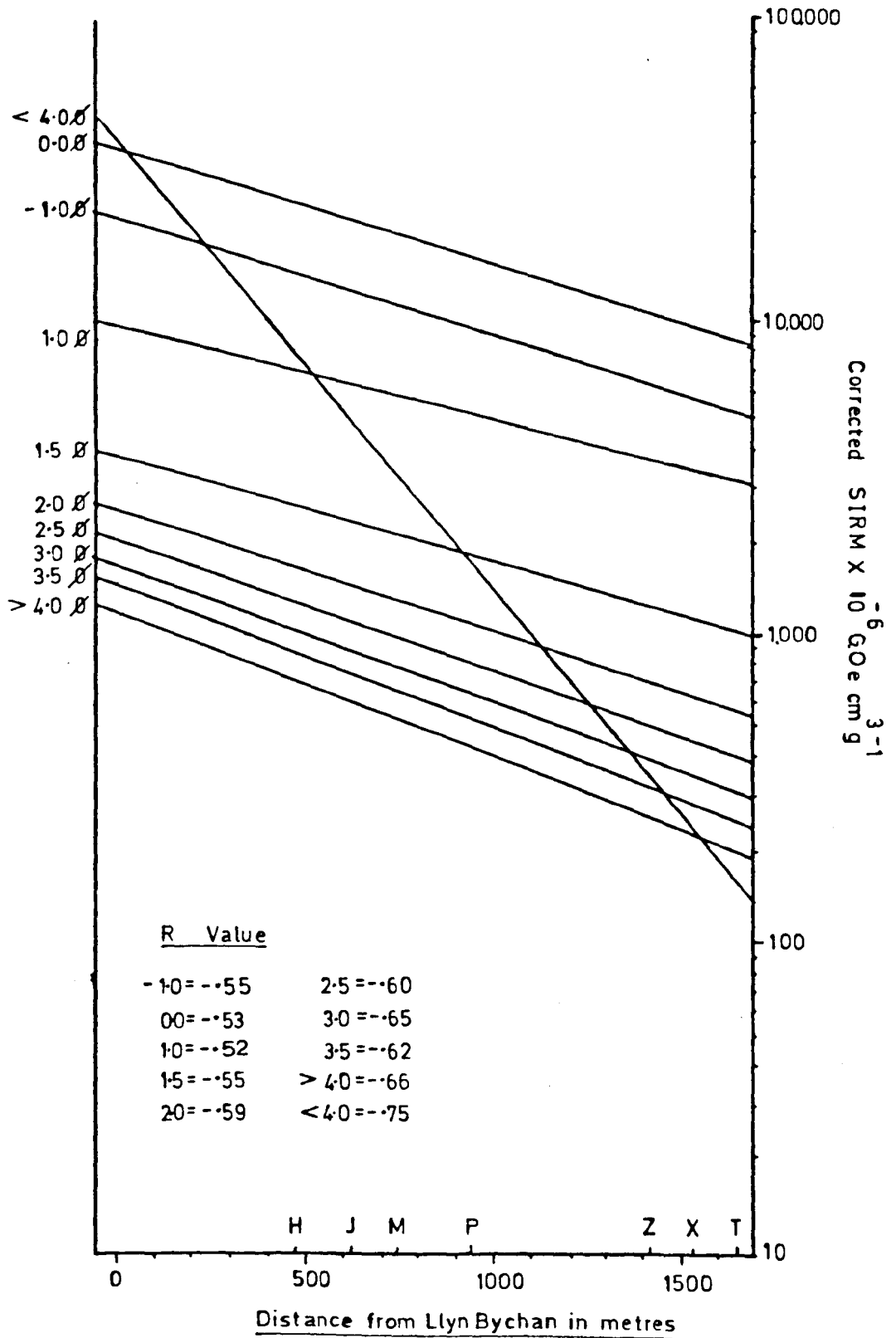


fig.2.15.3 Afon Abrach bedload rescaled S.I.R.M. regression lines.

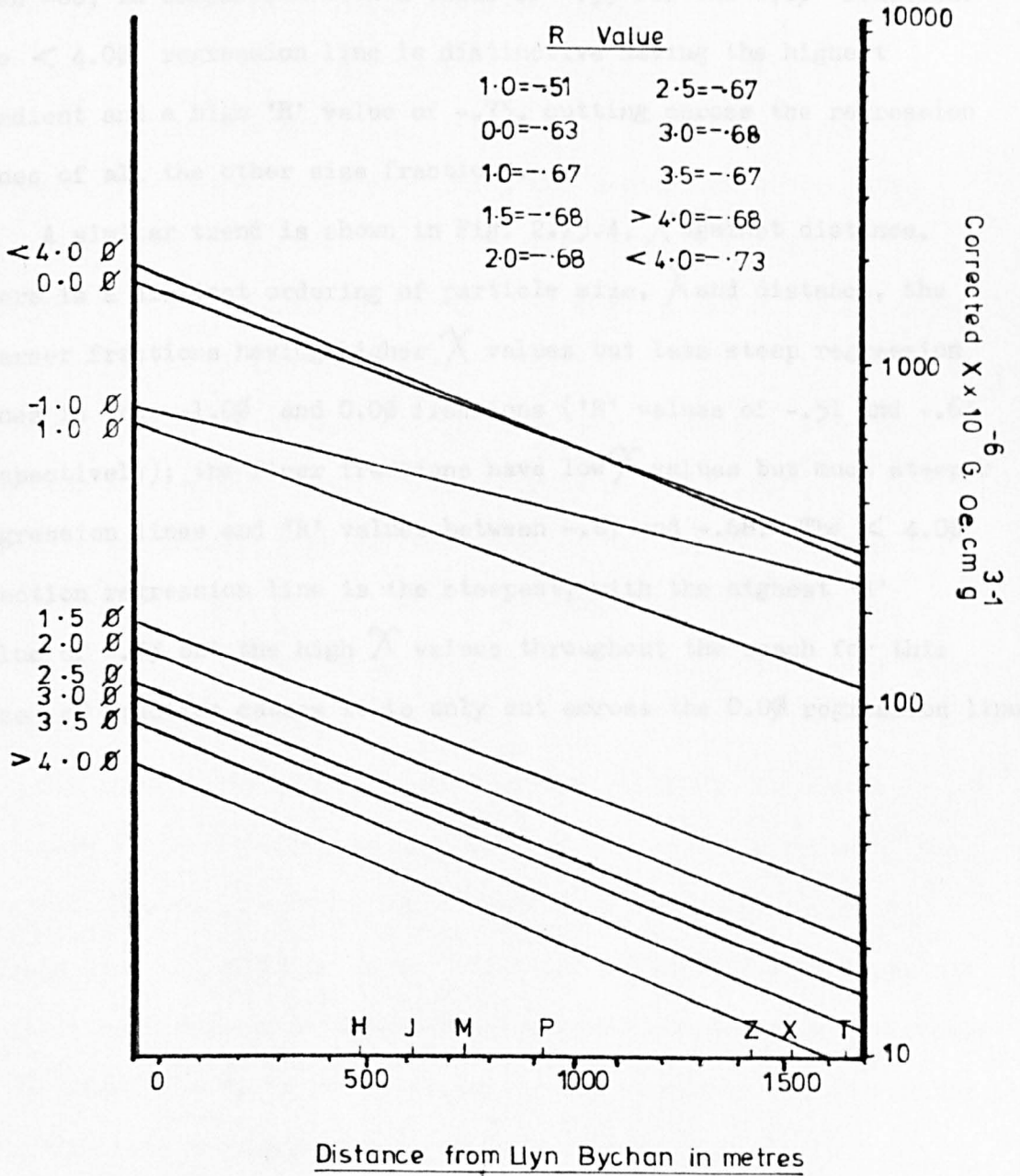


fig2.15.4 Afon Abrach bedload rescaled χ regression lines.

coarser fractions having higher S.I.R.M. values, down to the $> 4.0\phi$ fraction with lower S.I.R.M. values. However, the regression lines are steeper for the finer fractions as reflected in the greater 'R' values. The 2.5ϕ to $< 4.0\phi$ fractions have R values greater than -60 , in comparison with a value of $-.53$ for the 0.0ϕ fraction. The $< 4.0\phi$ regression line is distinctive having the highest gradient and a high 'R' value of $-.75$, cutting across the regression lines of all the other size fractions.

A similar trend is shown in Fig. 2.15.4, χ against distance. There is a distinct ordering of particle size, χ and distance, the coarser fractions having higher χ values but less steep regression lines in the -1.0ϕ and 0.0ϕ fractions ('R' values of $-.51$ and $-.63$ respectively); the finer fractions have low χ values but much steeper regression lines and 'R' values between $-.67$ and $-.68$. The $< 4.0\phi$ fraction regression line is the steepest, with the highest 'R' value of $-.73$ but the high χ values throughout the reach for this size of fraction causes it to only cut across the 0.0ϕ regression line.

DISCUSSION 2.16

The regression analysis shows that the χ and S.I.R.M. values decrease down the reach and away from the source of secondary ferrimagnetic minerals. This is believed to reflect some movement of magnetically enhanced material down the reach.

The high χ and S.I.R.M. values at shoal H in all size fractions indicate a shoal composition with a high proportion of secondary ferrimagnetic oxides, while the low values at shoal T indicate a smaller volume of magnetically enhanced material, especially in the finer fractions. The high χ and S.I.R.M. values in the larger size fractions for all shoals point to a high background χ and S.I.R.M. level which is probably due to primary magnetic minerals derived from the volcanic bedrock of the area. (section 2.2). The primary magnetic minerals have high χ and S.I.R.M. values and may be regarded as a natural highly magnetic residual component in the shoals of the reach upon which the declining trend away from the fire is superimposed.

The shoals, therefore, consist of two magnetic components :
A primary residual component derived from the volcanic rocks of the area and a second component due to secondary ferrimagnetic oxides derived from the burnt areas and which are relatively more important in the finer fractions. The natural residual component may be present in the finer fractions but is masked by the secondary magnetic minerals which dominate the finer fractions.

The nature of the movement of bedload material is outlined in Gregory and Walling (1973) and Morisawa (1974). The negative correlation of χ and S.I.R.M. and distance for the different size fractions indicates the movement of the enhanced material downstream. The steep regression line for the $< 4.0\phi$ fraction indicates that the fire influence is stronger in this fraction. The slope of the line may also indicate that in a high energy environment the fine material is quickly removed from the reach whereas the coarser fractions are only moved part of the way down the reach.

The distance decay effect is reflected in all the size fractions up to the 0.0ϕ fraction and may reflect the magnetic composition of the shoals sampled. It can be seen, therefore, that the magnetically enhanced secondary ferrimagnetic oxides are acting as a natural stream bedload tracer. The extent of the movement of the material in the reach is shown by the χ and S.I.R.M. values of the shoal which indicates the proportion of enhanced material in the shoal composition.

Despite the study being carried out in an uncontrolled and uninstrumented environment the results are well ordered and meaningful, showing the potential of using magnetically enhanced bedload as a stream bedload tracer.

CONCLUSIONS AND DISCUSSION 2.17

The Llyn Bychan case study has shown that in the burnt soils of the catchment.

(i) The production in the soil environment by the fire of secondary ferrimagnetic oxides that have been identified by various techniques as magnetite although of a non-stoichiometric form ($\text{Fe}_{2.9}\text{O}_4$) and with a magnetic component ranging from superparamagnetic to stable single domain.

(ii) The magnetic properties of the secondary ferrimagnetic oxides are typified by high χ and S.I.R.M. values, low S.I.R.M./ χ ratios and low coercivity of S.I.R.M. values. The degree of enhancement is dependant upon a number of factors, the most important of which is the availability of iron for conversion to a secondary ferrimagnetic form and the production within the soil of an environment suitable for their synthesis.

Around the burnt areas of Llyn Bychan the high χ and S.I.R.M. values indicate that during the fire optimum conditions were attained in the surface levels of the soil. Optimum conditions are high temperatures, possibly a strong reducing and oxidizing environment and a form of iron that can be converted into a secondary ferrimagnetic form (section 6.3).

Although the Llyn Bychan case study has identified the secondary ferrimagnetic oxide it does not necessarily follow that the end product cannot be maghemite. It is the author's opinion that the end product is dependant upon not only the soil environment created during the fire, but also the form of iron in the soil available for conversion. The iron available for conversion is not only dependant of pedogenic processes and soil type but also on vegetation type and climate. The

end product is therefore dependant on a complex interrelationship between the soil the environment and the fire created soil environment. These cannot be assumed to be the same for every site and fire.

Within the lake sediments it has been observed that the secondary ferrimagnetic material has entered the lake system and become incorporated into the lake sediment where it has formed a magnetically distinct layer. The magnetically enhanced lake sediment is typified by high χ , K and S.I.R.M. values, low S.I.R.M./ χ ratios and low $(Bo)_{CR}$ values.

The value of the magnetically distinct layer for limnological and palaeoecological studies is twofold : (i) It acts as an easily identifiable marker layer and time horizon (ii) It is an aid to core correlation within a lake basin.

Some of the pathways through which the secondary ferrimagnetic material has moved from the soils into the lake environment has been identified: (i) The small particle size of the enhanced material enabled the material to be physically lifted into the air by the fire upcurrents and distributed around the catchment. It is possible, therefore, that the magnetically enhanced material can be used as an atmospheric tracer to investigate the movement of material during fires and other events.

(ii) By wind erosion following removal of the vegetation cover by burning and before stabilisation by recolonisation by vegetation.

(iii) By increased streamflows after the fire event where the enhanced material could be used to study the amount of eroded material carried by the streams as opposed to their normal unenhanced load.

(iv) By soilcreep and gullying. The progress of this could easily be monitored by measuring the magnetic enhancement within the gully, soilcreep; the latter could be used as an indicator of its position and rate of progress.

(v) By snowmelt on the steepest slopes.

The bedload tracing of the magnetically enhanced material in the outflow stream of Llyn Bychan has identified the possible use of magnetically enhanced bedload material as a natural stream bedload tracer. The implications of this work have been followed up in a separate case study and are presented in Chapter 6.

LLYN GODDIONUON. A CASE STUDY. CHAPTER 3INTRODUCTION 3.1

Llyn Goddionduon (Grid Ref. SH753586) lies approximately 600m. to the south east of Llyn Bychan at a slightly lower altitude of 244m.O.D. (Fig. 2.1.1. plate 2). The lake covers 6.2 hectares and receives drainage from a 25 hectare catchment. Morphometrically the lake is a kettle hole type of formation with a maximum water depth of 6m. in a small trench which occupies less than 5% of the lake bed area. 50% of the present sediment surface lies between water depths of 0.75m. and 4.0m. Three small inflowing streams drain into the northern end of the lake. A small mire of about 6.0 hectares in extent at the southern end of the lake represents overgrowth of peat lying on marginal lake sediments.

The geology of the catchment is shown in Fig. 2.2.1 and is essentially similar to the Llyn Bychan catchment except that the area is dominated by the Llanrhychwyn slates and slates and shales of the upper Crafnant volcanic group.

Bloemendal (1977) has described the vegetation and land-use of the area in detail. The whole catchment is forested with coniferous trees of different ages, the dominant species being Sitka and Norway spruce, Scots and Lodgepole pine. In May 1951 the north-eastern area of the catchment was affected by a forest fire that eventually destroyed 50 hectares of the surrounding forest. Shaw, in an unpublished forestry report, describes the fire as inflicting serious and substantial damage to the soil of the affected area.

RESEARCH PROJECT AT LLYN GODDIONDUON 3.2

Llyn Goddionduon is the site of a research project evaluating the use of magnetic measurements for assessing sediment influx to a small lake. In 1977 an accurately surveyed grid of 130 minicores was sampled from the lake using a 1m. Mackereth cover. Whole core K measurements were performed on all the cores whilst in the field. Subsequent studies based on the extruded sediments have included single sample χ and S.I.R.M. measurements, coercivity of S.I.R.M. ($^{(Bo)}CR$), anhysteritic remanent magnetisation (A.R.M.) and the strength and direction of natural remanence magnetisation (N.R.M.) studies. Preliminary results from this study are published in Bloemendal et al., (op cit).

A multiple core correlation scheme along the lake is suggested on the basis of the use of various magnetic parameters. Two distinct magnetic peaks have been identified: one peak in the uppermost sediment is characterised by a high S.I.R.M./ χ ratio has been attributed to the 1951 forest fire.

Results

Fig. 3.2.1. plots the magnetic parameters of χ , S.I.R.M. and N.R.M. against depth for core 50/-43. Cesium 137 analysis was performed on samples from the core and the ^{137}Cs results are plotted on the same diagram. The magnetic profile of the core is typical of many of the cores taken from the lake.

The S.I.R.M. and χ values for the sediment samples below 20cm. are relatively low ($\chi < 10 \times 10^{-6} \text{G.Oe.cm}^3 \cdot \text{g}^{-1}$, S.I.R.M. $< 100 \times 10^{-6} \text{G.Oe.cm}^3 \cdot \text{g}^{-1}$)

but increase in the sediment sample shows that the peak χ and S.I.R.M. values in the top 10 cm of the sediment column ($\chi < 10.0 \times 10^{-6} \text{ pCi.g}^{-1}$, S.I.R.M. $< 250 \times 10^{-6}$) stratigraphically the top 10 cm of the sediment is different from the rest of the core as it is dominated by black material. The ^{137}Cs profile shows that the first presence of fallout could be dated to 1954 occurs at a depth of 5 cm in the sediment. (Redington, et al., 1978)

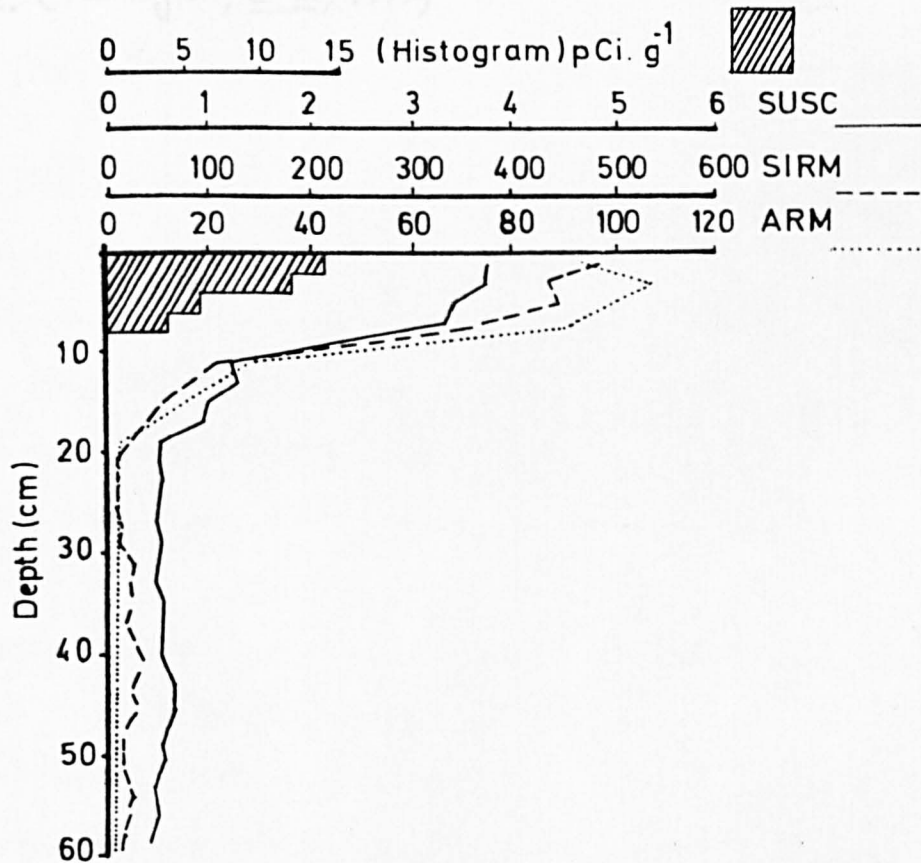


fig. 3.2.1 χ , S.I.R.M., H.R.M., and ^{137}Cs for Llyn Goddienduon core 50/-43

but increase in the sediment samples above 10cm to peak χ and S.I.R.M. values in the top 10cm of the sediment column ($\chi < c40.0 \times 10^{-6} \text{G.Oe.cm}^3 \cdot \text{g}^{-1}$, S.I.R.M. $495 \times 10^{-6} \text{G.Oe.cm}^3 \cdot \text{g}^{-1}$) Stratigraphically the top 10cm of the sediment is different from the rest of the core as it is dominated by black material. The ^{137}CS profile shows that the first presence of fallout cesium dated to 1954 occurs at a depth of 8cm in the sediment. (Pennington, etal, 1973)

DISCUSSION 3.3

Pollen analytical studies (Bloemendal, op cit) have confirmed that increases in ferrimagnetic mineral concentrations, identified by the high χ and S.I.R.M. values post date the partial afforestation of the catchment by exotic species of conifers in the 1930's. The occurrence of the 1954 ^{137}Cs level at 8cm, 2cm above the base of the most rapid increase in concentrations of magnetic oxides, places the age of the increase within the time range 1940-1954. Compatible with a direct correlation between the increase in the concentrations of magnetic minerals in the lake sediment, the 1951 forest fire and the production of secondary ferrimagnetic minerals in the soil.

The increase in the magnetic values in the top 10cm's of lake sediment is due to two possible mechanisms. Firstly the increase may be due to the input of large volumes of secondary soil ferrimagnetic minerals washed into the lake following the afforestation of the catchment before the 1951 fire. ^{Newson, (1980)} Secondly, it may be due to the input of secondary ferrimagnetic minerals formed in the soil at the time of the fire and moved into the lake sediment during and after the fire event. In light of the ^{137}Cs evidence the latter alternative is indicated and it is thought that the main area of deposition of the magnetically enhanced minerals occurred at the northern end of the lake near the zone of burning. (Bloemendal. pers. comm.).

CONCLUSION

The magnetic results from the Llyn Goddiondnon case study indicate that the top 10cm of the lake sediments are dominated by eroded soil ferrimagnetic minerals and magnetically enhanced secondary ferrimagnetic oxides that were formed during the 1951 forest fire. This suggests that the secondary ferrimagnetic oxides are persistent in the lake sediment environment over a time period of 26 years and are sufficiently magnetically distinct despite dilution by other magnetic minerals to allow a core correlation to be attempted on the basis of their magnetic properties.

CHAPTER 4LES LANDES. A CASE STUDYINTRODUCTION 4.1

The case study of the Llyn Bychan drainage basin has confirmed the formation of secondary ferrimagnetic oxides in the soils as a result of the 1976 forest fire. Magnetic measurements on lake sediment cores have shown that erosional processes have transported the oxides into the lake sediment where they are identified by high χ and S.I.R.M. values. Llyn Goddionduon has provided an insight into the persistence over time of the oxides in the lake sediment environment.

A catchment area was therefore needed which had been extensively damaged by a well documented forest fire at an earlier date. The 'Landes' in South-West France was considered to be an ideal site, with major fires in the 1940's culminating in the well documented disastrous fire in 1949. In addition, the area has a reasonably uniform lithology and two large lakes (étangs) with drainage basins that had been ravaged by the 1949 forest fire.

LOCATION AND PHYSICAL SETTING 4.2

The lakes of Biscarrosse and Sanguinet are situated on the sand covered Landes plateau, a vast 1,200,000 hectare triangular area in the south west of France, (44.13N,00.53W) spanning over 2° of latitude and almost 2° longitude. The triangular plateau is remarkably uniform in terms of topography, parent material, vegetation cover and soils. The littoral dunes and the Atlantic Ocean define the western limit of the triangle; to the east and north the Landes is bounded by the Garonne and by the Adour in the south (Fig.4.2.1).

The Landes plateau can be divided into two distinct regions:

- (i) in the west the dunes characterize the littoral zones;
- (ii) the area to the east of the coastal belts constitutes the true Landes plateau, on almost horizontal (with slopes of c.2°) plain of sand. From heights of more than 100m. in the east the plateau gently slopes to less than 20m. at the edge of the coastal dunes, a distance of over 60km. The monotony is broken by small clay hummocks 25 to 30m. in height and areas of continental dunes that cause undulations in the surface area.

A line of modern sand dunes rising to over 80m. in height and extending 8 to 9km. inland dominate the 225 km. long coastline from the Point de Grave in the north to the Adour in the south. Behind the modern dunes there is a discontinuous belt of ancient dunes which are frequently covered with deciduous forest or buried under a more recent sand cover.

Separating the littoral zone of dunes from the Landes plateau is a string of coastal lakes or 'étangs'. The lakes can be divided into two categories : those in the north which are deep (c. 24m) and have a tendency to be triangular in shape, and those in the south which are smaller and shallow (c. 2m deep). All the lakes display an

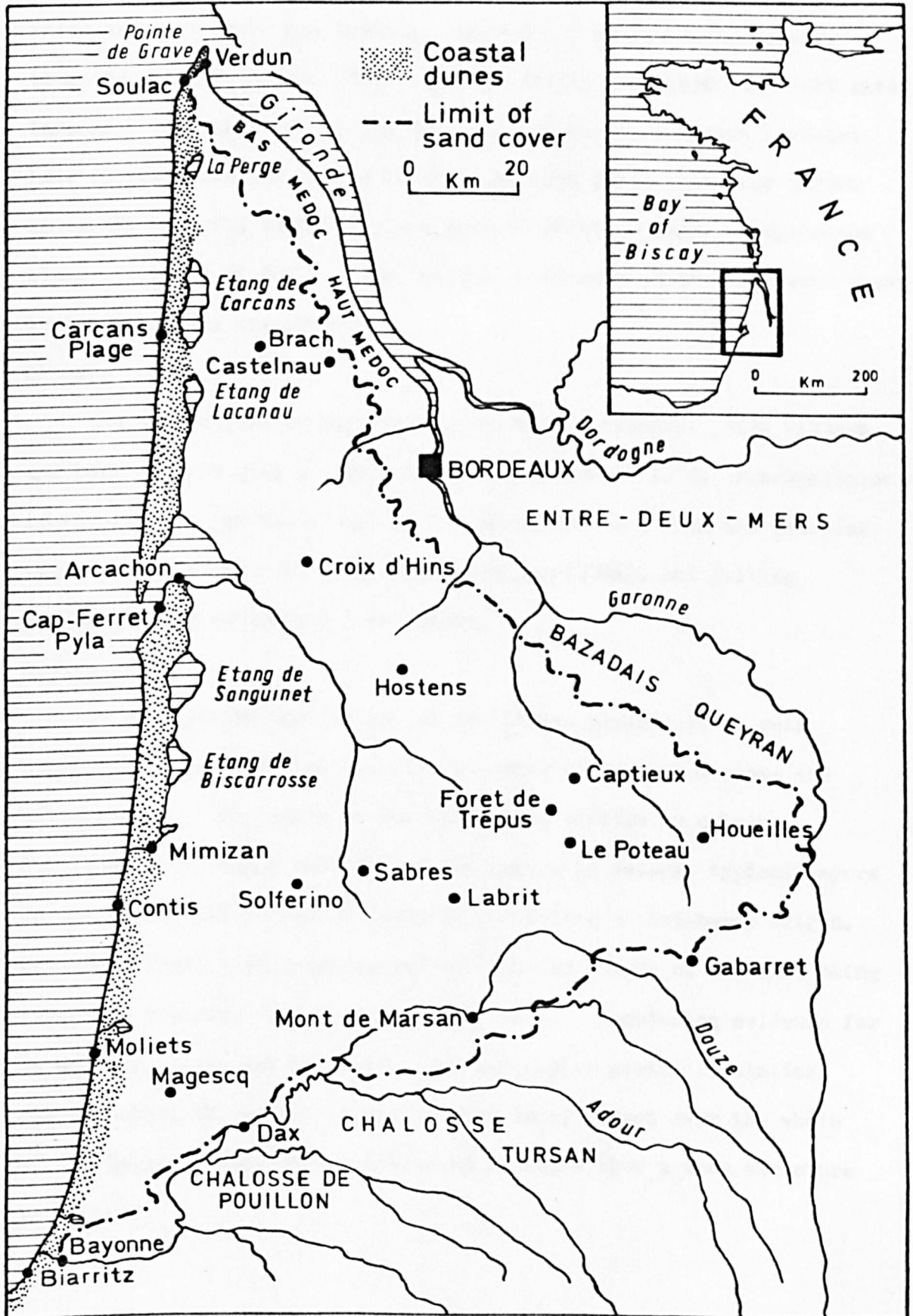


fig.4.2.1 Location of the Landes

interesting morphometric profile. the western slopes being steeper than the eastern slopes. Until quite recently the lakes were salt water lagoons, like the present day Bassin d'Archachon, but were isolated late in the Flandrian period by lines of sand dunes that were thrown up by the powerful westerly winds against offshore bars. Despite the close proximity of the sea the 'etangs' are fresh water lakes with water levels 20m. above sea level.

Climate

The Landes plateau experiences an oceanic climate. Mild winters and warm summers give a mean annual temperature of 12°C. Precipitation increases from the north east to the south west and from the interior westwards. Rainfall is seasonal, averaging 1000mm, and falling principally in autumn and late spring.

Geology

In considering the geology of the Landes plateau it is only necessary to consider the superficial cover of sand that masks the solid geology. The sands of the Landes are aeolian in origin. Cailleux (1952) found that 95% of the grains in several typical layers in the Landes all possessed features indicating a wind-borne origin. Houlsten (1968) also demonstrated the aeolian origin of the sand using frequency distributions and Friedman's tests. Convincing evidence for an aeolian origin can be seen in the landscape; gentle undulations corresponding in outline to the form of dunes extend over the whole of the Landes. Undulations dissected by roads show a dune structure in section.

The origins of the sand cover has provoked much discussion among french geomorphologists. There are two possible modes of origin.

(i) A marine origin, the sands having been transported inland from the coast by westerly winds (Duffart, 1900; Buffault, 1942).

(ii) A continental origin, the sands having been redistributed over the Landes from ancient valleys cut into the continental beds.

Léuêque (in Blayac, 1916).

Fabre (1905) favours the idea that both processes made substantial contributions to the generation of the large volume of sand. Enjalbert (1950) supports Duffart and Buffault but adds that the sand cover was deposited at a time when the sea was at a lower level than at the present day, or it was possibly rising. He further suggests that the phase of sand deposition was brought to a close by a climatic change during the Flandian period.

The extension of the sand cover has occurred since the early Flandrian and includes the restricted deposition of the sands of the modern dunes. Duffart (op.cit.) suggested that the ancient dunes were thrown up at the same time as, and for some time after, the Landes was being covered with sands originating from the coastal area. There was then a change to conditions which did not favour active dune formation and which was followed by the most recent period of dramatic dune invasion from the 14th to the 19th century, during which time the littoral forests were buried. Enjalbert (op.cit.) ascribes the new period of dune activity to a climatic change characterised by stronger winds and assisted by the burning practises of man in the coastal forests.

Description of the major soil types

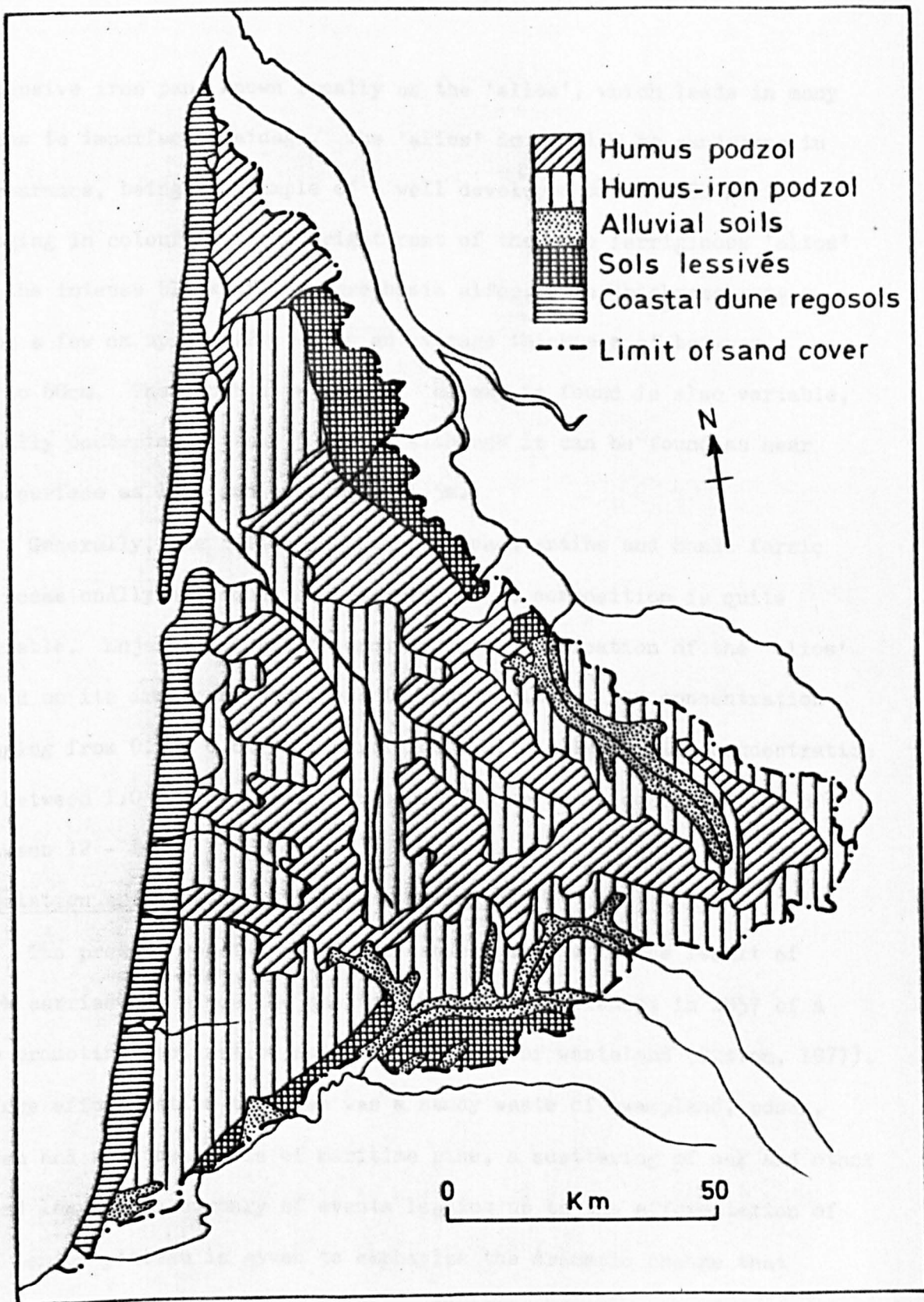
Fig. 4.2.2 maps the soils found in the Landes. A distinction can be made between the dune regosols of the coastal area and the podsols of the Landes plateau.

A division can also be made in the dune soils between the modern dune regosols and the ancient dune regosols. The latter group is found behind the former group which border the belt of unstable sand dunes. The modern dune regosols are infertile, possessing a shallow eluvial horizon passing straight into a C horizon (parent material). The soils have a high calcium carbonate content leading to a pH of almost 7. The soils are friable, possessing no real structure and consequently are prone to erosion unless stabilized by vegetation.

A deeper eluvial horizon characterizes the ancient dune regosols together with an increased organic matter content which gives the soil, a darker colour and a more developed structure. Increased leaching of the soil results in a lower pH, but the ancient dune regosols support a denser and more varied range of vegetation.

The podsol is the main soil group of the Landes plateau. Humus and humus-ferric indurated podsols form the majority of mature podsols, although iron-podsols are found in some sites. Generally the humus podsols are restricted to the poorly drained interflures. Gley-Podsols develop upon illuvial sands and gravels which are subject to severe water-logging during the winter, and humus-iron podsols develop on the better drained areas of the plateau.

A feature of the podsols of the Landes is the formation of an



Source. Houlston, 1968.

Fig. 4.2.2. Soils of the Landes.

extensive iron pan, known locally as the 'alios', which leads in many areas to imperfect drainage. The 'alios' is similar to sandstone in appearance, being an example of a well developed Bfe and Bh horizon ranging in colour from the bright rust of the pure ferruginous 'alios' to the intense black of the pure humic alios. Its thickness ranges from a few cm. up to 1.2m., with an average thickness of between 40 to 60cm. The depth at which the 'alios' is found is also variable, usually occurring between 30-40cm. although it can be found as near the surface as 10cm and as deep as 1.5m.

Generally, the 'alios' consists of sand grains and humic ferric or occasionally siliceous cements; the exact composition is quite variable. Enjalbert (op cit) produced a classification of the 'alios' based on its iron concentration: 1., Humic alios, iron concentration ranging from 0.1 - 0.8% 2., Ferruginous alios, iron oxide concentration of between 1.0 - 4.6%. 3., 'Garluche'., iron oxide concentration of between 12 - 16%

Vegetation and land-use history

The present vegetation of the Landes plateau is the result of work carried out since the passing by French Parliament in 1857 of a law promoting reclamation and afforestation of wasteland (Sutton, 1977). Before afforestation the area was a sandy waste of swampland, ponds, brush and scrubby stands of maritime pine, a scattering of oak and other broad leaves. A summary of events leading up to the afforestation of the Landes plateau is given to emphasize the dramatic change that has occurred in the study area since the dune fixation experiments of Bremon-tier. It was a result of his work between 1787 and 1793 that led to the successful afforestation of the area.

Dargan (1846, pp 292 in Woolsey, 1922) describes the Landes as an area of "acid sands, heather furze, clumps of pine and occasional flocks of sheep with shepherds on stilts. In summer the areas display drought and nakedness reminiscent of the deserts of Africa, but in winter they make a cold picture like the marshes of Siberia". The large areas of wasteland in France in the 18th Century led the government to try several approaches to rectify the problem in order to bring the land back into agricultural production. Clout (1969) emphasizes the magnitude of the problem. In 1761 a ten year tax exemption was allowed on lands that were improved by reclamation and indirectly led to Le Villers and Bremontiers reclamation attempts.

The coastal dunes of the Landes had been threatening to overwhelm Mimizan and Lege since the 14th Century, advancing at a rate of 20-27 m. per annum (Woolsey op cit). Le Villers in 1778 was the first to attempt the fixation of the dunes but it was not until Bemontier's experiments that the coastal dunes were successfully fixed.

The fixation of the dunes predates the drainage and afforestation of the interior Landes by some 70 years. The credit for this latter operation is given to the personal ingenuity of Chambrelant. In 1827 Chambrelant devised a drainage system for the Landes, thereby becoming the creator of the forest land use; by 1849 20,500 ha. had been reclaimed.

1857 saw the passing of the Defrichement laws by the French Parliament providing state legislation to enable the appropriation of any terrain in need of reclamation and providing for the construction of major drainage channels and canals. The law was enforced in 1865 when it was made compulsory that the area be reclaimed and the dunes fixed. Chambrelant's drainage system was completed in 1866. Fourcade (1909) estimated that by 1878 less than a tenth of the area awaited

improvement. Certainly between 1850 and 1879, the period of maximum reclamation, the amount of wasteland had decreased from 47% of the area in 1850 to 19% in 1879, 74,000 ha. having been afforested by 1891.

Behind the coastal forests the land was divided into 100ha. compartments and leased for resin tapping and for cutting. The forests were rotated every 70-80 years with 14-16 thinning cycles; the felled material was left to decay on the ground, being removed by burning when it was time to replant.

The tree most suited to the conditions of the Landes and used for the monoculture was Pinus pinaster. The tree is tolerant of siliceous soils and a good tap root system allows it to withstand the strong westerly winds. Such characteristics coupled with a rapid growth rate and high resin production makes the tree valuable to the pit prop, paper pulp and cellulose industries.

Fire has long been recognised as an important hazard to the forest, large fires occurring at Soustons and Messanges in 1822; but it was with the increased afforestation of the 19th century that the fire danger increased. An average of 3,500 ha of forest was destroyed by fire annually, but the drought years 1936 to 1952 led to a series of particularly severe fires, forcing the enclosure of the forest in 1945 and the introduction of regular forest patrols from 1946. Fig. 4.2.3 maps the area of the forest destroyed by fire in the years 1940-48 and the area ravaged by the disastrous fire of 1949.

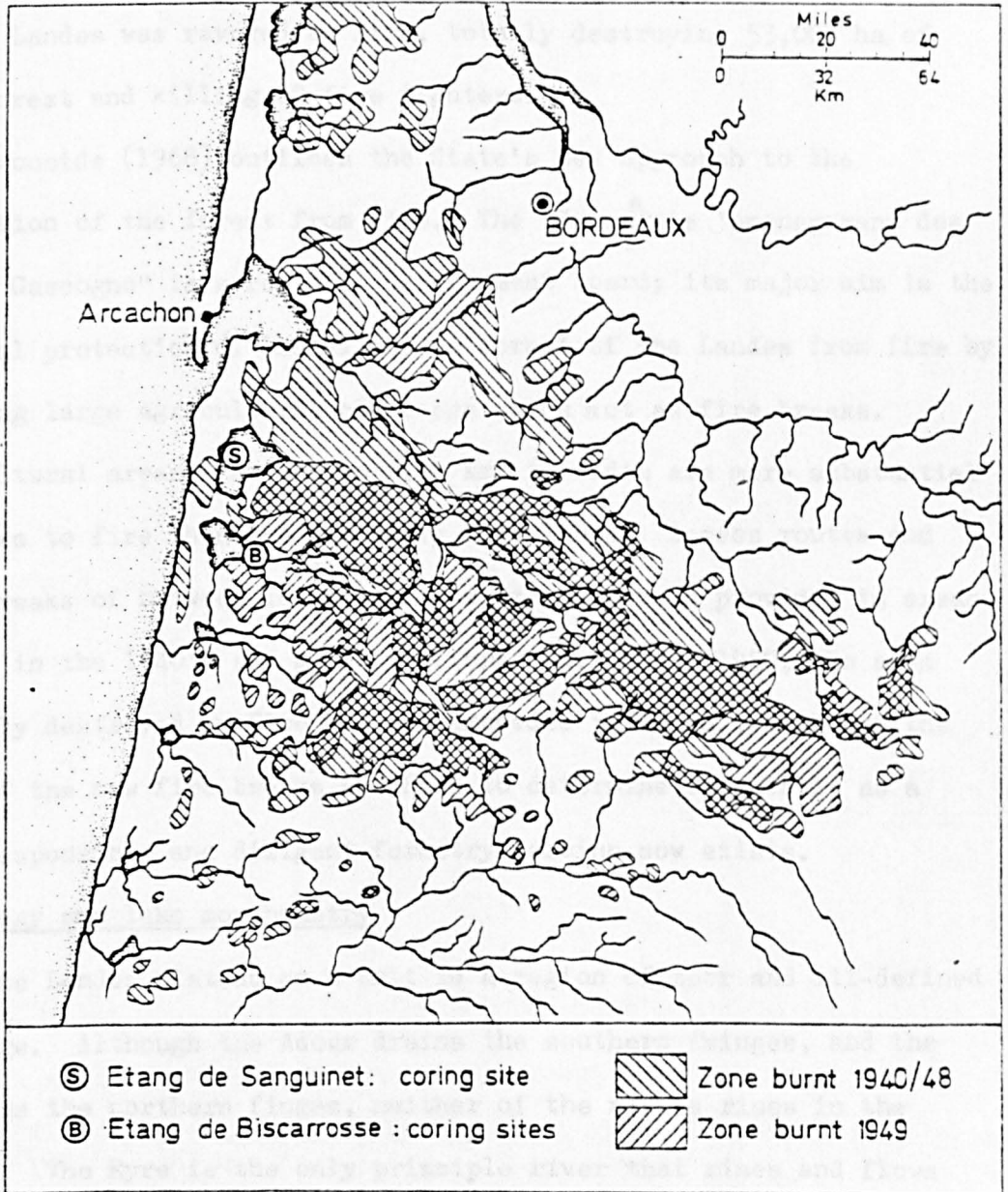


fig.4.2.3. Areas of the Landes destroyed by fire 1940-1948 and 1949.

Source: Carte de la Vegetation de la France.

Mont-de-Marsan No. 63, Bordeaux No.56 (1955)

Large areas of the Sanguinet drainage basin were burnt several times, however, it was the fire of 1949 that caused the maximum damage. Known locally as the "l'année rouge", the fires travelled up to 40km. in a day. Pinaud (1973) estimates that at the time of the Summer 1949, 132,000 ha. of the Landes was ravaged by fire, totally destroying 53,000 ha. of pine forest and killing 82 fire fighters.

Ironside (1968) outlines the State's new approach to the protection of the forest from fire. The "Campagne d'aménagement des Landes Gascogne" is a regional development board; its major aim is the physical protection of the extensive forest of the Landes from fire by creating large agricultural clearings which act as fire breaks. Agricultural areas from one to five km. in width are more substantial barriers to fire than the customary fire lanes. Access routes and fire breaks of between 16 to 50m. in width have been provided in areas burned in the 1940's and since reafforested. Since 1950, the area annually destroyed by fire has not exceeded 5,000 ha., although the role of the new fire breaks are hard to determine especially as a more responsible and diligent forestry service now exists.

Hydrology and lake morphometry

The Landes plateau as a unit is a region of poor and ill-defined drainage. Although the Adour drains the southern fringes, and the Garonne the northern fringes, neither of the rivers rises in the Landes. The Eyre is the only principle river that rises and flows through the Landes, draining into the Arcachon Basin from sources near Sabres and the Forêt des Trepus (Fig. 4.2.1).

Marshes are a common feature of the landscape as are the coastal lagoons. Further inland there are numerous small lakes, frequently arranged in small groups. However the construction of the canals and drainage systems of Chambrelant have improved the drainage of the Landes. Explanations for the inadequate drainage of the Landes point to the inadequate slope, the barrage effect of the coastal dunes and the impermeability of the alios as the main elements responsible.

Fig. 4.2.4 maps the hydrology of the two lakes studied; Lake Cazaux and Sanguinet, and Lake Biscarrosse and Parentis, the latter having the more extensive stream network. However, as for lake Sanguinet, the majority are artificial drainage channels dating from the work of Chambrelant.

The effect of the coastal dune system is to act as a barrage, diverting southwards the outflow from the lakes, and raising the water levels to 20m above sea level. The two lakes are connected by a canal. Table 4.2.1 gives the relevant data concerning the two lakes.

	<u>Length Km.</u>	<u>Breadth km.</u>	<u>Lake Area ha.</u>	<u>Catchment Area Km.</u>
Lake Sanguinet	11.2	9.95	59.3	225
Lake Biscarrosse	9.2	7.9	36.3	302

Due to the size of the two lakes a complete echo sounding was not performed and the basin morphometry is derived from Delebeque (1898). Figs. 4.25 and 4.2.6 confirm that the lakes have a similar assymetrical morphometry of a steeply dipping western edge and a shallow slope on the eastern edge.

THE BASIN MORPHOLOGY OF LAKE BISCARROSSE ST PARENTIS

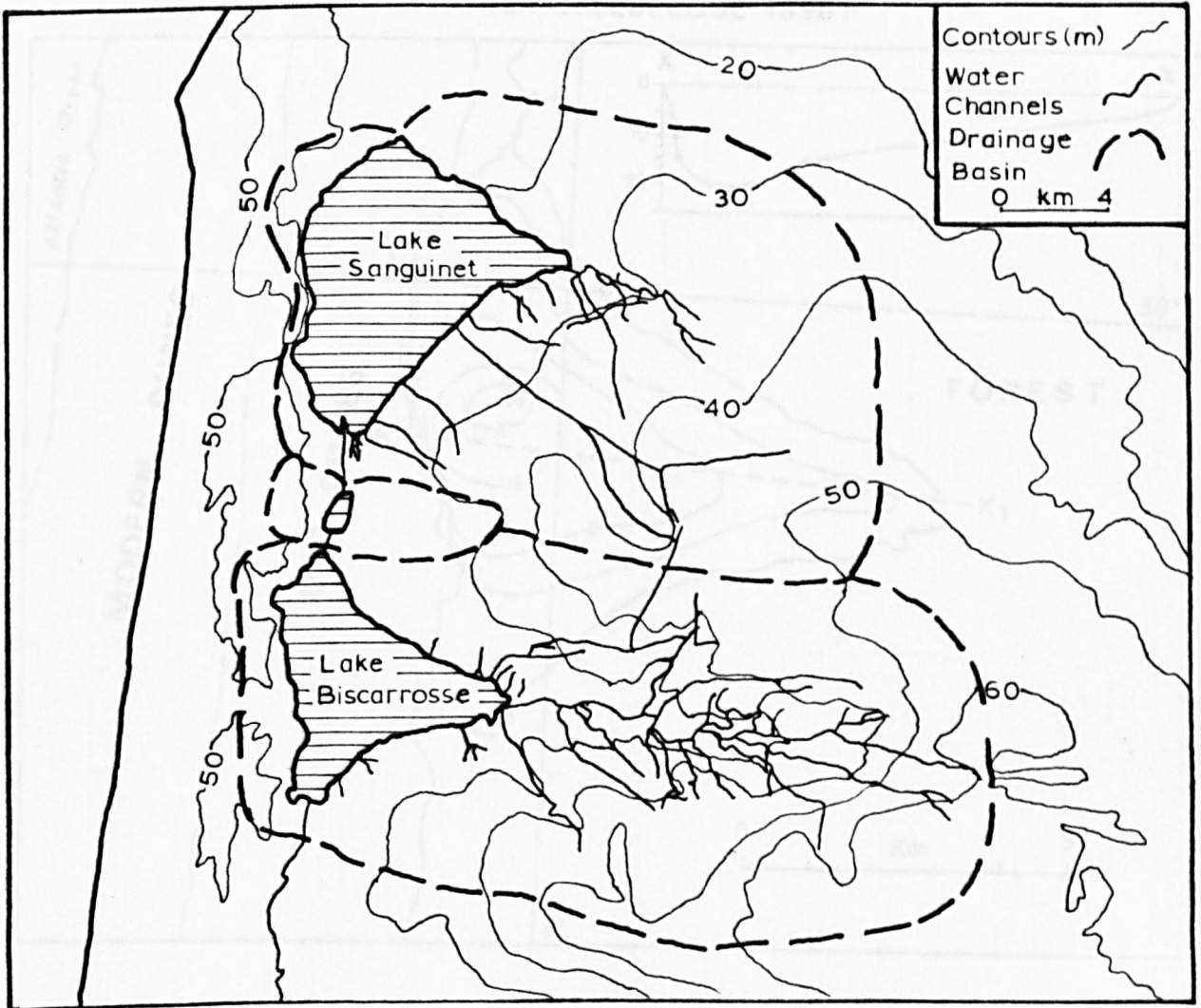


fig.4.2.4 Hydrology of Lake Biscarrosse and Lake Sanguinet

THE BASIN MORPHOLOGY OF LAKE BISCARROSSE ET PARENTIS
(AFTER DELEBECQUE 1898)

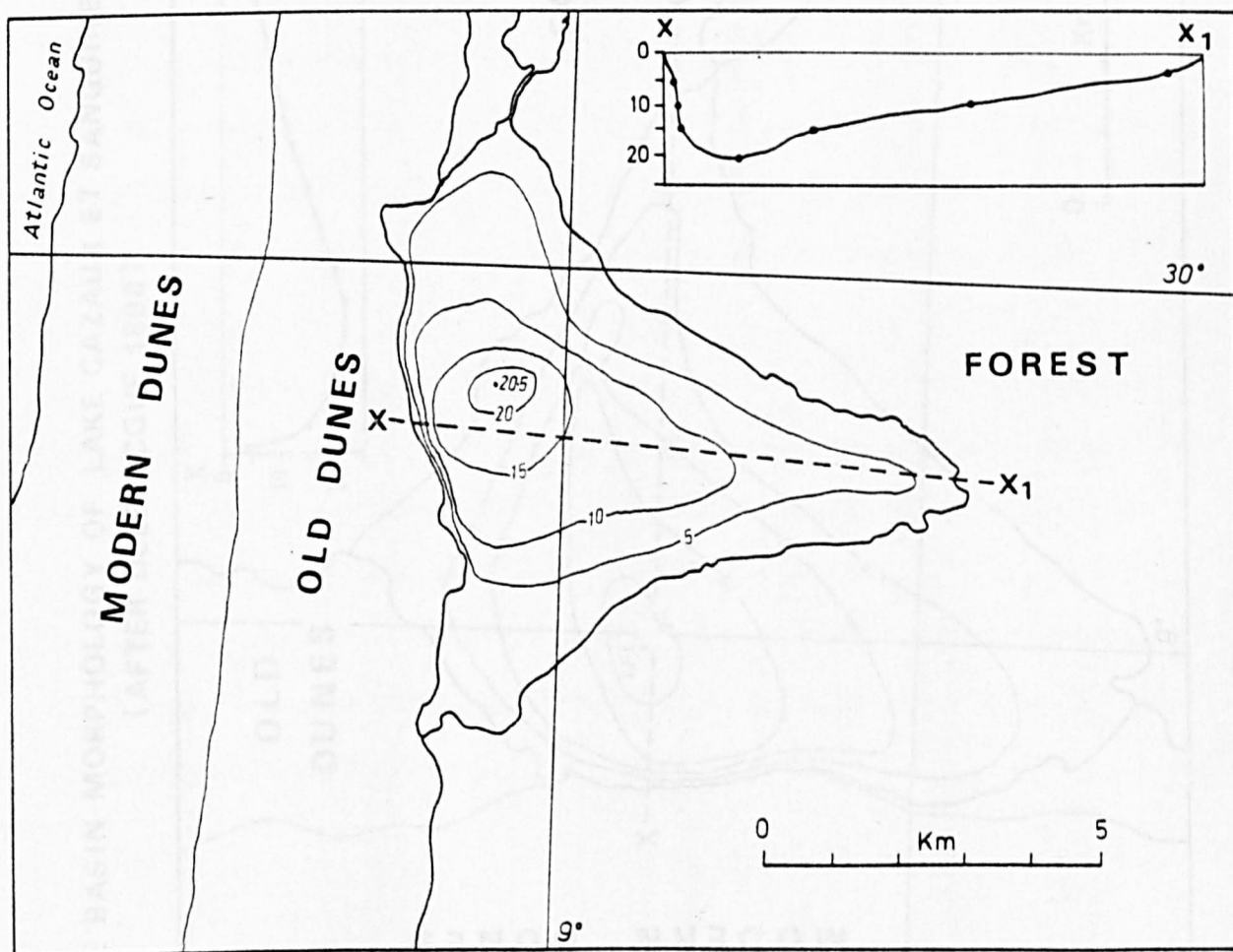


fig.
4.2.5

Morphometry of Lake Biscarrosse.

THE BASIN MORPHOLOGY OF LAKE CAZAUX ET SANGUINET
(AFTER DELEBECQUE 1898)

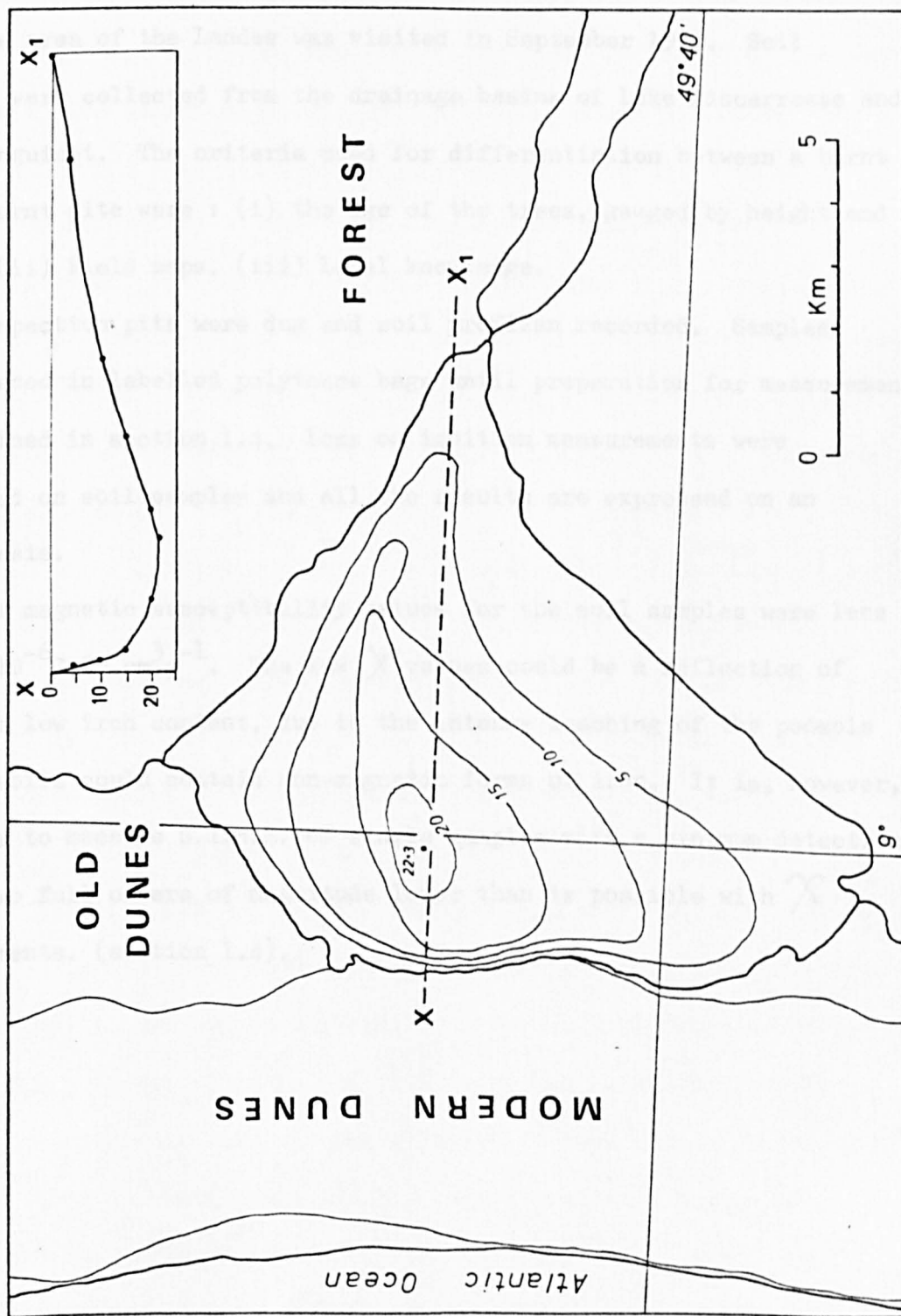


fig.4.2.6. Morphometry of Lake Sanguinet.

SOIL MAGNETISM 4.3Methodology

The area of the Landes was visited in September 1977. Soil samples were collected from the drainage basins of Lake Biscarrosse and lake Sanguinet. The criteria used for differentiation between a burnt and unburnt site were : (i) the age of the trees, gauged by height and girth. (ii) Field maps. (iii) Local knowledge.

Inspection pits were dug and soil profiles recorded. Samples were placed in labelled polythene bags until preparation for measurement as outlined in section 1.4. Loss on ignition measurements were performed on soil samples and all the results are expressed on an ashed basis.

The magnetic susceptibility values for the soil samples were less than $1 \times 10^{-6} \text{G.Oe.cm}^3 \cdot \text{g}^{-1}$. The low χ values could be a reflection of either a low iron content, due to the intense leaching of the podsols or the soils could contain non-magnetic forms of iron. It is, however, possible to measure S.I.R.M. of single samples with a minimum detection limit two full orders of magnitude lower than is possible with χ measurements. (section 1.4).

S.I.R.M. profiles for soils from the Lake Biscarrosse Catchment

Fig. 4.3.1 plots S.I.R.M. versus depth for the soil profiles sampled. A basic differentiation using the S.I.R.M. values can be made between the soils sampled from burnt and unburnt sites. The profiles from the burnt sites, with the exception of SB3 have S.I.R.M. values of greater than $150 \times 10^{-6} \text{G.Oe.cm}^3 \text{g}^{-1}$ in the top 10cm. corresponding to the zone of enhancement identified in the burnt Llyn Bychan soils (section 2.6). Soil profiles SB5 and SB6 have S.I.R.M. values exceeding $500 \times 10^{-6} \text{G.Oe.cm}^3 \text{g}^{-1}$ in this zone. Soil profile SB3 has a relatively low level of enhancement, $80 \times 10^{-6} \text{G.Oe.cm}^3 \text{g}^{-1}$, and may be due to the site conditions at the time of the fire being unfavourable for the maximum production of secondary ferrimagnetic oxides, or it may reflect a low iron content (see section 2.7).

The zone of maximum magnetic enhancement corresponds to the A horizon which contains the maximum near surface concentration of iron that is convertible to secondary ferrimagnetic forms. There are two possible sources of iron in the podsol: The iron may be found as a coating on the quartz grains or as iron released at the litter-mineral soil interface from the decay of organic matter.

Soil profiles SB1 and SB2 are from unburnt sites but SB2 must be regarded as more typical in respect of the S.I.R.M. profile. The site for soil profile SB1 was on a river bank, at Les Espanhangues Roudes Forges; the presence of large oak trees together with its proximity to the river indicated that it was unlikely to have been affected by the 1949 fire. However, the S.I.R.M. profile shows a degree of enhancement in the top 20cm. rising to a value of $97 \times 10^{-6} \text{G.Oe.cm}^3 \text{g}^{-1}$ at the surface. As the likelihood of the site having been burnt is minimal

SIRM/DEPTH FOR THE LAKE BISCARROSSE SOILS

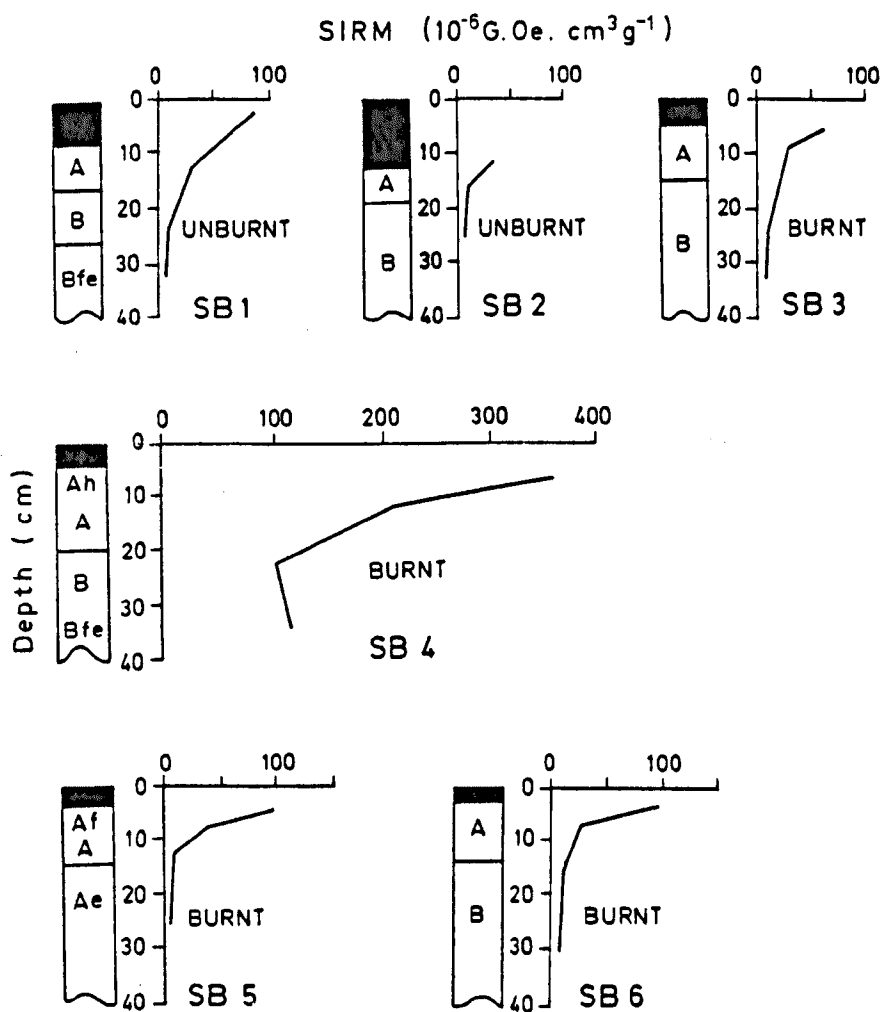


fig.

4.3.1 S.I.R.M. depth profiles for soil profiles from the Lake Biscarrosse catchment.

the increase in S.I.R.M. is probably due to one of two mechanisms or a combination of both: (i) As indicated by field notes the soil profile was not a true podsol rather a brown earth and this may have been subject to significantly different pedological processes than those which produce a true podsol. (ii) The proximity of the river together with the position of the sampling site on the floodbank may indicate that it has been subject to the deposition of magnetically enhanced material carried by floodwaters. (Walling *et al.*, *op cit*) which may have been deposited on the floodbank following the retreat of a flood.

Profile SB2 is regarded as typical of an unburnt soil, possessing a low level of magnetic enhancement ($37 \times 10^{-6} \text{G.Oe.cm}^3 \cdot \text{g}^{-1}$) in the top soil decreasing to $4.3 \times 10^{-6} \text{G.Oe.cm}^3 \cdot \text{g}^{-1}$ in the B horizon. Mullins (*op cit*) and Dearing (*op cit*) attribute such enhancement to natural pedogenic processes.

Soil profiles SB4, SB5 and SB6 display an average increase in S.I.R.M. of greater than one order of magnitude above the A horizon values of SB2. Soil profiles SB5 and SB6 show a pronounced decrease in S.I.R.M. with depth, attaining a similar low level (average of $4.2 \times 10^{-6} \text{G.Oe.cm}^3 \cdot \text{g}^{-1}$) below 20cm. From the profile description, SB4 had a Bfe horizon at 36cm., and the high S.I.R.M. value of $115.5 \times 10^{-6} \text{G.Oe.cm}^3 \cdot \text{g}^{-1}$ probably reflects the high content of oxidized iron associated with such a feature. All the other soil profiles from the drainage basin did not show any pronounced iron pan formation, or recognizable iron pan formation.

S.I.R.M. profiles for soils from the Lake Sanguinet catchment

Graphs of S.I.R.M versus depth for the soil profiles from the catchment are shown in Fig. 4.3.2. Generally the S.I.R.M. values for the Sanguinet soils are lower than those in the profiles collected from the Lake Biscarrosse drainage basin. However, the soils from the burnt sites display a similar trend of high S.I.R.M. values in the 'A' horizon over than those from unburnt sites. In the burnt profiles, the S.I.R.M. values decrease markedly below the 'A' horizon but are still

SPECIFIC SIRM DEPTH FOR SANGUINET SOILS

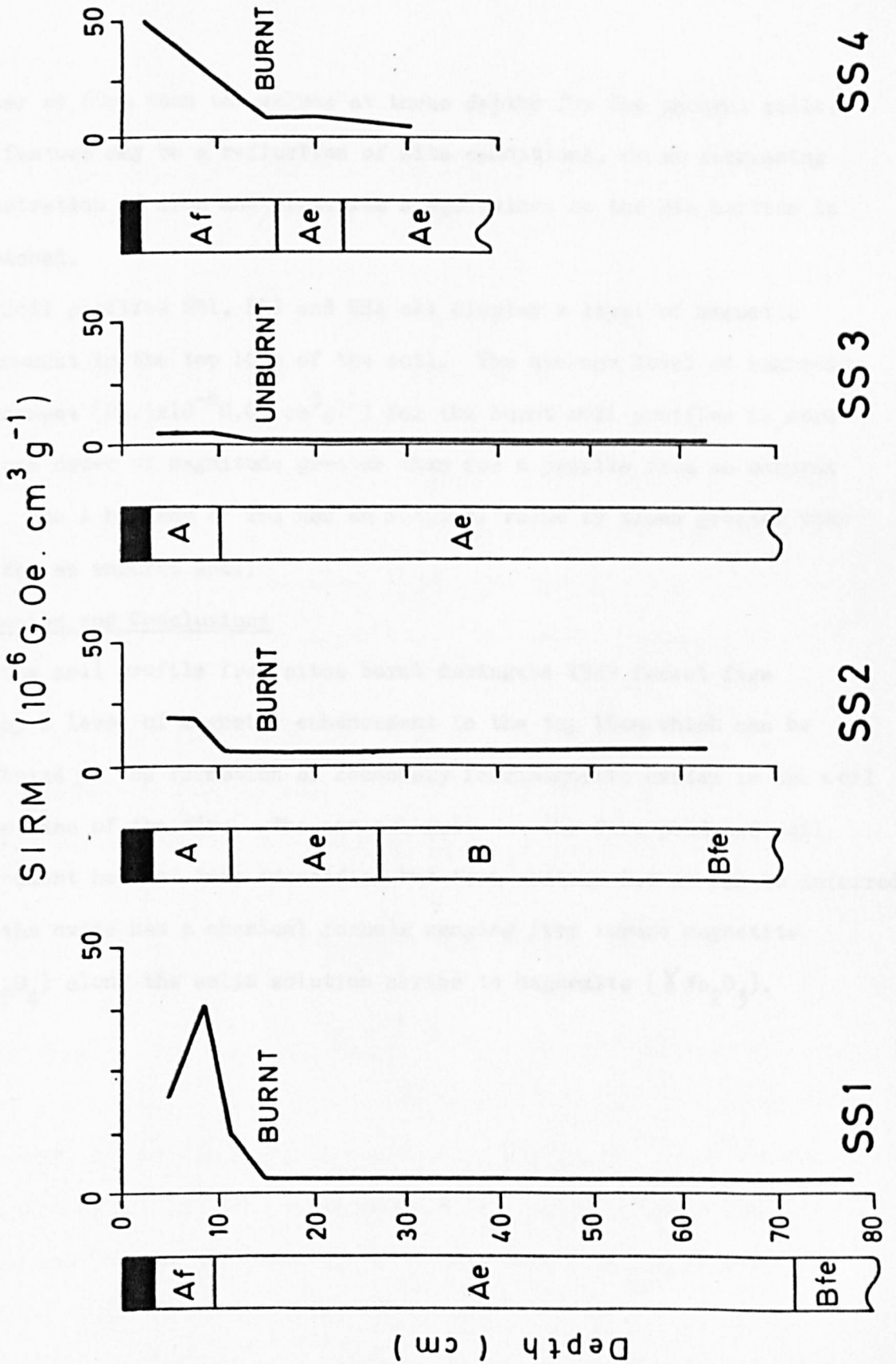


fig.4.3.2. S.I.R.M. depth profiles for soil profiles from the Lake Sanguinet catchment.

greater at 60cm than the values at these depths for the unburnt soils. This feature may be a reflection of site conditions, or an increasing concentration of iron and aluminium sesquioxides as the Bfe horizon is approached.

Soil profiles SS1, SS2 and SS4 all display a level of magnetic enhancement in the top 10cm of the soil. The average level of magnetic enhancement ($84.5 \times 10^{-6} \text{G.Oe.cm}^3 \text{g}^{-1}$) for the burnt soil profiles is more than one order of magnitude greater than for a profile from an unburnt site. The A horizon of SS4 has an S.I.R.M. value 19 times greater than that for an unburnt soil.

Discussion and Conclusions

The soil profile from sites burnt during the 1949 forest fire display a level of magnetic enhancement in the top 10cm which can be attributed to the formation of secondary ferrimagnetic oxides in the soil at the time of the fire. The mineral grown in the fire produced soil environment has not been identified but from section 2.8 it can be inferred that the oxide has a chemical formula ranging from impure magnetite ($\text{Fe}_{2.9}\text{O}_4$) along the solid solution series to maghemite ($\gamma\text{Fe}_2\text{O}_3$).

LAKE SEDIMENTS 4.4Methodology

A 1m. pneumatic Mackereth cover was used to retrieve 16 sediment cores from Lake Biscarrosse and 18 sediment cores from Lake Sanguinet during August 1977. Water depth was recorded at each coring site using an echo sounder. The positions of the coring sites were recorded using a triangulation method, whereby the boat's bearing to two easily identifiable stationary markers on the shore was taken at each site.

The majority of the cores were extruded into polythene bags in the field, the remainder being kept in the perspex core tubes for long core K measurements. The cores were later extruded for single sample χ and S.I.R.M. measurements, palaeobotanical analysis and radiometric dating.

The Lake Biscarrosse sediment cores were extruded in 1cm. slices to 10cm. and then in 2cm. slices to the end of the core. The Lake Sanguinet sediment cores were extruded in 0.5 cm. slices to 10cm. or until compact sand was encountered.

Samples were prepared for magnetic measurements as outlined in Section 1.4.

Sub samples for pollen and charcoal analysis were prepared according to the technique outlined by Faegri and Iverson (1964). 300 pollen grains was regarded as the minimum pollen count per level. Whole and broken saccate grains were counted separately. The broken curve was compiled by counting each bladder as half whether it was freely or singly attached to a whole or partial grain (Oldfield 1978c).

Charcoal pieces were measured and counted along with the pollen. The long 'A' and short 'B' axes were measured using a graticule, producing a total area of charcoal in mm^2 for each sample level.

The distinction between charcoal, organic and mineral matter was made using strict guidelines; although subjective they were rigorously adhered to.

Before being classified as charcoal the object under inspection had to be totally black and angular in appearance. These parameters were agreed before hand with Dr. K. Edwards (pers. comm.). Any spherical black object was disregarded as it could have been an atmospheric spherule derived from industrial sources (Oldfield et al., 1978b). Other authors, however, have included such particles in charcoal counts (see section 5.1).

Two cores, one from each lake, were selected for ^{210}Pb and ^{137}Cs dating. In order to minimize down carriage of sediment and smearing at the core edges, material for analysis was taken from the centre of the sample.

MAGNETIC RESULTS 4.5

Continuous core susceptibility results

Fig. 4.5.1 plots the continuous core K traces against depth for sediments from Lake Biscarrosse. Two peaks, A and B, can be identified in the 5 cores : Peak B is the dominant feature occurring between 10-20cm. in all the cores; peak A is found between 25 and 30 cm. The positions of the two peaks are at similar depths in all 5 cores measured indicate a fairly comparable sediment accumulation rate.

Fig. 4.5.2 locates the positions of the coring sites, all the cores were retrieved from the embayment at the eastern end of the lake. Attempts to collect cores from outside the embayment were unsuccessful.

Continuous core K is a rapid method of core correlation; however, due to its averaging tendency the technique is unable to resolve small variations between closely spaced sample levels. This feature, along with the problems associated with measuring K at the mud water interface, prevented a useful core correlation scheme from being constructed for the Lake Sanguinet cores. (The top 2-3cm. of the Lake Sanguinet sediment spans approximately 200 years). Fig. 4.5.3 locates the position of the coring sites for Lake Sanguinet. The wider areal spread of the sites also accounts for the difficulty in constructing a correlation on the basis of whole core K measurements, as it is impossible to correlate some of the deep water cores.

Single sample magnetic measurements

Magnetic susceptibility (χ) values for the sediment from the two lakes were too low to be meaningful, falling near the detection limits of the measuring apparatus. The S.I.R.M. values were adequate and have been used as an alternative to χ (section L3).

ETANG DE BISCARROSSE ET DE PARENTIS - Whole core magnetic susceptibility traces

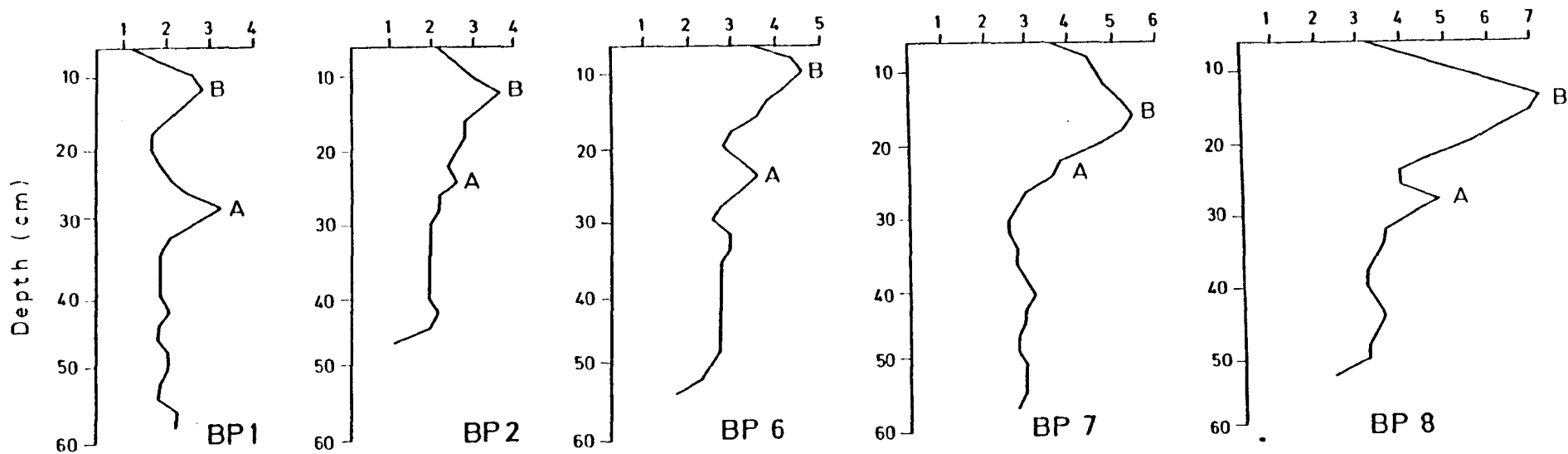


Fig 4.5.1 Continuous traces for Lake Biscarrosse cores BP1, 2, 6, 7, 8.

**LAKE BISCARROSSE
LOCATION OF LAKE SEDIMENT CORING SITES**

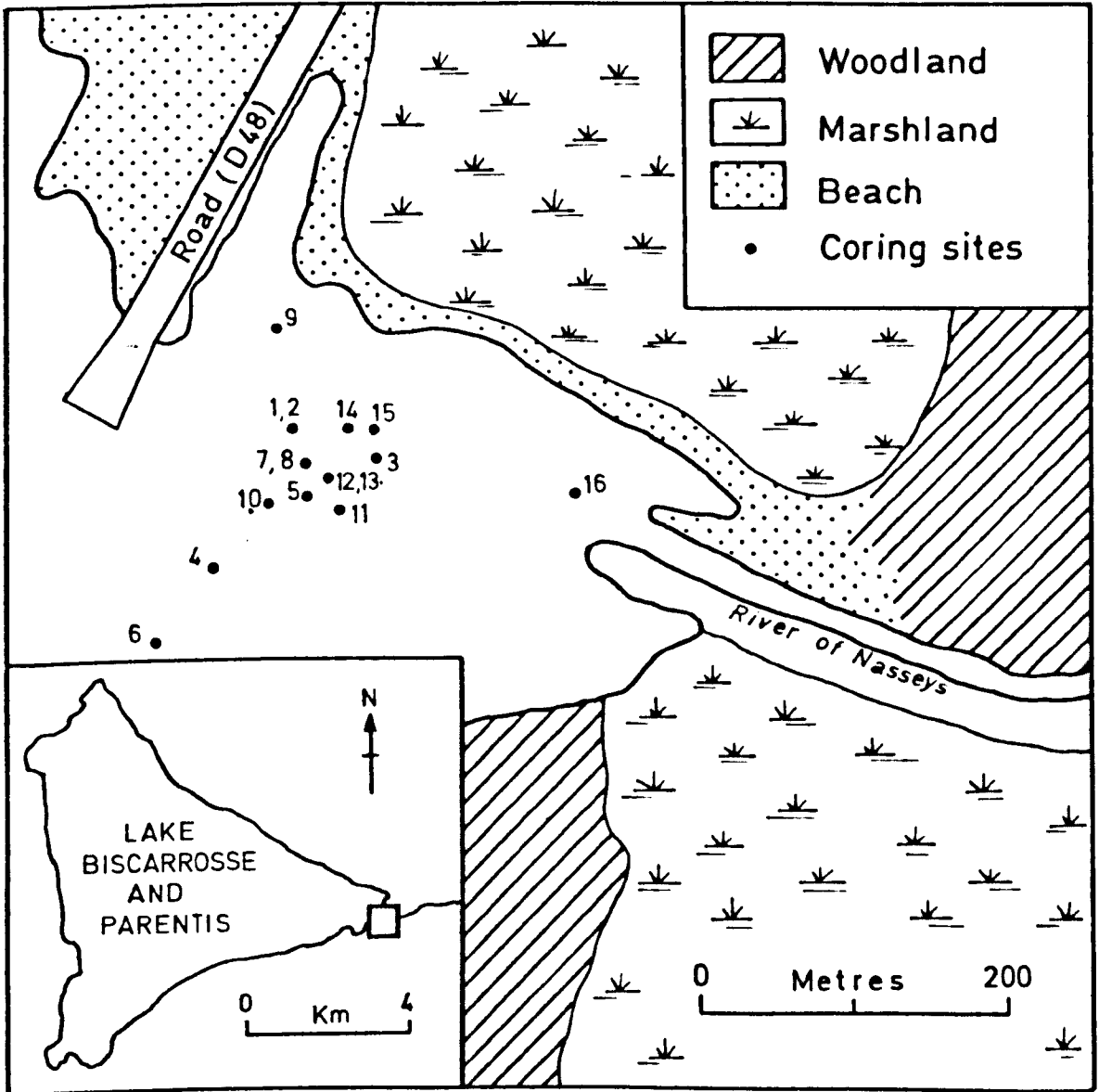


fig.4.5.2 Location of coring sites Lake Biscarrosse

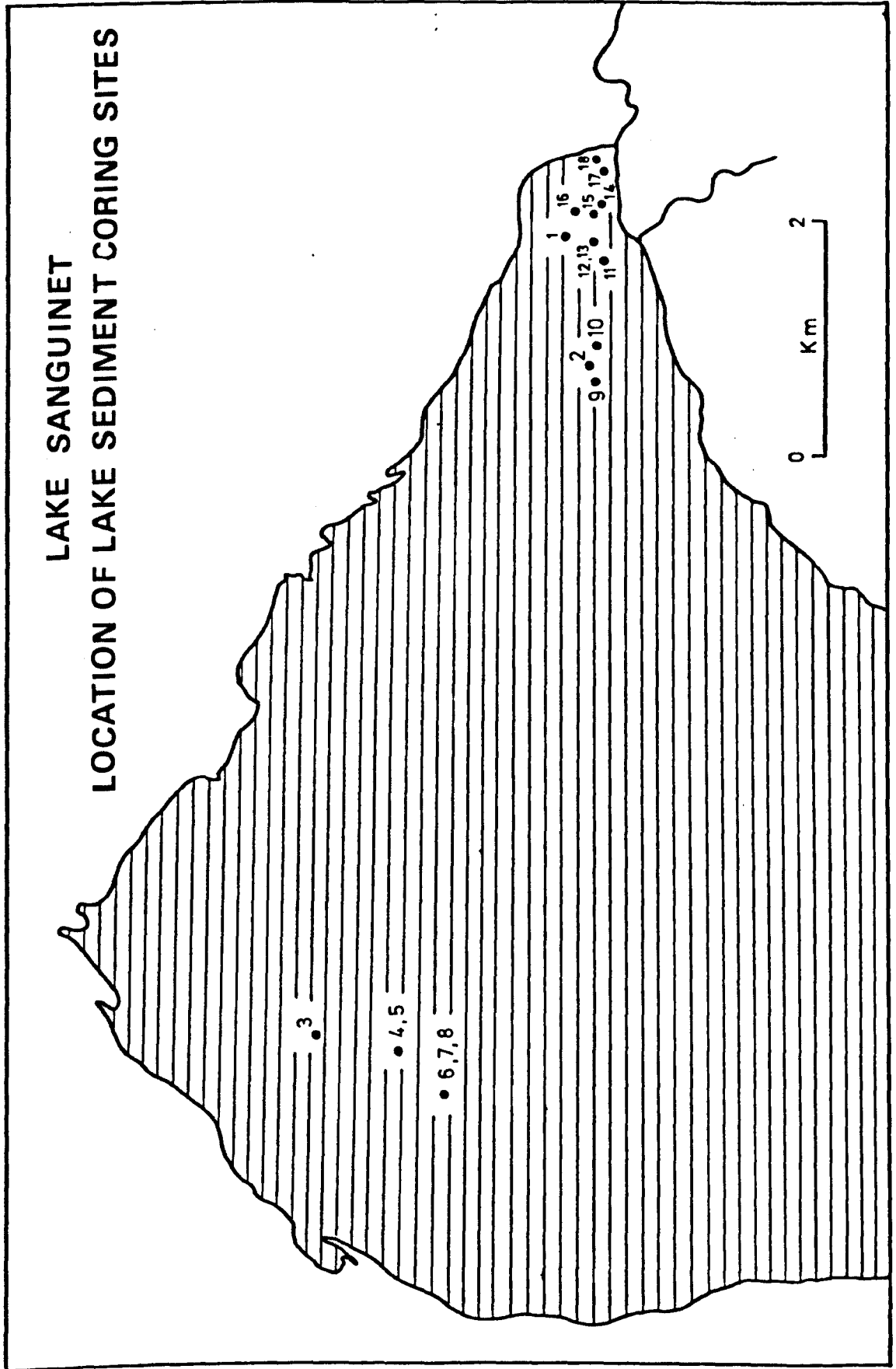


fig.4.5.3. Location of coring sites Lake Sanguinet.

Lake Biscarrosse sediments

Fig. 4.5.4 plots S.I.R.M. against depth for two lake sediment cores BP6 and BP9. Stratigraphically the cores can be distinguished by the position of the mud/sand interface: The transition is at 10cm. in core BP9 and 28cm. in core BP6 indicating that the sediment accumulation rate of BP6 is two to three times faster than that in core BP9. The position of core BP6, retrieved from a site opposite a potential sediment source (a drainage channel) (Fig. 4.5.2) accounts for the much faster accumulation rate.

The two cores can be correlated on the basis of the S.I.R.M. values; the prominent feature is peak B, at 12-14cm in BP6 and 5-6cm in BP9. The other peak S.I.R.M. values at A and C are present in both cores and provided a framework for correlation.

Core BP6 displays minimum S.I.R.M. values around a stratigraphic transition at 28cm. Peak A has S.I.R.M. values twice as high as for the transition zone but the values decrease to approximately $100 \times 10^{-6} \text{G.Oe.cm}^3 \cdot \text{g}^{-1}$ at 16cm. Peak B at 12-14cm. has an S.I.R.M. value of $1959 \times 10^{-6} \text{G.Oe.cm}^3 \cdot \text{g}^{-1}$, 20 times greater than the previous sample, and is the dominant feature of the core. Peak B is specific to a single sample, the adjacent sample being a whole order of magnitude lower. The remaining S.I.R.M. profile is characterized by a series of lesser peaks at 9-10 cm., 5-6 cm. and 2-3 cm., the values are \approx one quarter of those for the peak B value.

Core BP9 has a minimum S.I.R.M. value of $26 \times 10^{-6} \text{G.Oe.cm}^3 \cdot \text{g}^{-1}$ at the transition zone and a maximum value at peak B of $167 \times 10^{-6} \text{G.Oe.cm}^3 \cdot \text{g}^{-1}$. A smaller peak c occurs after a post peak B minimum value of $80 \times 10^{-6} \text{G.Oe.cm}^3 \cdot \text{g}^{-1}$.

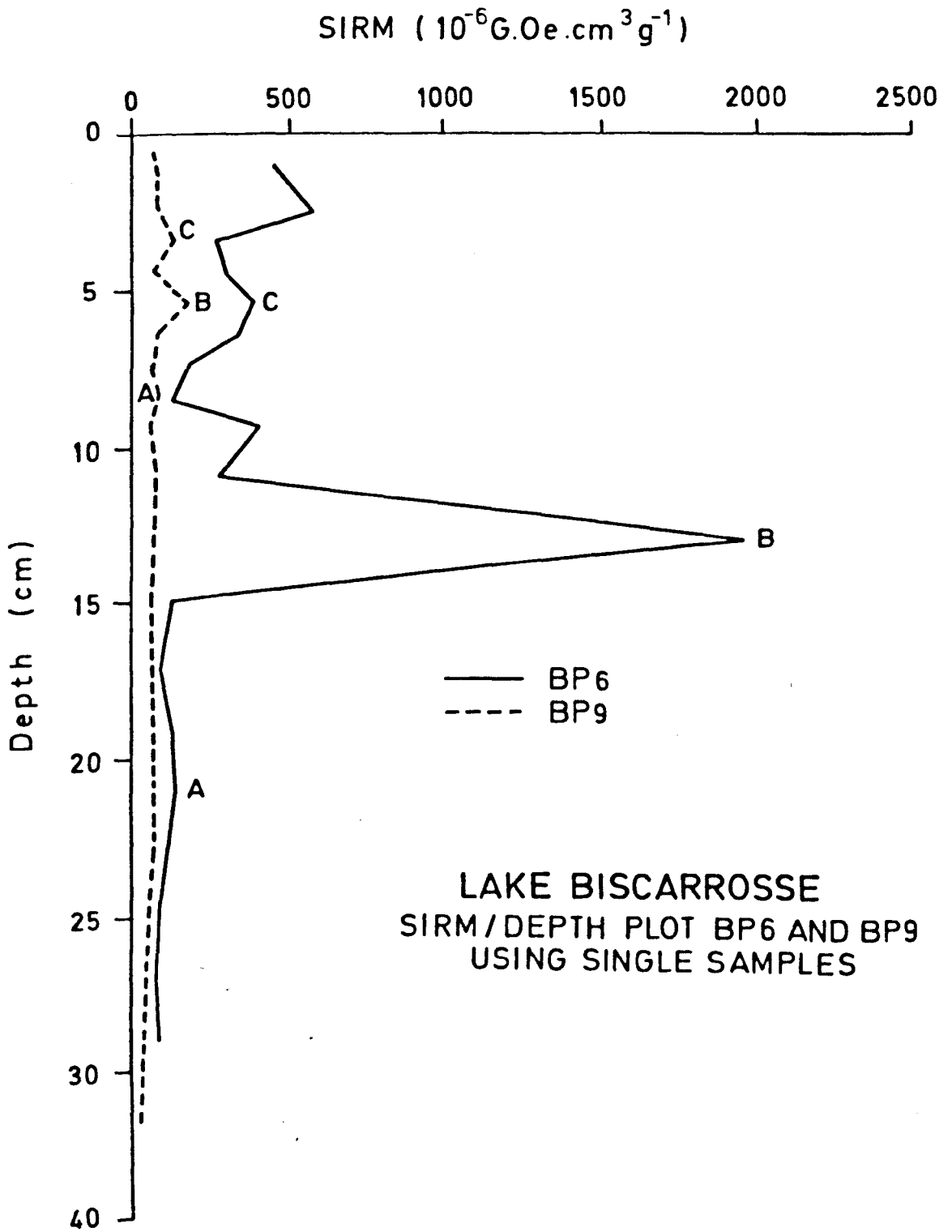


fig4.5.4 S.I.M. depth profile cores BP6 and BP9

Lake Sanguinet Sediments

Fig. 4.5.5 plots S.I.R.M. against depth for 3 sediment cores. Core S6 differs stratigraphically from the other cores; a sand-mud transition occurs between 2.0-2.5 cm. and magnetically the feature is reflected in the higher S.I.R.M. values for the samples below the transition. The sediment above the transition has a uniform S.I.R.M. profile until 0.0-0.5 cm. which has a S.I.R.M. value of $45 \times 10^{-6} \text{G.Oe.cm}^3 \text{g}^{-1}$. Core S6 was retrieved from a water depth of 20m. in the deepest part of the lake.

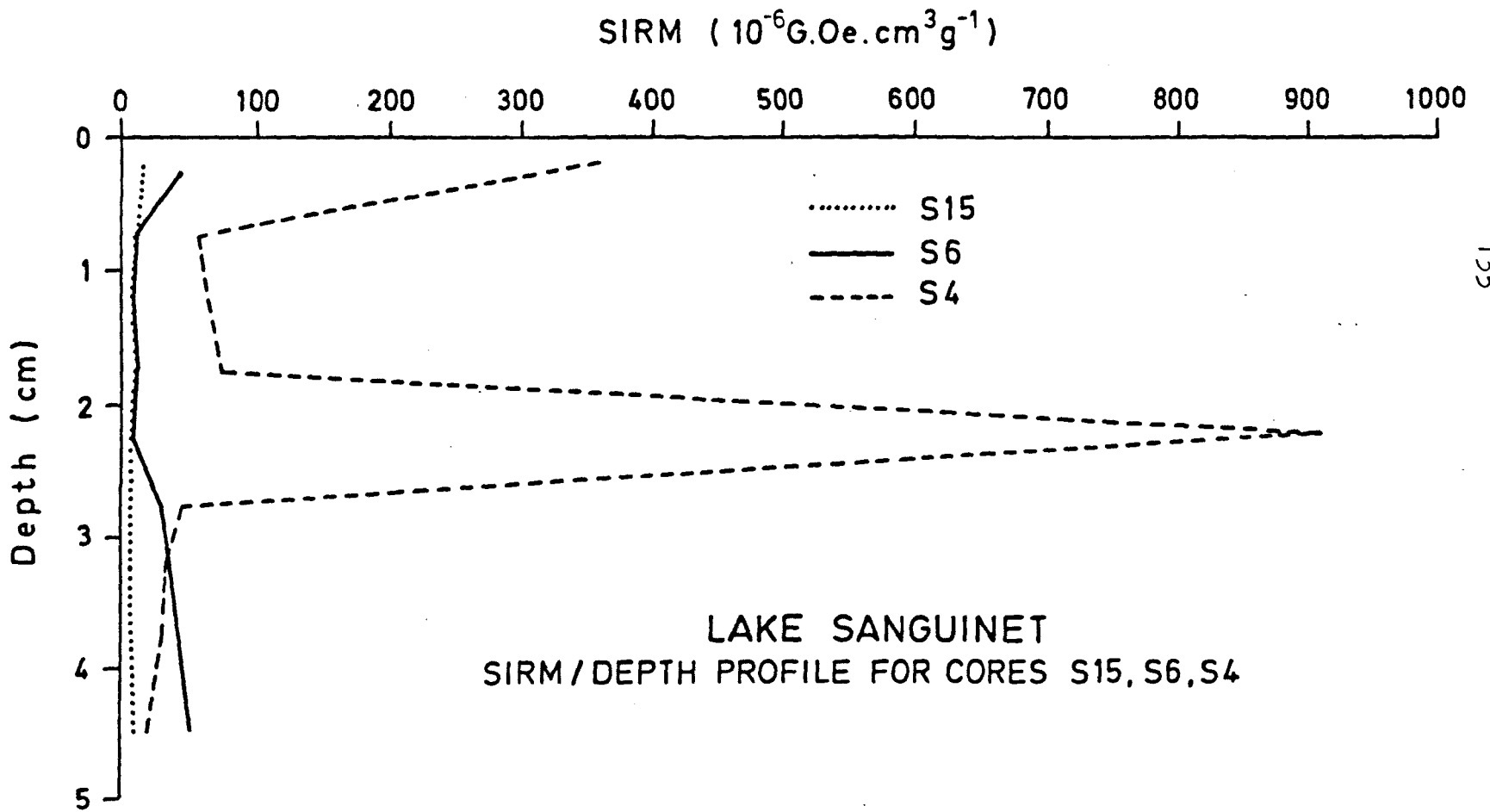
Core S15 is a shallow water core, from a depth of 5.5m. and was retrieved from a marginal position in the lake in relation to cores S6 and S4. The S.I.R.M. values below 3.0cm. are all below $10 \times 10^{-6} \text{G.Oe.cm}^3 \text{g}^{-1}$, but increase above this level to a maximum of $19 \times 10^{-6} \text{G.Oe.cm}^3 \text{g}^{-1}$ in the surface sample.

Core S4 is magnetically the most interesting of the cores that were subsampled for single sample S.I.R.M. measurements. The core is a deep water core from 19m. depth. The S.I.R.M. profile is dominated by the peak value of $905 \times 10^{-6} \text{G.Oe.cm}^3 \text{g}^{-1}$ at 2.0 to 2.5 cm. The S.I.R.M. peak is sample specific, the S.I.R.M. values of the samples immediately below and above this level are nearly two orders of magnitude lower than the peak value. The lowest S.I.R.M. values occur below 2.5 cm. whereas the values above 2.0 cm. are twice as high as the pre 2.5 cm. S.I.R.M. values. There is a substantial increase in S.I.R.M. to $353 \times 10^{-6} \text{G.Oe.cm}^3 \text{g}^{-1}$ in the top 0.0-0.5 cm.

Radiometric dating. ^{137}Cs and ^{210}Pb . 4.6

Penington *et al.*, (1973) and Ritchie *et al.*, (1973) have demonstrated the use of the atmospheric fallout of ^{137}Cs to date lake sediments a few decades in age. The dating procedure relies upon comparison of ^{137}Cs concentrations at different levels in the sediment with recorded variations in atmospheric ^{137}Cs levels since 1954.

fig.4,5.5. S.I.R.M. depth profile cores S4,S6 and S15.



^{137}Cs profiles may exhibit two significant peaks reflecting the onset of nuclear bomb testing in 1954 and the date of maximum ^{137}Cs fallout in 1963 (Digerfeldt et al., 1975).

The chronology of recent sediments can be further extended to about 200 years B.P. with the measurement of ^{210}Pb (half life 22.26 years). Results obtained by Oldfield et al., (1978b) indicate that consideration must be given to the degree of accelerated accumulation of sediment before an appropriate model can be assigned for calculating dates. The present calculations are based on the assumption of a constant rate of supply (C.R.S.) model as used by Appleby and Oldfield (1978) and opposed to the constant initial concentration (C.I.C.) model proposed by the majority of authors, e.g. Robbins and Edgington (1975); Pennington et al., (1976).

^{137}Cs and ^{210}Pb dating was performed on samples from cores BP6 from Lake Biscarrosse and S6 from Lake Sanguinet at the A.E.R.E., Harwell. It was considered that the onset of afforestation by Chambrelant and Bremon-tier in the 19th Century and the 1949 forest fire could be used to assess the accuracy of the two techniques, as well as to date the S.I.R.M. peaks in the two cores.

Results

Fig. 4.6.1 plots the ^{137}Cs concentrations together with S.I.R.M. versus depth for core PB6 from Lake Biscarrosse. Although it appears that there has been some downward diffusion of ^{137}Cs , the 1954 onset is clearly evident at 8-10cm., as in the 1963 maximum at 4-6 cm. The position of the peak S.I.R.M. value at 12-14 cm., only just below the 1954 level of ^{137}Cs increase is compatible with a date during the previous decade.

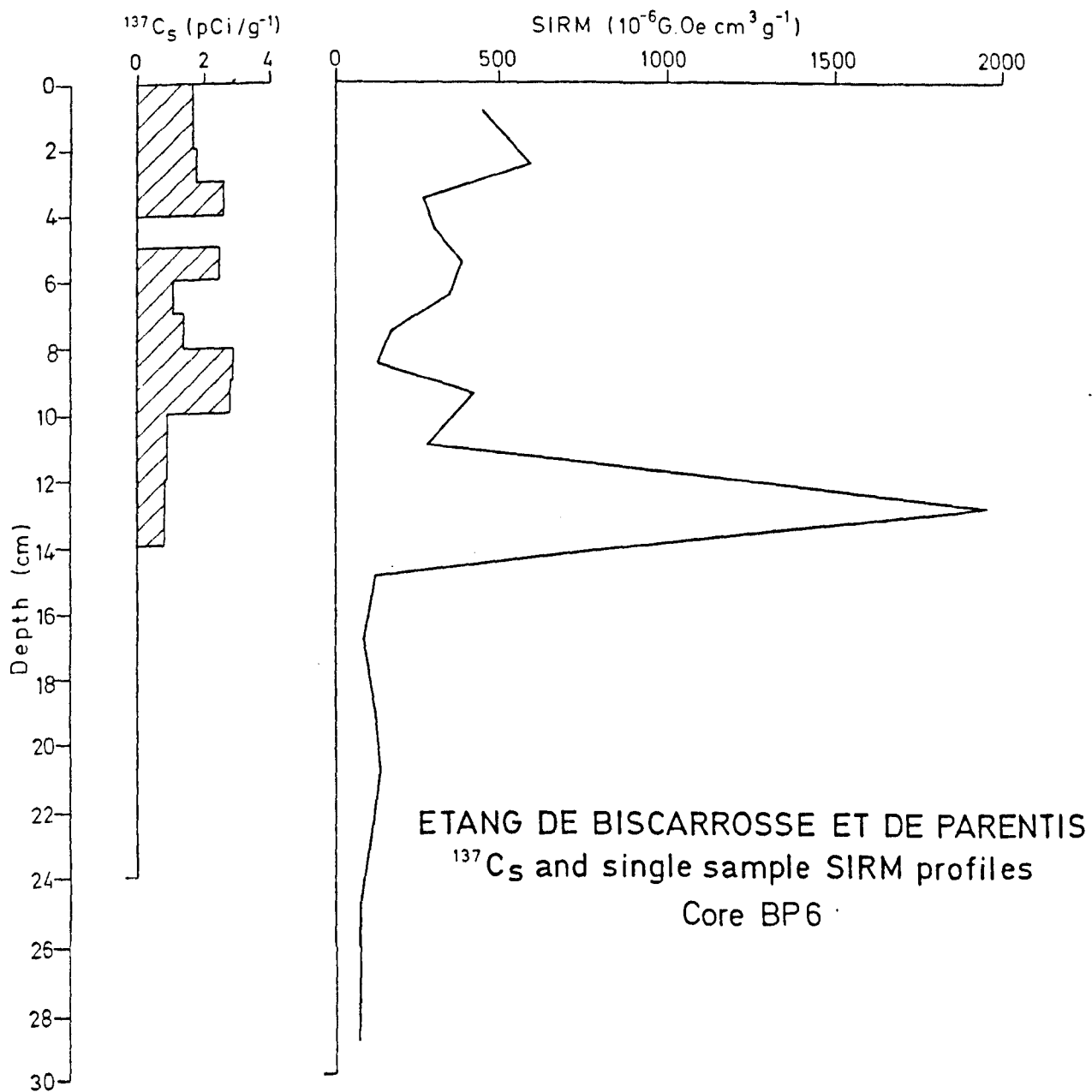


fig. 4.5.1

 ^{137}Cs Profile core BP6

In the Lake Sanguinet core the peak ^{137}Cs and S.I.R.M. values in the top 0.5 cm. of the sediment indicate a depositional history comparable to that of Lake Biscarrosse but preserved in sediments which have accumulated too slowly to permit detailed identification of the sequence of events during the last few decades.

Fig. 4.6.2 plots a ^{210}Pb age depth curve, accumulation rate and ^{137}Cs profiles for core S6. The ^{210}Pb age-depth curve dates quite accurately the beginnings of the dune fixation and afforestation period initiated by Bremonnier between 1787 and 1793 (section 4.2). Stratigraphically the event is marked by the mud/sand interface at 2.0-2.5 cm., corresponding to a minimum S.I.R.M. value. The slow depositional history of the sediments does not allow any firm inferences to be made about the 1949 fire event from the age-depth curve or the accumulation rate.

The ^{210}Pb based age-depth and dry mass sedimentation rate plots are not yet available for BP6 but preliminary estimates confirm a chronology of sedimentation comparable with the ^{137}Cs results and indicates a rapid acceleration in accumulation immediately after the fires of 1940's.

SANGUINET S6

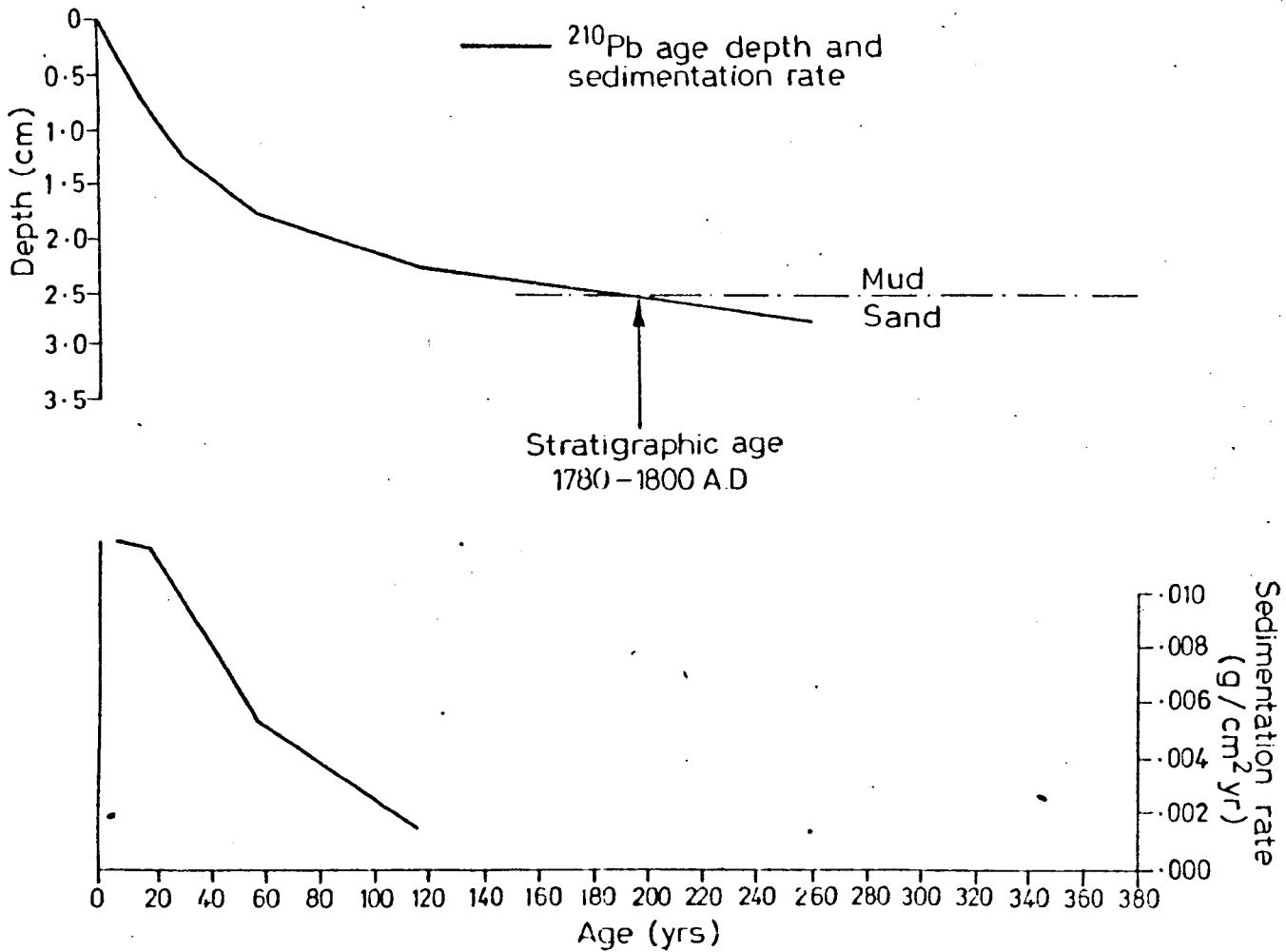


fig.4.6.2. ^{210}Pb , ^{137}Cs and sedimentation rate Core S6
(^{210}Pb dates are more accurate than the ^{137}Cs dates.)

POLLEN ANALYSIS 4.8

Pollen analysis was not approached with the aim of reconstructing a full vegetational history of the Landes but rather with the aim of identifying a level in the lake sediments that is attributable to the 1949 forest fire and of identifying the 18th century transition from a marshy wasteland to a pine monoculture.

Ahlgren and Ahlgren (op cit) in their comprehensive review article examining the ecological effects of fires pointed out the differing responses of vegetation types to fire. The conclusions from their evidence together with the evidence of other workers e.g. Heinselman (op cit); Frissel (1973); Cwyner (op cit); Swain (op cit) and Tolonon (1978) have been used in order to examine the pollen records of cores BP6 and S4 for evidence of the 1949 forest fire.

Typical responses of vegetation to a forest fire are a decrease in tree cover, with usually a rapid recovery of the pine species. The removal of the tree cover increases the amount of light penetration to the ground causing a general increase in the herbaceous flora. (Blaisdell, 1953). There are some herb species which, due to their preference for burned ground, are called 'fire followers'. Chamaenerion angustifolium is perhaps the most well known; however it is a poor pollen producer. Some members of the genus Rubus have also been recorded as fire followers (Heselman, 1916; Uggla, 1958). Pteridium aquilinum is another common colonizer after a fire. (McMinn, 1951).

The effects of a fire on a pine monoculture will be reflected in the percentage values for whole and broken pine grains, a minimum of whole pine grains associated with a peak in the relative proportion of broken pine grains will reflect an ecological disturbance such as a forest fire (Oldfield, 1978c).

A problem that may be encountered is that the reduced pollen production resulting from the destruction of vegetation by the fire may be more than offset, with respect to pollen influx to lake sediment, by increased erosion of polleniferous soil. (Pennington, 1979).

Lake Biscarrosse Pollen

Fig. 4.8.1 displays the total pollen diagrams for core BP6. The curve for whole pine grains reaches a minimum value of 12-14 cm. with the broken pine grains reaching a maximum at 10-12 cm. If the values are taken as a percentage of the total pine pollen sum then the maximum breakage percentage of 81% is at 12-14 cm. The tree species *Quercus*, *Betula* and *Corylus* decrease above the 12-14 cm. level, but the total sum of herbs has values of around 50% from 16 cm. to 8-9 cm. compared with a present day value of 35%, (at the top of the core). Many single taxa show a similar pattern; although the percentage values are low they may be regarded as useful. The taxa *Rumex maritimus*, Labiatae, Umbelliferae, Cruciferae, Ranunculaceae, Rosaceae and Compositae Liguliflorae and Tubiflorae all reach a maximum either at or above the 12-14 cm. level. Gramineae reaches a maximum at 12-14 cm. In all cases these taxa are more abundant at 12-14 cm. than below it.

In the Landes, the ericaceous species, *Erica scorparia*, *E. arborea*, *E. ciliaris* and *Calluna vulgaris* are all common. Together with being open ground colonizers they are reasonably fire tolerant. The abundance

of the Ericaceae increases dramatically from 14.3% at 12 - 14 cm. to 24% at 10 - 12 cm. indicating a quick recovery and re-colonization of burnt ground.

As a whole, the pollen diagram reflects the land-use change that has occurred in the region. The transition from a wasteland habitat to a pine monoculture is evident from 25 cm. upwards with decreasing representation of deciduous trees and herbs but with an increasing pine representation.

Lake Sanguinet pollen

Fig. 4.8.2 shows the total pollen diagram for core S4. The whole pine pollen curve reaches a minimum at 2.0 - 2.5 cm, corresponding to a maximum in the broken pine pollen curve. The other tree taxa, *Betula*, *Juglans* and to a lesser extent *Quercus* show a decrease at and above 2.0 - 2.5 cm. The herbaceous species increase above 2.0 - 2.5 cm. although this is not clearly reflected in the curve for the total sum of herbs. Individual taxa (*Lotus*, Labiatae, Campanulaceae, *Potentilla*, *Rumex*, *Artemisia* *Plantago major* and *P. media*) all increase after 2.0 - 2.5 cm. with the genus *Scrophularia* only being recorded at this level.

The 'fire follower' *Pteridium aquilinum* is absent at 2.5 - 3.0 cm. after being present in decreasing values from 4.5 - 5.0 cm., but reappears at 2.0 - 2.5 cm. The representation of cereal pollen can indirectly be used as a 'fire indicator'; no cereal pollen is recorded until above 1.5 - 2.0 cm. which corresponds to the post 1950 practise of using agricultural land for fire breaks (section 4.2).

The transformation of the area from a wasteland to a deforested area is reflected in the pollen diagram from 4.0 cm. upwards, with a decrease in the deciduous tree pollen and the Ericaceae pollen and an increase in pine pollen.

LAKE SANGUINET (Core S4)

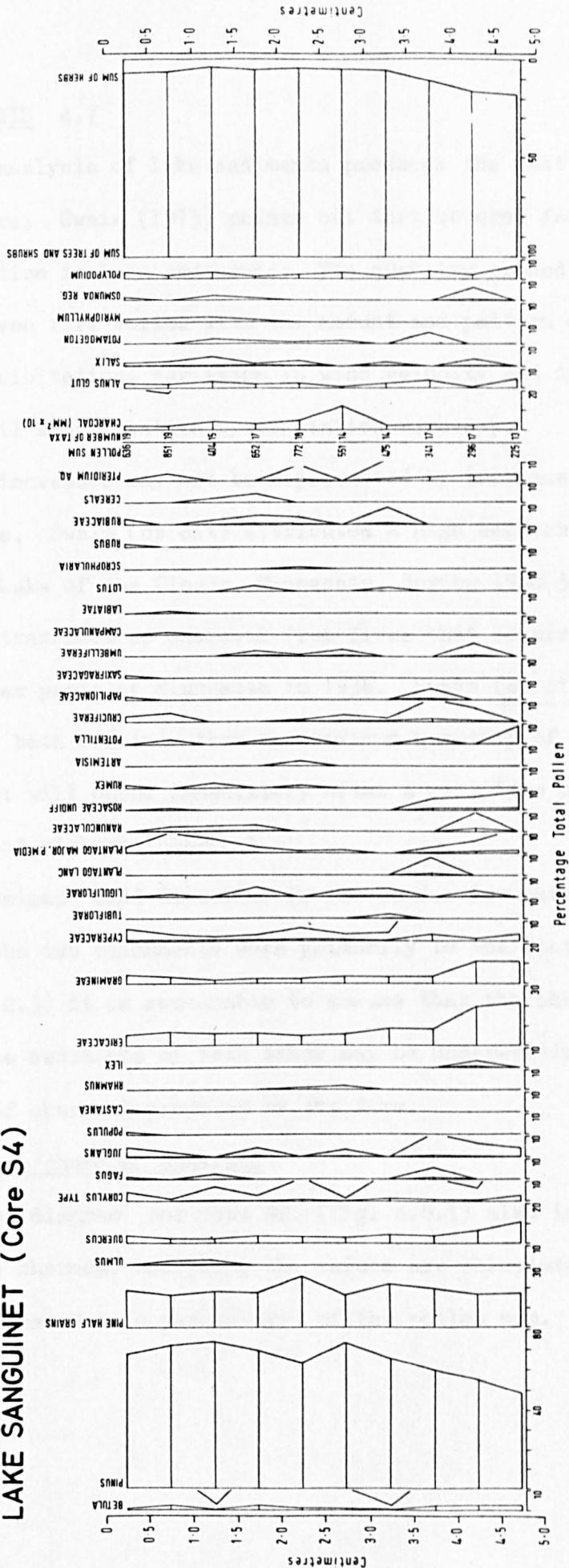


fig.4.8.2. Pollen and charcoal diagram core S4.

CHARCOAL ANALYSIS 4.7

Charcoal analysis of lake sediments produces the most direct evidence of fire, Swain (1973) points out that several factors affect its representation in lake sediments: The quantity eroded into a lake from a given fire varies with the amount and pattern of subsequent precipitation, variation in wind velocity and direction and the rate of soil stabilization by vegetation recovery.

Charcoal increases may not be represented by increases in other fire indicators. Swain (op cit) attributed a high sediment charcoal influx in the Lake of the Clouds, Minnesota, during 1930-39 AD. to long distance transport of charcoal from fires that occurred in Canada and other parts of Minnesota in 1936. Swain (op cit) and Cwyner (1978) both conclude that the maximum quantity of charcoal in the sediment will occur immediately after a real fire because of the abundance of airborne charcoal.

As the dominant wind direction in the Landes is westerly and the fires in the two catchments were primarily to the east of the Lakes (fig. 4.2.3) it is reasonable to assume that the charcoal peaks recorded in the sediments of both lakes may be under-estimates of the total volume of charcoal produced by the fire.

Lake Biscarrosse charcoal analysis

The pollen diagram for core BP6 (fig. 4.8.1) also includes the results of the charcoal analysis; the values are calculated in $\text{mm}^2 \times 10$ and expressed as a percentage of the pollen sum.

Apart from a high value of 10.4% (21.1mm²) at the surface there are two main peaks in the charcoal count. One of 9.8% (2.2mm²) at 22-24 cm. and the other of 10.3% (1.9mm²) at 12-14 cm. compared to an average background value of 3.3%. Charcoal values decrease steadily from 22-24 cm. but decline steeply from 12-14 cm. to a minimum value of 1.23% (0.4mm²) at 8-9 cm. indicating that the charcoal maximum at 12-14 cm. is sample specific.

Lake Sanguiret charcoal analysis

The pollen diagram for core S4 (fig. 4.8.2) includes the results of the charcoal analysis expressed in the same manner as for the Lake Biscarrosse count. The charcoal analysis for the core shows one peak of 12% (7.5mm²) at 2.5-3.0 cm. compared to an average background value of 3.1%. Higher general values are recorded at this level than before it and unlike BP6 there is no charcoal increase at the top of the core.

DISCUSSION 4.9

S.I.R.M., pollen and charcoal as evidence of fire.

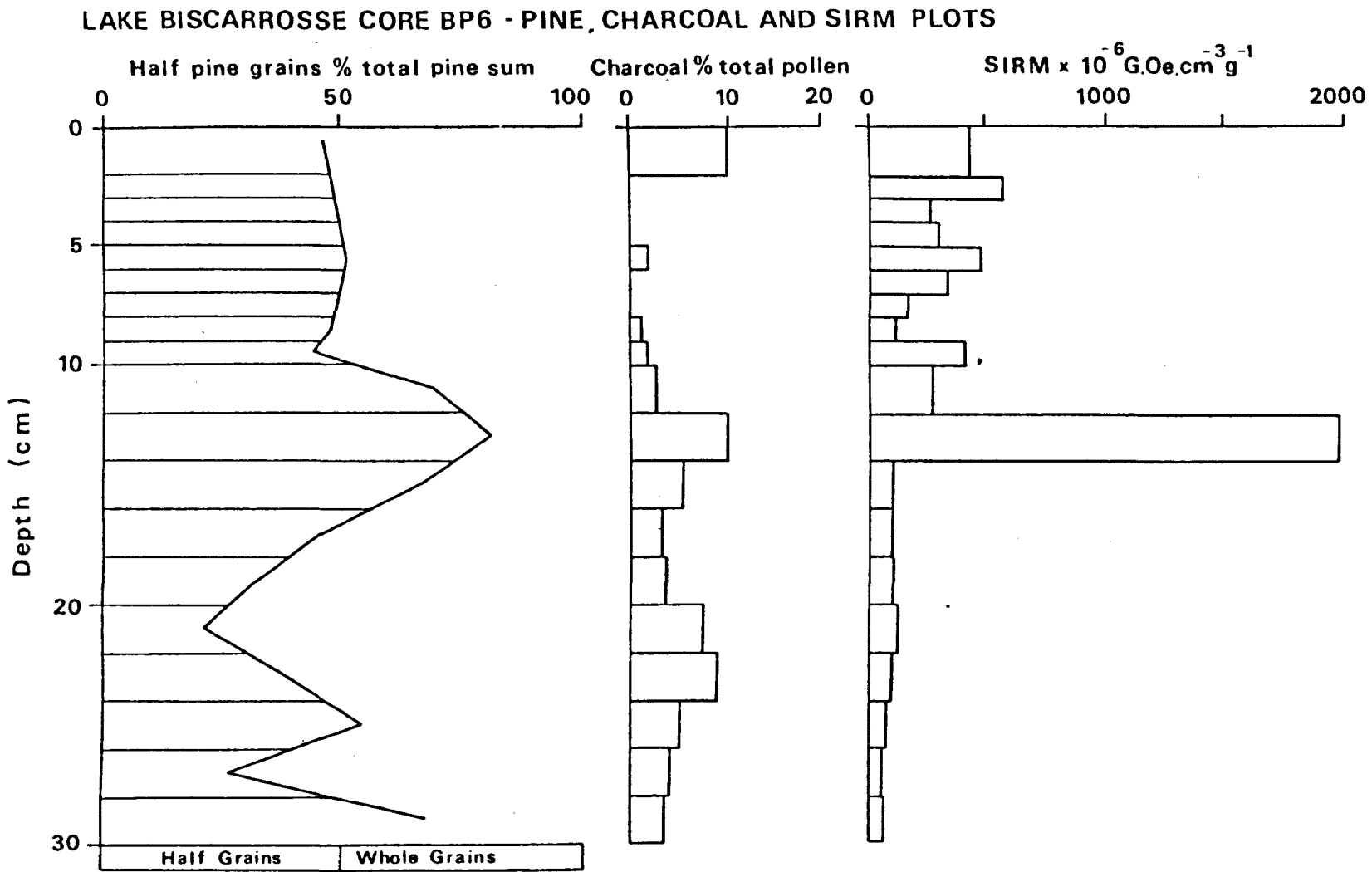
Lake Biscarrosse

Fig. 4.9.1 plots the main fire indicators of whole pine to broken pine ratio, charcoal and S.I.R.M. for core BP6. The synchronicity of the maximum charcoal peak, maximum pine pollen breakage ratio and S.I.R.M. at level 12-14 cm. can be interpreted as evidence of a forest fire. Other pollen indicators support this conclusion: the increase in the Ericaceae and herbaceous pollen content, together with a decrease in the tree species, indicates a removal of the tree cover. The consequent increase in the Ericaceae and herbaceous species is likely to be due to increased light levels and the availability of burnt ground for colonization. The charcoal peak at 12-14 cm., therefore, is direct evidence of a real forest fire especially as it correlates with the pollen fire indicators.

The peaks in charcoal at the surface and at 22-24 cm. do not correlate with the pollen fire indicators or with S.I.R.M; however an explanation can be offered: The increase in charcoal at the surface may reflect the present day use of the lake as a recreational resort with numerous campsites around the lake shores. The author expects that the recent increase in popularity of beach bonfire parties are a major source of the present day charcoal increases.

During the period of transition to a forested area it was normal to clear the vegetation by controlled burning, and this method remained in use up to at least the 1930's (Woolsey, op cit). The production of charcoal from this practise probably accounts for the 22-24 cm. charcoal peak together with the steady decline in charcoal levels after 22-24 cm. as the region became increasingly afforested. This contrasts with the sharp decline after the 12-14 cm. charcoal peak.

Fig. 4.9.1. Fire indicators and S.I.R.M. core BP6.



From the charcoal and pollen data we can distinguish a fire horizon at 12-14 cm. in the lake sediment; the synchronicity of the S.I.R.M. peak with the other fire indicators enables the peak S.I.R.M. value at 12-14 cm. to be considered a fire indicator.

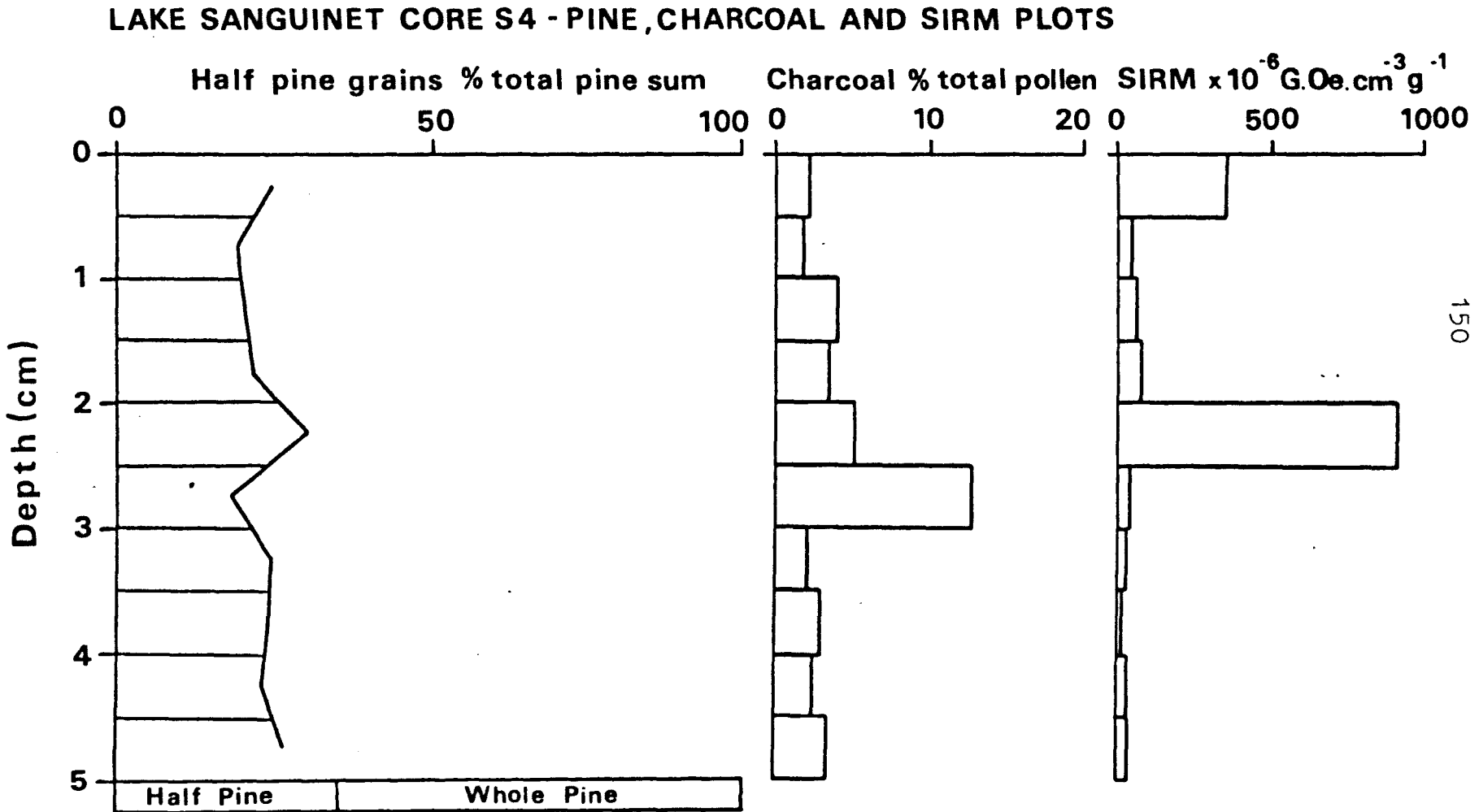
Lake Sanguinet

Fig. 4.9.2 plots the whole pine to broken pine ratio, charcoal and S.I.R.M. for core S4. The maximum pine breakage ratio is synchronous with the maximum S.I.R.M. value at 2.0-2.5 cm. but the maximum charcoal value occurs in the sample immediately prior to this level. The displacement of the charcoal peak probably reflects the immediate input of charcoal to the lakes from fires burning in the catchment before the pollen fire indicators and secondary ferrimagnetic minerals entered the lake.

The maximum charcoal value can therefore be considered associated with the maximum pine breakage ratio and S.I.R.M. peak at 2.0-2.5 cm., therefore indicating that all the three parameters are a function of the same ecological event.

Evidence for the occurrence of a forest fire comes directly from the charcoal analysis; core S4 has only one charcoal peak. The pollen analysis shows that the fire indicators of maximum pine pollen breakage ratio, decrease in tree pollen representation and increase in the herbaceous content of the flora indicate that the ecological event at 2.0 - 2.5 cm. was a forest fire. The synchronicity of the fire indicators and the correlation of the other pollen evidence with the S.I.R.M. peak at 2.0 - 2.5 cm. enable the S.I.R.M. peak to be considered as a fire indicator.

fig.4.9.2. Fire indicators and S.I.R.M. core S4.



Chronology

Having established from the charcoal and pollen evidence the likelihood that the S.I.R.M. peaks in both cores are attributable to a forest fire it is now possible to fit a chronology to the fire levels at 12-14 cm. in BP6 and 2.0-2.5 cm. in S4.

From documentary evidence the area suffered a series of small fires during the 1940's culminating in the devastating fire of 1949. The ^{137}Cs dating of core BP6 fixes the 1954 ^{137}Cs onset at 9-10 cm. just post-dating the S.I.R.M. peaks at 12.-14 cm., therefore making it compatible with a date during the previous decade of forest fires. The 1949 forest fire was the most extensive and damaging of the fires and it is correspondingly the event most likely to have produced the recorded responses in the charcoal, pollen and S.I.R.M. records. The peak S.I.R.M. value at 12-14 cm. can therefore be considered as dating largely from the 1949 fire event.

The pollen, charcoal and S.I.R.M. parameters at 2.0-2.5 cm. for core S4 are identical to the BP6 fire level making it possible to infer from the ^{137}Cs and ^{210}Pb dating that despite the slow and spatially variable sedimentation rate of Lake Sanguinet the S.I.R.M. peak in core S4 is attributable to the 1949 forest fire.

Persistence of the secondary ferrimagnetic oxides in the lake sediments

As shown in the Llyn Bychan case study (chapter 2) the peak S.I.R.M. values in the two cores are due to the input of magnetically enhanced secondary ferrimagnetic oxides by streams from the burnt soils in the catchment. The dating of the S.I.R.M. peaks at 1949 by radiometric analysis and indirectly by pollen and charcoal analysis indicates that the secondary ferrimagnetic oxides were formed in the soils at the time of the fire and were then transported into the lakes where they became incorporated into the lake sediments and persisted in the lake environment over a time span of at least 30 years.

CONCLUSIONS 4.10

From the case study of the Landes in South West France several conclusions can be drawn.

A. Soils

(i) Secondary ferrimagnetic oxides were produced in the soils at the time of the 1949 forest fire.

(ii) It is possible using S.I.R.M. measurements to distinguish between soils from burnt and unburnt sites in the catchments of the two lakes. However, some care must be used as the distinction is not always clear due to either a removal from the soil of the secondary ferrimagnetic minerals by erosion or natural enhancement in the topsoil from pedogenic processes.

(iii) The possibility of using S.I.R.M. as a means of identifying soils from burnt sites points to the persistence of the magnetically enhanced oxides in the soil environment over a timespan of at least 30 years. This is despite dilution by erosion or transformation of the oxides to another form by chemical or biogenic processes.

B. Lake Sediments

(i) Using the accepted techniques of pollen and charcoal analysis the S.I.R.M. peaks in the cores from Lake Biscarrosse and Lake Sanguinet have been identified as being the product of the 1949 forest fire: The high S.I.R.M. values are due to the erosion of secondary ferrimagnetic oxides, formed in the soils of the catchments, into the lakes where they have been incorporated into the lake sediments forming a magnetically distinct layer. The peaks in S.I.R.M. above 12-14 cm. in Lake Biscarrosse (BP6) are probably due to the continual input of the oxides into the lakes as the burnt areas are reforested releasing them from the soil as it is ploughed for replanting.

(ii) Using radiometric dating techniques and documentary evidence of the fire history of the area the S.I.R.M. peaks are ascribed to the 1949 forest fire. Thus the S.I.R.M. peak provides a dated horizon in the lake sediment column which can be used as a reference point for further analysis, and as a marker horizon to test the efficiency and accuracy of other dating techniques. It also provides a distinct horizon in the sediment facilitating rapid core correlation within the lakes.

(ii) Because the establishment of the S.I.R.M. peaks in the two lakes is attributable to the 1949 forest fire, it may now be possible to use the peaks in S.I.R.M. as an index of fires in a drainage basin with a known fire history. The advantages of using magnetic measurements as a fire index are considerable, when compared with the accepted techniques of pollen and charcoal analysis. Both of which are time consuming, laborious and sample destructive. The use of the magnetic samples for later pollen and charcoal analysis obviates the problems normally associated with using different techniques on different cores from the same lake.

(iv) The failure of the magnetic measurements to identify the controlled burning that was practised in both catchments and reflected in the pollen and charcoal curves in BP6 indicates that in the hydrological context of the Landes S.I.R.M. will only identify particularly devastating forest fires. Pollen and charcoal are subject to atmospheric transport, the secondary ferrimagnetic minerals much less so, their movement primarily being affected by stream transport. A forest fire recorded by S.I.R.M. peaks in lake sediments is therefore most likely to have taken place within the catchment of the lake, otherwise there is a significant

chance that the event would not be recorded in the magnetic record. However some atmospheric transport does occur but it is most probably locally over short distances. The detection of forest fires using magnetic measurements may therefore be less subject to problems of long distance transport associated with fire identification using the techniques of pollen and charcoal analysis.

LAKE LAUKUNLAMPI. A CASE STUDY. CHAPTER 5Introduction 5.1

In many environments fire plays an important part in the development and maintenance of the ecosystem. The importance of fire has been most studied in the context of the boreal ecosystem. The management programmes involving intensive fire controls in Itasca State Park, Minnesota, have resulted in a serious departure from natural conditions and have led to a reversal of fire suppression policies. (Frissel, op cit; Heinselman, 1973). Swain, (op cit) and Taylor (1973) offer the same conclusions for the Superior National Park and the Yellowstone National Park respectively.

To investigate the fire and vegetational histories of boreal ecosystems either dendrochronological records or lake sediments can be used. Frissel (op cit), Taylor (op cit), Cwynar (1979), Kilgore and Taylor (1979) working in the American Boreal environment have used tree ring studies to date fire scars back to the 17th century. Zackrisson (1977) working in the North Swedish Boreal forests has used fire scars to compile a fire history of the Vasterbotten Province spanning 600 years. Such studies are strictly limited by the availability of living trees and dead tree stumps and are also subject to the problems inherent in tree ring interpretation (FRITTS, 1976).

Lake sediment studies allow a more detailed vegetation and fire history to be compiled. Cwyner (1978) uses pollen and charcoal analysis to extend the fire history of the Barron Township, Algonquin Park, Ontario. Swain (op cit) investigated the annually laminated sediment of the Lake of the Clouds, Minnesota, and reconstructed the fire history for the past 10,000 years. Swain (op cit) used the frequency of occurrence of forest fires to determine moist and dry climatic phases.

Tolonon (op cit) uses charcoal and pollen analysis to record the land-use and fire history of the laminated sediments of Lake Ahvenianen, Southern Finland, as far back as 3022 BC. Huttenen (1980) interpreted the early land-use, especially the slash and burn cultivation in the commune of Lammi, southern Finland, using pollen and charcoal analysis.

The techniques of pollen and charcoal analysis are sample destructive, time consuming and tedious requiring in most cases a wide sampling interval with a consequent loss of resolution and an examination of the whole core before a total fire history can be constructed. Charcoal has similar transport qualities to pollen and it is possible that fires outside the lake catchment will be recorded in the lake sediments giving rise to a regional as well as a local fire history and a consequent miscalculation of fire frequency and periodicity.

The case studies of Llynau Bychan and Goddionduon and Lakes Biscarrosse and Sanguinet have shown that it is possible to detect forest fires in lake sediments from the identification of secondary ferrimagnetic oxides in the lake sediments where they form a magnetically distinct layer.

The case studies of the two French lakes have shown that the magnetic fire indicators of high S.I.R.M. values (and presumably high χ values) correlate with the known pollen and charcoal fire indicators and provide an accurate method for detecting forest fires which is both rapid and non-destructive. To explore the implications of the technique for studies of fire ecology the laminated sediments from a small lake in eastern Finland, with a long fire history were sampled.

LAKE LAUKUNLAMPI. PHYSICAL SETTING. 5.2

Lake Laukunlampi is a small kettle hole type lake in northern Karelia, Finland (63°36'N 29°9'E). The lake is situated in an area covered by glacio-fluvial deposits and lies at an altitude of 84 m. above sea level. Fig. 5.2.1 shows the drainage basin of the lake. The lake has a surface area of 8.5 ha. and a forested watershed of about 29 ha. A small quarry has been dug into the esker at the north end of the lake. The maximum water depth of the lake is 29 m., at present there is neither a visible outlet to the lake nor an inlet. Water therefore enters the lake by seepage. The lake is considered to be meromictic.

The forest types of the area belong to the southern Finnish Forest Type series (Kalela, 1961). The immediate surroundings of the lake are densely wooded, the steep slopes of the catchment support vegetation typical of the dry heath forests. Picea abies is dominant with stands of Pinus silvestris and some Betula verrucosa. The average age of the forest is around 80-90 years (tree ring dating). On lower levels, near the lake shore, stands of Alnus glutinosa, Betula and Populus tremula occur with individuals of Juniperus communis.

Land-use history.

The pattern and type of land-use practised in Karelia is well established from documentary and palaeoecological studies, Vuorinen (1978), Tolonon (op cit). Agriculture began with the widespread burning of the forests by man and the initiation of the slash-and-burn system. Vuorinen (op cit) has established the introduction of agriculture as beginning around 1400 A.D., although in southern Finland the agricultural phase began around 900 A.D. Huttunen (op. cit), Tolonon (op cit).

The slash-and-burn system was important for the production of rye, oats and flax in eastern Finland, where it is the oldest procedure in Finland's traditional crop cultivation. As a result of chemical and microbial changes in the soil caused by burning a substantial proportion of nutrients in the soil acquired a form readily available to cultivated crops. The latter quickly used up the nutrients thus liberated and the land was returned to forest growth after a short period of cultivation. The length of time for cultivation was dependent on the forest type, which governed the type of slash-and-burn method employed.

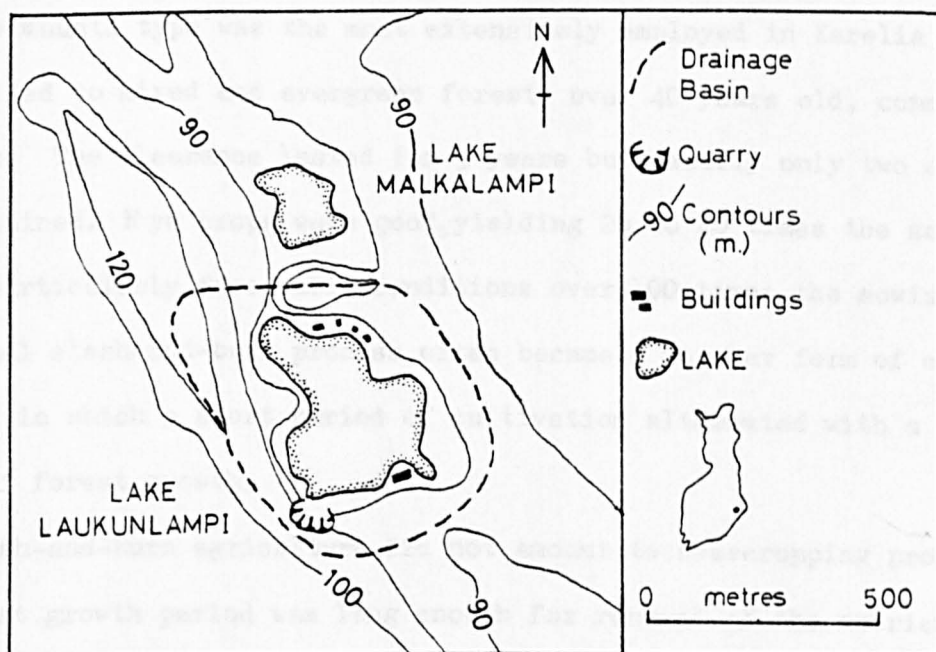


fig 5.2.1 Location Lake Laukunlampi

The slash-and-burn system was important for the production of rye, oats and flax in eastern Finland, where it is the oldest procedure in Finland's traditional crop cultivation. As a result of chemical and microbial changes in the soil caused by burning a substantial proportion of nutrients in the soil acquired a form readily available to cultivated crops. The latter quickly used up the nutrients thus liberated and the land was returned to forest growth after a short period of cultivation. The length of time for cultivation was dependant on the forest type, which governed the type of slash-and-burn method employed.

The Huuhta type was the most extensively employed in Karelia and was applied to mixed and evergreen forests over 40 years old, commonly 80 years. The clearance lasted for 3 years but usually only two crops were obtained. Rye crops were good, yielding 20 to 40 times the sowing and in particularly favourable conditions over 100 times the sowing. The normal slash-and-burn process often became a regular form of crop rotation in which a short period of cultivation alternated with a long period of forest growth.

Slash-and-burn agriculture did not amount to overcropping provided the forest growth period was long enough for renewal of the nutrient reserves, i.e. at least 25 years. As settlement grew denser in the 18th century there developed a shortage of adequate extensive forests and the slash-and-burn system turned into overcropping. Slash-and-burn agriculture effectively stopped around 1900 A.D. when there was a movement towards enclosure of the fertile lake edges and an increase in the importance of forestry.

Local documentary evidence has shown that Lake Laukunlampi was used as a retting lake from around 1700 A.D. onwards. The flax grown around the shores of Kirkkoselkä was soaked in the waters of Lake Laukunlampi.

The practise of flax retting ceased around the beginning of the 19th century. Vuorinen (op cit) has indicated that the practise of flax retting brings about a eutrophication of the lake and in the Lake Laukunlampi core corresponds to an area of brown organic sediment spanning 30cm. from 28cm. to 58cm. (see section 5.4).

Since the end of agriculture in the catchment around 1900 A.D. the only disturbance in the watershed has been the opening of the esker at the north end of the lake for quarrying around the 1930's and the construction of buildings around the lake in postwar years.

METHODOLOGY 5.3

The uppermost sediment sequence from the deepest part of the lake was sampled by freezing the sediment in situ. Freezer coring has been used by several workers and a description of the technique is given in Swain (op cit). The lake sediments were sampled in 1977 and in 1978 from a hole in the ice using an ice-corer of a post box design (Huttunen and Merilainen, 1978). The corer consists of a large flat rectangular box which is packed with dry ice and allows a large unmixed sediment sample to be collected on one face.

The sediment was removed from the corer in the laboratory and cleaned up to remove any contamination that may have occurred. Cleaning the core with hot water 'brings out' the laminated structure of the sediment. The sediment core was sliced into strips 100cm. by 5cm. for ease of sampling.

A varve count was performed on the sediment core. Due to the narrowness of some of the Laminae the core was subsampled every 2.5 mm, which in the middle and lower parts of the core corresponded to approximately 7 years of sediment. It was possible to subsample individual laminae in the top 16cm. of the sediment core.

A stainless steel razor blade was used to subsample the core, great care was taken to avoid cross contamination of subsamples. The sediment column was kept frozen during subsampling and necessitated the whole procedure being carried out in a cold room at -5.0°C . Every hour the column was placed in a freezer at a temperature of -20.0°C for approximately 30 minutes to refreeze the thawed area. The whole core was subsampled in this manner; the samples were placed in numbered watertight polythene containers until preparation for magnetic measurements (section 1.4). Due to the low weights of the samples (approx. 0.1 gm.) it was impossible to carry out χ measurements, and so S.I.R.M. measurements were used as a substitute for χ .

After magnetic measurement the samples were prepared for palaeoecological analysis, i.e. charcoal, pollen and diatom analysis which are being performed at the Karelian Institute, Finland and University College London.

RESULTS 5.4

The lake sediment is laminated, the laminae consisting in general, of a thin black layer following a pale layer and a grey layer. Within the black layer Chrysophyceae cysts and black spheres are abundant. The pale bandings are composed mainly of diatom frustules, the grey or grey brown layers consist mainly of organic detritus. Saarnisto et al., (1977) and Vuorinen (op cit) working on laminated sediment with a similar structure concluded that the laminae reflect the seasonal changes of the lake production and deposition of mineral matter. A dark-light couplet represents one year. The brown zone from 28cm. to 58cm. consists almost entirely of fibrous plant remains.

Magnetic results

Fig. 5.4.1 plots the S.I.R.M. profile for single samples against depth; the sediment structure is also shown. The laminae count for the sediment core spans 600 years, the base of the sediment dating from 1400 A.D.

The S.I.R.M. profile divides the sediment column into two components:

- (i) the recent sediment above 25cm. dating from 1900 A.D. to the present day, and
- (ii) the remaining sediment below 25 cm. dating from 1900 A.D. to 1400 A.D.

The topmost sediment is dominated by a peak S.I.R.M. value of $1070 \times 10^{-6} \text{ G.Oe.cm.}^3 \text{g}^{-1}$ at 20.0cm. with the prominent S.I.R.M. peaks above this level attaining values of less than $500 \times 10^{-6} \text{ G.Oe.cm.}^3 \text{g}^{-1}$ for individual laminae above 18cm.

The second component can be subdivided into the S.I.R.M. profile above 43 cm. to 25 cm. and the S.I.R.M. profile from 43 cm. to 80 cm. Below

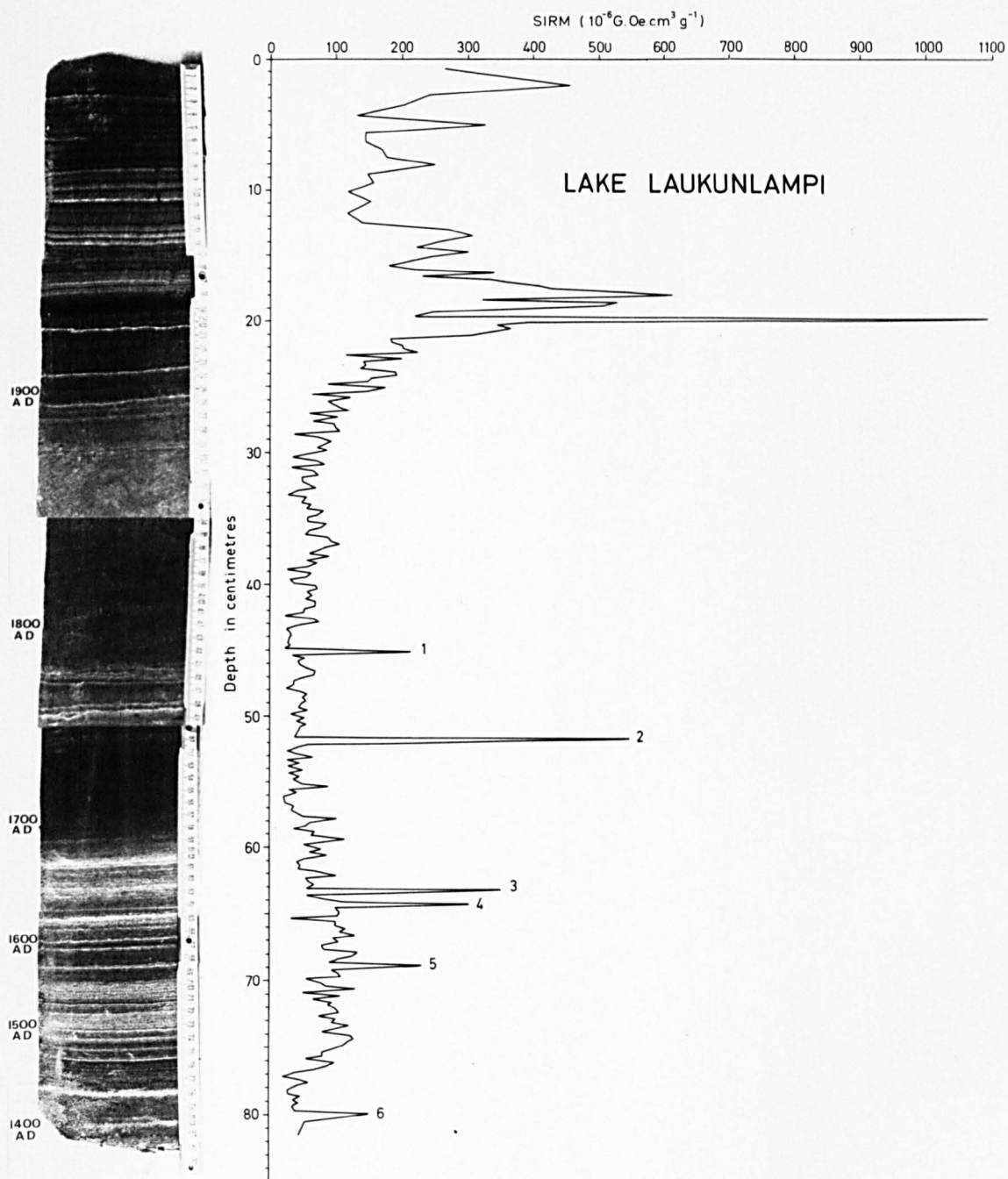


fig 5.4.1. SIRM PROFILE FOR THE SEDIMENT CORE

43 cm. (1800 A.D.) the magnetic profile for the sediment is characterized by prominent S.I.R.M. peaks with values above $150 \times 10^{-6} \text{G.Oe.cm}^3 \text{g}^{-1}$. Peaks 3 and 4 have S.I.R.M. values of over $300 \times 10^{-6} \text{G.Oe.cm}^3 \text{g}^{-1}$ with peak number 2 reaching $547 \times 10^{-6} \text{G.Oe.cm}^3 \text{g}^{-1}$. All the S.I.R.M. peaks are sample specific. The sediment between the prominent peaks in S.I.R.M. is characterized by lesser more frequent S.I.R.M. peaks with values of approximately $48 \times 10^{-6} \text{G.Oe.cm}^3 \text{g}^{-1}$. Table 5.4.1 lists S.I.R.M. depth and time interval between the major S.I.R.M. peaks; this ranges from 12 years to 138 years. The average time interval between the intermediate S.I.R.M. peak is approximately 14 years.

Above 40cm. the sediment, dating from 1800 to 1900 A.D. is characterized by smaller S.I.R.M. peaks with values of around $90 \times 10^{-6} \text{G.Oe.cm}^3 \text{g}^{-1}$ and which have a time interval between the S.I.R.M. peaks of between 6 -8 years.

PEAK NO.	DEPTH cm.	S.I.R.M. $\text{G.} \times 10^{-6} \text{G.Oe.cm}^3 \text{g}^{-1}$	Time between S.I.R.M. peaks
1	45.125	215	93
2	51.875	547	138
3	63.375	351	12
4	64.375	303	54
5	68.375	228	132
6	79.875	151	

TABLE 5.4.1

Fig. 5.4.2 plots the sedimentation rate in mm. yr^{-1} against depth for a sediment core sampled the previous year to the core used for magnetic analysis. Below 50cm. the average sedimentation rate is less than 1mm. yr^{-1} , above this level the sedimentation rate increases to greater than 2mm. yr^{-1} , decreasing to 1.25mm. yr^{-1} in 1950 above which it increases to 7.5mm. yr^{-1} in the modern sediment.

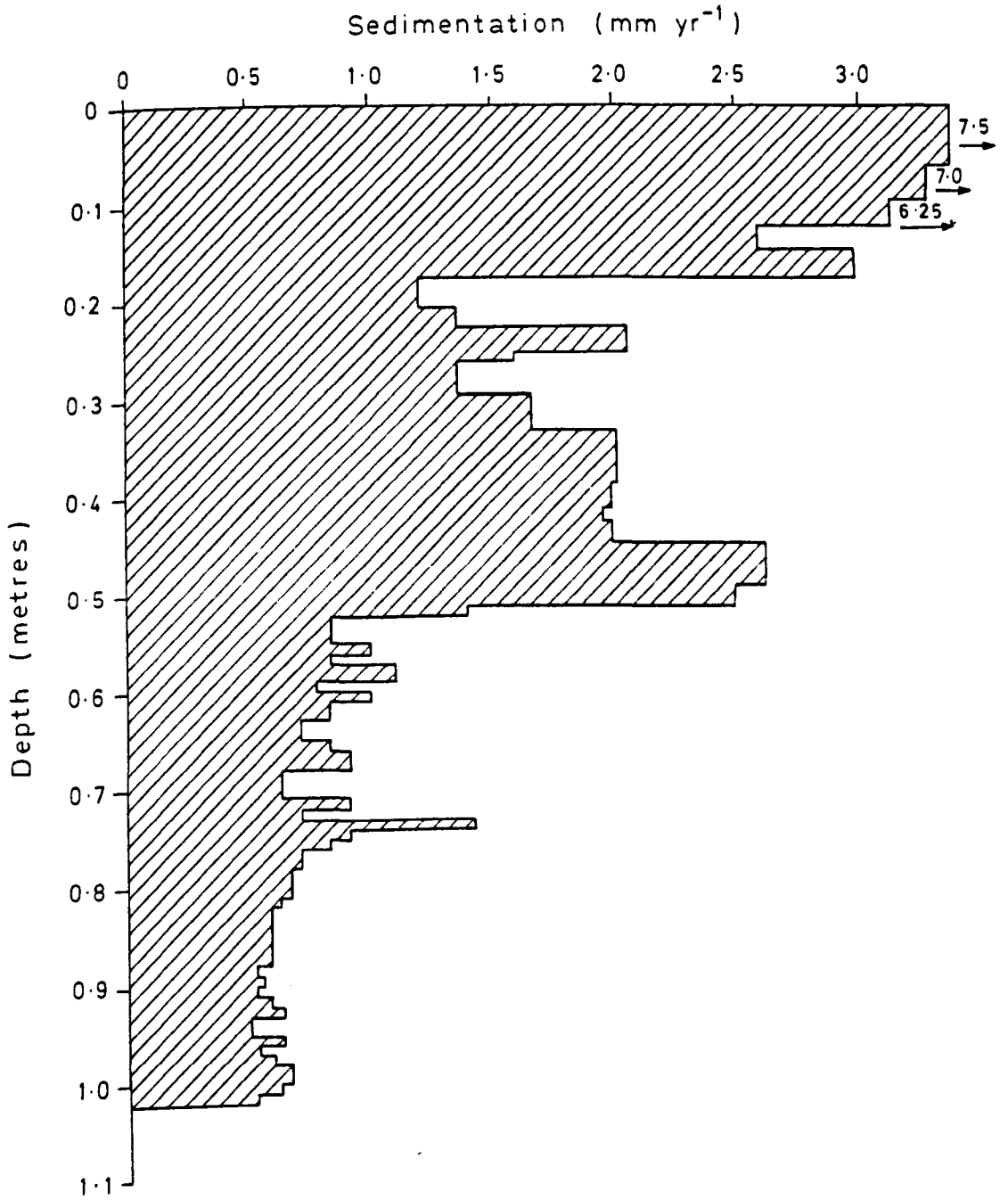


fig.5.4.2 Sedimentation rate (mm. yr.) depth curve for core

The same sediment core was subsampled every 0.5 cm. from a depth of 40 cm. to 75 cm. the following year and measured for S.I.R.M. The samples were measured for S.I.R.M. on magnetometers at Liverpool University. This equipment produces values 50-60% of those produced on the Edinburgh University magnetometers. The S.I.R.M. values for the 0.5 cm. set of samples are therefore lower than the 0.25 cm. set of samples.

Fig. 5.4.3 plots the 0.25 cm. sample derived S.I.R.M. curve and the 0.5 cm. sample derived S.I.R.M. curve. Despite the averaging effect produced by using 0.5 cm. samples and the lower values produced on the Liverpool University magnetometers it can be clearly seen that the majority of major S.I.R.M. peaks identified by the 0.25 cm. samples (notably peaks 1,2,3 and 4 (Fig. 5.4.1)) are not reproduced in the 0.5 cm. samples.

S.I.R.M. peaks of such magnitude in relation to the background S.I.R.M. levels should be identified in both sets of samples. As the 0.25 cm. S.I.R.M. peaks are not found in the second 0.5 cm. set of samples it immediately suggests that the first set of samples suffered some contamination. The similarity in trends of the 0.25 cm. S.I.R.M. curve with the 0.5 cm. S.I.R.M. curve (i.e. relatively high S.I.R.M. values in the lower half of the sediment column and relatively low S.I.R.M. values in the upper part of the column) suggests that contamination has only occurred in a few samples.

During sampling and measuring great care was taken at all times to prevent contamination from occurring. The contamination, therefore, is totally unexpected and the author feels that the only possible sources of contamination can be microscopic particles shed from the sampling instrument and the possible use of contaminated foam packing.

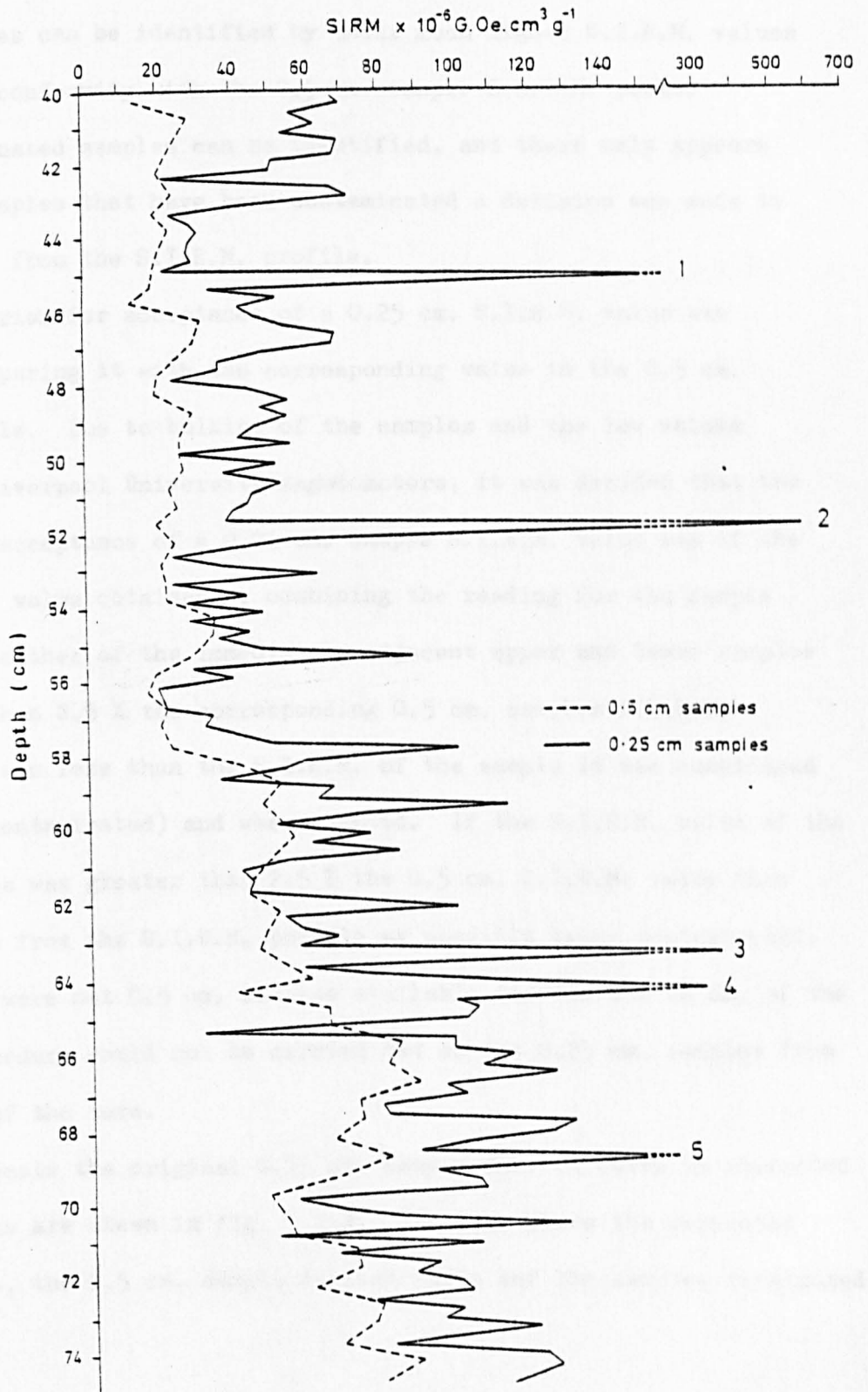


fig. 5.4.3. S.I.R.M. results 0.25 and 0.5 cm. samples Lake Laukunlampi sediments.

By comparing the two sets of data it can be seen that the contaminated 0.25 cm. samples can be identified by their much higher S.I.R.M. values and their non-conformity with the 0.5 cm. sample S.I.R.M. peaks. As the contaminated samples can be identified, and there only appears to be a few samples that have been contaminated a decision was made to eliminate them from the S.I.R.M. profile.

The criterion for acceptance of a 0.25 cm. S.I.R.M. value was applied by comparing it with the corresponding value in the 0.5 cm. S.I.R.M. profile. Due to bulking of the samples and the low values given on the Liverpool University magnetometers, it was decided that the criterion for acceptance of a 0.25 cm. sample S.I.R.M. value was if the average of the value obtained by combining the reading for the sample with that for either of the immediately adjacent upper and lower samples was not more than 2.5 X the corresponding 0.5 cm. samples S.I.R.M. value. If it was less than the S.I.R.M. of the sample it was considered real (i.e. uncontaminated) and was accepted. If the S.I.R.M. value of the 0.25 cm. sample was greater than 2.5 X the 0.5 cm. S.I.R.M. value then it was omitted from the S.I.R.M. profile as possibly being contaminated.

As there were not 0.5 cm. samples available for the top 40 cm. of the core this procedure could not be carried out on the 0.25 cm. samples from the top part of the core.

On this basis the original 0.25 cm. sample derived curve is corrected and the results are shown in fig. 5.4.4. The fig. shows the corrected 0.25 cm. curve, the 0.5 cm. sample derived curve and the samples eliminated

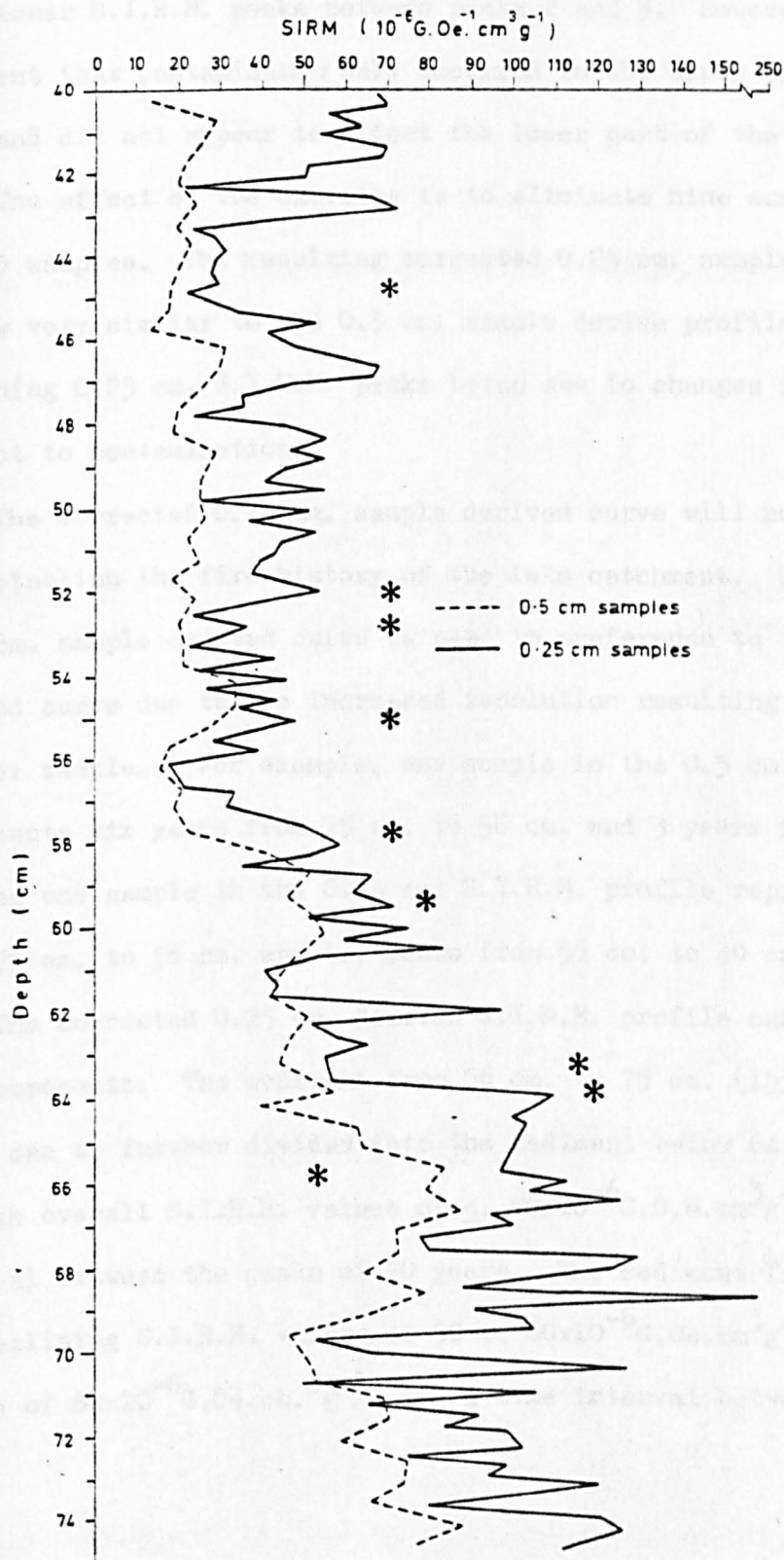


fig.5.4.4. Corrected S.I.R.M. 0.25cm. samples and 0.5cm. samples. Rejected samples shown by a star.

(identified by a star). It can be seen that the original 0.25 cm. S.I.R.M. peaks 1,2,3 and 4 are eliminated as being contaminated along with several of the lesser S.I.R.M. peaks between peaks 2 and 3. However it is also apparent that contamination only occurred in the upper part of the sediment core and did not appear to affect the lower part of the sediment core.

The effect of the exercise is to eliminate nine samples out of a total of 140 samples. The resulting corrected 0.25 cm. sample derived profile is now very similar to the 0.5 cm. sample derive profile with the remaining 0.25 cm. S.I.R.M. peaks being due to changes in the lake catchment and not to contamination.

The corrected 0.25 cm. sample derived curve will now be used to try and establish the fire history of the lake catchment. The corrected 0.25 cm. sample derived curve is used in preference to the 0.5 cm. sample derived curve due to the increased resolution resulting from using smaller samples. For example, one sample in the 0.5 cm. S.I.R.M. profile represents six years from 75 cm. to 56 cm. and 3 years from 56 cm. to 40cm. Whereas one sample in the 0.25 cm. S.I.R.M. profile represents three years from 75 cm. to 56 cm. and 1.7 years from 56 cm. to 40 cm.

The corrected 0.25 cm. derived S.I.R.M. profile can be divided into two components. The sediment from 56 cm. to 75 cm. (1550 A.D. - 1700 A.D.) which can be further divided into the sediment below 64 cm. characterized by high overall S.I.R.M. values of $\underline{c.} 80 \times 10^{-6} \text{G.O.e.cm.}^3 \text{g}^{-1}$ with a time interval between the peaks of 20 years. The sediment from 64 cm. to 56 cm. has declining S.I.R.M. values of 50 to $60 \times 10^{-6} \text{G.Oe.cm.}^3 \text{g}^{-1}$ with peak S.I.R.M. values of $80 \times 10^{-6} \text{G.Oe.cm.}^3 \text{g}^{-1}$ and a time interval between the peaks of 21 years.

The second component from 56 cm. to 40 cm. (1700 A.D. to 1800 A.D.) is characterized by low background S.I.R.M. values of c. 30 to 40 $\times 10^{-6} \text{G.Oe.cm}^3 \text{g}^{-1}$ with S.I.R.M. peaks ranging in value from 40 to 70 $\times 10^{-6} \text{G.Oe.cm}^3 \text{g}^{-1}$. The time interval between the S.I.R.M. peaks is approximately ten years.

Discussion 5.5

The following discussion will only involve the corrected S.I.R.M. 0.25 cm. sample derived profile from 40 cm. to 75 cm.

The interpretation of the fire history from the S.I.R.M. profile is subjective, in that an attempt is made, on the evidence of the previous case studies to infer that S.I.R.M. peaks can be used as indicators of burning episodes. The periodicity of the S.I.R.M. peaks may be regarded as indirect evidence of a slash-and-burn system of agriculture as the only probable regular ecological disturbance in the catchment was the slash-and-burn system of agriculture. To fully establish the relationship between S.I.R.M. and the fire history of the catchment detailed local documentary evidence is needed to verify the type and length of rotation and the number of forest plots in the catchment that were involved in the agricultural system.

Relating the S.I.R.M. profile to the land-use history of the lake basin, then the lower part of the sediment column from 64 cm. to 75 cm. corresponds to the period when the slash-and-burn system of agriculture was correctly utilized. The peak S.I.R.M. values may relate to the slash-and-burn practises, with the 20 year time interval between the peaks possibly indicating forest rotation in the catchment. The high background S.I.R.M. values for this part of the core may relate to high temperature fires: The long forest regeneration period of 80 years (section 5.2) would allow a large litter fuel source to accumulate and would result in high temperature controlled fires which would produce local hotspots in the soils of the catchment. The zones would then act as source areas for the erosion of magnetically enhanced secondary ferrimagnetic oxides.

It is the authors opinion that the enhanced material would probably enter the lake during the spring snowmelt when runoff in the catchment would be at its highest. There is therefore a probable reduction in the S.I.R.M. peaks through dilution by non and less magnetic minerals as each sample spans at least three years in this part of the sediment column.

The sediment from 56 cm. to 64 cm. has relatively high S.I.R.M. values and a time interval between the S.I.R.M. peaks of 21 years and may relate to the end of the efficient use of the slash-and-burn system and the start of the misuse of the forests (i.e. shorter forest regeneration periods). The lower overall S.I.R.M. values in comparison with the section below it may be due to the increased use of the slash and burn system resulting in decreased litter fuel sources available to burn. The lower temperature fires would therefore probably not produce large amounts of magnetically enhanced oxides in the soil and consequently result in the lower overall S.I.R.M. values for this part of the sediment column. The slightly higher accumulation rate for this section compared with the lower part of the core (Fig. 5.4.2) may also indicate this.

The sediment from 56 cm. to 40 cm. relates to the period of overcropping of the forest by the slash-and-burn system and is reflected in the lower background S.I.R.M. values and lower S.I.R.M. peak values and a time interval between the peaks of 10 years. The shorter length of time allowed for forest regeneration would result in less fuel available to burn and therefore lower temperature fires and consequently a much smaller volume of secondary ferrimagnetic oxides being produced in the soil.

This section of the core is also typified by a greatly increased sedimentation rate which reflects both the overcropping of the forest by slash-and-burn practices and the use of the lake for flax retting.

Additional magnetic measurements are planned on the larger samples and hopefully on 0.25 cm. samples. The magnetic parameters of S.I.R.M./ χ and $(B_0)_{CR}$ should make identification of fire horizons and contamination much easier.

Conclusions 5.6

The case study has shown that it is possible from a lake with a long fire history to produce a meaningful S.I.R.M. profile.

On the basis of the evidence from the previous case studies the S.I.R.M. peaks that occur in the sediment below the 1800 A.D. level can probably be attributed to the slash-and-burn system of agriculture that dominated the Lake Laukunlampi drainage basin. The effect of the fires would be to produce in the soils secondary ferrimagnetic oxides which would be washed into the lake after the spring snowmelt. When overcropping became dominant the effect of decreasing the time interval between the rotation period would be to decrease the amount of litter fuel available for burning and therefore lower temperatures which can be seen in the lower S.I.R.M. values for this section of the sediment column.

The time interval between the S.I.R.M. peaks is consistent with the documentary evidence for the slash-and-burn system as practised in this region of Finland.

Pollen and charcoal analysis are at present in progress on the 0.25 cm. samples and although not conclusive the preliminary results support the corrected S.I.R.M. profile indicating a relationship between S.I.R.M. and palaeobotanical fire indicators.

The benefits of measuring the magnetic properties of the samples before pollen and charcoal analysis are performed are numerous.

- (i) The magnetic measuring procedure is rapid and non sample destructive enabling the same samples to be used for pollen and charcoal analysis.
- (ii) The magnetic measurements may identify possible fire horizons in the sediment enabling a selection of the samples for pollen and charcoal analysis to be made.

(iii) The production of secondary ferrimagnetic oxides in the burnt soils and their subsequent erosion into the lake results only in fires specific to a lake catchment being recorded in the sediment. Pollen and charcoal analysis reflect both the regional and local occurrence of forest fires and may result in erroneous conclusions.

(iv) In a lake with annually laminated sediments the measurement of magnetic properties allows a rapid estimate of the occurrence of forest fires in a boreal ecosystem and the periodicity of such fire events. Swain (op cit) attributes an increase in fire frequency to a change in climate, therefore magnetic profiles of lake sediments may provide a rapid method of distinguishing 'dry' and 'moist' climatic periods.

The importance of fire in many ecosystems has long been known, but the accepted techniques of pollen, charcoal and chemical analysis along with dendrochronology are time consuming and labourious. Magnetic analysis of the sediments can provide a complimentary technique that decreases the time interval usually associated with producing results from the accepted technique by the nature of its sample spotting abilities.

The corrected S.I.R.M. profile for the Lake Laukunlampi sediments and its implications to fire frequency and periodicity studies are preliminary and require fuller and thorough magnetic, pollen and charcoal analysis to be performed on the samples before any definite conclusions can be drawn.

PLYNLIMON. A CASE STUDY. CHAPTER 6INTRODUCTION 6.1

The problems and ranges of techniques concerned with the tracing and monitoring of the movement of stream bedload is well documented in Gregory and Walling (1973). There is as yet no single effective technique for tracing the movement of stream bedload through the size ranges from large cobbles ($>0.05\text{m}$) to fine silt ($<500\mu\text{m}$).

The current techniques widely used range from simple painted stone studies to the more expensive and complex flourescent and radioactive tracing studies.

Painted stone studies are only really viable when studying the movement of the larger grain sizes. The technique can be upgraded by using different colours for the various grain sizes that are being studied. The technique has several limitations, the major problem being the recovery of the painted stones. Leopold et al., (1966) successfully demonstrated the use of painted stones in the Vigil Network experiments.

Flourescent tracers have been successfully used in estimating sediment transport rates and for studying dispersion, sorting and mean particle velocities. The technique involves coating the sediment with a flourescent dye and a vinyl binder. Rathbun et al., (1971) have demonstrated the effectiveness of the technique in sand-dominated streams near Bernardo, New Mexico. Flourescent tracers suffer from similar limitations to painted stones; the problem of recovery of the treated material and additional problems of fixing the flourescent dye and the removal of the dye by abrasion during the experimental run constitute strict limitations to the use of the techniques.

Radioactive labelling studies are expensive to set up and require expensive equipment to trace the movement of the treated bedload. Radioactive labelling can be achieved by either irradiating natural or artificial particles in a reactor or by coating the particles with a radioactive substance such as Iridium 192 solution (Hubbell and Sayre, 1965). With larger grain sizes the material to be used has to be drilled and a radioactive plug inserted and sealed into the hole (Kidson and Carr, 1962).

In all cases the half life of the radioactive substance should be related to the duration of the transport phenomena under study. However, the longer the duration of the study the longer the half life of the material to be used has to be, with a consequent increased danger of contamination to both the worker and the environment. Fluorescent tracers can also pose several environmental problems.

The possibility of using the natural magnetic enhancement that occurs in soils as a suspended sediment source tracer has been successfully demonstrated in the Exe catchment. (Oldfield et al, op. cit; Walling et al, op.cit).

The previous case studies have successfully demonstrated the tracing of downstream and within-catchment movement of magnetic minerals as a result of natural forest fires. The study of the bedload material in the Llyn Bychan outflow stream (section 2.15) provided the initial stimulus for the use of magnetically enhanced bedload as a natural stream tracing technique.

To fully ascertain the usefulness of the magnetic technique a more systematic and controlled study is required. Two drainage

ditches in an instrumented catchment in the Plynlimon area of mid-Wales, an area of homogenous lithology, were chosen as the site for the case study.

SITE DESCRIPTION 6.2

The Institute of Hydrology's research station at Plynlimon (G.R. 892860) covers the upper reaches of the rivers Severn and Wye. The major elements of the catchment landscape are ridges and shelves formed by outcropping gritstones. Upper and middle peneplains appear as broad interfluves mantled by blanket peat; the glaciated valleys between them have been infilled by slope material and then re-incised so that today the dominant control on the stream channels is bedrock.

The bedrock of the area is a homogenous lithology of Silurian shales and mudstones which are poor in magnetite and hematite but rich in paramagnetic forms of iron, making the area an ideal site for any magnetic study using enhanced magnetic properties. The suite of soils in the area range from podsoles to brown earths and gleys with the flat hill tops and valley bottoms characterised in general by peat deposits.

Fig. 6.2.1 locates the Severn catchment and the two drainage channels used in the experiment, Lower Tan and Lower Tan A. The Severn catchment differs from the adjacent Wye catchment in its land-use; the ^{Severn} catchment has over 67% of its area forested. A more detailed account of the physiography, deposits and vegetation of the Plynlimon catchments can be found in Newson (1976).

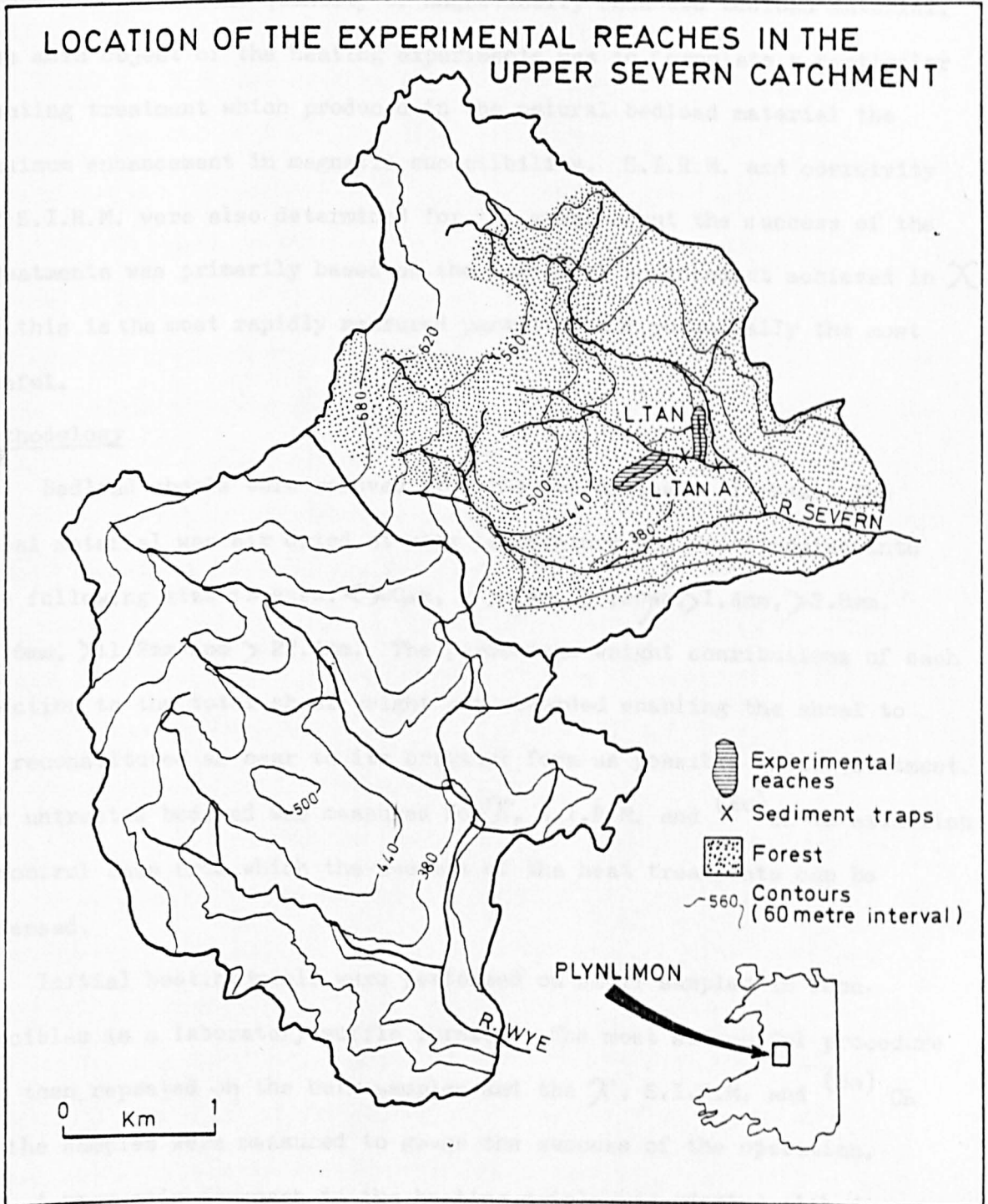


fig. 6.2.1 Location of test reaches.

HEATING EXPERIMENTS 6.3

Before the tracing experiments could begin it was necessary to produce a sufficient quantity of magnetically enhanced bedload material. The main object of the heating experiments was to formulate a particular heating treatment which produced in the natural bedload material the maximum enhancement in magnetic susceptibility. S.I.R.M. and coercivity of S.I.R.M. were also determined for the samples but the success of the treatments was primarily based on the degree of enhancement achieved in χ as this is the most rapidly measured parameter and potentially the most useful.

Methodology

Bedload shoals were removed from the two drainage ditches. The shoal material was air dried at room temperature and fractionated into the following size classes: $< 500\mu\text{m}$, $> 500\mu\text{m}$, $> 710\mu\text{m}$, $> 1.4\text{mm}$, $> 2.8\text{mm}$, $> 5.6\text{mm}$, $> 11.2\text{mm}$ and $> 22.4\text{mm}$. The percentage weight contributions of each fraction to the total shoal weight was recorded enabling the shoal to be reconstituted as near to its original form as possible after treatment. The untreated bedload was measured for χ , S.I.R.M. and $(B_0)_{CR}$ to establish a control base from which the success of the heat treatments can be assessed.

Initial heating trials were performed on small samples in 10cc. crucibles in a laboratory muffle furnace. The most successful procedure was then repeated on the bulk samples and the χ , S.I.R.M. and $(B_0)_{CR}$ of the samples were measured to gauge the success of the operation.

A pragmatic approach to the heating trials was adopted with five main variables being altered according to the success of the previous treatment. The variables that were altered were : (i) temperature, (ii) length of time at that temperature, (iii) rate of heating (iv) rate of cooling, (v) the presence of a reducing or oxidizing environment in the furnace.

RESULTS

Table 6.3.1 lists the χ and S.I.R.M. of the different size samples at two contrasting temperatures, 200°C. and 800°C. The natural χ and S.I.R.M. is also listed as are the degree of enhancement in χ and S.I.R.M. achieved at 800°C. The samples were toasted in a muffle furnace for 30 minutes after being rapidly heated to this temperature. The samples were rapidly cooled after toasting.

In all cases an increase in χ of over 1800 times the normal value is achieved, with increases in S.I.R.M. ranging from 423 to 1663 times the normal value. Enhancement in S.I.R.M. begins to occur in the fine fractions before 200°C with the growth of hematite, then with the combustion of organic matter at higher temperatures magnetite begins to be produced and is reflected in the higher χ values. Fig. 6.3.1 plots χ (on a logarithmic scale) against temperature for the samples, demonstrating the increase in χ at lower temperatures in the grain sizes less than 700 μ m. Maximum magnetic enhancement in χ in all the size classes is attained at 800°C. Above 800°C the samples anneal resulting in a loss of enhancement.

Fig. 6.3.2 demonstrates the effects of rate of heating and the presence of a reducing environment on magnetic enhancement. Bulk samples were used and the results indicate that to produce maximum magnetic enhancement in S.I.R.M. and χ in all the size fractions the following procedure is required: A rapid heating of the sample to 800°C, the material is maintained at 800°C for 30 minutes followed by a rapid cooling to room temperature.

Sets B, C and D all show that rapid heating is required but that the presence of organic matter may not be important. Set A, slow rate of heating and cooling and no organic matter shows minimum enhancement in S.I.R.M. and χ after the treatment. Additional studies have indicated that the presence of organic matter does not appear to be

<u>SIZE</u>	<u>NATURAL</u>		<u>200°C</u>		<u>800°C</u>		<u>ENHANCEMENT</u>	<u>S.I.R.M. 800</u>
	\bar{X}	S.I.R.M.	\bar{X}	S.I.R.M.	\bar{X}	S.I.R.M.	$\bar{X}/800/\bar{X}_0$	<u>S.I.R.M. 0</u>
<500 μ m	6.3	214	7.2	529	20,700	91,980	3280	430
500-700 μ m	6.3	164	7.2	731	18,000	69,300	2857	423
0.7-1.4 mm	6.3	88	6.3	164	16,200	56,700	2751	644
1.4-2.8 mm	6.3	50	5.4	25	13,950	41,580	2214	832
2.8-5.6 mm	6.3	25	6.3	25	11,700	35,280	1857	1411
5.6-11.2 mm	6.3	25	6.3	25	12,600	41,580	2000	1663
>11.2 mm	7.2	25	6.3	25	14,400	36,540	2000	1462

TABLE 6.3.1

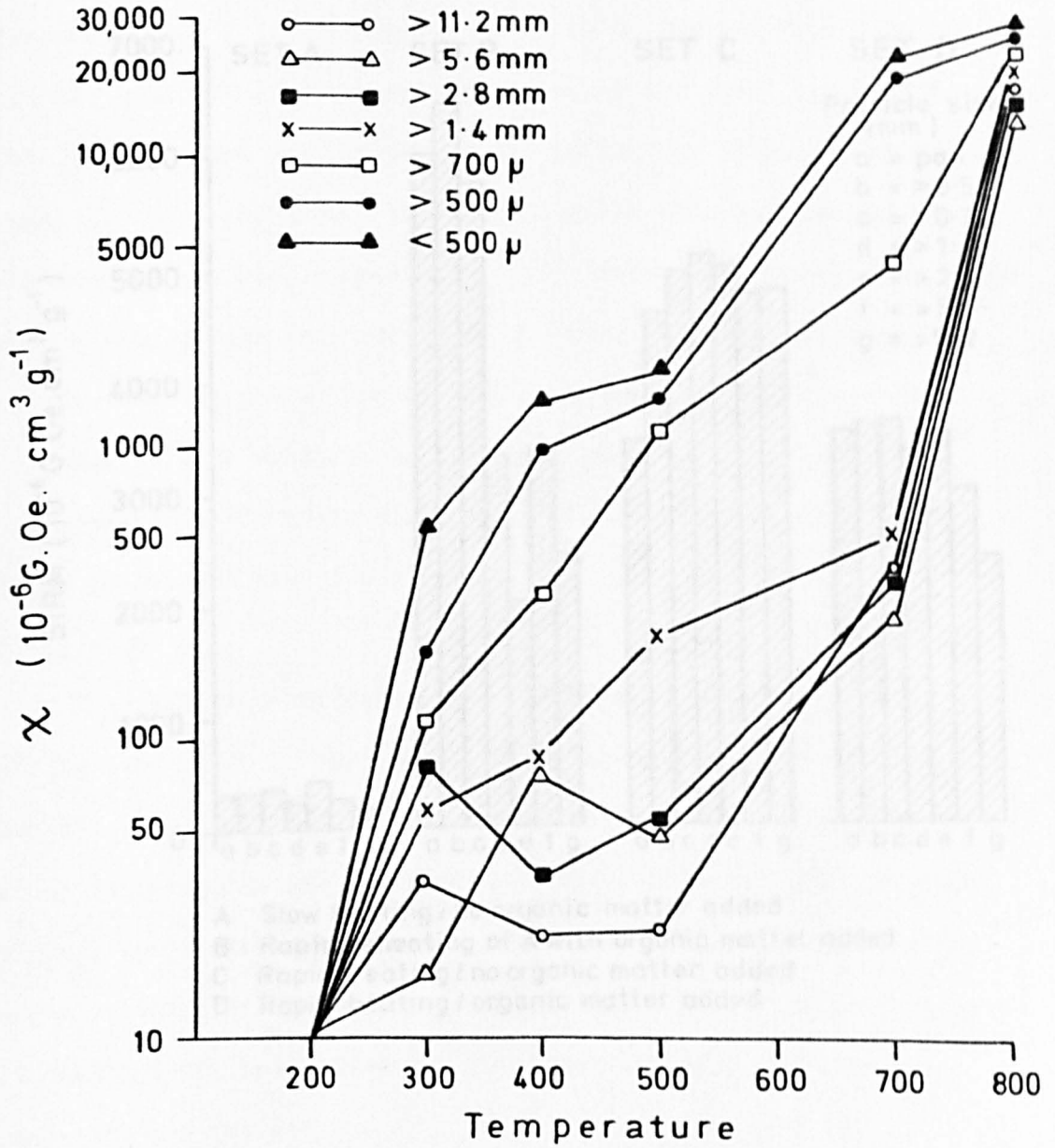


fig. 6.3.1 χ against temperature for toasted material.

PLYNLIMON BEDLOAD
EFFECTS OF ALTERNATIVE 'TOASTING' PROCEDURE

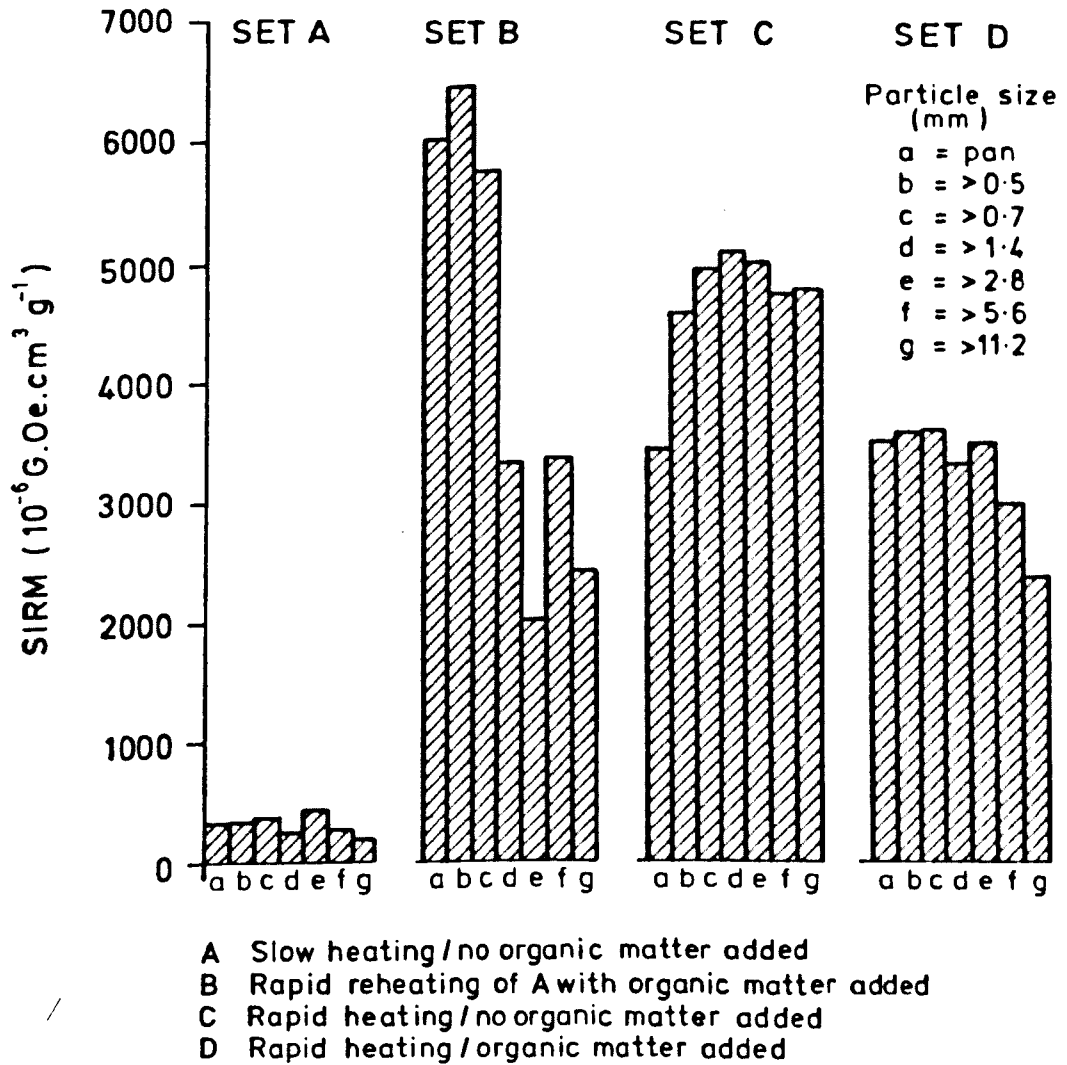


fig. 6.3.2 Effects of alternative toasting procedures.

crucial to maximum magnetic enhancement. (S.I.R.M. values are shown in preference to χ due to difficulties encountered on the equipment measuring such high χ values).

Fig. 6.3.3 plots χ against the different particle sizes for the toasted bedload that were used in the pilot study. The material was toasted at 800°C for 30 minutes after being rapidly heated to 800°C and quickly quenched to room temperature after heating. Due to the large bulk of the samples the ovens at the Pilkingtons Research Laboratory, Ormskirk, were employed. The diagram shows that maximum magnetic enhancement has been achieved only in the smaller grain sizes. The χ of the larger size fractions are, however, at least one order of magnitude greater than the untoasted bedload.

Due to time constraints it was decided that the levels of enhancement achieved in all the size fractions were sufficiently great to proceed with the pilot study.

Discussion

The full range of variables contributing to the success or failure of the production of maximum magnetic enhancement in χ and S.I.R.M. has not been systematically studied. The approach adopted in this study is pragmatic and designed to achieve an acceptable compromise between the degree of enhancement, bulk of material treatable and costs in terms of time and resources. The heating treatment adopted at Pilkingtons, was considered to be satisfactory although as indicated not perfect.

Oldfield et al (in press) have adopted a more systematic approach in studying the effects of different heat treatments on the production

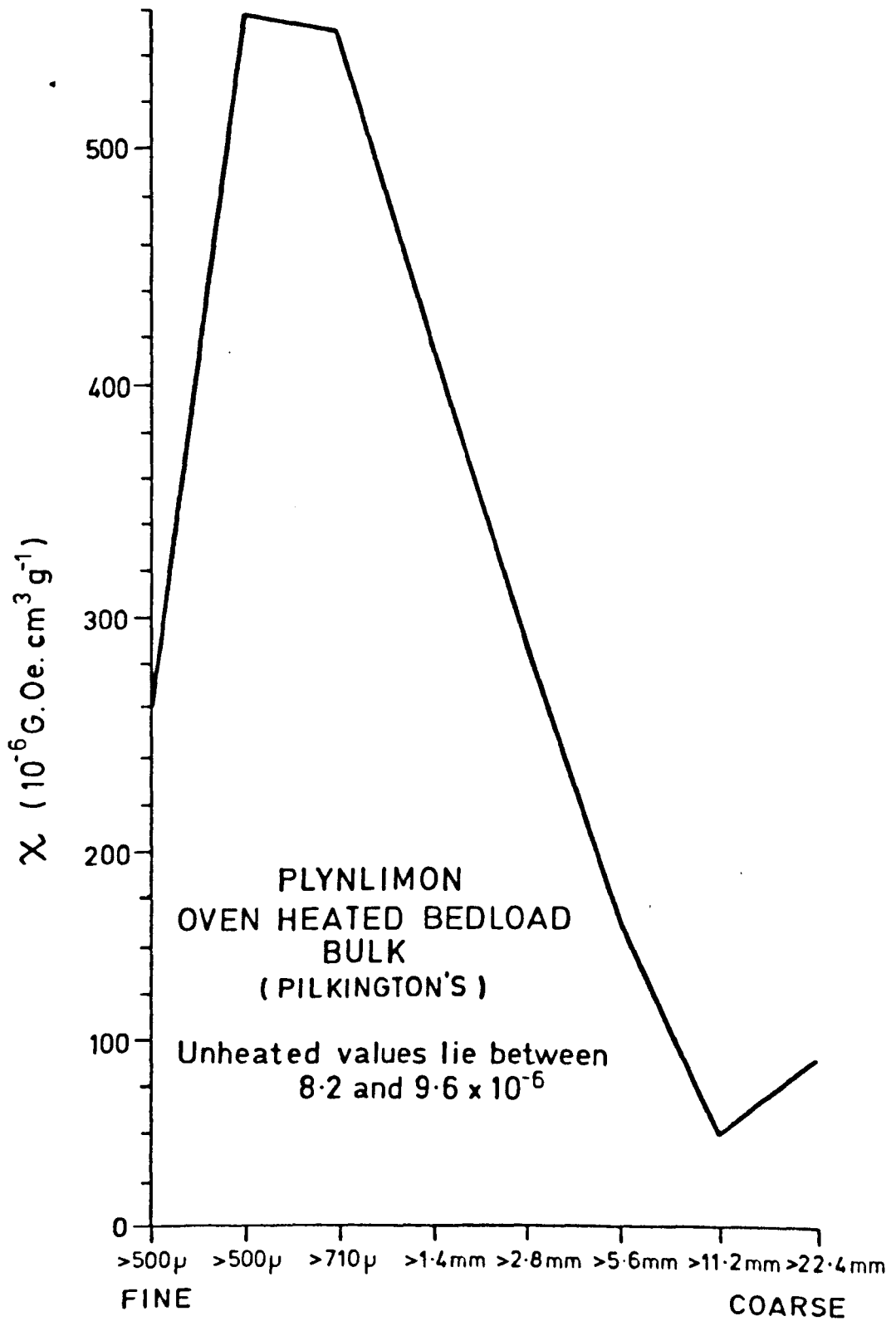


fig. 6.3.3 χ / grain size for toasted bedload used in the pilot study.

of maximum magnetic enhancement. They have investigated more fully the effects of the heat treatments on the magnetic mineralogy of the bedload samples: The dominant processes affecting the magnetic mineralogy during heating are firstly the growth of single domain magnetite followed by the formation of superparamagnetic magnetite, probably by both the breakdown of single domain magnetite and the growth of new crystals simultaneously with the formation of hematite. The fine magnetic particles dominate most of the magnetic properties of the heat-treated samples although hematite is produced in greater abundance.

PILOT STUDY 6.4Methodology

The treated bedload from the Pilkington experimental run was emplaced in streams Lower Tan A and Lower Tan in early November 1978 (Fig. 6.2.1). The treated shoals were recreated as near to their original form as possible on a percentage weight basis of the different size fractions. The two reaches were chosen because of stream bedload traps that were positioned approximately 200m. downstream of each shoal. The bedload traps were emptied after 'flood' events on the 4/12/1978 and the 9/1/1979. Lower Tan A is a fast eroding stream and had moved a sufficient amount of bedload for the bedload trap to be emptied after a minor flood event on the 27/11/78.

The trapped bedload material was air dried at room temperature and fractionated into 8 different size classes. Initially four 10cc aliquots of the different size fractions were measured for χ and S.I.R.M; however, the large volumes of trapped material in relation to the small samples measured introduced a sampling error. In the larger size fractions the sampling error was particularly significant where it became a matter of chance if the 10cc sample measured, contained a toasted pebble and was therefore not representative of the sample as a whole.

Subsequent measurements of the trapped material were made using a Littlemore Susceptibility Bridge Type 780 which enabled 250g. aliquots to be measured at a time allowing the whole of the trapped material to be measured. These results are used. Percentage dilution factors were compiled by measuring the χ of known dilutions of toasted material to untoasted bedload producing a dilution curve against which the χ

of the trapped material can be related, in order to ascertain the degree of dilution by untoasted bedload.

The χ of the trapped material was measured in the manner described and percentage dilution factors were obtained for each size fraction after each bedload trap emptying.

Results

Fig. 6.4.1 uses the control and mean toasted χ values in each size range to plot χ versus percentage concentration for each size range. The steeper slopes on the finer fractions reflect the greater degree of magnetic enhancement achieved during the toasting procedure, e.g. a value of around $20 \times 10^{-6} \text{G.Oe.cm}^3 \cdot \text{g}^{-1}$ for size fraction $> 710 \mu\text{m}$ indicates a 98% dilution of the toasted material by untreated material, whereas a χ value of around $10 \times 10^{-6} \text{G.Oe.cm}^3 \cdot \text{g}^{-1}$ indicates a 98% dilution factor for the 11.2 size range.

Fig. 6.4.2 plots the estimation of percentage concentration of the enhanced material for three size fractions; $> 710 \mu\text{m}$, 2.8mm and 11.2mm for the Lower Tan January 1979 emptying. The control, toasted and trap emptying χ values are given for each size fraction. In all cases χ values are higher than the χ of the control material indicating a percentage concentration of toasted material ranging from less than 1% for the finer fractions to greater than 1% for the coarsest fraction.

The low estimated mean concentration of 1.9% for the 11.2mm size fraction is due to the relatively low level of enhancement after toasting. However, the presence of at least one 250g sample with a χ value twice the control value confirms that magnetically enhanced toasted material is being detected.

PLYNLIMON BEDLOAD

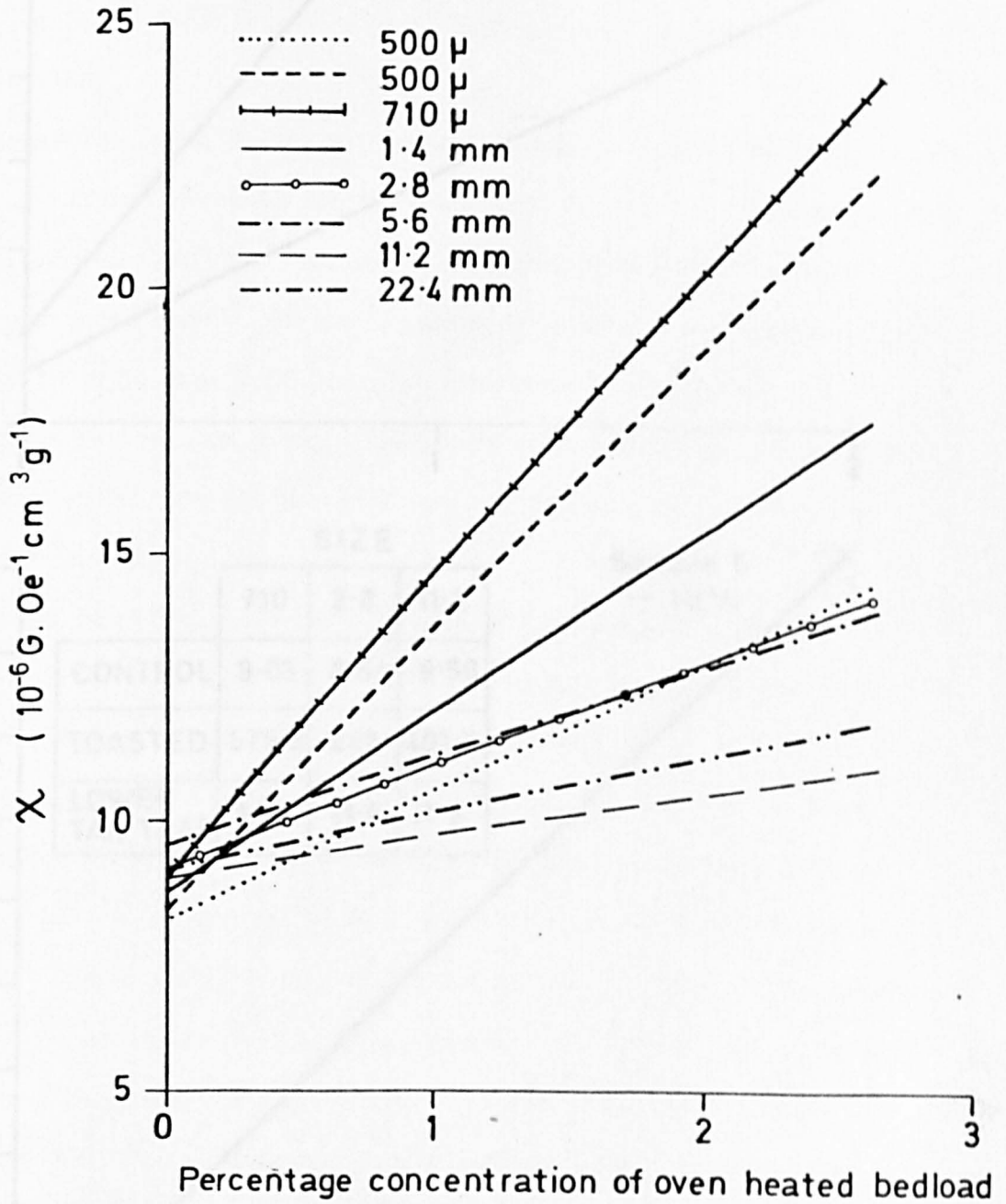


fig.6.4.1. Control/mean χ values for each size range versus percentage concentration.

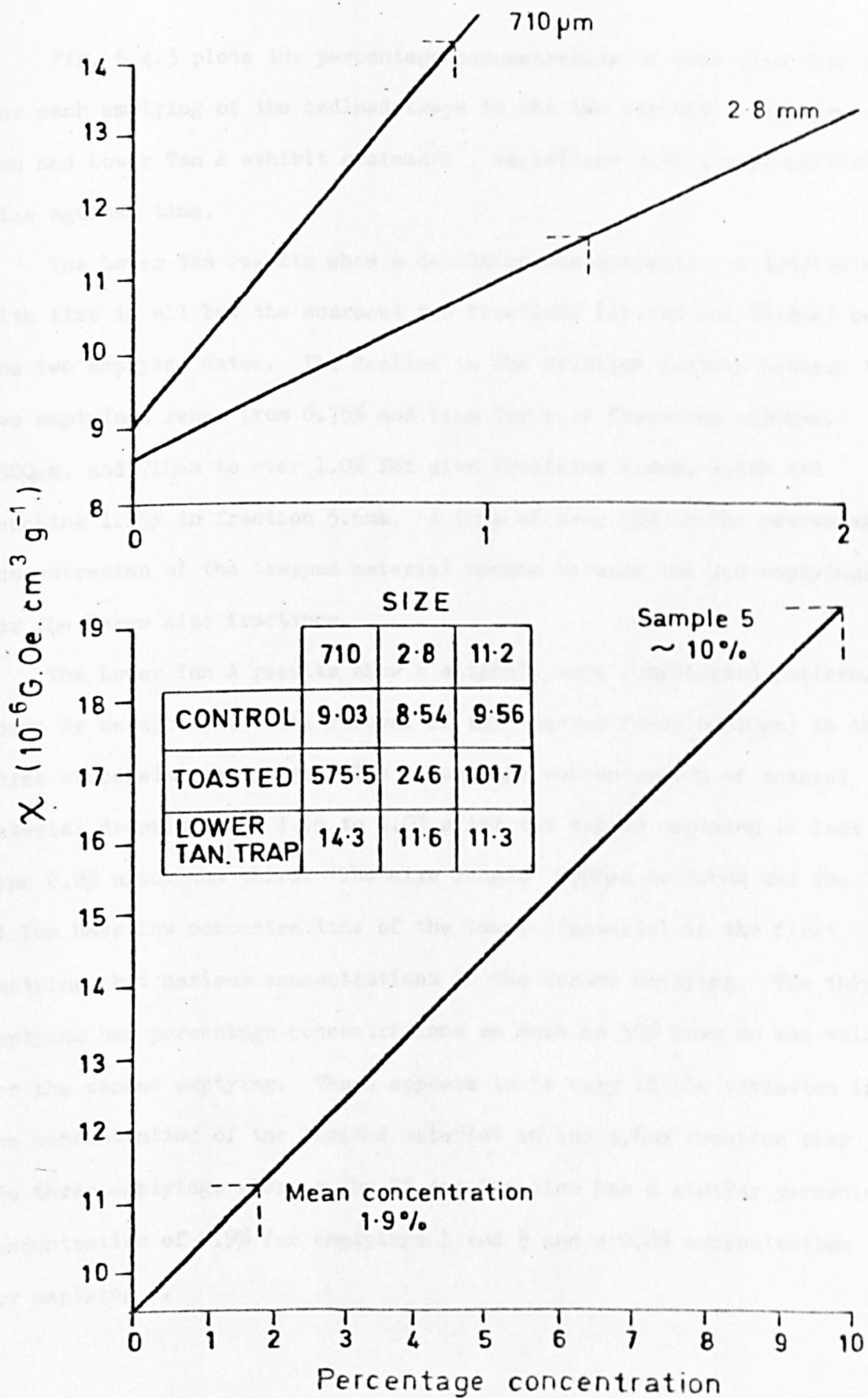


fig 6.4.2 Estimated percentage concentration of enhanced material size ranges 710 μm , 2.8 mm, and 11.2 mm.

Mean concentrations are shown by the dotted line.

Fig. 6.4.3 plots the percentage concentration of each size fraction for each emptying of the bedload traps in the two streams. Both Lower Tan and Lower Tan A exhibit systematic variations with stream particle size against time.

The Lower Tan results show a declining concentration of toasted material with time in all but the coarsest two fractions (11.2mm and 22.4mm) between the two emptying dates. The decline in the dilution factors between the two emptyings range from 0.75% and less for size fractions $<500\mu\text{m}$, $>500\mu\text{m}$, and $>710\mu\text{m}$ to over 1.0% for size fractions 1.4mm, 2.8mm and reaching 1.25% in fraction 5.6mm. A drop of over 50% in the percentage concentration of the trapped material occurs between the two emptyings for the large size fractions.

The Lower Tan A results show a slightly more complicated pattern. There is an apparent total removal of the toasted fines ($<500\mu\text{m}$) in the three successive emptyings. The percentage concentration of toasted material dropping from 1.4% to 1.0% after the second emptying to less than 0.2% after the third. The size ranges $>500\mu\text{m}$ to 5.6mm and the 11.2mm have low concentrations of the toasted material in the first emptying, but maximum concentrations in the second emptying. The third emptying has percentage concentrations as much as 50% down on the value for the second emptying. There appears to be very little variation in the concentration of the toasted material in the 5.6mm fraction over the three emptyings whereas the 22.4mm fraction has a similar percentage concentration of 0.9% for emptyings 1 and 3 and a 0.6% concentration for emptying 2.

Discussion

The interpretation of the sediment results indicate a differential movement of particle size with time in both systems. The interpretation of the results from Lower Tan are relatively straightforward. The 4/12/1978 flood event was the largest and the most significant.

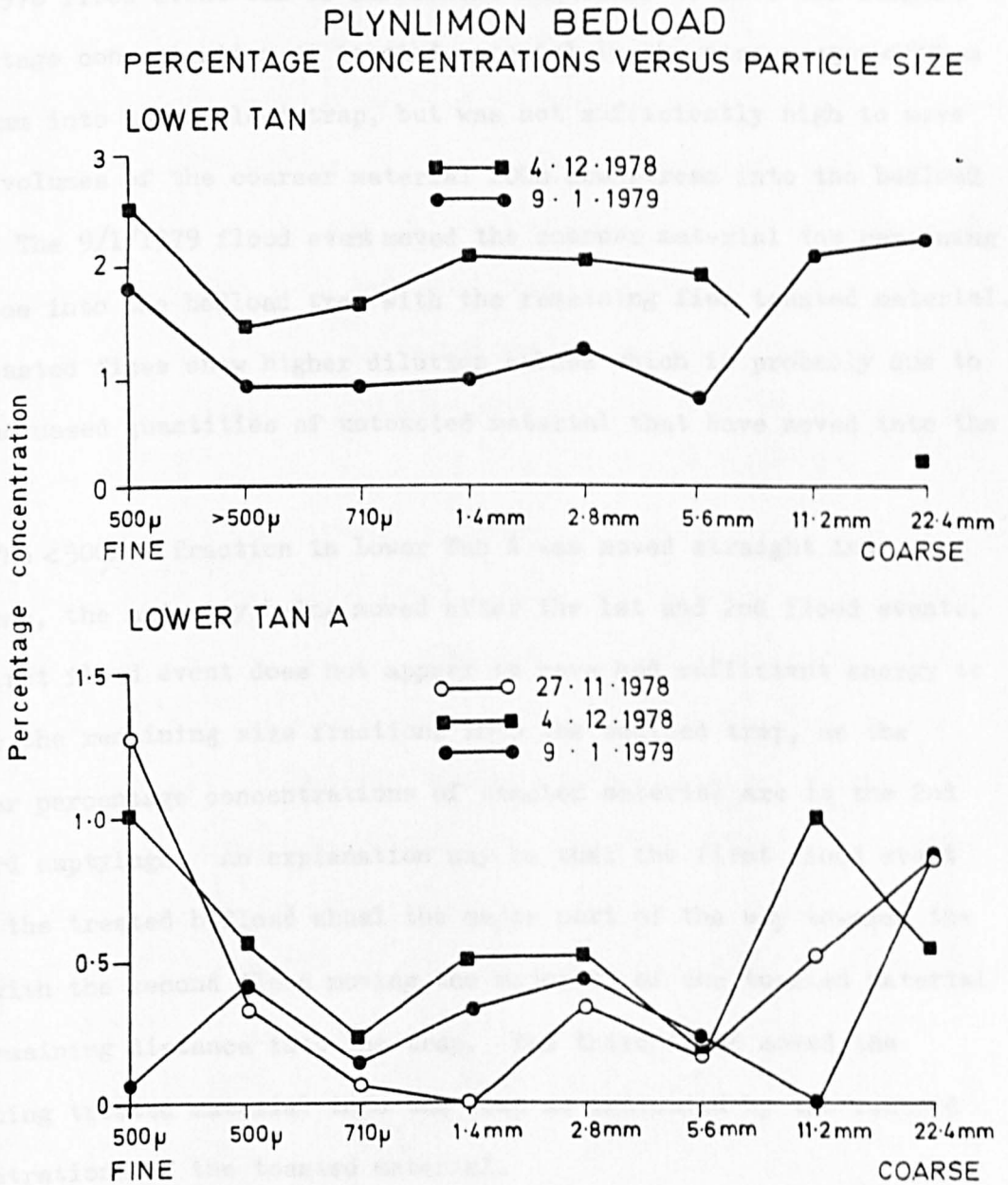


fig 6.4.3 Percentage concentrations for each fraction at each trap emptying. L. Tan and L. Tan A.

Discussion

The interpretation of the magnetic results indicate a differential movement of particle size with time in both streams. The interpretation of the results from Lower Tan are relatively straight forward. The 4/12/1978 flood event was of sufficient magnitude to move the largest percentage concentration of toasted material in the size ranges $<500\mu\text{m}$ to 5.6mm into the bedload trap, but was not sufficiently high to move large volumes of the coarser material 200m. downstream into the bedload trap. The 9/1/1979 flood event moved the coarser material the remaining distance into the bedload trap with the remaining fine toasted material. The toasted fines show higher dilution values which is probably due to the increased quantities of untoasted material that have moved into the trap.

The $<500\mu\text{m}$ fraction in Lower Tan A was moved straight into the trap, the majority being moved after the 1st and 2nd flood events. The first flood event does not appear to have had sufficient energy to remove the remaining size fractions into the bedload trap, as the greater percentage concentrations of toasted material are in the 2nd and 3rd emptyings. An explanation may be that the first flood event moved the treated bedload shoal the major part of the way towards the trap with the second flood moving the majority of the toasted material the remaining distance into the trap. The third flood moved the remaining treated material into the trap as indicated by the reduced concentrations of the toasted material.

The greater dilution of the treated material in Lower Tan A is a result of faster erosion and consequently much larger volumes of trapped natural, unenhanced, material from further upstream.

The results from both streams indicate that there still may be a certain amount of toasted material to be moved into the traps from the points of emplacement after the 9/1/1979 emptying, the last in the pilot study run.

The aim of the study was not primarily to provide an insight into the physics of bedload movement in the two streams, but to assess the feasibility of using magnetically enhanced bedload as a tracing technique.

The results indicate that it is possible, once the optimum toasting conditions have been established, to produce maximum magnetic enhancement in χ of between 2-3 orders of magnitude greater than the control bedload samples. In the pilot study maximum magnetic enhancement had not been established in the coarser fractions but due to the low χ of the bedload material the levels of enhancement were sufficient to be detected even when greatly diluted by untreated bedload.

The results from the pilot study have demonstrated that by toasting the natural stream bedload so as to radically alter the magnetic properties, it is possible to use the toasted material as a natural stream bedload tracer. However, some slight modification of the transport properties may result from the change in bulk density and shattering of the larger size fractions that occurs after toasting.

CONCLUSIONS 6.5

Within the constraints of the pilot run it has been demonstrated that magnetically enhanced natural bedload can be successfully used as a tracing technique. Despite some awkward logistical problems that are mainly concerned with the toasting procedure the magnetic technique offers several advantages over other techniques (section 6.1) although it has some limitations.

1. The use of natural bedload material that has been magnetically enhanced effectively reduces any problems that may result from changes in the transport dynamics of the stream arising from the introduction of artificial or foreign tracing mediums.
2. The enhanced magnetic properties of the toasted material are persistent and therefore of immense value in long-term tracing experiments, and could prove valuable alternatives to radioactive tracers. However, in short term studies the persistence of the treated material could pose a problem. No further studies using magnetic material could be embarked upon until all the toasted material from the previous trials had been totally removed from the test reach.
3. Due to the high levels of magnetic enhancement that can be achieved by the correct toasting procedure the treated material can be detected in very low concentrations, making it an important tracing technique in fast eroding streams and streams that carry large volumes of bedload material.

By being able to detect extremely low concentrations of toasted material Newson (1980) in a progress report, has demonstrated that it is possible, using a Whites Metal Detector, a Pulsed Induction Meter or a Bartington Meter to detect the treated material in transit. Enabling the distance moved by the enhanced bedload after each flood event to be monitored.

4. The technique offers great potential for increased sophistication. By using additional magnetic parameters coupled with the ability to selectively toast different size ranges it may be possible to fingerprint the different size fractions enabling complex tracing studies to be mounted.
5. The technique is inexpensive in terms of producing the tracer and in monitoring its progress and recovery of the material.
6. The magnetic technique is a safe and non-destructive to both the worker and the environment.
7. The relative success of the pilot study has indicated the potential of the technique in larger scale studies. A more extensive, systematic and detailed study is at present in progress using the magnetic bedload technique to trace bedload movement in the upper reaches of the River Severn.

However, the technique has only been proved in a well instrumented catchment with a magnetically favourable lithology and it is possible that in areas with a complex magnetic lithology the technique will not be as successful.

Because of the cheapness and relative ease with which the technique can be used, research in less magnetically favourable areas is in progress.

CHAPTER 7SUMMARY AND GENERAL CONCLUSIONS

(i) The study has utilized several magnetic parameters (χ , S.I.R.M. $(B_0)_{CR}$ and S.I.R.M./ χ ratio) to examine the effects of forest fires on the sediment source-lake sediment linkages in lake catchments. All the measurements are rapid, inexpensive and non-sample destructive. The review of the evidence suggests that burning produces in the soil magnetically enhanced secondary ferrimagnetic oxides. The study may essentially be regarded as in two parts : the first part examined the production of the secondary ferrimagnetic minerals in the soil and their movement via the source-sediment linkages. The second part examined the persistence of the secondary ferrimagnetic oxides within the lake and the soil environment.

(ii) In the soils of the Llyn Bychan catchment the production of the secondary ferrimagnetic minerals was shown to occur as a result of the heating of the soils by the forest fire. The secondary ferrimagnetic oxides were shown to have distinctive magnetic properties characterized by high χ and S.I.R.M. values, typically 2 to 3 orders of magnitude greater than unburnt soil values, low S.I.R.M./ χ ratios and low coercivities of S.I.R.M. $(B_0)_{CR}$ (typically 100-200 Oe).

The magnetic studies identified the oxides as magnetite with the Mössbauer spectra identifying the mineral as an impure non-stoichiometric form characterized by the formula $Fe_{2.9}O_4$. The magnetic properties of the oxide are shown to be dominated by a superparamagnetic form of iron together with a stable single domain and viscous component.

(iii) The main source-sediment linkages have been studied using the magnetic parameters and have identified the main pathways as soil creep following the loosening effects of rain splash. Sheet erosion was magnetically identified in several profiles e.g. TB23 and BY2, gully erosion from pockets of unstructured material typified by high χ and S.I.R.M. values. The highest increases in χ and S.I.R.M.

are shown to be in orange/pink material which relate to soil mineral horizons rich in forms of iron convertible to the enhanced secondary ferrimagnetic form. Sediment samples from stream traps not only indicated an input of magnetically enhanced minerals by these sources but also an output from the lake system down the outflow stream.

(iv) Within the lake environment the χ and S.I.R.M. results from the sediments in the lake bottom trap indicate the input of secondary ferrimagnetic oxides into the lake from sources in the catchment. The lake sediment cores have shown that the secondary ferrimagnetic oxides from a magnetically distinct layer at the mud-water interface that is easily and rapidly identifiable. Resampling of the lake sediments has shown the continual input of magnetically enhanced material into the lake and the persistence of the secondary ferrimagnetic oxides at or near the mud-water interface.

(v) The magnetic study of the bedload shoals in the outflow stream, Afon Abrach, indicates a loss of enhanced material from the lake catchment. The correlation of the χ of the particle sizes with distance downstream pointed to the use of naturally enhanced material as a stream bedload tracer. The Plynlimon case study is a direct result of these observations and successfully demonstrated, in a magnetically ideal situation, the use of artificially magnetically enhanced bedload material as a tracing medium.

The second part of the study was primarily concerned with examining the persistence of the secondary ferrimagnetic oxides in the lake and soil environment.

(vi) The enhanced magnetic properties are shown to be persistent over time in the soil environment. The magnetic studies of the soils from the Landes catchments have shown the feasibility of differentiating between burnt and unburnt soils on the basis of enhanced S.I.R.M. values in the top few centimetres of the burnt soils.

(vii) The identification in the sediments of Lakes Goddienduon, Biscarrosse and Sanguinet of a magnetically distinct layer, characterised by χ and S.I.R.M. values at least one order of magnitude greater than the normal values, indicates the persistence of the secondary ferrimagnetic oxides in the lake environment. Pollen and charcoal analysis of the Landes lake sediments identified the peaks in S.I.R.M. as being attributable to a forest fire with documentary and radiometric dating indicating temporal association with the 1949 forest fire.

(viii) The establishment of a dated magnetically distinct layer in the lake sediments enabled a core correlation scheme to be constructed and provides a known datum from which to assess the reliability and accuracy of other dating techniques. It also provides a marker for further sedimentation and limnological studies.

(ix) An effort was made to investigate more fully the potential of the technique to detect past forest fires in lake sediments. The sediments of a small lake with a long fire history were sampled. The magnetic results from the Lake Laukunlampi sediments have indicated the use of the technique in determining the periodicity and fire frequency in the catchment over the past 600 years. The use of magnetic indicators in detecting fire levels in the sediments by their non-destructive nature allows palaeoecological analysis to be performed on the identified samples thereby reducing the length of time normally associated with such studies. The S.I.R.M. results show the persistence of the secondary ferrimagnetic oxides in the lake environment over 600 years.

Further research

Further research stemming from the results of the study are now in progress.

(i) A recently burnt lake catchment, Llyn Geirrionydd (North Wales) is the site of an extensive study in which the movement of secondary

ferrimagnetic oxides from burnt soils into the lake sediments is to be quantitatively monitored. Three lake sediment traps have been placed in position in order to investigate the lake sedimentation rate, and erosional studies on burnt slopes have been set up to assess the rate of removal of the burnt soil by wind, soil and water erosion.

(ii) The use of the magnetic technique as a rapid method of identifying past forest fires is to be further studied by magnetically examining lake sediments with a known fire history on the basis of results from pollen and charcoal analysis.

(iii) The use of the magnetic bedload tracing technique is being extensively investigated in stream sediment studies at present under way in the Wye and Severn catchments. An effort is also being made to assess the usefulness of the technique in areas where the lithology is not so favourable for magnetic studies.

APPENDIX 1

Magnetic extracts were prepared in the following manner. The sample was dispersed in de-ionised water and placed in a 1 litre burette. A strong magnet was positioned above the tap touching the glass sides of the burette and the suspension was allowed to slowly drip out into a beaker. The magnetic grains in the suspension are attracted to the sides of the burette, where the magnet touches, and remain on the sides after all the suspension has drained out. The tap is then closed and the magnet removed. The magnetic extract is then flushed out of the burette with de-ionised water into a beaker. The procedure is repeated numerous times so as to attain a pure as magnetic extract possible.

APPENDIX 2

The lake bottom sediment trap is shown in Fig. 8.2. The trap essentially consists of two compartments; the outer compartment is divided into two quadrants. The inner compartment is higher than the outer compartment in an effort to reduce any input into the trap by re-suspension, which may occur in the outer compartments. Håkanson (1976) explains the need for extensive walls to reduce the input of resuspended material but also warns to the dangers of creating eddies in the water over the trap and subsequent removal of the trapped sediment.

The trap was weighted by four concrete blocks. To orientate the trap the apparatus was designed to slide over a central shaft constructed of square cross sectional drainpipe which was hammered into place in the deepest part of the lake. The trap was orientated in relation to the drainpipe and gently placed on the lake bottom with the aid of lifting lines. A collar was placed around the square cut-out to minimize re-suspension through the opening into the inner compartment.

The lifting lines were bouyed below the water surface, the trap being raised over the central shaft emptied and re-orientated onto it again before emplacement.

The trap was designed to investigate any preferred direction in sedimentation in the catchment. Two outer compartments were orientated towards the burnt half of the catchment and two to the unburnt half (Fig. 2.11.6). The central compartment would only catch material falling directly into the trap and not any material that may roll down the slopes of the trench (Fig. 2.2.3) and be recorded in the outer compartments.

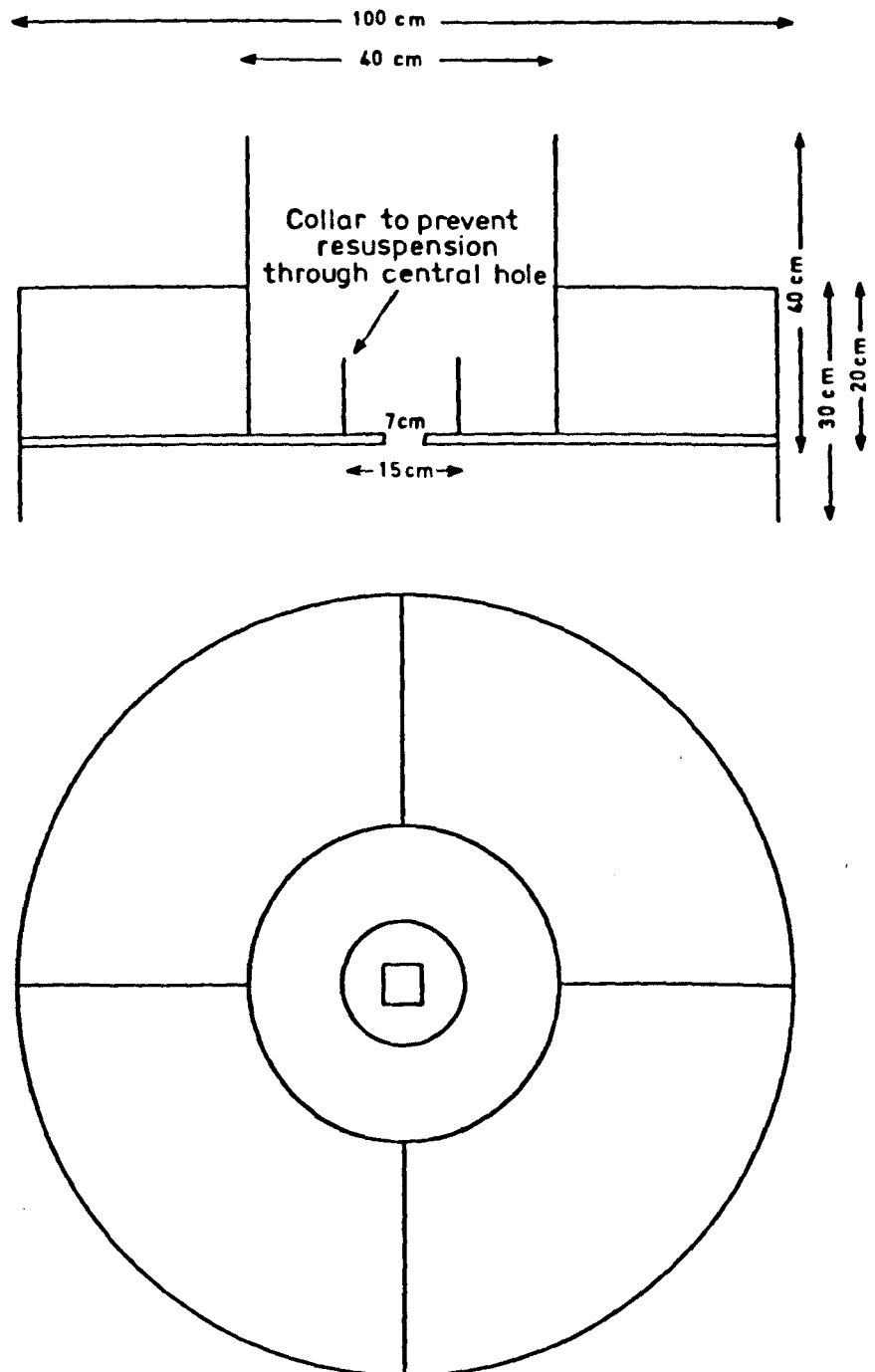


fig. 8.2 Lake Bottom sediment trap

APPENDIX 3

Fig. 8.3 shows the design of the stream sediment traps. The traps are of a simple design consisting of a 5 litre polythene bottle with the lid removed, the opening serving as an inlet and a small outlet hole drilled in the bottom. The bottle is attached to two wooden stands and placed in the stream with the inlet pointing upstream.

A large volume of water flows into the trap, where the outlet only allows a small volume of water to exit, causing the water velocity in the trap to reduce, thereby depositing its suspended sediment load.

Traps were placed in the burnt inflow, unburnt inflow and the outflow stream (Fig. 2.13.1). Emptyings were attempted as a regular basis but vandalism reduced the programme to two emptyings.

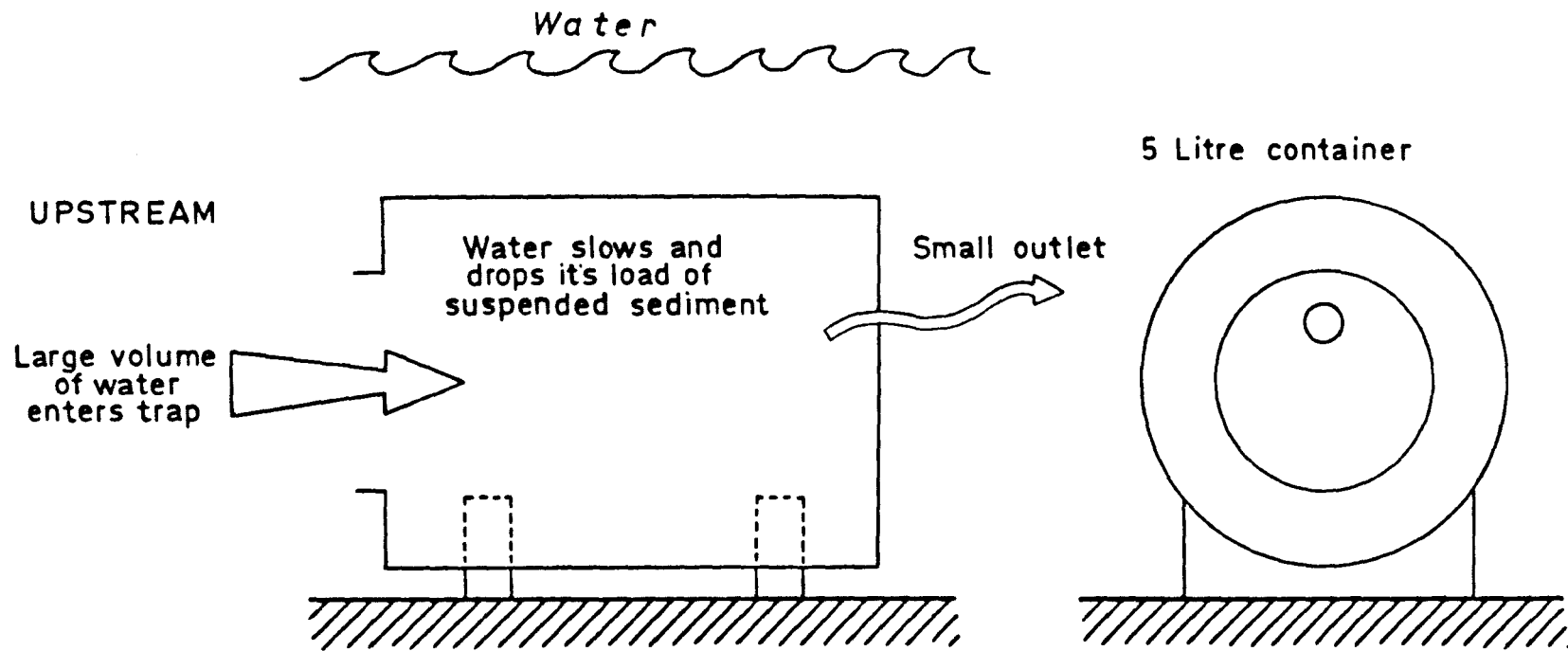


Fig. 8.3 Stream sediment trap

APPENDIX 4

Some of the authors publications

- Rummery. T.A., Bloemendal. J., Dearing. J.A., (1979) The persistence of fire induced magnetic oxides in soils and lake sediments.
 Oldfield. F., and Thompson. R.
Annls. Geophys. 35
- Longworth. G., Becker. L.W., Thompson. R., (1979) Mossbauer effect and magnetic studies of secondary iron oxides in the soil.
 Oldfield. F., Dearing. J.A., and Rummery. J.A.
J. Soil. Sci. 30
- Thompson. R., Bloemendal. J., Dearing. J.A., (1980) Environmental applications of magnetic measurements.
 Oldfield. F., Rummery. T.A., Stober. J.C.,
 and Turner. G.M.
Science 207

The persistence of fire-induced magnetic oxides in soils and lake sediments

by

T.A. RUMMERY, J. BLOEMENDAL, J. DEARING and F. OLDFIELD

Department of Geography, University of Liverpool, Liverpool, U.K.

R. THOMPSON

Department of Geophysics, University of Edinburgh, Edinburgh, U.K.

ABSTRACT. — *Measurements of magnetic susceptibility (χ) and saturation isothermal remanent magnetization (SIRM) have been carried out on soils recently subject to the effects of major forest fires, and on lake sediments which include material eroded from the burnt soils. The results confirm that the secondary ferrimagnetic minerals formed as a result of heating may persist both in the soils and in the sediments derived from them. This accords with the predictions of Le Borgne in his early studies of soil magnetism.*

Demonstration of the persistence of fire-induced magnetic oxides in sediments has implications for the study of sediment sources, landuse history and erosion rates, for core correlation and for the interpretation of natural remanent magnetization (NRM).

RESUME. — *Des mesures de la susceptibilité magnétique (χ) et de l'aimantation rémanente isotherme à saturation ont été effectuées sur des sols soumis récemment aux effets de feux de forêts importants, et sur des sédiments lacustres qui contiennent des matériaux provenant de l'érosion des sols brûlés. Les résultats confirment que les minéraux ferrimagnétiques secondaires formés par chauffage peuvent persister à la fois dans les sols et les sédiments qui en dérivent. Ceci est en accord avec les prédictions de Le Borgne des ses premières études sur le magnétisme des sols.*

La démonstration de la persistance des oxydes magnétiques induits par le feu dans les sédiments a des implications pour l'étude des sources de sédiments, l'histoire de l'utilisation des terrains et les taux d'érosion, pour la corrélation des carottes et pour l'interprétation de l'aimantation rémanente naturelle (ARN).

1. Introduction

In documenting the formation of secondary ferrimagnetic oxides in or near the surface of a wide variety of soils, Le Borgne (1955) noted the possibility of their survival in soils and also their subsequent transport and survival in sediments:

"Le constituant magnétique de néoformation présent dans les sols est stable dans les conditions naturelles, sauf, toutefois, dans les sols très humides où le fer est mobilisé par les fermentations, puis entraîné par le drainage. Lorsque le sol reste sur place, ses propriétés magnétiques se conservent et on les retrouve dans les sols fossiles.

Par contre, le départ des éléments superficiels sous l'action de l'érosion laissera un sol de susceptibilité réduite et ces effets de l'érosion seront d'autant plus sensibles que les fractions fines sont les plus magné-

tiques. Si les particules entraînées ne subissent pas d'autre action que celle de l'air et de l'eau, ces propriétés des sols superficiels doivent se retrouver dans les sédiments qu'ils fournissent, d'où l'application, signalée dans l'introduction, des propriétés magnétiques du sol aux recherches archéologiques. D'un point de vue plus général, l'étude des propriétés magnétique des sédiments peut apporter des données expérimentales concernant les rapports entre la pédogénèse et la genèse des sédiments".

Mullins (1977) in his comprehensive review of studies of soil magnetism concludes that secondary ferrimagnetic oxides may form at or near the soil surface as a result of any one or more of the following processes:

- (i) the effects of fire,
- (ii) the dehydration of lepidocrocite,

(iii) the alternate oxidation and reduction of initially paramagnetic iron compounds in natural pedogenic processes.

(iv) low temperature oxidation of magnetite to maghaemite.

Strong though often circumstantial field evidence exists for the importance of both the first and third of these mechanisms. Following Le Borgne, the resulting mineral has usually been identified as impure maghaemite, $\gamma\text{Fe}_2\text{O}_3$. Recent studies using Mössbauer and thermomagnetic analyses indicate that both maghaemite and magnetite may be formed in the soil.

The present paper deals with sites with a well documented history of burning and considers evidence for the persistence of fire-induced magnetic oxides both in the soil and in lake sediments derived from them. The question of persistence arises from recent studies of the magnetic properties of lakes (Thompson *et al.* 1975; Oldfield *et al.* 1978a) and stream sediments (Oldfield *et al.* in press) and of peats (Oldfield *et al.* 1978b). These studies have demonstrated the successful application of non-destructive magnetic measurements for core correlation, as well as for identifying sediment sources within both streams and lakes.

Ferrimagnetic spinel-type oxides dominate the magnetic properties of many of these sediments. In some cases, especially where the bedrock of the source areas either lacks magnetic forms of iron or where it is dominated by canted anti-ferromagnetic fine grained haematite cement, the incorporation and persistence in the sediments of secondary oxides resulting from the magnetic enhancement of topsoil seems likely though this possibility has not previously been systematically evaluated. The present paper reports the formation and fate of secondary magnetic oxides resulting from well dated and documented heath and forest fires in four lake drainage basins.

2. Llyn Bychan, North Wales

Llyn Bychan (Fig. 1) lies in an area of Ordovician Slates. An extensive forest fire in August 1976 destroyed heathland and forest along the western flank of the lake and burnt off areas of shallow peat and raw humus to expose the underlying mineral layers to the action of intense heat under at least partially reducing conditions. Mössbauer effect studies on the burnt soil confirm that here the ferrimagnetic material in both the bulk samples and magnetic extracts is magnetite. (Longworth *et al.* in press).

Figure 2 shows down-profile variations in χ at a site where burnt soil had, within 8 months of the fire, become buried by rapidly eroding surface material from upslope. Figure 3 plots saturation isothermal remanent magnetization (SIRM) down a 1 m sediment

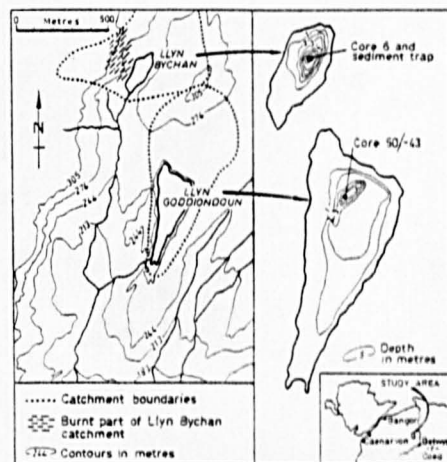


Fig. 1

Location of Llyn Bychan and Llyn Goggiionduon, N. Wales.

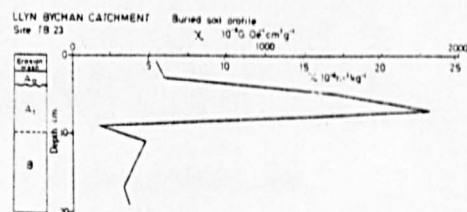


Fig. 2

Soil profile from the Llyn Bychan catchment. Magnetic susceptibility vs depth in a soil burnt in August 1976 and subsequently buried by eroded material from upslope.

core from the centre of Llyn Bychan obtained in December 1976, 4 months after the fire. The core, taken with a pneumatic Mackereth minicorer (Mackereth, 1969) preserves a perfect mud-water interface at the top. The low and relatively constant susceptibility values of all but the top 2 cm lie in sediment accumulated over many centuries. The uppermost material has SIRM values 20 times greater than the mean value below and represents material blown and washed into the lake during the fire and the ensuing few months. A lake-bed sediment trap was emplaced in December 1976 in the centre of the lake at the coring point, and raised in June 1977. The trap consisted of four quadrants and a raised central section and was orientated. The SIRM of trapped material in each compartment shows that magnetically enhanced material has

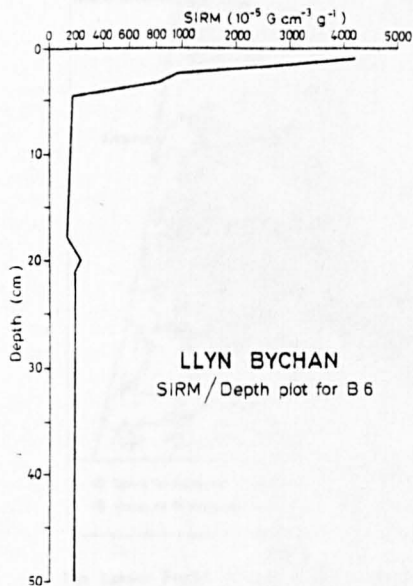


Fig. 3

Sediment core from the centre of Llyn Bychan. Specific saturation Isothermal Remanent Magnetization vs depth.

continued to contribute the bulk of the suspended particulate input to the site subsequent to the fire. Specific susceptibility and SIRM measurements on stream bed-load derived from the burnt areas give values 10 to 40 times greater than those of unburnt substrate and confirm the downstream movement of fire-enhanced magnetic material.

3. Llyn Goddionduon, North Wales

This lake lies less than 1 km from Llyn Bychan (Fig. 1). An extensive fire in an area of Forestry Commission Plantation on the eastern shore of the lake occurred in 1952. A grid of 150 sediment cores obtained from the lake in 1977 included many with a major increase in χ , SIRM, and anhysteretic magnetization (ARM) in black sediment forming the top 10-20 cm of the profile. Figure 4 illustrates these increases in core 50/-43. Pollen-analytical studies (Bloemendal, 1977) confirm the dramatic increase in ferrimagnetic mineral concentrations post-dates the partial afforestation of the catchment by exotic conifers which began in the mid-late 1930's. ^{137}Cs dating of the profile shows that the first presence of fall-out Caesium, dated to 1954 (Pennington *et al.* 1973;

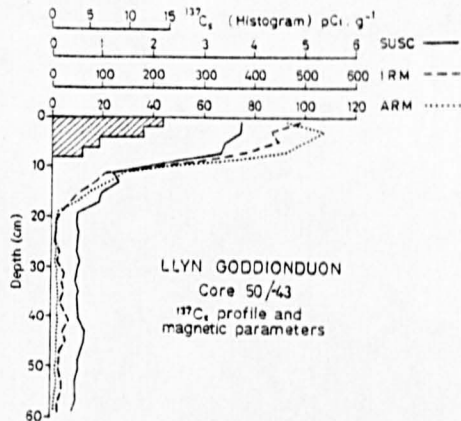


Fig. 4

Llyn Goddionduon, Core 50/-43. Caesium-137 concentrations and magnetic parameters for single samples down a 60 cm long sediment core.

Ritchie *et al.* 1973) occurs at 8 cm, 2 cm above the base of the recent most rapid increase in the concentration of magnetic oxides. These data therefore place the age of the increase within the time range 1940 to 1954 and are compatible with a direct correlation between the increase in concentration of magnetic minerals in the lake sediments and the forest fire.

4. The Landes, South West France

During the 1940's extensive forest fires occurred in the then almost ubiquitous commercial stands of *Pinus pinaster* which had been established from 1850 onwards on the Quaternary outwash sands of the region (Fig. 5). These fires culminated in the major burn in the summer of 1949 which destroyed a vast area much of it in the drainage basins of the Etang de Sanguinet and the Etang de Biscarosse et de Parentis. Many of the tracts of soil which were burnt during the 1940's can still be readily distinguished both by reference to published maps and from the age structure of the surviving pine stands. Figure 6 plots SIRM vs. depth for a variety of burnt and unburnt soil profiles from the catchments of the Etang de Sanguinet, and the Etang de Biscarosse et de Parentis. Figure 7 plots whole core susceptibility measurements (cf. Thompson *et al.* 1975) for cores from the Etang de Biscarosse et de Parentis and confirms the presence of peak values of χ in the upper part of most cores. Core BP6 was chosen for ^{137}Cs and ^{210}Pb dating as well as for more detailed single sample magnetic and pollen-analytical study. Single sample SIRM values for this core are

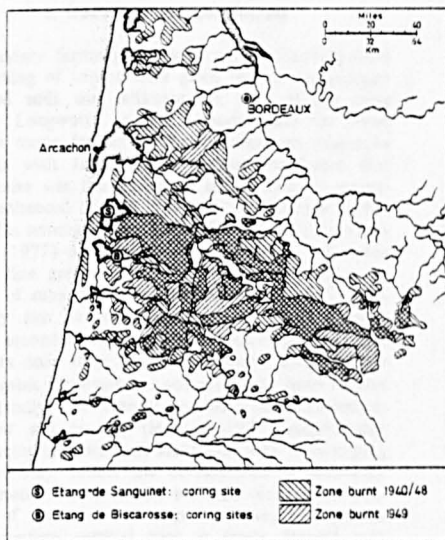


Fig. 5

The Landes Region of S.W. France locating the Etang de Sanguinet and the Etang de Biscarosse et de Parentis in relation to the areas affected by major forest fires.

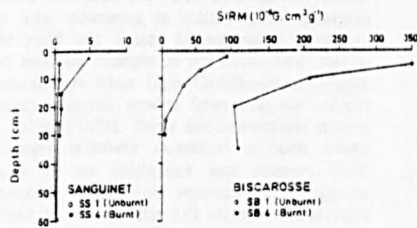


Fig. 6

Soil profiles from burnt and unburnt areas in the Landes region. SIRM vs depth.

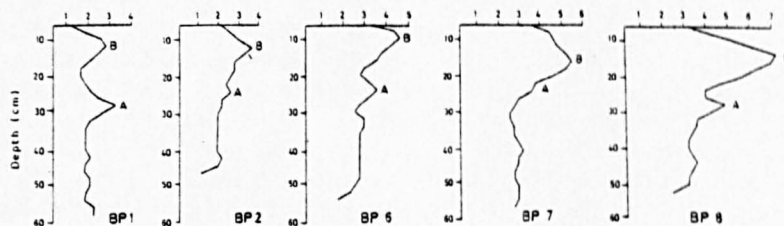


Fig. 7

Whole core susceptibility profiles from the Etang de Biscarosse et de Parentis.

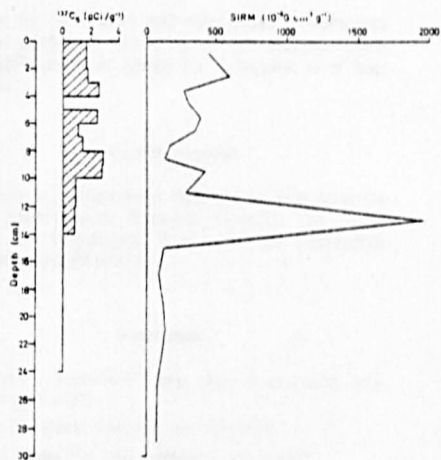


Fig. 8

Caesium-137 concentrations and SIRM vs depth for Core BP 6, Etang de Biscarosse et de Parentis.

plotted in Figure 8 which also records the ^{137}Cs profile. The position of the peak SIRM values at 12-14 cm, only just below the 1954 level of ^{137}Cs increase is compatible with a date during the previous decade of forest fires. Analyses of charcoal concentrations and pollen content, including pine pollen breakage ratios (cf. Oldfield, 1978) confirm the coincidence between the level of peak SIRM and the forest fires.

In the Etang de Sanguinet, peak ^{137}Cs and SIRM values in the top 0.5 cm of the record indicate a depositional history comparable to that at Biscarosse but preserved in sediments which have accumulated too slowly to permit detailed identification of the sequence of events during the last few decades. The results of stratigraphic and ^{210}Pb analysis confirm that the last 250 y is represented by only 2.5 cm of sediment.

5. Discussion and Conclusions

Secondary ferrimagnetic iron oxides resulting from the burning of topsoil have given rise to magnetically enhanced soils and sediments in each of the areas studied. Longworth *et al.*'s demonstration (in press) that the oxide formed at Llyn Bychan was magnetite contrasts with Le Borgne's original conclusion that maghaemite was the dominant spinel form in magnetically enhanced topsoil. The sum of evidence so far, much of it summarised in Mullins (1977) and Longworth & Tite (1977) suggests that the enhanced iron oxide is very fine grained ($< 1 \mu\text{m}$), frequently impure as a result of substitution e.g. by Mg, Al, Na or Ti ions, and may also be non-stoichiometric. The persistence of the secondary ferrimagnetic oxides in soils and sediments once they have been formed either by fire or pedogenic processes has not previously been studied systematically. Consistently low levels of enhancement in gleyed soil profiles (Mullins, 1977) suggest that the reducing environments associated with waterlogging may not only inhibit the development of secondary ferrimagnetic oxides in soil but also lead to the conversion of some to non-magnetic forms. The present results confirm survival both in freely drained soils and in lake sediments at least over a timespan of decades. Taken together with studies of secondary magnetic minerals in suspension as part of the river-borne particulate load (Oldfield *et al.* in press) the present results reinforce the value of magnetic measurements in lake sediments as indicators of variations in sediment yield and source in response to environmental and land-use changes in the catchment. Remanence measurements from Llyn Goddionduon suggest that secondary minerals eroded from soils are carriers of natural, stable, PDRM. These and comparable studies of much longer sediment sequences in lakes where the bedrocks of the catchment lack primary ferrimagnetic minerals suggest that secondary ferrimagnetic oxides formed at or near the soil surface in the ways

described by Le Borgne and subsequent authors may not only contribute the bulk of the magnetic input to the sediments but persist on timescales of at least 10^3 years.

Acknowledgements

We wish to acknowledge financial support from the Natural Environment Research Council, The Royal Society, the Leverhulme Trust and the Universities of Liverpool and Edinburgh.

References

- Bloemendal J., Unpublished Thesis, Dept. of Geography, Univ. of Liverpool, 1977.
- Le Borgne E., *Annals. Geophys.*, 11, 399, 1955.
- Longworth G. and M.S. Tite, *Archaeom.*, 19, 3, 1977.
- Longworth G., L.W. Becker, R. Thompson, F. Oldfield, J. Dearing and T.A. Rummery, *J. Soil Sci.*, in press.
- Mackereth F.J.H., *Limnol. Oceanogr.*, 14, 145, 1969.
- Mullins C.E., *J. Soil Sci.*, 28, 223, 1977.
- Oldfield F., *Pollen et Spores*, 20, 167, 1978.
- Oldfield F., J. Dearing, R. Thompson and S.E. Garrett-Jones, *Polish Arch. f. Hydrobiol.*, 25, 321, 1978a.
- Oldfield F., R. Thompson and K.E. Barber, *Science*, 199, 679, 1978b.
- Oldfield F., T.A. Rummery, R. Thompson and D.E. Wailing, *Water Resources Research*, in press.
- Pennington W., R.S. Cambay and E.M. Fisher, *Nature, Lond.*, 242, 324, 1973.
- Ritchie J.C., J.R. McHenry and A.C. Gill, *Limnol. and Oceanogr.*, 18, 254, 1973.
- Thompson R., R.W. Battarbee, P.E. O'Sullivan and F. Oldfield, *Limnol. and Oceanogr.*, 20, 687, 1975.

MÖSSBAUER EFFECT AND MAGNETIC STUDIES OF SECONDARY IRON OXIDES IN SOILS

G. LONGWORTH¹, L. W. BECKER¹, R. THOMPSON², F. OLDFIELD³, J. A. DEARING³
and T. A. RUMMERY³

Summary

Simple, rapid and non-destructive measurements of magnetic properties (magnetic susceptibility, saturation isothermal remanent magnetization and coercivity of isothermal remanence) coupled with more time consuming and sophisticated analyses such as thermomagnetic and Mössbauer effect studies, provide a basis for identifying forms of iron oxide present in the soil.

At two of the sites studied, Caldy Hill, Merseyside, and Llyn Bychan, N. Wales, the secondary ferrimagnetic oxide formed in surface soil as a result of recent forest fires is shown to be non-stoichiometric magnetite approximating to the formula $Fe_{2.9}O_4$. No evidence for the presence of maghemite was found in any of the soil samples from these sites or in soils from the Annecy region of S.E. France.

Introduction

NUMEROUS studies record the formation of secondary ferrimagnetic iron oxides in soils developed on sedimentary rocks. In a recent review article, Mullins (1977) summarises evidence for the origin, nature and composition of the oxides so formed and concludes that several possible mechanisms are involved, including burning, dehydration of lepidocrocite, and the alternate wetting and drying normally involved in pedogenesis. He cites several authors who have used a variety of techniques to identify the ferrimagnetic minerals in soils but recommends caution in evaluating the conclusions reached (p. 234). Although Neumeister and Peschel (1968), and Vadyunina and Kovtun (1974) claim to have identified magnetite, the majority of authors, whether on the basis of experimental methods designed to simulate the pedogenic processes inferred (e.g. Tite and Mullins, 1971, Taylor and Schwertmann, 1974), X-Ray diffraction studies or, more recently, Mössbauer effect studies (Longworth and Tite, 1977), have followed Le Borgne (1955, 1960) in identifying the mineral resulting from enhancement by thermal and/or chemical transformation as maghemite.

Recent studies of magnetic minerals in lake sediments suggest that they provide not only a rapid means of core and sample correlation but also a powerful tool in differentiating types and sources of allochthonous input (Thompson *et al.*, 1975; Oldfield *et al.*, 1978). Evaluating and interpreting the contribution to lake sediments of secondary magnetic minerals formed in the soil depends in part on a further understanding of their origin, nature and chemical composition as well as their persistence, in the soil itself, during transport and in the depositional environment of the lake.

¹ Mössbauer Group, AERE, Harwell.

² Department of Geophysics, University of Edinburgh.

³ Department of Geography, University of Liverpool.

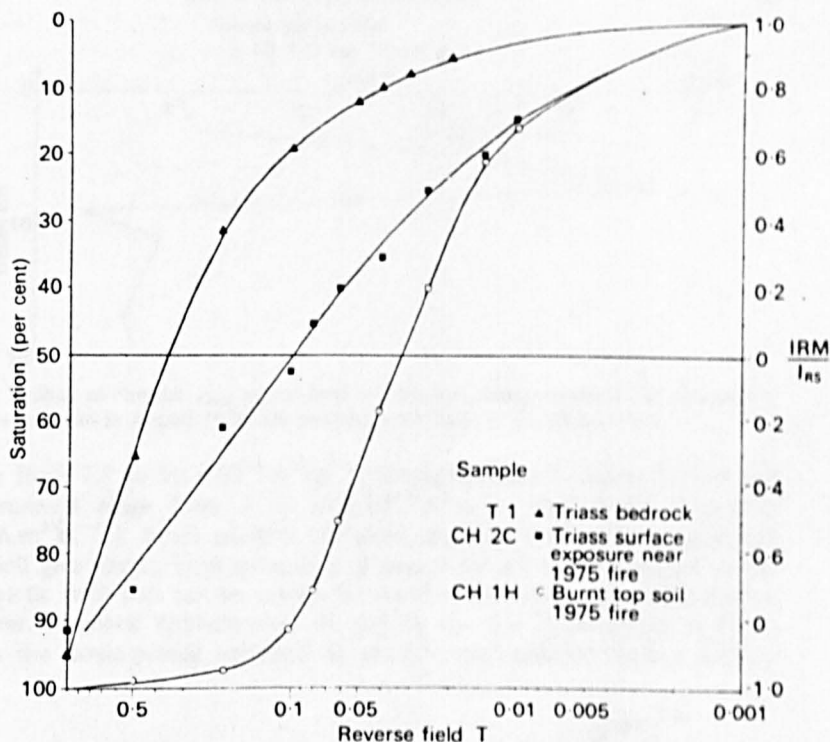


FIG. 1. Caldly Hill. Coercivity of IRM (B_{CR}) profiles for unweathered bedrock (T1), and for the finest particle size fraction ($<63 \mu\text{m}$) taken from a partially weathered rock face close to the edge of the burnt area (CH2C) and from burnt topsoil (CH1H).

0.02T pointing to the presence of ferrimagnetic oxides. In higher reversed fields the spectra diverge in a manner consistent with dominance of the burnt soil extract by fine grained ferrimagnetic magnetite/maghemite and the parent material by fine grained antiferromagnetic haematite. The failure of the soil extract to saturate in a reversed field of 0.1T probably indicates the survival of a significant amount of haematite in the soil sample (*cf.* Table 3), though proportionally much less than exists in the parent material. The susceptibility data and the B_{CR} profiles may be interpreted as reflecting the partial transformation of antiferromagnetic haematite cement within the parent material into ferrimagnetic iron oxides largely if not entirely as a result of burning.

Llyn Bychan

A substantial part of the lake's catchment was burnt in a major fire during August 1976. This provided an opportunity to study the nature of the magnetic minerals formed during the fire, their persistence in the soils and their incorporation into stream and lake sediments. Over thirty samples were taken from soils in the burnt and unburnt parts of the catchment in addition to several from stream bedloads as well as cores from the lake sediments.

Specific susceptibilities for parent material derived from local mining waste, from the base of soil profiles and from the bed-load of streams draining unburnt

SECONDARY IRON OXIDES

97

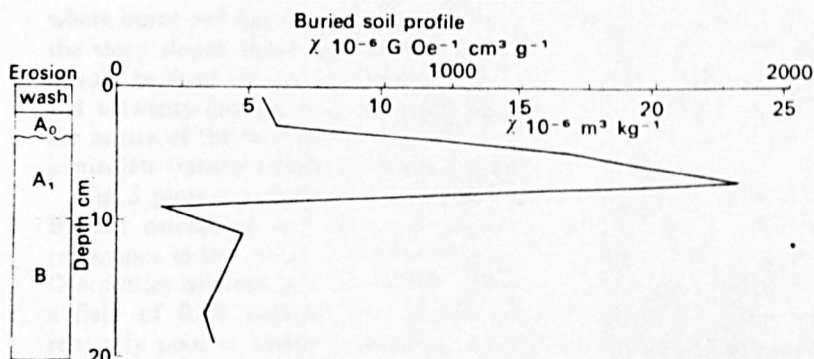


FIG. 2. Llyn Bychan catchment. I_{RS} values from a burnt and subsequently buried soil profile; fire occurred in August 1976; the samples were taken in December 1976.

areas ranges from 7.5 to $90 \times 10^{-8} \text{ m}^3 \text{ kg}^{-1}$. Susceptibilities for burnt surface soil (0–2 cm) material range from 1 to $33 \times 10^{-6} \text{ m}^3 \text{ kg}^{-1}$, (I_{RS} from 9 to over $50 \times 10^{-3} \text{ A.m}^2 \text{ kg}^{-1}$). Small pockets of baked, exposed and highly magnetized orange subsoil give rise to local anomalies of over 1000 nT in the strength of the earth's magnetic field and can be readily detected *in situ* using a portable Proton Magnetometer. Magnetic enhancement of soil by the fire is illustrated in Fig. 2 which plots the down-profile variation in specific susceptibility from a locality

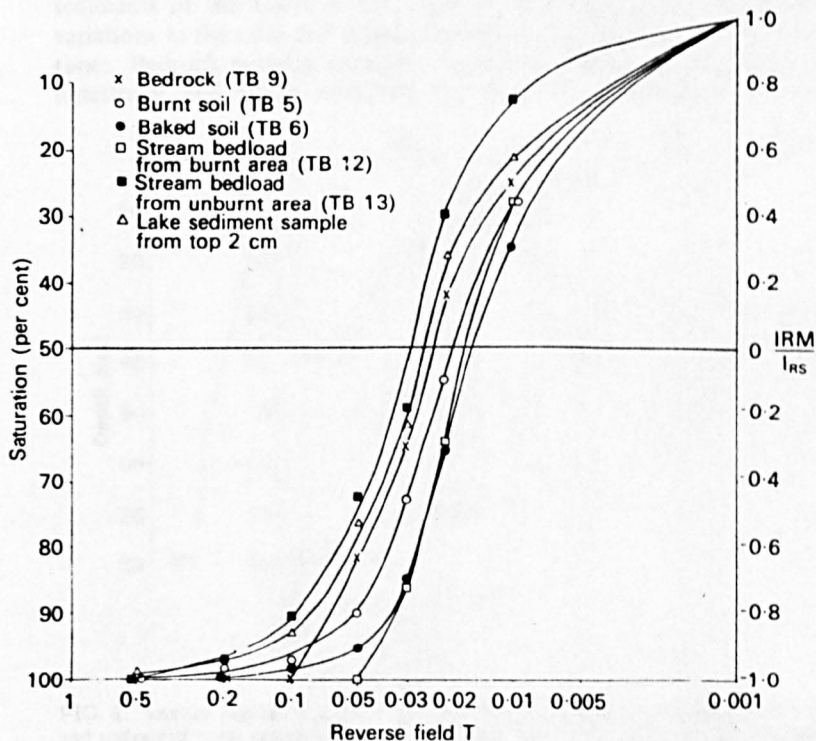


FIG. 3. Llyn Bychan catchment. Coercivity of IRM (B_{cR}) profiles for a variety of materials.

where burnt soil had been subsequently covered over as a result of rapid erosion on the steep slopes above which have been stripped bare of vegetation by the fire. Stream bedload derived from the burnt areas has enhanced susceptibility values, and a twenty-fold increase in I_{RS} in the top 2 cm of a sediment core taken from the centre of the lake in November following the August fire points to the almost immediate transfer of some burnt material to the lake bed.

Fig. 3 plots coercivity of I_{RS} profiles for a selection of samples from the Llyn Bychan catchment and lake. All show a rapid change in isothermal magnetic remanence in low fields and all become 90% to 100% saturated in a field of 0.1T. Coercivities between 0.01 and 0.04T coupled with the high percentage saturation in a field of 0.1T indicate that all the material measured, even the bedrock, is relatively poor in antiferromagnetic minerals (*cf.* Table 3). Burnt soil and stream bedload samples derived from the fire show the lowest coercivities (0.01 to 0.2T) and are fully saturated in fields at or below 0.1T. These features, together with the greatly increased χ and I_{RS} values associated with the fire, point to the formation of secondary ferrimagnetic oxides from soils and parent material, iron rich, but initially poor in both ferrimagnetic and antiferromagnetic minerals. Mössbauer samples TB3 and TB7 are from the top 5 cm of burnt soil, TB1 from the bedload of a stream draining an area of exclusively unburnt soil.

Annecy

Several hundred soil, stream and bedrock samples have now been studied from the region as part of a larger project designed to use magnetic minerals both in the sediments of the Lac d'Annecy and in its drainage basin as an aid to estimating variations in the rates and types of erosion resulting from land use changes in recent times. Bedrock samples from the region are almost entirely diamagnetic Jurassic limestones and either weakly or non-magnetic shales, with susceptibility values

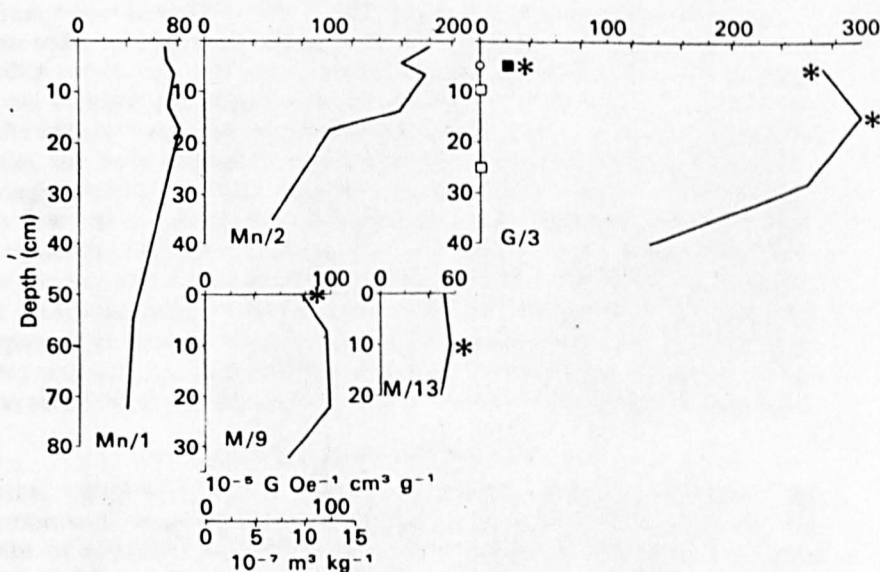


FIG. 4. Annecy region. Magnetic susceptibility profiles from a representative series of bulk soil and extracted rock samples; the samples used for further study are identified with an asterisk. For washed rock fragments from G/3, \circ is calcareous, \blacksquare non-calcareous and \square both types.

SECONDARY IRON OXIDES

99

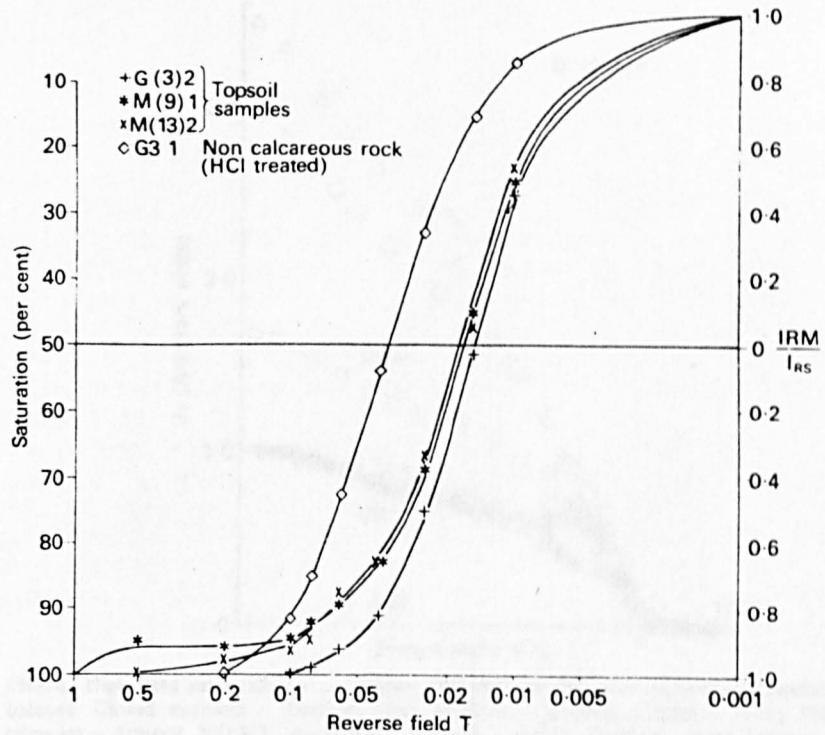


FIG. 5. Annecy region. Selected coercivity of IRM (B_{CR}) profiles for topsoil and rock samples.

ranging from ~ 6 to $12 \times 10^{-8} \text{ m}^3 \text{ kg}^{-1}$. Soil samples often have susceptibility values at least an order of magnitude higher than the associated bedrock. Fig. 4 shows susceptibility values for soil and bedrock samples illustrative of these generalizations and includes measurements from the two profiles G/3 and M/13 which yielded the magnetic extracts for thermomagnetic study. Fig. 5 plots B_{CR} for three soil samples, one from each of the soil profiles plotted in Fig. 4, as well as for the most strongly magnetic bedrock fragment measured. The three soil samples show uniformly low coercivities (0.02T) though two remain unsaturated at 0.1T indicating a significant haematite content. The rock sample has a much higher coercivity and remains only 70% saturated in a reversed field of 0.1T. The susceptibility and IRM data point to the transformation in the soil of weakly or non-magnetic iron compounds to strongly ferrimagnetic forms. For the magnetic enhancement of the Annecy soils, it is not yet possible to estimate the relative importance of former burning as part of land management, as against more gradual pedogenic processes.

Thermomagnetic experiments

Magnetite, maghemite and haematite exhibit different variations of magnetization with temperature. Pure magnetite has a Curie point of 850K, the Curie point of haematite is 950K, whilst pure maghemite inverts to haematite around 550–700K.

The soil extracts were subjected to a heating and cooling cycle in air in a steady magnetic field of 1.4T, while their magnetization was monitored on a horizontal

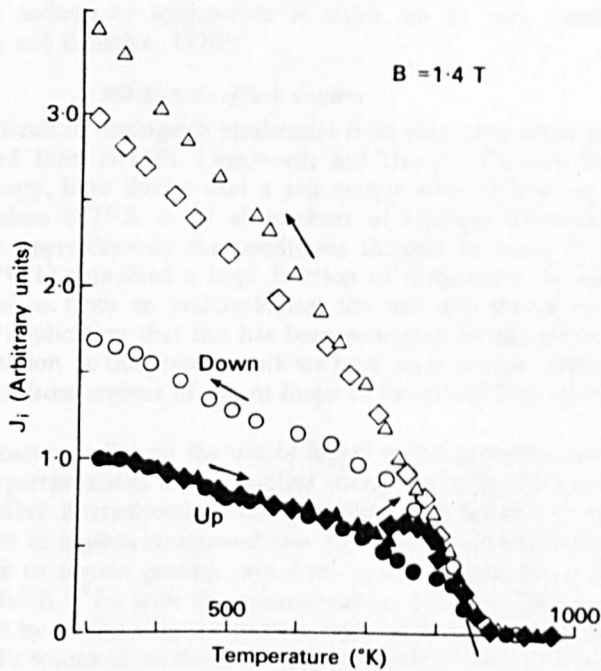


FIG. 6. High field susceptibility (J_i) against temperature changes measured on translation Curie balance. Closed symbols - heating; open symbols - cooling. Circles - Caldy Hill extract; triangles - Ancey M/13/2; diamonds - Ancey - G/3/1. Original, room temperature high field susceptibility normalized to starting value of 1.0.

translation Curie balance. Each heating cycle was made at a rate of about 20° -per minute. The results are shown in Fig. 6.

The Caldy Hill magnetic extract shows a clear Curie point near 850K. On cooling, the thermomagnetic curve is seen to be non-reversible. At room temperature the increase in magnetization is 70 per cent above the original value. This increase has resulted from paramagnetic material or antiferromagnetic haematite being converted at high temperature to ferrimagnetic magnetite. The non-magnetic residue shows an increase of around 2500 per cent above the initial room temperature magnetization following the cycling to 1000K.

Thermomagnetic curves for Ancey samples G3/1 and M 13/2 are similar to those from Caldy Hill. However, there is an increase in magnetization with increasing temperatures in both samples near 720 K. This increase is due to growth of magnetite and complicates an estimation of the Curie point of the natural extract. But again a value close to 850 K is most probable. The increases, after thermal cycling, above the initial room temperature magnetizations, are 200 per cent and 250 per cent for the magnetic extracts for G3/1 and M13/2 respectively.

The thermomagnetic properties of all three extracts can be satisfactorily explained by magnetite being the dominant magnetic carrier. The high Curie point suggests that the magnetite is reasonably free from impurities. The thermomagnetic experiments shows that maghemite is most unlikely to be an important magnetic mineral in these samples because both in natural (e.g. Lowrie, 1974) and artificial samples it typically inverts on heating in air to iron minerals of lower magnetization. Mag-

hemite doped with sodium or magnesium is stable up to very much higher temperatures (Stacey and Banerjee, 1974).

Mössbauer effect studies

Although it is difficult to distinguish maghemite from magnetite when present in impure finely divided form in soils, Longworth and Tite (1977), with the use of Mössbauer spectroscopy, have shown that a soil sample after undergoing a laboratory heating procedure (825 K in an atmosphere of nitrogen followed by air) designed to simulate approximately the conditions thought to occur in the field (Tite and Mullins, 1971) contained a large fraction of maghemite. In addition a sample of topsoil taken from an archaeological site was also shown to contain maghemite with the implication that this has been produced by the action of fires during the site occupation. In the present work we have made similar measurements on soil samples taken from regions of recent forest or heathland fires and from the Annecy region.

Mössbauer spectroscopy relies on the use of highly monochromatic gamma rays to measure the tiny perturbations of the nuclear energy levels by the surrounding electrons, the hyperfine interactions, which give rise to an absorption spectrum which is characteristic of a given compound (see e.g. Greenwood and Gibb, 1971). The effect is specific to certain gamma rays from certain radioactive isotopes of which the most useful is ^{57}Fe with the gamma ray at 14.4 keV. The absorption spectrum is measured by modulating the gamma ray energy via the Doppler effect by mounting the ^{57}Fe source on an electromagnetic vibrator. The soil samples may be used directly as absorbers, there being sufficient ^{57}Fe in the soil to give a measurable spectrum. In such soils the iron occurs both as free iron oxides and as substitutional impurities in the clay minerals, so-called structural iron.

The hyperfine interactions may be divided into three types, the isomer shift, electric quadrupole interaction and the magnetic hyperfine interaction. Of these the isomer shift displaces the centroid of the Mössbauer spectrum, while with ^{57}Fe the latter two interactions split the Mössbauer line into either a doublet or a six line pattern respectively. The quadrupole doublet occurs for example when the iron atoms sit on sites of non-cubic symmetry, such as those of structural iron, while the magnetic iron oxides each give rise to a six line pattern, whose splitting is determined by the magnetic hyperfine field. When the oxides are finely divided (<300 Å) they may behave as superparamagnets in a Mössbauer measurement (see e.g. Kündig *et al.* 1966). When the hyperfine field direction changes at a rate of $>10^8 \text{ s}^{-1}$, the magnetic splitting is destroyed and the spectrum reverts to a single line or quadrupole doublet. The Mössbauer spectrum is also sensitive to the presence of impurity atoms via their effect (e.g. on the hyperfine field) so that it is frequently difficult to distinguish the different iron oxides in soils on the basis of their Mössbauer spectra. In the work of Longworth and Tite (1977) it was shown that the application of a large magnetic field to the soil samples could be used to distinguish ferrimagnetic and antiferromagnetic oxides.

Experimental method

The soil samples were sieved through a 125 μm sieve and dispersed in vacuum grease to make absorbers approximately 100 mg cm^{-2} . In this way absorbers were prepared from the original material and from the material after magnetic separation. The Mössbauer spectra were measured using a source of about 50 mCi ^{57}Fe .

TABLE 2

Hyperfine parameters derived from fits to room temperature spectra of soil samples. H is the hyperfine field, S is the isomer shift, Q the quadrupole interaction given by the difference in separation between lines 1 and 2 and 5 and 6 in a combined magnetic and quadrupole spectrum. Δ is the splitting of the quadrupole doublet

Sample	Magnetic components				Non-magnetic components		
	H (T)	S (mm s ⁻¹)	Q (mm s ⁻¹)	Relative area	Δ (mm s ⁻¹)	S (mm s ⁻¹)	Relative area
TB1	-	-	-	-	0.80	0.18	63%
					2.60	1.07	37%
TB3	51.7	0.27	0.36	12%	0.88	0.26	59%
	49.3	0.23	0.16	16%	2.40	1.00	6%
	45.7	0.49	0.04	7%			
TB7	51.5	0.27	0.24	7%	0.82	0.26	51%
	49.4	0.26	0.12	23%	2.72	0.95	7%
	46.0	0.25	0.04	16%			
Caldy Hill	51.4	0.26	0.32	44%			
	48.9	0.19	0.12	28%	0.76	0.23	12%
	45.8	0.56	0.04	16%			
Annecy	49.2	0.27	0.31	24%	0.61	0.24	18%
					2.65	1.00	12%

diffused into rhodium foil and a conventional constant acceleration Mössbauer spectrometer (obtainable from Harwell Scientific Services). Spectra were recorded at room temperature, at 4.2 K using a liquid helium cryostat and at 4.2 K with a field of 3T applied to the absorber in a direction parallel to that of the gamma ray beam (Figs. 7-11). The spectra were fitted to Lorentzian lineshapes using a least squares minimisation routine. The derived hyperfine parameters are tabulated in table 2 and the fits are shown as solid lines in the figures. Also included for comparison with the 4.2 K spectra are similar spectra for pure bulk oxides.

Results and discussion

Comparison of Figs. 7 and 8 illustrates the effectiveness of the magnetic separation technique for samples from Annecy, Llyn Bychan (TB3 and TB7 both samples of burnt surface soil) and Caldly Hill (1976 burn), through the observed increase in the percentage Mössbauer absorption. This increase is less for TB1, a stream bedload sample from an unburnt part of the Llyn Bychan catchment. Here the material is either paramagnetic or superparamagnetic at room temperature. The increased Mössbauer absorption is due mainly to the removal of some of the non-iron compounds which, while not producing any Mössbauer absorption, will increase the background (photoelectric) absorption.

We consider first those room temperature spectra which contain six line magnetic patterns, Annecy, TB3, TB7 and Caldly Hill, the last three of which are directly associated with recent burning. Apart from these magnetic components (1) there are three other components. Component (2) is a central quadrupole doublet whose amplitude is seen to decrease on cooling the samples to 4.2 K. At the same time the relative amplitude of the magnetic component increases. Such a feature

SECONDARY IRON OXIDES

103

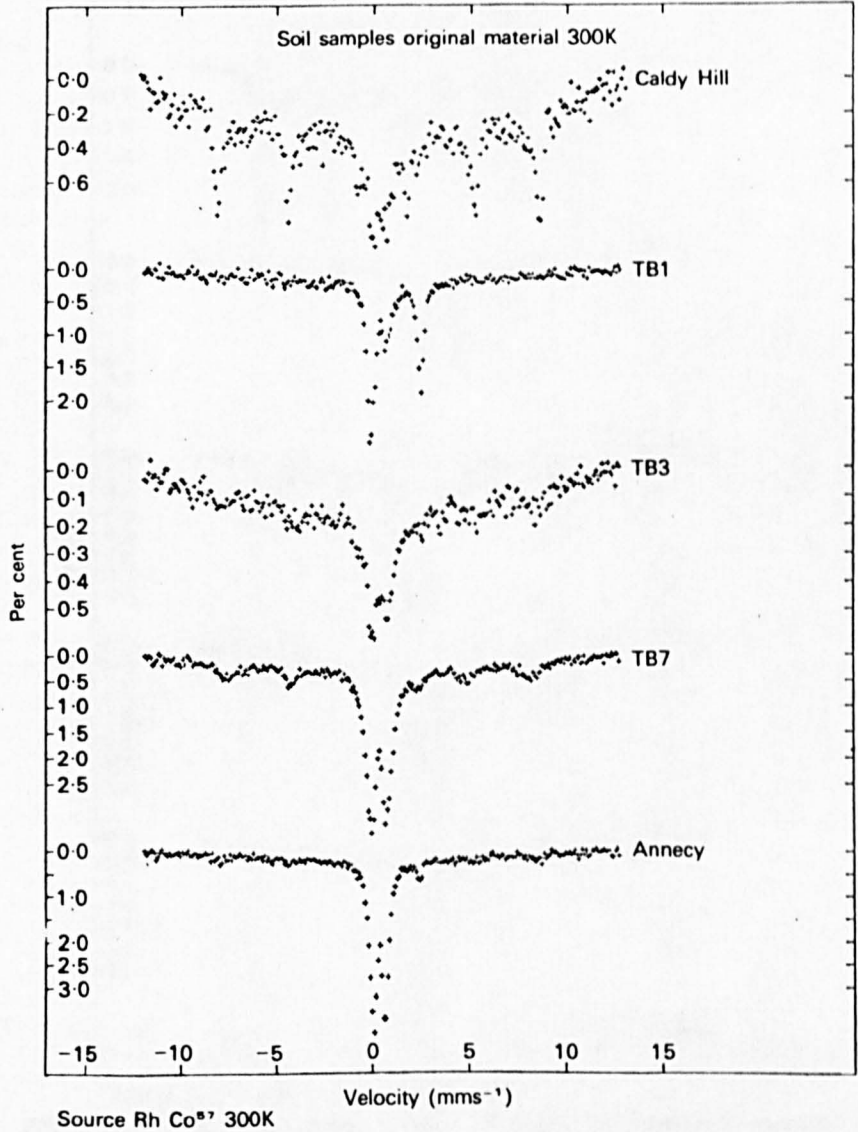


FIG. 7. Iron-57 Mössbauer spectra at room temperature for original samples. The zero of the velocity scale refers to the isomer shift of iron metal. The Caldly Hill sample and the Llyn Bychan samples TB3 and TB7 are from surface soils (0–2 cm) burnt in 1976. Llyn Bychan sample TB1 is stream bedload from an unburnt area.

suggests that at room temperature at least part of the quadrupole doublet is due to a superparamagnetic iron oxide, while at 4.2 K the rate at which the magnetisation and hence the hyperfine field directions are flipping, has decreased sufficiently for a magnetic pattern to be observed for those iron atoms. The fact that both a superparamagnetic (2) and a magnetic (1) pattern are observed at 300 K

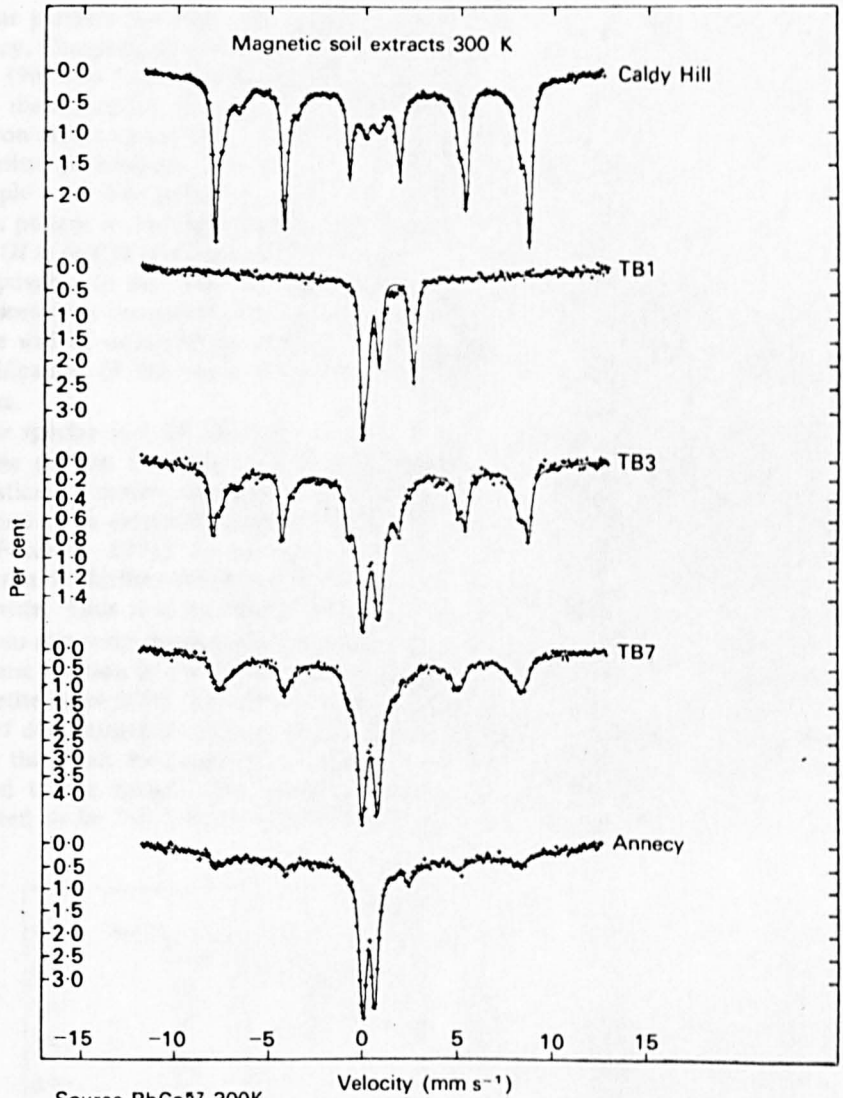


FIG. 8. Iron 57 Mössbauer spectra at room temperature for magnetically separated extracts. The solid line indicates the least squares fit to the data points.

is due to a range in the particle sizes present. It is known that the spin flip frequency depends also on the particle size. Thus we conclude that the average oxide particle size increases in the sequence Annecy, TB7, TB3 and Caldly Hill. The remainder of the 300 K doublet, component 3, and essentially all the 4.2 K doublet, is due to structural ferric material which has a very similar splitting to that of the superparamagnetic doublet (2). In addition there is a weak quadrupole doublet (4) (splitting 2.5 mm s^{-1}), due to structural ferrous ions (see particularly the TB1 spectrum).

The magnetic patterns observed at 300 K may in fact be fitted to three sets of

six line patterns for TB3, TB7 and Caldly Hill (Fig. 9), and one six line pattern for Annecy. Comparison of the observed parameters with those of iron oxides (Kündig *et al.* 1966 and Volenik *et al.* 1975), suggests that one pattern arises from haematite while the remaining two are produced by magnetite. It is known that in magnetite the iron atoms sit on two different types of site giving rise to two differing sets of hyperfine parameters. The relative area under a given Mössbauer pattern, for example a six line pattern, is approximately proportional to the number of iron atoms present in the respective compound on that site. For pure magnetite the area ratio ($H \cong 46\text{T}/H \cong 49\text{T}$) is 2 while the observed ratio is about 0.6 (Table 2). Thus it is possible to say that the magnetite deviates from stoichiometry and may be represented by the approximate formula $\text{Fe}_{2.9}\text{O}_4$. The remaining sites on the spinel lattice will be occupied by vacancies and/or impurity atoms. This completes the identification of the room temperature magnetic components in the Mössbauer spectra.

The spectra at 4.2K (Fig. 10) were fitted to two quadrupole doublets and one six line pattern in order to determine the amount of structural iron. No more sophisticated model was used since the spectrum for pure magnetite at this temperature is extremely complex having at least six six-line patterns (Rubinstein and Forester, 1971). In the present samples the magnetite is impure and the spectrum is further complicated by the presence of overlapping lines due to haematite. Thus it is extremely difficult to use the 4.2 K spectra to distinguish between magnetite/maghemite and haematite in soil samples. We have seen that the magnetic fraction in the 300 K spectra has been identified as being due mainly to magnetite (except for the Annecy sample) (Table 3), and thus we now need some way of determining the nature of the superparamagnetic component. It is possible to do this from the behaviour of the 4.2 K spectra when a large magnetic field is applied to the sample. The relative areas of the six line magnetic patterns are expected to be 3:2:1:1:2:3 where the 3d spins and hyperfine field directions are

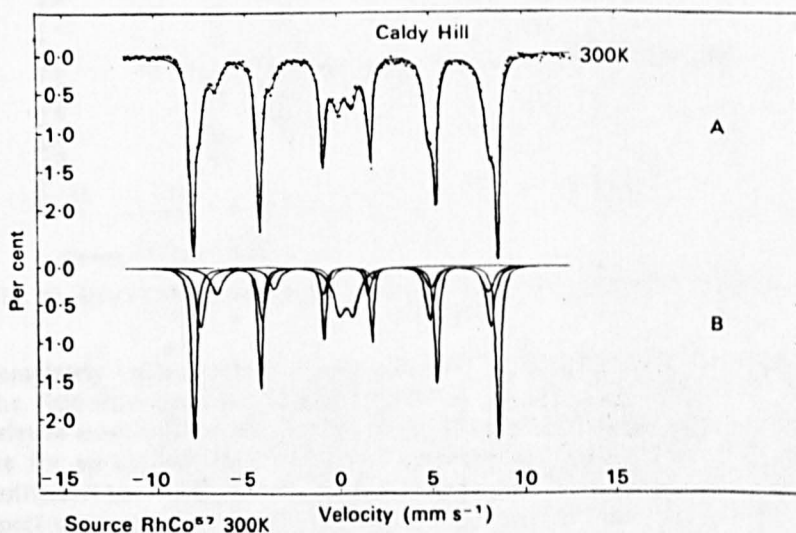


FIG. 9. Iron-57 Mössbauer spectra at room temperature of Caldly Hill samples: A: total fit (as Fig. 8), and B: subsidiary fits for individual compounds.

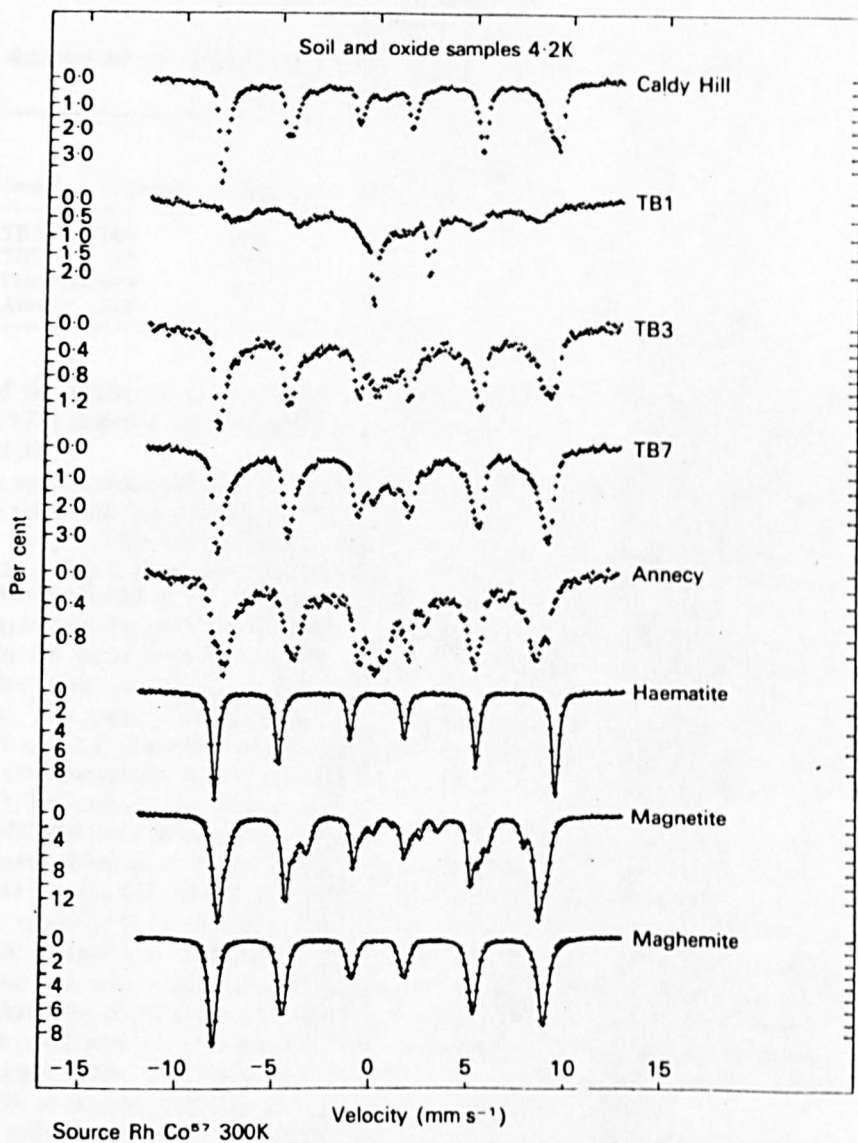


FIG. 10. Iron-57 Mössbauer spectra at 4.2 K for magnetically separated samples and for oxide standards.

completely random e.g. in a unmagnetised ferromagnet or antiferromagnet. If all the field directions are aligned parallel to the gamma ray direction, then these relative areas become 3:0:1:1:0:3. This will occur for ferrimagnets such as magnetite for an applied field $\gtrsim 1$ T but in general the internal field directions in an antiferromagnet will be unchanged in such an applied field. For this case the spectrum is expected to be unchanged as far as the area ratios are concerned. Thus the two oxides may be distinguished by applying a large external magnetic field. There is one complication however, in that when a ferrimagnetic oxide is finely

SECONDARY IRON OXIDES

107

TABLE 3
Assignment of relative areas from different phases in the Mössbauer spectra

Sample	Haematite	Magnetite	Superparamagnetic iron	Structural iron	
				Ferric	Ferrous
TB3	18%	34%	29%	15%	4%
TB7	3%	39%	41%	10%	7%
Caldy Hill	44%	44%	7%	5%	—
Annecy	24%	—	46%	18%	12%

divided the alignment of spins may not be complete (Coe, 1971). Longworth and Tite (1977) observed patterns with relative areas of 3:1:1:1:3 for such oxides in a field of 3T.

The spectra observed here at 4.2 K in a parallel field of 3T (Fig. 11) were fitted to one set of six lines in order to determine the relative areas of components 2 and 5. For samples TB3, TB7, Caldly Hill and Annecy these were found to be about 1.1, 1.1, 1.5, and 1.2. The predicted intensity for Caldly Hill is approximately $44/88 \times 1$ (magnetite) + $44/88 \times 2 = 1.5$ (haematite) as observed. It is assumed that the superparamagnetic component is magnetite, as is the room temperature magnetic fraction. In the same way if it is assumed that all the superparamagnetic oxide is magnetite then relative areas 1.2, 1.0 and 1.3 are predicted for TB3, TB7 and Annecy. This assumption gives the closest agreement with the observed values of 1.1, 1.1 and 1.2. Thus the relative areas due to magnetite in Table 3 after inclusion of the superparamagnetic fraction will be 63 per cent, 80 per cent and 46 per cent for TB3, TB7 and Annecy respectively.

Finally the room temperature spectrum for TB1 is seen to contain no magnetic component although at 4.2 K about 40 per cent of the total area is made up of a magnetic component. At this temperature the hyperfine field has a value of 48.3T with a quadrupole interaction $Q = 0.36 \text{ mm s}^{-1}$. A smaller amplitude for the magnetic pattern was observed at 77 K which suggests again a superparamagnetic behaviour but with a much smaller particle size than in the other soil samples. It is likely that even at 4.2 K the spin flip rate is not sufficiently slow for the full value of the hyperfine field to be observed. The appearance of the spectrum in an applied field suggests that this component is due to an antiferromagnetic oxide, either haematite or possibly goethite ($H = 50.5 \text{ T}$ at 4.2 K for bulk material).

The soil samples are shown to contain a mixture of iron oxides and structural iron. For samples TB3, TB7, Caldly Hill and Annecy the relative component areas due to magnetite are 63 per cent, 80 per cent, 51 per cent and 46 per cent and due to haematite 18 per cent, 3 per cent, 44 per cent and 24 per cent. The spectra observed for the magnetite component suggests a deviation from stoichiometry, i.e. an approximate formula $\text{Fe}_{2.9}\text{O}_4$. The identification of magnetite is based on the interpretation of the room temperature spectra where its expected contribution is straightforward. There is no evidence for maghemite in these spectra.

Conclusions

Susceptibility, I_{RS} and B_{CR} measurements indicate that in the three areas studied magnetic enhancement has taken place in the soils as a result either of

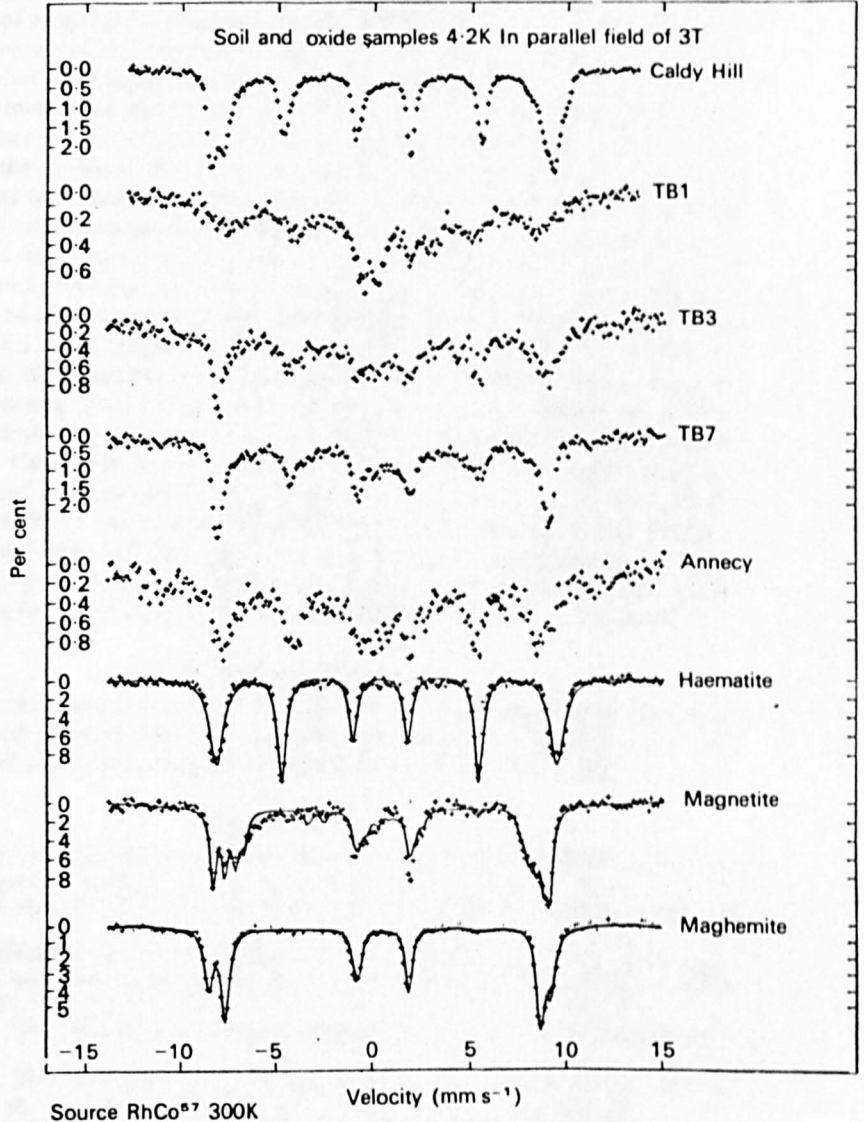


FIG. 11. Iron-57 Mössbauer spectra at 4.2 K with an applied field of 3T in the gamma ray direction, for magnetically separated samples and for oxide standards.

burning or, perhaps in the Ancecy soils, more gradual pedogenic processes. In each area, B_{cR} spectra profiles in particular indicate qualitative differences between parent material and enhanced topsoil. These qualitative differences, taken together with the increased susceptibility values, point to the conversion of either non-magnetic or antiferromagnetic forms of iron into strongly ferrimagnetic oxides.

Thermomagnetic studies on magnetically enhanced soils from Caldly Hill and Ancecy, and Mössbauer effect studies on soils from Caldly Hill and Llyn Bychan concur in demonstrating that the resultant mineral is magnetite. This conclusion

differs from that reached by the majority of authors who have studied secondary ferrimagnetic oxides in soils and, following Le Borgne (1955, 1960), have inferred the formation of maghemite. Evidence for the relative purity and for the deviation from stoichiometry of the secondary magnetite identified in the present studies remains somewhat conflicting though not irreconcilable; the results of the thermomagnetic experiments are not incompatible with pure stoichiometric Fe_3O_4 whereas the Mössbauer results clearly indicate a degree of non-stoichiometry. Taken together with the previous Mössbauer studies of Longworth and Tite (1977) and unpublished thermomagnetic experiments on soils used in their studies (Thompson, pers. comm.) it seems reasonable to conclude provisionally that secondary ferrimagnetic oxides resulting from the chemical transformation of iron compounds in soils and bedrock, whether by fire or more gradual pedogenic processes, may occupy a range of positions close to the solid solution series between stoichiometric magnetite (Fe_3O_4) and maghemite ($\gamma\text{Fe}_2\text{O}_3$), and may moreover be affected by varying degrees of impurity as a result of isomorphic substitution of iron by commonly occurring soil cations such as sodium and aluminium. Conclusions derived from Mössbauer effect studies with regard to the non-ferrimagnetic components of the Caldly Hill and Llyn Dychan and Annecy samples are compatible with those derived from the magnetic measurements (cf. Figs. 1 and 3 and Table 2).

The combination of rapid, non-destructive measurements such as I_{RS} and B_{CR} with more sophisticated but also more time consuming thermomagnetic and Mössbauer effect studies on selected samples can be seen to provide an effective means of characterizing both ferrimagnetic and non-ferrimagnetic forms of iron in soils.

Acknowledgements

We are especially indebted to Mr. P. A. James, Dept of Geography, Liverpool, for supplying soil samples and accompanying information from the Annecy area. We should also like to acknowledge useful discussions with Dr. M. S. Tite.

REFERENCES

- COEY, J. M. D. 1971. Noncollinear spin arrangement in ultra fine ferrimagnetic crystallites. *Phys. Rev. Lett.*, 27, 1140-2.
- GREENWOOD, N. N. and GIBB, T. C. 1971. *Mössbauer spectroscopy*. London: Chapman & Hall.
- KÜNDIG, W., BÖMMEL, H., CONSTABARIS, G., and LINDQUIST, R. H., 1966. Some properties of supported small $\alpha\text{-Fe}_2\text{O}_3$ particles determined with the Mössbauer effect. *Phys. Rev.* 142, 327-33.
- LE BORGNE, E., 1955. Abnormal magnetic susceptibility of the topsoil *Annls. Geophys.* 11, 399-419.
- LE BORGNE, E. 1960. The influence of fire on the magnetic properties of soil, schist and granite. *Ibid.* 16, 159-96.
- LONGWORTH, G., and TITE, M. S. 1977. Mössbauer and magnetic susceptibility studies of iron oxides in soils from archaeological sites. *Archaeometry*, 19, 3-14.
- LOWRIE, W. 1974. Oceanic basalt magnetic properties and the Vine and Matthews hypothesis. *J. Geophys.* 40, 513-36.
- MOLYNEUX, L. 1971. A Complete Result Magnetometer for measuring the Remanent Magnetization of rocks. *Geophys. J. R. astr. Soc.* 24, 429-34.
- and THOMPSON, R. 1973. Rapid measurement of the magnetic susceptibility of long cores of sediment. *Ibid.* 32, 479-81.
- MULLINS, C. E. 1977. Magnetic susceptibility of the soil and its significance in soil science -- a review. *J. Soil Sci.* 28, 223-46.
- NEUMEISTER, H., and PESCHEL, G. 1968. Magnetic susceptibility of soils and Pleistocene sediments in the neighbourhood of Leipzig. *Albrecht - Thaer - Arch.* 12, 1055-72.

- OLDFIELD, F., DEARING, J., THOMPSON, R., and GARRETT-JONES, S. E. 1978. Some magnetic properties of lake sediments and their possible links with erosion rates. In *Proceedings of the second International Symposium on Palaeolimnology*. Pol. Arch. f. Hydrobiol. 25, 321-31.
- RUBINSTEIN, M. and FORESTER, D. W. 1971. Investigation of the insulating phase of magnetite by NMR and the Mössbauer effect. *Solid State Comm.* 9, 1675-8.
- STACEY, F. D., and BANERJEE, S. K. 1974. *The physical principles of rock magnetism*, p. 92. Amsterdam: Elsevier.
- TAYLOR, R. M., and SCHWERTMANN, U. 1974. Maghemite in soils and its origin. I Properties and observations on soil maghemites and II Maghemite synthesis at ambient temperature and pH 7. *Clay Minerals*, 10, 289-310.
- THOMPSON, R., BATTARBEE, R. W., O'SULLIVAN, P. E., and OLDFIELD, F. 1975. Magnetic susceptibility of lake sediments. *Limnol. and Oceanogr.* 20, 687-98.
- TITE, M. S., and MULLINS, C. E. 1971. Enhancement of the magnetic susceptibility of soils on archaeological sites. *Archaeometry*, 13, 209-19.
- VADYUNINA, A. F., and KOVTUN, V. Ya. 1974. Magnetic susceptibility of the separates of some soils. *Soviet Soil Sci.* 6, 106-10.
- VOLENIK, K., SEBERINI, M., and NEID, J. 1975. A Mössbauer and X-ray diffraction study of nonstoichiometry in magnetite. *Czech. J. Phys.* B25, 1063-71.

(Received 14 April 1978)

Environmental Applications of Magnetic Measurements

R. Thompson, J. Bloemendal, J. A. Dearing, F. Oldfield
T. A. Rummery, J. C. Stober, G. M. Turner

In 1831 Faraday (1) demonstrated that movement of a magnet could produce an electric current. With the development of modern electronics, it has become possible to utilize the connection between magnetism and electricity to rapidly and easily measure many magnetic parameters of weakly magnetic natural

magnetic susceptibility, while the ratios between various magnetic parameters provide information about the types of magnetic grains present and their size. Concentrations of magnetic grains as low as 1 part in 10^6 can readily be measured. Although detailed and often sophisticated analyses of several properties are

Summary. A wide range of examples of the application of magnetic measurements to environmental studies illustrate the advantages of magnetic techniques over conventional methods. Magnetic measurements, in both the field and the laboratory, are particularly useful for reconnaissance work because of their speed and flexibility. Quantification as well as simple diagnosis of the transformation and movement of magnetic minerals within and between the atmosphere, lithosphere, and hydrosphere is practical. Techniques of investigating intrinsic and mineral magnetic properties, in addition to paleomagnetic remanence, are described in subjects as diverse as meteorology, hydrology, sedimentology, geophysics, and ecology.

minerals. Measurements of the magnetic properties of materials such as rocks, soils, sediments, and atmospheric particulates provide information of immense value in a wide spectrum of disciplines. The magnetic analyses are often made with a speed many orders of magnitude faster than is attainable with conventional methods of environmental analysis. This article illustrates the application of a range of rapid, simple, nondestructive, magnetic measurements to problems in geophysics, meteorology, climatology, hydrology, limnology, oceanography, sedimentology, geomorphology, soil science, ecology, and land-use studies.

The concentration of magnetic minerals in a sample can be estimated from its

necessary to determine the precise magnetic composition of a sample, a wealth of information can be obtained from a few simple parameters.

Initially, we illustrate the application of three principal parameters, chosen for their diversity and speed of measurement. The first parameter, susceptibility or magnetizability, χ , can be measured on rock, soil, and sediment samples weighing 0.1 to 100 grams, on whole sediment cores, or even on exposures in the field. The air-cored coil bridge system used produces weak alternating fields (< 1 millitesla) of high frequency (~ 10 kilohertz). The second parameter, "saturation" isothermal remanence magnetization (SIRM), is measured on a

sensitive magnetometer after placing a 0.02- to 20-g specimen in a strong, uniform, d-c magnetic field (1 tesla) produced by a conventional electromagnet. Only tens of seconds are needed for both the magnetization process and the remanence measurement. Several kinds of sensitive magnetometers, including flux gates, astatics, spinners, and cryogenics, are admirably suited for isothermal remanence measurement (2). The third parameter, remanent coercivity, B_{rH} —that is, the reverse d-c field required to reduce the SIRM to zero—provides a rapid method of distinguishing common natural magnetic minerals. Minerals of the corundum structure, such as hematite, have remanent coercivities above 0.2 T. Minerals of the spinel structure, such as magnetite, have remanent coercivities below 0.05 T. The B_{rH} of magnetite varies from 50 mT for grains 1 micrometer in diameter to less than 20 mT for grains exceeding 100 micrometers. Ten measurements of isothermal remanent magnetizations (IRM's), grown in increasing reverse field strengths, are sufficient to define a complete magnetization curve including the remanent coercivity.

The ratio of the first two parameters, $SIRM/\chi$, provides a very quick first approach to monitoring the changes in magnetic mineral type or size in a suite of samples. For hematite, $SIRM/\chi$ is greater than 200 kiloamperes per meter, and for magnetite it varies from 1.5 to about 50 kA/m as the grain size decreases. Materials with a high superparamagnetic content have $SIRM/\chi$ ratios below 0.01 kA/m. Combinations of magnetic minerals in natural assemblages complicate this simple picture, but they may often be recognized by other magnetic analyses. For example, a combination of fine magnetite and ultrafine (~ 10 nanometers) superparamag-

R. Thompson is a lecturer and J. C. Stober and G. M. Turner are research students in the Department of Geophysics, University of Edinburgh, Edinburgh EH9 1JZ Scotland. F. Oldfield is a professor of geography and J. Bloemendal, J. A. Dearing, and T. A. Rummery are research students in the Department of Geography, University of Liverpool, Liverpool L69 3BX England.

netic magnetite would have a $SIRM/\chi$ ratio similar to that of coarse magnetite, but its coercivity of remanence would be higher as the ultrafine material only contributes to χ and not to the $SIRM$ or B_{CR} .

The transformations and movement of magnetic minerals within and between the atmosphere, lithosphere, and hydrosphere are summarized in Fig. 1. The magnetic measurements outlined above can be applied to materials within all phases at or near the boundary layers.

They can thus be used to identify, characterize, and quantify the transformations and fluxes portrayed. In this way, especially in view of the sensitivity of iron compounds to both natural and anthropogenic environmental processes, crucial contributions to a wide range of disciplines and to interdisciplinary studies of environmental system linkages become possible. Case studies illustrating magnetic analyses of materials from different compartments and linkages in Fig. 1 are described below.

Atmosphere

Magnetic measurements provide a basis for quantifying and differentiating atmospheric particulates. Figure 2 shows atmospheric input to peat at several locations in western Europe. Time control is provided by a variety of methods (3-5). Where this is precise enough to allow deposition rate calculations, the results are expressed as weight of magnetite deposited per square meter per year (Fig. 2a). Not only do the profiles of $SIRM$ versus depth or age provide a history of particulate atmospheric pollution at each site, but spatial variations in the post-1840 magnetite influx per square meter can be identified and related to the proximity of major domestic and industrial sources (Fig. 2b). In addition, B_{CR} spectra allow differentiation of the dominant source of atmospheric particulates in contemporary samples.

By applying both $SIRM$ and B_{CR} measurements to longer peat profiles and to ice core samples, it should be possible to trace long-term qualitative and quantitative variations in particulate input. It should also be possible to identify major spatial and temporal variations in atmospheric particulate sources and compare empirical evidence with dust-veil indices reconstructed from historical records. The speed and ease with which magnetic measurements of lake sediments and peats can be used to confirm and extend correlations based on volcanic ash sequences have been demonstrated by studies of lake sediments from the New Guinea highlands (6).

The evidence available so far identifies anthropogenic and volcanic processes as the dominant sources of atmospheric magnetic particulates and thus has important implications for understanding the origin of magnetic minerals in deep-sea sediments. At present, these sources, together with terrestrially derived material resulting from dust storms, fires, and wind erosion, appear to predominate by orders of magnitude over the cosmic flux of extraterrestrial magnetic minerals (3).

Lithosphere

In many contexts, lithospheric sources of magnetic minerals predominate over atmospheric ones. Not only does the bedrock often yield primary magnetic minerals, but paramagnetic or weakly magnetic forms of iron, weathering out of parent material, may be transformed to persistent ferrimagnetic forms by fire or more gradual soil formation processes

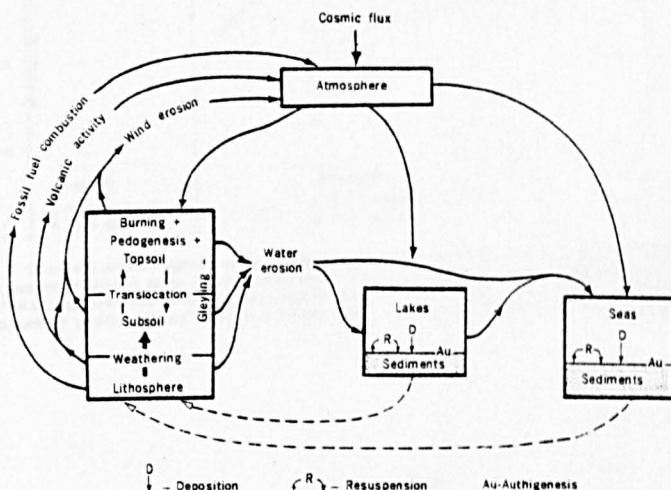


Fig. 1. Simplified model of the movements of magnetic minerals between the atmosphere, lithosphere, and hydrosphere.

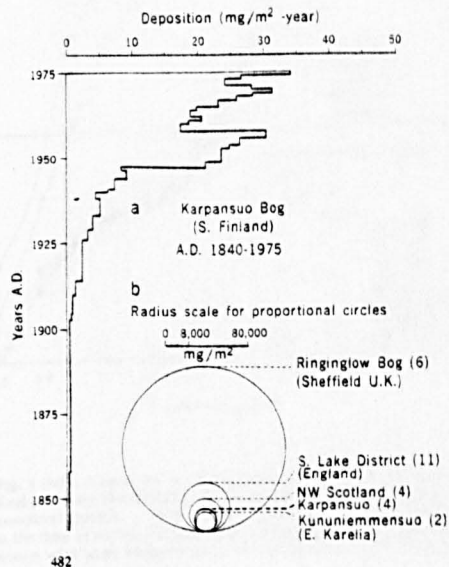


Fig. 2. Atmospheric deposition of magnetic minerals. (a) Yearly deposition of magnetite at Karpansuo Bog, Finland. (b) Spatial variation of total magnetite deposition after 1840 (after the first phase of the industrial revolution); the amount, expressed as milligrams per square meter, is represented by the area of each circle. The number of peat profiles used to calculate the post-1840 influx per square meter at each locality is shown in parentheses.

(7-10). These transformations are most readily detected as an increase in χ at or near the soil surface. A firmer basis for this has been established by B_{CR} curves from topsoil and parent material from a variety of bedrock types. The ferrimagnetic minerals formed by "enhancement" in the soil have been identified by

x-ray diffraction, thermomagnetic measurements, and Mössbauer effect studies as either impure maghemite (11) or non-stoichiometric magnetite (9). The down-profile variations in magnetic properties and their spatial variations provide evidence for previous forest fires (9, 10), land-use history (7, 12), and soil erosion

(Fig. 3) on a wide range of parent materials.

It follows that magnetic measurements can often be diagnostic of the source of particulates once these pass into the drainage system of an area. Identifying the source of stream-borne particulates has proved difficult by nonmagnetic

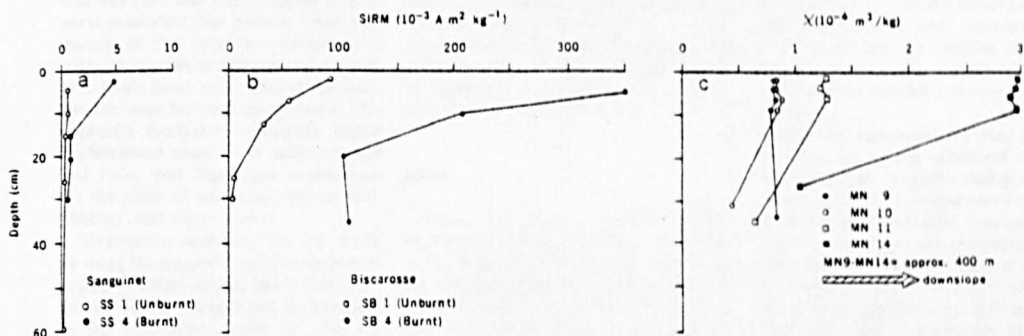


Fig. 3. Down soil profile magnetic variations for three localities in France. (a and b) Plots of SIRM against depth for burnt and unburnt profiles on Quaternary outwash sands in the Landes region. Note the enhancement of SIRM by production of ferrimagnetic minerals caused by burning. (c) Plot of χ against depth for profiles on a cultivated hillside on Jurassic limestone bedrock at Le Bois in the Montmin Valley near Annecy. The enhancement of susceptibility from the near-zero values of bedrock depends on position on the slope and land use.

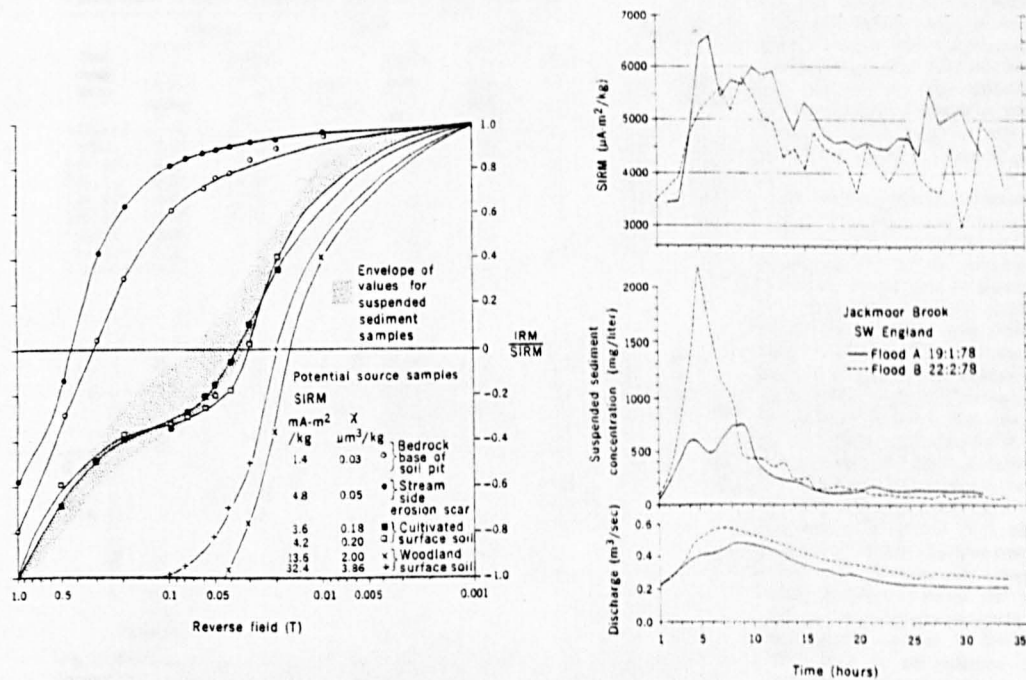


Fig. 4 (left). Coercivity of remanence spectra of bedrock, soils, and suspended sediments from an instrumented catchment in southwestern England. Note the similarity of the suspended sediment spectra to those of cultivated surface soils and their contrast with those of bedrock and woodland topsoils. Fig. 5 (right). Variation in SIRM of suspended sediment during two floods of Jackmoor Brook. Note the increase in SIRM at the time of increased runoff and sediment concentration and the lag in peak SIRM values compared with the hydrograph. This pattern is consistent with some channel scour during the rising stage of the hydrograph followed by increasing importance of surface runoff.

methods since the techniques available for differentiating materials yielded by contrasting processes such as topsoil erosion or channel scour are costly and time-consuming. Figures 4 and 5 show how, in an instrumented catchment in southwestern England, the dominant source of suspended sediment can be identified magnetically not only in a general way (13), but with a degree of temporal resolution that permits some estimation of the relative importance of different sources at different stages within a single flood event and at the comparable stage between flood events. This approach facilitates potentially highly sophisticated analyses of sediment type and yield, with significant implications for the study of soil loss, channel morphology, and water quality.

River-borne sediments can be traced by using the magnetic enhancement generated by either natural forest fires or artificial heating in a reducing environment in the laboratory (Table 1). The en-

hanced ferrimagnetic material can be used as an artificial tracer not only for suspended sediment but also for bed load, which is often exceptionally difficult to trace effectively by established techniques. With an artificially enhanced tracer, downstream dilutions of 1 part in 500 can be detected on 100-g bed-load samples with portable susceptibility bridges, or even on bed load in situ with metal detectors of the type used by treasure hunters. The insight into storage and delivery rates arising from such studies is important for studies in fluvial geomorphology and hydrology.

Lakes

Where the magnetic minerals yielded by erosion from a catchment contribute to the sediment of a lake, the down-profile variation in magnetic properties provides a rapid basis for core correlation and for the quantification and character-

ization of sediment influx (12). Figure 6 illustrates such core correlations based on magnetic whole-core volume susceptibility (κ) scanning for ten cores from Loch Lomond. Clear correlations between sediments from shallow (AIM8) and deep (TOM4) water are found, as well as between cores from near the head (GUM19) and the outflow (RPM1) of the loch. Cores GUM19 and RPM1 are more than 20 kilometers apart, separated by a pronounced trench extending to 200 m below sea level and a chain of islands with a narrow threshold of only 10-m water depth.

Magnetic measurements may also be used to date recent sediments (14-16). As an example, magnetic dating of these widely separated Lomond cores is based on magnetic declination measurements (16) (Fig. 7). These paleomagnetic direction variations are a signature of ancient geomagnetic field direction changes, which were locked into the sediment close to the time of deposition. The locking process in Lomond is due to physical stabilization of single-domain magnetite grains with diameters on the order of 1 μm . This process of postdepositional remanent magnetization involves grains that had a natural remanence before their deposition. Another possible remanence process is one in which authigenic grains acquire a fresh magnetization, in the ambient geomagnetic field direction, by growing through a critical volume. For spherical magnetite grains this critical blocking diameter is about 30 nanometers.

The stable remanence directions (Fig. 7) have been used to date the sediment by matching the oscillations with a master geomagnetic secular variation curve. In Britain three types of master curve have been used. First, the most recent secular changes have been recorded at magnetic observatories. Records at London began in A.D. 1576. Magnetic declination moved from 11°E, as recorded by Sir Martin Frobisher at that time, to 0°E in A.D. 1660. King Charles II, among others, noted the zero declination (17, 18). The horizontal direction continued to change and passed through a westerly maximum of 24° in A.D. 1815, while it is now about 7°W and changing much more slowly (18). Second, the observatory record has been extended back to A.D. 1000 by archeomagnetic studies (19). Paleomagnetic records for before A.D. 1000, dated by palynological changes and carbon-14 age determinations, provide a third type of master curve. The A.D. 1815 westerly maximum of the observatory records can be recognized in all the Lomond cores (Fig. 7). Lower-

Table 1. Enhancement in natural stream bed load. Material was "toasted" in a muffle furnace for 30 minutes. Note the enhancement in different particle-size fractions. Enhancement of SIRM begins to occur in fine fractions before 200°C with growth of hematite; with combustion of organic matter at higher temperatures, magnetite begins to be produced.

Size range (mm)	Natural		200°C		800°C		Enhancement	
	χ (10^{-8} m ³ /kg)	SIRM (10^{-3} A m ² kg ⁻¹)	χ (10^{-8} m ³ /kg)	SIRM (10^{-3} A m ² kg ⁻¹)	χ (10^{-8} m ³ /kg)	SIRM (10^{-3} A m ² kg ⁻¹)	χ_{900} / χ_0	SIRM ₉₀₀ /SIRM ₀
<0.5	0.07	0.17	0.08	0.42	23	73	350	440
0.5- 0.7	0.07	0.13	0.08	0.58	20	55	300	430
0.7- 1.4	0.07	0.07	0.07	0.13	18	45	260	650
1.4- 2.8	0.07	0.04	0.06	0.02	15	33	230	840
2.8- 5.6	0.07	0.02	0.07	0.02	13	28	210	1200
5.6-11.2	0.07	0.02	0.07	0.02	14	33	250	1400
>11.2	0.08	0.02	0.07	0.02	16	29	230	1200

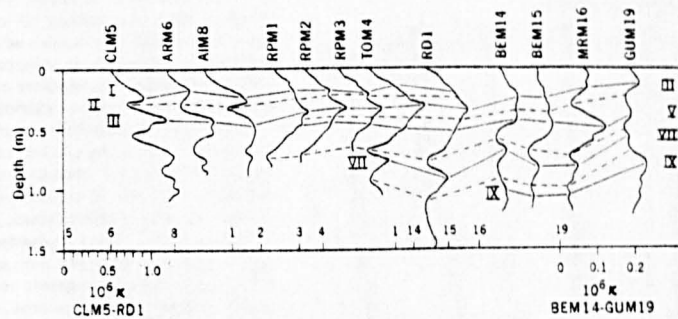


Fig. 6. Whole-core susceptibility traces for surface cores from Loch Lomond, Scotland. The locality code and number are given for each core (for example, CLM5). Susceptibility maxima are identified by odd Roman numerals and joined by solid lines. Susceptibility minima have even Roman numerals and are joined by dashed lines. The origin of the susceptibility scale for each core trace is indicated by a vertical tick on the lower axis and identified by the core number (6 refers to core ARM6). The susceptibility scales for cores CLM5 through RD1 and cores BEM14 through GUM19 are also given on the lower axis.

amplitude fluctuations of the archeomagnetic record (19) can also be distinguished, and the easterly turning point (D), dated at 1000 years ago, is also present in all the longer Lomond sequences. The κ variations of Fig. 6 match and reinforce the magnetic dating correlations. The speed of whole-core remanence measurements (10 centimeters per minute) (20) makes them very attractive when many cores are to be dated.

Extension of the whole-core magnetic correlation and dating technique to a grid spanning a whole lake makes accurate measurements of total sedimentation in a closed basin practical for the first time. Bloemendal *et al.* (21) illustrate this with data from a 130-core grid obtained from the sediment of Llyn Goddionduon, northern Wales, during a 2-week spell of fieldwork. Whole-core κ sensing was completed and the results were plotted in graphical form during the same period at temporary laboratory facilities close to the lakeside. Correlation of the profiles, using additional magnetic parameters, together with pollen and radiometric dating (^{14}C , ^{137}Cs , and ^{210}Pb), provides a rapid basis for quantifying material input to the sediments on a whole-lake basis. This, in turn, can be more realistically related to whole-catchment denudation than results based on extrapolation from a few cores analyzed by conventional, time-consuming methods.

Since the fluctuations in susceptibility result from changes in the concentration of magnetic minerals, they provide a basis not only for core correlation but for sedimentological interpretations, as heavy minerals, including magnetite, are sorted during transport and concentrated in sediments according to their hydrological properties. For example, in Loch Lomond magnetic concentration is related to the particle size of the sediment (22). The coarse silt fraction has a low concentration of magnetite, thus coarser, silty horizons are associated with low susceptibility values. The changes in particle size distributions result from environmental changes in the drainage basin—for example, variations in the relative importance of erosion of topsoil. This Lomond model of bulk susceptibility fluctuations helps to account for the linkage, first observed in Lough Neagh, between changes in pollen indicators of human activity (such as grasses, bracken, and plantains) and the susceptibility of limnic deposits (23).

In many lakes with catchments dominated by bedrock as diverse magnetically as ferrimagnetic-rich basalt and diamagnetic limestone, a strong direct link, similar to that observed in Loch Lomond

and Lough Neagh, has emerged between the increased concentration of ferrimagnetic minerals in the sediment and accelerated erosion resulting from forest clearance and farming. In each of these cases, the most likely explanation for the link involves a shift from a sedimentation regime dominated by channel-derived material to one in which the supply from channel sources becomes relatively less important as loosened and exposed surface material transported by overland flow becomes increasingly significant. Wherever reliable time control is available (and this is coming increasingly from paleomagnetic direction measurements), acceleration in dry mass sediment accumulation accompanies the assemblage of evidence for human impact and soil loss.

Although the pattern of magnetic concentration and composition in a lake sediment is produced by local land-use variations, an underlying regional pattern can be discerned. For example, three Finnish lakes (Fig. 8, a to c) and one lake from southern Sweden (Fig. 8d) show a similar pattern of steadily de-

creasing magnetic concentration during the last 9000 years. In contrast, British records (Fig. 8, e to g) show much more within-core variation and more pronounced increasing concentration trends over the last 5000 years. These differences in ferrimagnetic mineral concentration between Scandinavian and British postglacial sites would become greater if the rates of sediment accumulation were taken into account and viewed in terms of the weight, or volume, of ferrimagnetic minerals accumulated per square meter per year (a flux density). This further exaggeration would arise because the χ peaks occur at times of high accumulation rate. We account for the pattern of Scandinavian χ variations as resulting from processes associated with interglacial maturation of soils and vegetation in the absence of man, as described by Mackereth (24), coupled with a declining allocthonous contribution to the lake sediments until very recent land-use changes, such as forest clearance and settlement, caused χ to rise again. Greater disturbance of the landscape in Britain by man, particu-

Fig. 7. Whole-core relative declination logs for three surface cores from Loch Lomond, Scotland. The susceptibility maxima from Fig. 6 are shown as short horizontal bars and confirm the correlations of the relative declination logs. The magnetic ages correspond to the declination turning points A to F.

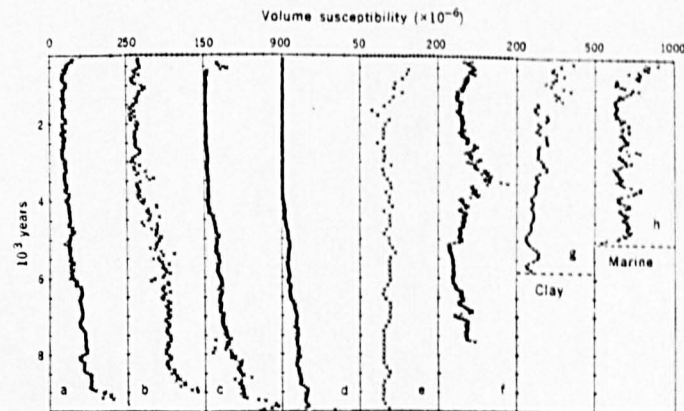
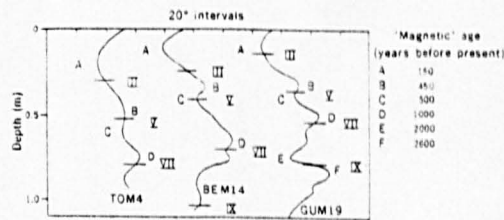


Fig. 8. Volume susceptibility logs for four Scandinavian and four British lake sediment cores: (a) Paajarvi, (b) Ormarjarvi, (c) Vuokonjarvi, (d) Hjortsjon, (e) Lake Windermere, (f) Lough Catherine, (g) Lough Neagh, and (h) Loch Lomond.

larly after the decline of the elms (*Ulmus*) (25), would similarly account for the more variable magnetic record.

Climatic Shifts

On a longer time scale, the magnetic mineral types and concentrations reflect the weathering, pedogenic, and denudational regimes prevailing through the major climatic shifts of the Pleistocene. Magnetic measurements can provide rapid insight into the nature of these shifts, their effect of weathering, soil development, and erosion rates, and their expression in the sedimentary record. Preliminary studies confirm paleoclimatic linkages in environments as diverse as northwest England (26), tropical Africa, and northern Queensland (27). The time scales of variation differ by an order of magnitude and the climatic regimes reflected span the range from arctic-alpine to humid tropical.

Prospect

Laboratory magnetic analyses have been shown to have many applications to a wide range of disciplines associated with environmental problems. The importance of these magnetic techniques will probably be further extended by the development of sensitive instruments capable of measuring, in the field, both magnetic remanence and magnetic susceptibility.

References and Notes

1. M. Faraday, *Philos. Trans. R. Soc. London* (1832), pp. 125-162.
2. D. W. Collinson, *Rev. Geophys. Space Phys.* 13, 659 (1975).
3. F. Oldfield, R. Thompson, K. E. Barber, *Science* 199, 679 (1978).
4. F. Oldfield, P. G. Appleby, R. S. Cambray, J. D. Eakins, K. E. Barber, R. W. Battarbee, G. R. Pearson, J. M. Williams, *Oikos* 33, 40 (1979).
5. P. Pakarinen and K. Tolonen, *Suo* 28 (pt. 1), 19 (1977).
6. R. Thompson and F. Oldfield, *Phys. Earth Planet. Inter.* 17, 303 (1978).
7. E. Le Borgne, *Ann. Geophys.* 11, 399 (1955).
8. C. E. Mullins, *J. Soil Sci.* 28, 223 (1977).
9. G. Longworth, L. W. Becker, R. Thompson, F. Oldfield, J. A. Dearing, T. A. Rummery, *ibid.* 30, 93 (1979).
10. T. A. Rummery, J. Bloemendal, J. Dearing, F. Oldfield, R. Thompson, *Ann. Geophys.* 35, 103 (1979).
11. G. Longworth and M. S. Tite, *Archaeometry* 19, 3 (1977).
12. F. Oldfield, *Prog. Phys. Geogr.* 1, 460 (1977).
13. T. A. Rummery, R. Thompson, D. E. Walling, *Water Resour. Res.* 15, 211 (1979).
14. D. Ninkovitch, N. D. Opdyke, B. C. Haezen, J. H. Foster, *Earth Planet. Sci. Lett.* 1, 476 (1966).
15. N. D. Opdyke, *Rev. Geophys. Space Phys.* 10, 313 (1972).
16. F. J. H. Mackereth, *Earth Planet. Sci. Lett.* 12, 332 (1971).
17. L. A. Bauer, *Phys. Rev.* 3, 34 (1899).
18. S. R. C. Main and E. C. Bullard, in preparation.
19. M. J. Aitken, *Philos. Trans. R. Soc. London Ser. A* 269, 77 (1970).
20. L. Molyneux, R. Thompson, F. Oldfield, M. E. McCallan, *Nature (London)* 237, 4 (1972).
21. J. Bloemendal, F. Oldfield, R. Thompson, *ibid.* 280, 40 (1979).
22. R. Thompson and D. J. Morton, *J. Sediment. Petrol.* 49, 801 (1979).
23. R. Thompson, R. W. Battarbee, P. E. O'Sullivan, F. Oldfield, *Limnol. Oceanogr.* 20, 687 (1975).
24. F. J. H. Mackereth, *Philos. Trans. R. Soc. London Ser. B* 250, 165 (1966).
25. H. Godwin, *History of the British Flora* (Cambridge Univ. Press, Cambridge, ed. 2, 1975).
26. F. Oldfield, J. Dearing, R. Thompson, S. E. Garget-Jones, *Pol. Arch. Hydrobiol.* 28, 321 (1978).
27. A. P. Kirshaw, *Nature (London)* 251, 222 (1974).

APPENDIX 5

Identification of cores
used for analysis.

LOCATION	CORE NUMBER.	STORED	USED FOR MAGNETIC MEASUREMENTS.	USED FOR PALAEO- ECOLOGICAL ANALYSIS.	USED FOR RADIONETRIC DATING.
LLYN BYCHAN	LB1		X		
	LB2		X		
	LB3		X		
	LB4		X		
	LB5		X		
	LB6		X		
	B79:1		X		
	B79:2		X		
	B79:3		X		
	B79:4		X		
	B79:5		X		
<u>LES LANDES</u> LAKE BISCARROSSE	BP1		X		
	BP2		X		
	BP3	X			
	BP4	X			
	BP5	X			
	BP6			X	X
	BP7			X	
	BP8			X	
	BP9			X	
	BP10	X			
	BP11	X			
	BP12	X			
	BP13	X			
	BP14	X			
	BP15	X			
	BP16	X			
LAKE SANGUINET	S1	X			
	S2	X			
	S3	X			
	S4			X	X
	S5	X			
	S6			X	
	S7	X			
	S8	X			
	S9	X			
	S10	X			
	S11	X			
	S12	X			
	S13	X			
	S14	X			
	S15			X	
	S16	X			
	S17	X			
	S18	X			

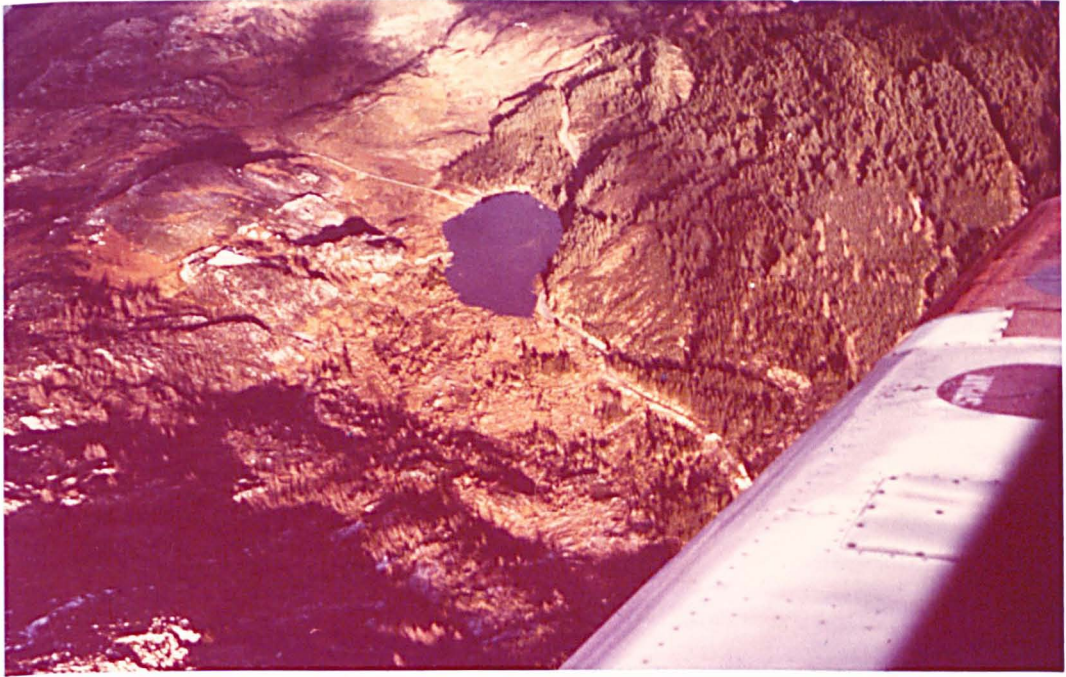


Plate 1 Llyn Bychan study area.



Plate 2 Llyn Goddionduon study area.

- Ahlgren. I.F., and Ahlgren. C.E., (1960) Ecological effects of forest fires.
Bot. Rev., 26, pp 483-533
- Appleby. P.G. and Oldfield. F. (1978) The calculation of lead - 210 dates assuming a constant rate of supply of unsupported ²¹⁰Pb to the sediment.
Catena, 5., No. 1. pp 1-8
- Beaton. J. D. (1959) The influence of burning on the soil in the timber range area of Lac Le Jeune, British Columbia.
Can. J. Soil Sci., 39., pp 1-11
- Blakemore. R. (1975) Magnetotactic Bacteria.
Science, 190 pp 377-379
- Blaisdell. J. P. (1953) Ecological effects of planned burning of sage bush grass range on the Upper Snake River Plains.
U.S. Dept. Agr., Tech. Bull. 1075 pp 1 - 35
- Blayac J. (1916) Contribution a l'etude du sol des Landes de Gascogne.
Annls. Geogr. 25 pp. 23 - 46
- Bloemendal. J. (1977) Palaeoecological studies in a small upland drainage basin in Caernarvonshire.
Unpublished thesis. University of Liverpool
- Bloemendal. J., Oldfield. F., and Thompson. R. (1979) Magnetic measurements used to assess sediment influx at Llyn Goddionduon.
Nature 250 pp 50 - 53

- Borman. F.H., Likens. G.E., and
Eaton. J.S.
(1969) Biotic regulation of particulate
and solution losses from a forested
ecosystem.
Bioscience 19, pp 600 - 610
- Buffault. P.
(1942) Histoire des dunes maritimes
de la Gascogne
Edition Dulmas.
- Cailleux. A.
(1952) Recentes variations du niveau
des mers et des terres.
Bull. Soc. Geol. Fr., Ser. 6. Vol.2 pp135
- Clout. H. D.
(1969) Country Planning in Gascony.
Scott.Geogr. mag., 85, pp 9-16
- Connaughton. C.A.
(1935) Forest fires and accelerated
erosion.
J. For. 33. pp 751 - 2
- Cwynar. L.C.
(1978) The recent fire history of
Barron Township Algonquin Park, Ontario.
Can. J. Bot., 55. pp 1524-1538
- Cwynar. L.C.
(1979) Recent history of fire and
vegetation from laminated sediment
of Greenleaf Lake. Algonquin Park,
Ontario.
Can. J. Bot., 56. pp.10 - 21
- Dearing. J. D.
(1979) The application of magnetic
measurements to studies of particulate
flux in lake-watershed ecosystems.
Unpublished Ph. D. thesis,
University of Liverpool.

- Delebecque. A. (1898) Les Lacs Francais
Paris Chamerot et Renourad.
- Digerfeldt. G., Battarbee. R.W.,
and Bengtsson. L. (1975) Report on annually laminated
sediment in Lake Järslasjön, Nacka,
Stockholm.
Geol. For. - Stockh. Forh., 97,
pp 29-29-40.
- Dryness. C.T. and Youngsberg. C.T. (1957) The effect of logging and
slash-burning on soil structure.
Soil Sci. Soc. Amer. Proc., 21,
pp 444 - 447
- Dryness. C. T. (1965) Soil surface conditions following
tractor and high-lead logging in the
Oregon Cascades.
J. For. 63, pp 272 - 5
- Dryness. C. T. (1967) Erodibility and erosion potential
of forest watersheds.
(In International Symposium on Forest
Hydrology)Ed. Sopper. W.E., and Lull H.W.
Pergamon press.
- Duffart ch. (1900) Origines des sables ayant
contribué aux formations eoliennes
quaternaires qui caracterient le
plateau lanclaire et la côte de
Gascogne.
- Dunlop D. J. (1972) Magnetite : Behaviour near the
single domain threshold.
Science (N.Y.) 176, pp 41-43

- Dunlop D. J. (1973) Superparamagnetic and single-domain threshold sizes in magnetite. J. Geophys. Res., 78 pp 1780-1793
- Eakins. J.D., and Morrison R.T. (1977) A new procedure for the determination of Lead-210 in lake and marine sediments. Atomic Energy Research Establishment Report 8475 LONDON H.M.S.O.
- Elpatievsky. M.P., Runiantsev. S.P., and Yarmelovich. B. K. (1934) Methods of slash disposal to forest types. U.S. Forestry Service Translation.289
- Enjalbert H. (1950) Observations morphologiques Les Landes de Gascogne. Les Gorges due Ciron et le Karst de Casteljaloux. Revue Geogr. Pyrenees S.-Ouest. 21 pp 5-42
- Fabre. L. A. (1905) Le sol de la Gascogne. La Geographie. Paris p. 42
- Faegri. K. and Iverson J. (1964) Textbook of pollen analysis Blackwell, Oxford.
- Feitknecht. W. (1965) The oxidation of finely divided Fe_3O_4 and iron. Colloques, Int. Cent. Natn. Tech. Scient. 122. pp 121 - 126
- Fitzpatrick. R. W. and Le Roux J. (1975) Pedogenic and solid solution studies on iron titanium minerals. Proc. Int. Clay Conf., Mexico City pp. 585 - 599
- Fourcade. A. (1909) De la mise en valeur des Landes de Gascogne. Résultat économiques de la loi du 19 Juin 1857
Doctorate thesis, Bordeaux

- Fredriksen. R. L. (1970) Comparative water quality-natural and disturbed systems pp. 125-137 (in) Forest land-uses and stream environment Dreyon state Univ., School of Forestry. Corvallis, Oreyon Eds. Krygier.J.R. and Hall. J. D.
- Frissel S. S. (1973) The importance of fire as a natural ecological factor in Itasca State Park. Minnesota. Quat. Res. (NY). 3. pp 329-382
- Fritts. H. C. (1976) Tree rings and climate Academic press (New York and London).
- Fuller. W. H. (1955) Effects of burning on certain forest soils of Northern Arizona. Forest. Sci. 1. pp 44-50
- Gould S. J. (1979) A natural precision designer. Bacteria with built in magnets reveal biologie's meticulous engineering. New. Sci., pp 446-447
- Graham I.B.G. and Scollar. I. (1976) Limitations on magnetic prospecting in archaeology imposed by soil properties. Archaeo - Physika. 6, pp 1-124
- Gregory K. J. and Walling D. E. (1973) Drainage basin form and process, a geomorphological approach Edwards Arnold.
- Håkanson, L. (1976) A bottom sediment trap for recent sedimentary deposits. Limnol. Oceanogr. 21 pp. 170-174

- Heinselmann. M.L. (1973) Fires in the virgin forests of the Boundary Waters Canoe Area, Minnesota.
Quat. Res., 3. pp. 329-382
- Hendricks. B.A. and Johnson. J. M. (1944) Effects of fire on steep mountain slopes in Central Arizona.
J. Agr. Res., 32 pp 631-644
- Heselman. H. (1916) Omvara skogsforyngringsatgarders inverkan pa saltpeterbildningen i marken och dess betydelse for barrskogens foryngring.
English summary in J. Ecol., 7 pp. 213
- Heyward. F. (1938) Soil temperatures during forest fires in the Longleaf pine region.
J. For. 36 pp 478-491
- Heyward. F. (1939) The relationship of fire to stand composition of Longleaf pine forests.
Ecology 20, pp. 287-304
- Hibbert A. R. (1967) Forest treatment effects on wateryields.
in. International Symposium on Forest Hydrology. pp. 527 - 543
Ed. Sopper, W.E. and Lull. H.W.
Pergamon press.

- Hotbie. J.E. and Likens. G.E. (1973) Output of phosphorous, dissolved organic carbon, and fine particulate carbon from the Hubbard Brook Watersheds. Limn. Oceanogr., 18 pp 734 - 742
- Houlston R. M. (1968) Pedogenesis and soil development in the Landes des Gascogne.
Unpublished thesis. University of Manchester
- Howells. M. F., Francis. E.H., Leveridge. B.E., and Evans C.D.R. (1978) Classical areas of British geology: Capel Curig and Betws-y-Coed.
H.M.S.O.
- Hubbell.D.W. and Syre.W.W. (1965) Application of radioactive tracers in the study of bedload movement.
Proc. Federal Inter Agency Sedimentation Conf. 1963.
U.S.D.A. Misc. publ., 970, pp 569-578
- Huttunen. P and Merilainen J. (1978) New freezing device providing large unmixed sediment samples from Lakes.
Ann. Bot. Fenn. 15, pp 128-130
- Huttunen. P. (1980) Early land-use, especially the slash and burn cultivation in the commune of Lammi, Southern Finland, interpreted mainly using pollen and charcoal analyses.
Acta Bot. Fenn. 113 pp 1-45
- Ironside. R. G. (1968) Rural renovation in Les Landes, south-west France: A french regional development experiment.
Cah. Geogr. Queb. 27. pp 365-380

- Isaac. L.A. and Hopkins. H.G. (1937). The forest soil of the Douglas Fir region and the changes wrought upon it by logging and slash burning.
Ecology. 18 pp 264-279
- Kalela (1961) Waldvegetationzonen Finnlands und ihre Klimatischen Paralleltypen.
Arch. Soc. Vanamo 16 (suppl). pp 65-83
- Kidson. C. and Carr. A.P. (1962) Marking beach material for tracing experiments.
Proc. A.S.C.E.J. Hyd. Div., 88 pp 43-60
- Kilgore B.M. and Taylor D. (1979) The fire history of a sequoia-mixed conifer forest.
Ecology 60 pp 129-142
- Komarek. E. V. (1970) Controlled burning and air pollution : an ecological review.
Proc. Tall Timbers Fire Ecology Conf. (Texas) pp 141-173
- Komarek. E. V. (1973) Further remarks on controlled burning and air pollution.
Proc. Tall Timbers Fire Ecology Conf. (Florida) pp 274-282
- Krammes. J. S. (1970) Erosion from mountainside slopes after fire in southern California.
U. S. Forest and Range Expt. Sta. Res. Note. 171 pp 8
- Le Borgne. E. (1955) Susceptibilité magnétique anormale du sol superficial.
Annls. Geophys., 11. pp 399 - 419

Le Borgne. E.

(1960) Influence du feu sur les propriétés magnétiques du sol et due granite.

Annls. Geophys., 16 pp 159-195

Leopold L. B., Emmett W. W. and Myrick R. W.

(1966) Channel and hillslope processes in a semi arid area. New Mexico.

U.S. Geol. Survey Professional Paper 352 G

Liddle M. J.

(1974) A survey of twelve lakes in the Gwydyr Forest region of Snowdonia.

Unpublished thesis. University College North Wales.

Likens G. E., Bormann. F. H., Johnson. N.M., Fisher D. W. and Pierre. R.S.

(1970) Effects of forest cutting and herbicide treatment on nutrient budgets in the Hubbard Brook Watershed Ecosystem.

Ecol. Monogr. 40 pp 23-47

Likens. G. E., and Bormann F. H.

(1974) Effects of forest clearing on the northern hardwood forest ecosystem and its biochemistry.

In. Proc. First Internal Cong. Ecol. (Hague)

Likens. G. E. and Davis M. B.

(1975) Postglacial history of Mirror Lake and its watershed in New Hampshire. U.S.A. An initial report.

Verh. Intl. Verein. Limnol., 19 pp 982-993

Longworth. G., Becker. L.W., Thompson R. Oldfield F., Dearing J.A., and Rummary T.A.

(1979) Mössbauer effect and magnetic studies of secondary iron oxides in soils.

J. Soil. Sci. 30 pp 93-110

- McElhinney. M.W. (1973) Palaeomagnetism and plate tectonics.
Cambridge University Press. London.
- McMinn R.G. (1951) The vegetation of a burn near Blaney
Lake B.C.
Ecology. 32(1) pp 135-140
- Mackereth F. J. H. (1958) A portable core sampler for lake
deposits.
Limnol. Oceanogr., 3 pp 81
- Molyneux L. (1971) A complete result magnetometer for
measuring the magnetic susceptibility of
long cores of sediment.
Geophys J.R. astr. Soc., 32 pp 479-481
- Molyneux L. and Thompson R. (1973) Rapid measurement of the magnetic
susceptibility of long cores of sediment.
Geophys. J. R. astr. Soc. 32 pp 429-434.
- Morisawa. M. (1973) Streams their dynamics and morphology
McGraw - Hill. New York.
- Mullins. C. E. (1974) The magnetic properties of the soil
and their application to archaeological
prospecting.
published Ph. D. thesis in Archeo-Physika.,
5. pp 143-347.
Rheinland Verlag. Bonn.
- Mullins. C. E. (1977) Magnetic susceptibility of the soil
and its significance in soil science:
A review.
J. Soil Sci., 28 pp 223-246

- Mutch. R. W. (1970) Wildland fires and ecosystems. -
A hypothesis.
Ecology. 51. pp 1046- 1051
- Newson. M. (1976) The physiography and vegetation of the
plynlimon catchments.
Institute of Hydrology Rep., No. 43
- Newson. M. (1980) Erosion and deposition by rivers.
M.A.F.F. funded project 73.
Unpublished first progress report. (January).
- Oades. J. M. and Townsend. W.N. (1963) The detection of ferromagnetic minerals
in soils and clays.
J. Soil. Sci., 39 pp 179-187
- Oldfield F. (1977) Lakes and their drainage basins as
units of sediment - based ecological study.
Prog. Phys. Geog., 1. (3) pp 460-504
- Oldfield. F., Dearing J.D.,
Thompson R. and Garret-Jones S. (1978a) Some magnetic properties on lake
sediments and their possible links with
erosion rates.
Pol. Arch. Hydrobol., 25 1/2 pp 321-331
- Oldfield. F., Thompson R., and Barber. K. E. (1978 b) Changing atmospheric fallout of
magnetic particles recorded on recent
ombotrophic peat sections.
Science. 199 pp 679-680
- Oldfield. F. (1978 c) Pollen analysis of recent sediments
from two lakes near Halifax. Nova Scotia.
Canada.
Pollen Spores. 20 pp 167-175
- Newson. M. (1980). The erosion of drainage ditches and its
effect on bedload yield studies in Mid-Wales:
Reconnaissance case studies.
Earth Surface Processes. 5 pp. 275-290.

- Oldfield. F., Rummery. T. A., Thompson R. and Walling D.E. (1979) Identification of suspended sediment sources by means of magnetic measurements: Some preliminary results.
Wat. Res. Research. 15 pp 211-218
- Oldfield. F., Thompson. R. and Dickson. D.P.E. (1980) Artificial enhancement of stream bedload : A hydrological application of superparamagnetism.
D.E.P.I. (in press)
- O'Reilley. W. (1976) Magnetic minerals in the crust of the earth.
Rep. Prog. Phys. 39 pp 857-908
- Parry. L. G. (1965) Magnetic properties of dispersed magnetic powders.
Phil. Mag., 11., pp 303-312
- Pennington. W., Cambray. R.S. and Fisher. E.M. (1973) Observations on lake sediment using fallout Cs¹³⁷ as a tracer.
Nature Lond., 242 pp 324-326
- Pennington. W. (1979) The origin of pollen in lake sediments: an enclosed lake compared with one receiving an inflow stream.
New Phytol. 83 (1) ppl89-213
- Pinaud. A. M. (1973) La Foret Landaise.
Revue Geogr Pyrénées S-Ouest. 44 pp 207-224
- Rathbun. R.E. and Nordin.C.E. (1971) Tracer studies of sediment transport processes.
Proc. A.S.C.E. J. Hydr. Div., HY9. pp 1305-16

- Rich. L. R. (1962) Erosion and sediment movement following a wild fire in a ponderosa pine forest of central Arizona.
U.S. Forest Serv. Rocky Mtn. Forest and Range Expt. Sta Res. Note. 76 pp 12
- Ritchie. J. C., McHenry. J. R. (1973) Dating recent reservoir sediments. and Gill. A.C. Limnol.Oceanogr., 18 pp 254 - 263
- Robbins. J. A. and Edgington D.N. (1975) Determination of recent sedimentation rates in Lake Michigan using Pb-210 and Cs137. Geochem. et Cosmo Acta 39 pp 285-304
- Rummery. T. A., Bloemendal, J (1978) The effects of fire on soil and and Oldfield. F. sediment magnetism.
Geophys. J. R. Astr. Soc., 53
- Rummery. T.A. Bloemendal. J., (1979a) The persistence of fire induced Dearing. J.D., Oldfield. F., magnetic oxides in soils and lake sediments. and Thompson R. Annls. Geophys. 35 pp 103
- Rummery. T.A., Oldfield. F., (1979b) Magnetic tracing of Stream bedload. Newson. M., and Thompson. Geophys. J.R. astr. Soc., 57 pp 278-279
- Saarnisto. M., Huttunen. P., (1977) Annual lamination of sediments in and Tolonen. K. Lake Lovojärvi, southern Finland, during the past 600 years.
Ann Bet. Fenn. 14 pp 35-45
- Scheffer. F., Meyer. B., and (1959) (Magnetic measurements as aids in the Babel. U. determination of iron oxides in the soil).
Beitr. Miner. Petrogr., 6 pp 371-387
- Schoeffer. V. J. (1973) Some physical relationships of fine particulate smoke.
Proc. Tall Timbers Fire Ecology. Conf. (Florida) 13

- Schwertmann. U. and Taylor R.M. (1976) Iron oxides.
In. Minerals in the soil environment Am.
Soc. Agron Publication.
- Shaw D. (1971) The Gwydyr Forest in Snowdonia.
H.M.S.O.
- Stacey. F.D. and Banerjee. S.K. (1974) The physical principles of rock
magnetism.
Elsevier. Amsterdam.
- Stober. J.C. and Thompson R. (1979) Magnetic remanence acquisition in
finnish lake sediments.
Geophys. J.R. Astr. Soc., 57 pp 727-739
- Sutton. H. D. (ed.) (1977) Themes in the historical geography
of France.
Ch: 8. Reclamation of wasteland during the
18th and 19th centuries.
Academic Press. London.
- Swain. A.M. (1973) A history of fire and vegetation in
north-eastern Minnesota as recorded in lake
sediments.
Quat. Research. 3. pp 383-396
- Swain. A. M. (1978) Environmental changes during the past
2000 years in northern Wisconsin : Analysis of
pollen, charcoal and seeds from varved lake
sediments.
Quat. Research. 10 pp 55-68
- Tarling. D. H. (1971) Principles and applications of
palaeomagnetism.
Chapman and Hall. London.

- Tarrant. R. F. (1956) Effects of slash burning on some physical soil properties.
Forest Sci., 2 pp 18-22
- Taylor D. L. (1973) Some ecological implications of forest fire control in Yellowstone National Park Wyoming.
Ecology. 54 pp 1394-1396
- Taylor. R. M. and Schwertmann. U. (1974) Maghemite in soils and its origins.
Clay Minerals. 10 pp 299-310
- Teidemann. A.R. and Helvey J.D. (1973) (abstract) Nutrient ion losses after fire and fertilization in eastern Washington.
Am. Inst. Biol. Sci. (annual meeting)
- Thompson R. (1974) Palaeomagnetism.
Sci. Prog., Oxford. 61 pp 349-373
- Thompson. R. Battarbee. R. W. (1975) Magnetic Susceptibility of lake sediments.
O'Sullivan.P.E. and Oldfield F. Limnol. Oceanogr. 20 pp 687-698
- Thompson R. and Oldfield F. (1978) Evidence for palaeomagnetic secular variation in lake sediments from the New Guinea Highlands.
Phys. Earth. Planet. Inter., 17 pp 300-306
- Thompson R. and Morton. D. J. (1979) Magnetic susceptibility and particle size distribution in recent sediments of the Loch Lomond drainage basin. Scotland.
J. Sed. Pet., 49 pp 810-812
- Thompson R., Bloemendal. J. (1980) Environmental applications of magnetic measurements.
Dearing J. Oldfield. F.,
Rummary. T.A., Stober. J.C. Science 207 pp 481-486
and Turner G. M.

- Tite. M.S. and Mullins.C.E. (1971) Enhancement of the magnetic susceptibility of soils on archaeological sites.
Archaeometry. 13 (2) pp 209-219
- Tite M.S. and Lillington.R.E. (1975) The effect of climate on the magnetic susceptibility of soils.
Nature. 256 pp 565 - 566
- Tolonon.M. (1978) Palaeoecology of annually laminated sediments in Lake Ahvendinen. S. Finland.
Pts. 1 -111
Ann. Bot. Fenn. 15 pp 177-240
- Ugglä.E. (1958) Ecological effects of fire on north Swedish Forests.
Almquist and Wiksells Boktryckeri A.D.
Uppsala 1-8
- Vadyunina. A. F. and Babanin. V.F. (1972) Magnetic susceptibility of some soils in the U.S.S.R.
Soviet Soil. Sci., 4 pp 588-599
- Vines. R. J. (1973) Bush fire smoke and air quality.
In. Prac. Tall Timbers Fire Ecology Conf.
(Florida) 13 pp 303-8
- Vuorinen. J. (1978) The influence of prior land use as the sediments of a small lake.
Pol. Arch. Hydrobiol. 25 pp 443-451
- Walcott. C., Gould. J.M. and Kirschvink. J. L. (1979) Pigeons have magnets.
Science 205 pp 1027-1029
- Walling. D.E. Peart. M.R. and Thompson. R. (1979) Suspended sediment sources by magnetic measurements.
Nature. 281 pp 110-113

- Wallis, J.R. and Willen D.W. (1963) Variation in dispersion ratio, surface aggregation ratio and texture of some California surface soils as related to soil forming factors. Internat. Assoc. Sci. Hydrol., 8 pp 48-54
- Whittaker. E. (1963) Temperatures in heath fires. J. Ecol., 49 (3) pp 709-716
- Willen. D. W. (1965) Surface soil textural and potential erodability characteristics of some southern Sierra Nevada Forest Sites. Soil Sci. Soc. Amer. Proc., 29 pp 213-218
- Woolsey. T. S. (1920) Studies in French Forestry
Ch. 8 Forestry in the Landes.
John Wiles and Sons. N.Y.
- Wright R. F. (1976) The impact of forest fire on the nutrient influxes to small lakes in north eastern Minnesota. Ecology. 57 pp 649 - 663
- Zackrisson. O. (1977) Influence of forest fires on the North Swedish boreal forest. Oikos. 29 pp 22-32

ADDENDA.

- Oldfield, f. Tolonen, K. (IN PRESS) History of particulate atmospheric pollution from magnetic measurements in dated Finnish peat profiles.
- Thompson, R.

AMBIO.